THE UNIVERSITY
of EDINBURGH

5-Nitrofurans and ALDH: implications for a novel therapeutic approach in cancer

By

Richard Crispin

Doctor of Philosophy

Edinburgh Cancer Research UK Centre, IGMM
University of Edinburgh
2017

Declaration

I declare that this thesis has been composed by myself, Richard Crispin, and that the work has not be submitted for any other degree or professional qualification. I confirm that the work submitted is my own, unless otherwise stated. All work included that was not performed by me has been used with permission and I confirm that appropriate credit has been given within this thesis, where reference has been made to the work of others.

Signed.....

Date.....

Abstract

I hypothesise that cancer cells with high aldehyde dehydrogenase ($ALDH^{high}$) activity present a new therapeutic target and will be selectively sensitive to 5-nitrofuran pro-drugs.

Cancers are heterogeneous and contain subpopulations of $ALDH^{high}$ cells with tumour initiating potential. ALDH enzymes metabolize toxic aldehydes, and are highly expressed in somatic and cancer stem cells (CSCs), although their function in CSCs is not fully understood. In a small molecule screen coupled with target ID, Zhou *et al*. (2012) recently discovered that clinically active 5-nitrofurans (5-NFNs) are substrates of ALDH2. 5-NFNs are a class of pro-drug widely used to treat bacterial and parasitic infections, where their relative specificity is driven by nitroreductases, but little is known about the enzymes that bio-activate 5-NFNs in humans. Recent clinical cancer research has found that the 5-NFN, nifurtimox, has anti-cancer properties and it is currently in Phase 2 clinical trials for neuroblastoma and medulloblastoma (ClinicalTrials.gov Identifier: NCT00601003), however the mechanism underlying this anti-cancer activity is unknown.

In melanoma and other cancers, ALDH1A1 and ALDH1A3 are highly expressed in CSCs. I demonstrate the anti-cancer activity of 5-NFNs in cancer cell lines, where they express high sensitivity to 5-NFNs in cell viability assays (A375 melanoma cells EC_{50} = 867nM). To test if ALDH1 enzymes are substrates of 5-NFNs, I performed *in vitro* activity assays by monitoring NADH production (λ = 340nm). I found that the clinically available 5-NFNs, nifuroxazide and nifurtimox, in addition to our own newly synthesised 5-NFNs, are competitive substrates for human ALDH1A3 activity *in vitro* ($P < 0.05$). Notably, nifuroxazide is not a substrate for ALDH2, suggesting that nifuroxazide may show selectivity toward ALDH1. Enzymatic assays with purified human ALDH2, demonstrate that ALDH2 requires NAD^+ for bio-activation of 5-NFNs. Consistent with these assays, I found that 5-NFNs are competitive substrates for ALDH activity in melanoma cells by Aldefluor™, with 5-NFNs displaying a prolonged competitive inhibition of ALDH activity compared with the known inhibitor, DEAB. Importantly, no-nitro control compounds show no activity toward ALDH enzymes *in vitro* or in culture. Kinetic living-cell imaging (IncuCyte ZOOM®) reveals that a subpopulation of ALDH1A3 siRNA transfected A375 cells

are protected from 5-NFN toxicity ($P > 0.05$) and cell death (DRAQ7™: $P < 0.0001$), demonstrating a functional role for ALDH1A3 in mediating 5-NFN activity in cancer cells. In contrast, A375 cells overexpressing ALDH1A3 by cDNA transient transfection were hypersensitive to 5-NFNs ($P < 0.001$), determined by Muse™ cell viability. Computational docking studies reveal that 5-NFNs have the potential to fit within the interior of the ALDH enzymatic cavity and interact with the catalytic cysteine, thereby offering a potential mechanism for 5-NFN bio-activation. Finally, in collaboration, we show a unique interaction between 5-NFNs and ALDH using mass spectrometry and have initiated protein crystallography trials.

My work demonstrates a novel and biologically relevant 5-NFN-ALDH interaction in cancer cells. I propose 5-NFNs have the potential to target $ALDH^{high}$ CSCs within a tumour and advance the repurposing of clinical 5-NFN pro-drug antibiotics as anti-cancer therapeutics.

Lay Abstract

5-nitrofurans (5-NFNs) are a class of antibiotic drugs used in the treatment of both bacterial and parasitical infections. Recently, nifurtimox, a WHO essential medicine for the treatment of parasitical Chagas disease, has been found to have anti-cancer activity in childhood brain cancers. As clinical trials continue for the use of nifurtimox to treat these cancers, the mechanism for this anti-cancer activity remains unknown. It is important to define the targets and mechanism of 5-NFN therapy in order to determine those patients that will most benefit from treatment in the future. Our lab has recently discovered that 5-NFNs can target cells with high aldehyde dehydrogenase (ALDH) expression. ALDH is a family of enzymes that metabolise toxic aldehydes produced by the body through growth and diet, which can otherwise lead to DNA damage. Like in normal tissues, cancers are heterogeneous, where there exists a subpopulation of cells that exhibit stem-cell like characteristics. These cells, dubbed cancer stem cells (CSCs), are typically more resistant to chemotherapy, thought to be the primary driver in cancer relapse, and reported to have high expression of ALDH enzymes. We hypothesise that the anti-cancer activity seen with nifurtimox is driven by targeting ALDH enzymes in cancer cells.

In melanoma, high levels of ALDH ($ALDH^{high}$) also mark CSCs. Here I demonstrate the anti-cancer activity of 5-NFNs in cancers, including melanoma, where 5-NFNs can promote cancer cell death. I report that new 5-NFNs compounds, as well as current clinical 5-NFNs, can target ALDH enzymes, where the clinical 5-NFN, nifuroxazide, shows some specificity towards the ALDH1 isoform - the ALDH enzymes most associated with cancer. As well as being able to target these $ALDH^{high}$ cells, I show that 5-NFNs can also inhibit the activity of ALDH1 enzymes in melanoma cell cultures, where ablating ALDH activity has been shown to make cancers more sensitive to chemotherapies. By decreasing the expression of ALDH1 enzymes in melanoma cells, we show that melanoma becomes more resistant to 5-NFNs, where there was significantly less cancer cell death upon treatment. In parallel, by overexpressing ALDH1 enzymes in these melanoma cells, I demonstrate hypersensitivity to 5-NFNs also. Through computer simulations, it was revealed that 5-NFNs have the potential to strongly bind or 'fit' in the active site of ALDH enzymes, offering a mechanism for 5-NFN inhibition of ALDH enzymes. Finally, working in

collaboration at The University of Edinburgh, we discover that 5-NFNs can irreversibly inhibit ALDH activity, offering a dual function for these 5-NFN compounds.

We demonstrate a novel mechanism that can both selectively target and kill ALDH^{high} cancer cells coupled with irreversible inhibition of ALDH enzymes, where the clinical 5-NFN, nifuroxazide, may exhibit specificity towards the ALDH enzymes most expressed in cancer. Here, I propose the repurposing of 5-NFN antibiotics as a potential future treatment for cancer.

Acknowledgements

Firstly, I need to thank my fantastic supervisor, Liz Patton, for all your continued support and guidance, and for giving me this amazing opportunity to begin with. I want to thank you for all the time you spared, working to help make my project a success. Your supervision has been the backbone of my project and I am so proud to watch as both the ALDH story and ALDH team grows.

I also have to thank my second supervisor, Asier Unciti-Broceta, for all the guidance with my chemistry and all the pints down the pub. Both sharing your knowledge and always being extremely optimistic has made my time working with your lab hugely enjoyable, and I am grateful to have been given the opportunity to be part of 2 fantastic labs during my project.

I also have to thank the rest of my thesis committee, Neil Carragher, Val Brunton and Charlie Gourley, for all your guidance and support throughout.

I need to thank everyone in the Patton Lab, both past and present. The support has been exceptional and paramount to the success of my project. From teaching me how to do PCRs for the first time to troubleshooting experiments that randomly didn't work, I am so grateful. I thank you for the friendships, the laughs and the scientific support throughout.

I want to thank all the chemists too for their patience in helping me with my chemistry, through the confusing NMRs and the never ending quest to remove DMF, it's been a blast and I loved being considered a member of your lab. I especially want to thank Craig, Jason and Sam for all the great cinema trips turned nights out and horrible mornings after at work – we had some good times.

And also, I'd like to thank everyone from Neil Carragher's lab, especially Alison, John and Karen, for always helping me when things went awry and for constantly putting up with me stealing your food.

To all the amazing people who worked with me at The University of Edinburgh: Martin Waterfall, Lizzie Freyer, Alex von Kriegsheim, Jimi Wills, Martin Wear, Matt Nowicki, Liz Blackburn and Douglas Houston. And to my fantastic collaborators: Dave Adams, Marco Ranzani, Thomas Hurley, Daria Mochley-Rosen, Che-Hong Chen and everyone at OakLabs. The work you contributed to this project has helped make it such a success, so thank you.

To my parents, I have to thank you for everything. Supporting me even when you you're still not quite sure exactly what I'm doing. Without you guys, I wouldn't be where I am today and I want to thank you for always being there, regardless.

I really want to thank everyone at the Edinburgh University Kickboxing Club for being my family away from home all these years. From the sketchy driving to the trips to A&E, it's been the best times and it makes me incredibly sad to have to (finally) leave you guys.

And of course I need to thank the rest of my family, friends and colleagues for continually being there over the last 8 years. I've truly loved my time here, but it would not have been without such an amazing community of people, so thank you.

Sist men ikke minst, må jeg takke Nathalie Spockeli, min glade nordmann. Du var den med kompetente, entusiastiske, hardt arbeidende æres-studenten jeg kunne ha fått jobbe med. Du ble ikke bare veldig godt kjent med alle du arbeidet med, du kontinuerlig overgikk deg selv i evne og ferdighet. Det var en sann glede å ha deg i laboratoriet og du var kjært savnet av alle når du dro (spesielt for tapet av den evige forsyningen av norsk sjokolade!). Jeg håper du fortsetter å følge din lidenskap for vitenskap, men du vil uansett alltid bli ansett som en fantastisk forsker av meg. Men viktigst av alt så vil jeg takke deg for å være min beste venn. Gjennom våre opp- og nedturer (og når jeg alltid vant over deg i '8 Out of 10 Cats Does Countdown'!), var du alltid min klippe og den personen jeg snudde til for råd, samtaler, feiring og moro. Du er den mest omsorgsfulle, godhjertede personen jeg vet om, du kan alltid få meg til å smile og jeg ser tilbake med glede på dagen vi møttes på Starbucks den solfylte september ettermiddagen. Fra hver grettene telefonsamtale til hvert bekymringsfrie eventyr, jeg håper jeg alltid vil ha deg som min bestevenn. Jeg ville ikke vært hvor jeg er i dag, eller blitt den jeg er, uten deg i livet mitt. Så fra bunnen av mitt hjerte, takk.

Contents

Chapter 1

Introduction

1.1 ALDH and Cancer Stem Cells

1.1.1 Function of ALDH enzymes in normal physiology

The aldehyde dehydrogenase (ALDH) superfamily is a group of enzymes responsible for metabolising toxic aldehydes. Aldehydes are continually produced in our bodies through metabolism of amino acids, lipids, carbohydrates, vitamins and steroids, as well as being accumulated through growth and diet.[1] One common example is the production of acetaldehyde in the liver as result of drinking alcohol (ethanol), which is then broken down by hepatic ALDH2.[2] Aldehydes are highly reactive electrophilic species, which, when left unchecked, can form adducts with organic macromolecules such as DNA, lipid membranes and proteins, in turn promoting DNA damage, cancer development and stem cell failure.[3,4]. ALDH enzymes catalyse the metabolism of these toxic aldehydes from the body through $NAD(P)^+$-dependant irreversible oxidation into their carboxylic acid conjugates (**Figure 1.1**), which are less harmful to the body and can be excreted safely. Although ALDH plays a crucial role in detoxifying aldehydes from the body, some of the carboxylic acid intermediates produced, such as retinoic acid (RA) or γ-aminobutyric acid (GABA), are essential for normal physiology and embryonic development.[1] For instance, conversion of retinal to retinoic acid by ALDH1A enzymes is important for the regulation of gene expression needed for growth and development,[5] or synthesis of GABA by ALDH9A1 in the regulation of the dopaminergic pathway.[2,6] Many ALDH enzymes also have essential, non-catalytic functions, such as in the formation of crystallins in the eye or acting as binding proteins for both endogenous and exogenous compounds required for normal physiology and homeostasis.[7] So it is unsurprising that ALDH functionality, in particular through ALDH1 driven retinoic acid signalling, is quintessential in mediating embryogenesis, development, cell proliferation, differentiation and survival.[2]

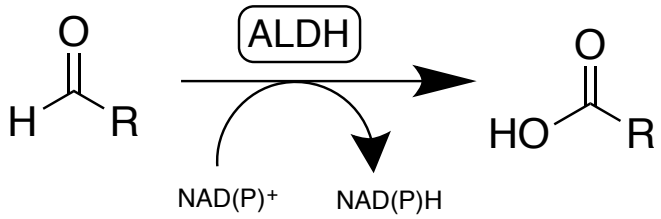

Figure 1.1: Enzymatic action of ALDH enzymes. ALDH catalyses the irreversibly oxidation of the aldehyde carbonyl to the carboxylic acid conjugate through hydride transfer to couple the reduction of co-factor, $NAD(P)^+$ to NAD(P)H.

The ALDH superfamily is evolutionarily conserved, with isoforms represented in all 3 factions of the taxonomic tree.[8] In the eukaryotic genome, ALDH expression is highly diverse across species with 24 ALDH families currently characterised. In humans, there are 19 distinct ALDH isoforms, all with different substrate specificities and physiological functions (**Table 1.1**).[2] ALDH enzymes contain 3 domains, a $NAD(P)^+$ co-factor binding domain, a catalytic binding domain and a linker region, important for oligomer formation. ALDH enzymes are non-functional as single monomers, and as such, the formation of dimer, tetramer or hexamer complexes from homo-ALDH subunits are important for enzyme functionality.[9] This is paramount in the ALDH2*2 mutation, present in approximately 8% of the human population. Primarily localised in persons of Eastern Asian descent, this single point mutation (G→A) substitutes lysine in place of glutamic acid (E487K). Although both the catalytic and co-factor binding domains remain unaltered, the resultant mutation promotes the formation of a disordered α-helix, integral for ALDH dimer formation (**Figure 1.2**).[10] The consequent incorporation of mutant ALDH2*2 subunits into ALDH2 tetramer complexes, ablates normal ALDH2 activity, and individuals with this mutation exhibit alcohol intolerance and have increased risk of cancer, stroke, cardiac disease and neurodegenerative diseases, such as Parkinson's.[10] Although the latter is most likely as a result of inefficient production of aldehyde-derived neurotransmitters, the majority of these risk factors are associated with acetaldehyde accumulation.

ALDH enzymes all share highly conserved residues important for normal functionality. ALDH activity relies on a highly conserved catalytic cysteine (Cys302 in ALDH1 and ALDH2) to facilitate hydride transfer from the substrate aldehyde to co-factor $NAD(P)^+$.[2,11,12] $NAD(P)^+$

co-factor binding occurs via an initial interaction with the Rossmann fold (a glycine rich loop between an α-helix and β-sheet), where, coupled with a conformational change, activates the catalytic cysteine residue in order to attack the aldehyde carbonyl. It is the act of co-factor binding that activates the enzyme to enable hydride transfer and, in most ALDH isoforms, dissociation of NAD(P)H resets catalytic activity.[11]

ALDH	Preferred aldehyde	Additional functions and characteristics
ALDH1A1	Retinal	Ester hydrolysis; binds androgen, cholesterol, thyroid, daunorubicin, and flavopiridol; corneal and lens crystallin; oxidizes DOPAL, acetaldehyde
ALDH1A2	Retinal	High affinity for LPO-derived aldehydes
ALDH1A3	Retinal	High affinity for LPO-derived aldehydes
ALDH1B1	Acetaldehyde	May protect the cornea from UV-light
ALDH1L1	10-Formyltetrahydrofolate	Binds acetaminophen
ALDH1L2	Unknown	Induced by the anti-inflammatory agent indomethacin
ALDH2	Acetaldehyde	Ester hydrolysis; nitroglycerin bio-activation, oxidizes LPO-derived aldehydes; binds acetaminophen
ALDH3A1	Aromatic, aliphatic aldehydes	Ester hydrolysis; scavenges ROS; UV-filter; corneal crystallin; oxidizes LPO-derived aldehydes; regulation of cell-cycle
ALDH3A2	Fatty aldehydes	Insulin regulates gene expression
ALDH3B1	Unknown	Oxidizes LPO-derived aldehydes
ALDH3B2	Unknown	Unknown
ALDH4A1	Glutamate γ-semialdehyde	Ester hydrolysis; may mitigate oxidative stress
ALDH5A1	Succinate semialdehyde	May be involved in neurotransmission efficiency
ALDH6A1	Malonate semialdehyde	Esterase activity; only known human CoA-dependent ALDH
ALDH7A1	α-Aminoadipic semialdehyde	Closely related to plant osmoregulatory protein; may regulate cell cycle
ALDH8A1	Retinal	Oxidizes LPO-derived aldehydes and acetaldehyde
ALDH9A1	γ-Aminobutyraldehyde	Oxidizes betaine, acetaldehyde and DOPAL; involved in carnitine biosysnthesis; esterase activity
ALDH16A1	Unknown	Unknown
ALDH18A1	Glutamic γ-semialdehyde	Unknown

Table 1.1: Characterisation of all human 19 ALDH isoforms. Described are the preferred substrate aldehyde of each isoform and other physiological functions of each ALDH enzyme, both catalytic and non-catalytic. Table adapted from Marchitti *et al.* (2008).[2]

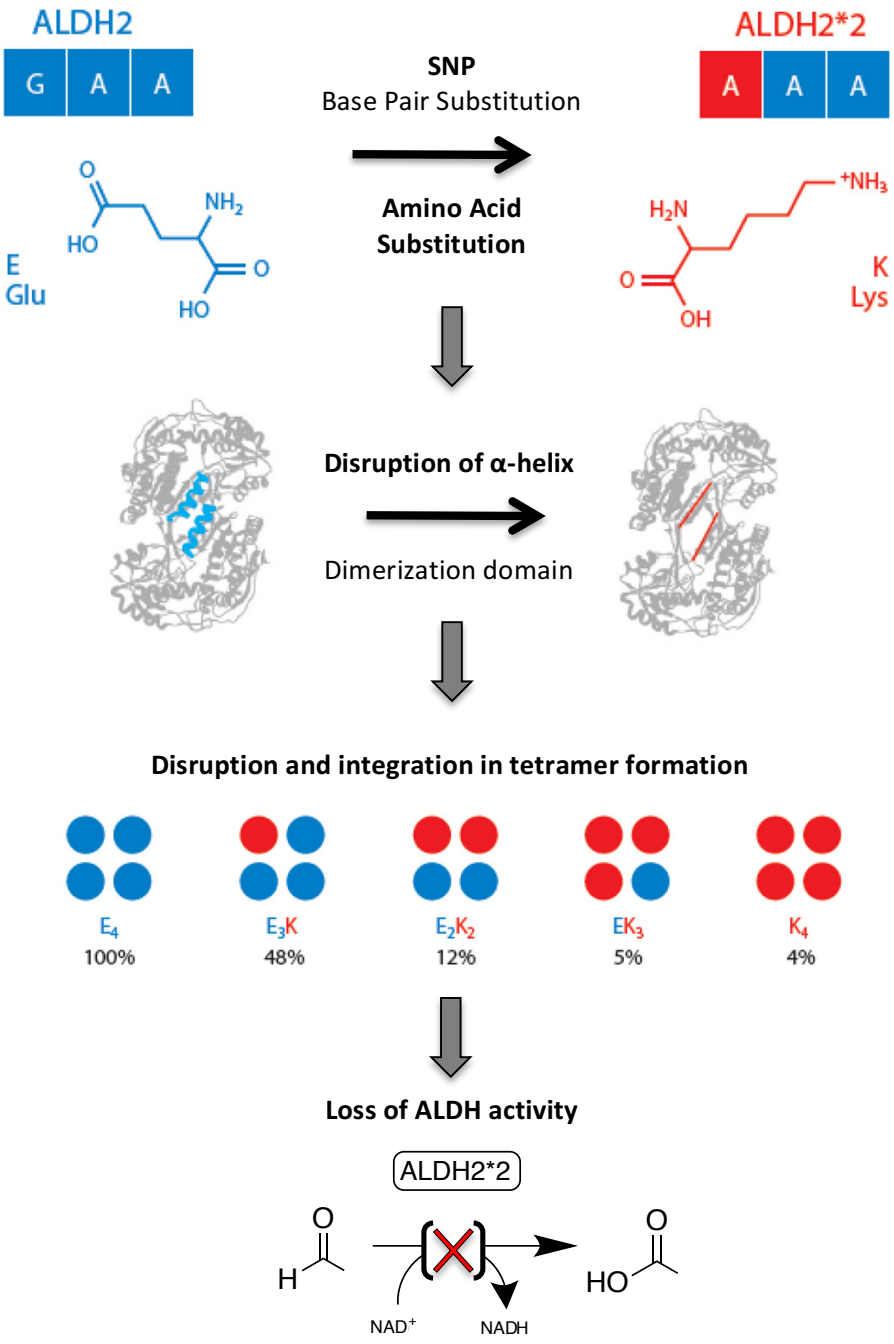

Figure 1.2: Effect of ALDH2*2 mutation of normal enzymatic function. ALDH2*2 mutation is a single point mutation involving substitution of guanine (G) to adenine (A), in turn, resulting in the substitution of glutamic acid (E) to a lysine (K) residue. This amino acid substitution causes the disruption of the α-helix structure in the domain important for dimerization. Incorporation of ALDH2*2 monomers in ALDH tetramer complexes ablates activity, where ALDH activity decreases per each ALDH2*2 subunit incorporated. The incorporation ablates the catalytic conversion of acetaldehyde to acetate via NAD^+ reduction. Figure adapted from Gross *et al.* (2015).[10]

1.1.2 ALDH and stem cells

ALDH enzymes, although having a well-described role in normal physiology, are also well established stem cell markers. Being first described in blood, $ALDH^{high}$ umbilical blood cell populations were shown to be enriched in hematopoietic progenitor cells, or hematopoietic stem cells (HSCs).[13] $ALDH^{high}$ cells were determined by Storms *et al.* (1999) in the first described use of the Aldefluor™ assay, a flow cytometry assay relying on the specific conversation of the fluorescent marker, BODIPY-aminoacetaldhyde (BAAA), to its negatively charged BODIPY-aminoacetate conjugate by ALDH, leading to fluorescent accumulation. Using this method, they demonstrated that these $ALDH^{high}$ umbilical blood cells were depleted of differentiated cell populations (e.g. mature T-cells, natural killer cells and markers for myeloid, erythroid, and platelet populations) and enriched for another HSC marker, CD34.[13] ALDH as a marker for HSCs and neural stem cells has now been well established,[14] so it is expected other cell types will also share this characteristic marker. The work from Ginister *et al.* (2007) has highlighted this, where they reported an $ALDH^{high}$ subpopulation in mammary epithelial tissue, isolated through the same Aldefluor™ technique as before, which exhibited stem like properties. They were also able to describe a corresponding $ALDH^{high}$ population in malignant breast cancer, correlating ALDH expression with poor clinical outcome.[15] From this, increased ALDH activity, particularly ALDH1A1, was shown to be a marker for several stem and progenitor cell populations including, neural stem and progenitor cells, colonic stem cells and adipose-derived mesodermal stem cells.[16,17]

Although the function of ALDH activity in stem cells is not fully understood, it is likely that retinoic acid signalling is an important factor, considering the consistency of ALDH1 enzymes specifically being highlighted as stem cell markers. Retinoic acid is essential in the differentiation of cells, where binding of all-*trans*-retinoic acid, a product of ALDH1 biosynthesis, to retinoic acid receptors (RAR) and retinoid X receptors (RXR) expressed on target cellular nuclei, causes haematopoiesis, tissue patterning and cellular development.[18,19] ALDH inhibition in HSCs resulted in decrease retinoic acid activity and delayed differentiation.[20] It has also been suggested that ALDH1 and retinoic acid signalling play an important role in regulation of self-renewal in HSCs, especially as ALDH1 inhibition seemed to directly down-regulate transcription factors, such as HOXB4, associated with

HSC self-renewal.[14,20] Perhaps the role ALDH enzymes play in cellular detoxification and their ability to protect cells against oxidative stress may also provide an important role in promoting stem cell longevity,[14] where loss of ALDH expression or function can lead to a wide spectrum of disease severities.[2,10] Similarly, an interesting report found that isolated $ALDH^{high}$ bone marrow cells injected into patients with ischemic heart failure exhibited beneficial cardiac functionality 6-months after treatment, highlighting the use of ALDH-determined stem cells as a future therapeutic option.[21]

Aldehyde detoxification by ALDH enzymes plays an important role in Fanconi anaemia. It has been reported that the Fanconi anaemia gene, *Fancd2*, has a functional role in protecting cells from aldehyde toxicity,[22] and indeed, chicken DT40 B *Fancd2*$^{-/-}$ cells were hypersensitive to formaldehyde and acetaldehyde treatment. Critically, Patel and his team discovered that *Aldh2*$^{-/-}$*Fancd2*$^{-/-}$ murine pups had disrupted haematopoiesis upon continued ethanol exposure, leading to bone marrow failure, and consequently leukaemia; likely through the lack of ALDH2 in HSCs offering vital aldehyde detoxification.[22] A recent study by Garaycoechea *et al*. (2012) reported an important synergy between ALDH2 expression and the Fanconi anaemia DNA-repair pathway in protecting HSCs from aldehyde toxicity, where Fancomi anaemia driven bone marrow failure is likely caused by aldehyde accumulation.[4] They highlighted the importance of *Fancd2* in mediating sensitivity to aldehydes, where DNA repair pathways are likely to be important in HSC survival. They describe synthetic lethality of double knock-out (*Aldh2*$^{-/-}$*Fancd2*$^{-/-}$) HSCs upon aldehyde exposure, where aldehyde metabolism is quintessential in maintaining the HSC pool.[4] This is validated by the fact that the HSC pool is significantly diminished upon double knock-out of *Aldh2* and *Fancd2*; where knock-out of *Aldh2* only significantly inhibited bone-marrow repopulation, and a likely cause of the haematological cancers associated with Fanconi anaemia.[4] A further synergy between ALDH2 and FANCD2 has been reported in embryonic development, where double *Aldh2*$^{-/-}$*Fancd*$^{-/-}$ embryos were not viable unless maternal ALDH2 was present for catabolism of aldehydes and oxidative agents in order to protect the foetuses.[23] This highlights the functional importance for ALDH2 being required (both internally or maternally) in embryogenesis, particularly when DNA crosslink repair pathways are deficient. But crucially, when maternal ALDH2 is present during gestation, embryogenesis is rescued, however the HSC pool is still impaired.[23]

1.1.3 ALDH as a marker for cancer stem cells

Many cancers have now been described to display certain heterogeneity and hierarchy, where there exists a sub-population within the cancer cell bulk that exhibits stem-like behaviours, these are coined cancer stem cells.[24] Cancer stem cells (CSCs) are a small sub-population of cancer cells that possess the tumorigenic potential to give rise to both tumorigenic and non-tumorigenic progeny.[25] The proposed CSC model describes CSCs as tumour initiating cells, where they propagate the differentiation of heterogeneous non-tumorigenic cancer cells that constitutes the bulk of the tumour through establishment of progenitor cells that can further differentiate (**Figure 1.3**).[24,26] However, unlike in normal tissue, it is the CSCs only that have the capacity to self-renew, making them essential in both the initiation and maintenance of a tumour.[27] CSCs are often described as resistant to conventional chemo-therapeutics; whether that is through upregulation of such genes as the multi-drug resistant gene (MRP),[28] increased expression of mechanisms to evade drug toxicity, including increase of ATP-binding cassette (ABC) transporters to essentially pump the drugs out of the cell.[29] Another likely source of CSC chemo-resistance may lie in their low-proliferative potential, where therapeutics targeting rapidly diving cell populations will leave CSC subpopulations essentially unaffected.[27] It is hypothesised that where cancers have relapsed after conventional chemo-therapeutic treatment, it is the chemo-resistant CSCs that repopulate the regressed tumour, in many cases presenting resistance to original course of therapy.[26,27] This tumorigenic potential of CSCs coupled with their resistance to conventional therapies makes treatment of relapsing tumours increasingly difficult, on top of any somatic mutations that may occur during therapy to help drive repopulation. The 'gold-standard' assay for detection of CSCs is through serial *in vivo* transplantation into immunodeficient mice, where only the tumorigenic potential of CSCs will give rise to cancer populations.[27] CSCs currently have no universal marker, with many cancer types (or even subtypes) differing in markers for CSCs, such as CD271 in melanoma[30] or $CD34^{+}CD38^{-}$ in acute myeloid leukaemia,[31] however, even these prove dependant on the individual patient phenotype.

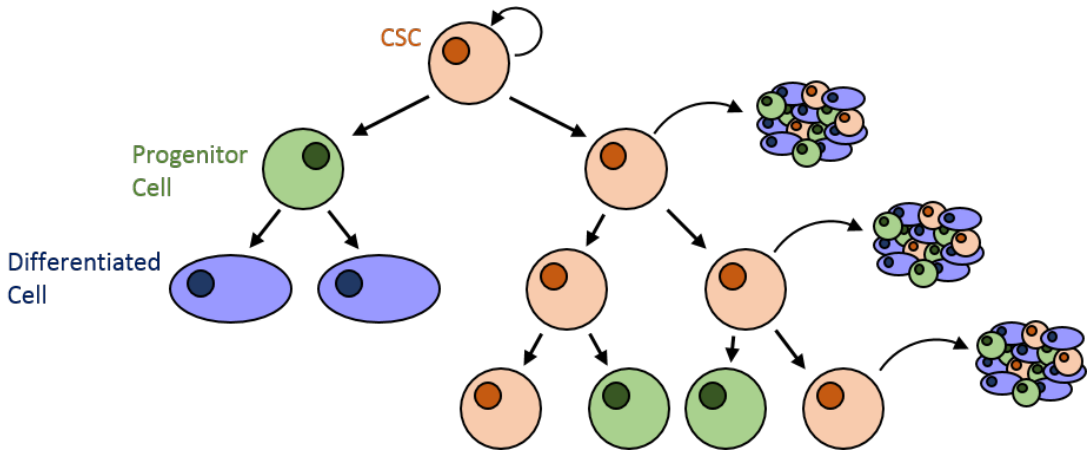

Figure 1.3: Schematic detailing the cancer stem cell (CSC) model. CSCs can differentiate to give rise to progenitor cells as well as further CSC formation. Progenitor cells can drive the production of further differentiated cells, with low tumorigenicity, encompassing the tumour bulk. Only CSCs have the ability to both self-renew and drive the re-population of tumour bulk. Schematic adapted from Reya *et al*. (2001).[24]

ALDH activity has recently become a focus in cancer due to its prevalence in many cancers,[32,33] including melanoma,[34,35] colorectal,[36] pancreatic,[37] lung,[38] breast,[15] ovarian,[39] glioblastoma[40] and neuroblastoma.[41,42] The ALDH^{high} subpopulation of cells within a tumour have been shown to exhibit CSC-like properties such as chemo-resistance[43,44] and increased tumorigenicity.[34] ALDH is now on the verge of being labelled a universal functional CSC marker,[44,45] and in colorectal cancer especially, the ALDH^{high} subpopulation overlapped sufficiently enough with CD44, a well-established CSC marker in this cancer, that the ALDH^{high} subpopulation presented as a niche within CD44 cell subpopulation themselves, suggesting ALDH may serve as a more accurate marker for CSCs in colorectal cancer.[36] ALDH^{high} subpopulations are thought to be involved in mediating metastasis in a number of cancers.[46] In breast cancer, the transplantation of ALDH^{high}CD44^{+}CD24^{-} cells into NOD/SCID/IL2γ^{null} mice matched the metastatic behaviour observed in patients.[47] Cancers that have higher level of ALDH expression correlate with poor clinical outcome, and a number of studies reveal the success of using ALDH expression as a prognostic marker to predict the response to treatment and clinical progression,[39,48,49] primarily dependant on ALDH1A1 or 1A3. ALDH1A1 has consistently been deemed to be a universal CSC marker across all cancer types,[31,44] however other ALDH isoforms have been demonstrated as CSC

markers also, dependant on specific cancer type.[45] For instance, in neuroblastoma, it is reported that ALDH1A2 is the key driver of CSC-potential,[42] and ALDH3A1 mediates tumorigenesis in prostate cancer.[50]

Summarised in **Table 1.2**, it is clear that ALDH as a CSC marker is dynamic and complex, mirroring the wide variances seen between cancer types. Specific ALDH expression relies heavily on the tumour sub-type, however the exact function for this upregulation is largely unknown. In head and neck squamous cell carcinomas, the $ALDH^{high}$ CSC subpopulation was highly enriched in patients with Fanconi anaemia, reporting more aggressive and resistant tumours as a direct correlation.[51] The link between Fanconi anaemia and cancer has been well established, in particular regarding BRCA2 mutations and breast cancer,[52] suggesting ALDH provides protection against the increase in DNA damaging agents as a result of Fanconi anaemia, and in turn, promoting more aggressive tumours.

ALDH	Cancer type	Source	Cancer-related function
ALDH1A1	All cancer types	-	Biomarker for CSC, drug resistance
ALDH1A1	Ovarian	A2780/CP70 ovarian cancer cell line	Cell cycle regulation, DNA repair network signalling
ALDH1A2	Prostate	Transgenic adenocarcinoma mouse prostate model	Reduced expression in prostate cancer in comparison with normal tissue. Retinoid metabolism
ALDH1A2	Acute myeloid leukaemia (AML)	K562S + K562AC cell lines	High expression and resistance to Ara-C
ALDH1A2	Neuroblastoma	Neuroblastoma primary tumours	Chemo-resistance
ALDH1A3	Gallbladder	Squamous cell/adenosquamous carcinomas and adenocarcinomas	Poor prognosis, high expression in advanced disease
ALDH1A3	Bladder	Non-muscle invasive bladder cancer primary tumours	Decreased expression and aggressive clinicopathological characteristics
ALDH1A3	Breast	MDA-MB-468, SKBR3, MDA-MB-435, BT-20, MCF7, T47D, and MDA-MB-231 breast cancer cell lines	Correlation to tumour grade and metastasis
ALDH1A3	Glioblastoma	Primary glioblastoma tissues	Hypermethylation associated with better prognosis
ALDH1A3	Melanoma	A375 melanoma cell line + malignant melanoma primary tumours	Cell cycle arrest, apoptosis and decreased viability

Continued on next page

ALDH	Cancer type	Source	Cancer-related function
ALDH1A3	Prostate	Human prostate cancer epithelial cells	Androgen-responsive, retinoic acid biosynthesis
ALDH1A3	Prostate	Human prostate cancer epithelial cells	Androgen-responsive, retinoic acid biosynthesis
ALDH1B1	Colon, lung, breast and ovary	Human adenocarcinomas of colon, lung, breast and ovary	Biomarker for colon cancer
ALDH2	Leukaemia	K562 chronic myeloid leukaemia (CML) cell line	Drug resistance, cell proliferation
ALDH3A1	Breast, lung, and glioblastoma	A549 and CCD-13Lu lung cancer cell lines, SF767 glioblastoma cell line and MCF-7 breast cancer cell line	Drug resistance, CSC, cell proliferation
ALDH3B1	Breast	MDA-MB-231 breast cancer cell line	Tyrosine metabolism, downregulation by PGGc
ALDH3B1	Renal and liver	ALDH3B1-transfected human embryonic kidney (HEK293) cells, HepG2 liver cancer cell lines and A549 lung cancer cell line	Protective against oxidative stress
ALDH4A1	Glioblastoma	U373MG human glioblastoma cell line	Induced by overexpression of p53, protective against oxidative stress
ALDH5A1	Hepatoma	HuH7 hepatoma cell line	Not known
ALDH5A1	Renal cell carcinoma (RCC)	RCC patient tissue and HNF4α-mutated HEK239 embryonic kidney cell line	Possible regulation by HNF4α, deregulated in RCC
ALDH5A1	Breast ductal carcinoma *in situ* (DCIS)	MCF10.DCIS, SUM102 and SUM225 brest DCIS cell lines	Differentially overexpressed
ALDH6A1	Normal breast epithelium versus MCF-7 cancer cell line	MCF-4 breast cancer cell line vs MTSV1.7 non-tumorigenic breast epithelium cell line	RA metabolism in MTSV1.7 versus MCF-7 cell lines
ALDH7A1	Renal cell carcinoma (RCC)	RCC4 renal cell carcinoma cell line	Regulated by pVHLd, does not affect cell growth or motility
ALDH7A1	Prostate	PC-3M-Pro4 human prostate cancer cell line	Knockdown impairs migration and reduces metastases in animal model
ALDH10 (ALDH3A2)	Oesophageal squamous cell carcinoma (ESCC)	ESCC patient tumour tissues with del 17p13.3-p11.1	LOHe in this specific patient population

Table 1.2: Specific ALDH enzymes in their roles as cancer stem cell markers. The ALDH isoform associated as a cancer stem cell marker varies depending on cancer type. While ALDH1A1 remains conserved across all cancers, other ALDH isoforms appear to mark cancers differently and vary in functionality. Table adapted from Pors & Moreb (2014).[45]

In many reports, there is a heavy emphasis on ALDH upregulation in conjunction with drug resistance,[45] but the exact mechanism in which this occurs is still not fully understood in many cases. The correlation between ALDH expression and drug resistance has been observed in the majority of tumour types and in patients with resistant tumours also,[44] linking ALDH expression to poor clinical prognosis as a consequence. The association between ALDH and drug resistance has long been described,[53] where Moreb *et al*. (2000) initially described the functional role for ALDH1A1 in mediating 4-hydroperoxycyclophosphamine (4-HC) resistance in tumours, by sensitising K562 leukemic and A549 lung cancer cells to 4-HC upon ALDH1A1 knock-down.[54] ALDH^{high} cancer cells, isolated through Aldefluor™ driven FACS, were consistently highly resistant to the conventional chemotherapeutics, where it was demonstrated that sensitivity to treatment was restored upon ALDH inhibition or knock-down in lung, breast, melanoma and gastric carcinoma tumours.[43,55-57] Meng *et al*. (2013) further showed the expression of ALDH1 increased in A2780 ovarian cells upon synthetic induction of cisplatin resistance,[39] where a distinct ALDH1^{high} subpopulation was established. This was also reported in pancreatic xenographs, where treatment with gemcitabine, an anticancer nucleoside pro-drug, enriched the tumour population for ALDH expression, as well as other CSC markers.[58]

Although the exact functional role and mechanism ALDH1 enzymes play in CSC chemo-resistance remains unclear, Raha *et al*. (2014) demonstrated that the ALDH^{high} CSC subpopulation of MET-amplified gastric carcinoma cells were resistant to the MET kinase inhibitor, crizotinib, in an otherwise highly sensitive cancer cell line.[43] In these resistant ALDH^{high} cells, they reported having higher levels of oxidative stress upon treatment with crizotinib, and cell death was induced as a result of ROS overexposure, when coupled with inhibition of ALDH.[43] This highlights ALDH providing a protective role in chemo-resistant CSCs, where ALDH1 specifically contributes to protection against DNA damage within the CSC niche. This suggests the increase in chemo-sensitivity upon ALDH inhibition is driven primarily by increased oxidative stress, rather than ALDH enzymes directly contributing to the mechanism of chemo-resistance. Similarly, mesenchymal glioma stem cells are reported to have higher levels of ALDH1A3, associated with resistance to radiotherapy, where, upon non-lethal doses of radiotherapy, the non-mesenchymal glioma stem cell populations will switch their phenotype to increase expression of ALDH1A3.[59] This highlights a functional role of ALDH1A3 in mediating resistance to radiotherapy, where the ability of ALDH1A3 to

protect the glioma stem cell population against oxidative stress, mediated by radioactive-bombardment, is a likely mechanism for this resistance.

ALDH enzymes have also been shown to have a functional role in facilitating chemo-resistance by directly metabolising drugs or their active intermediates.[60,61] ALDH enzymes have been reported in the catabolism of an important class of chemotherapeutic pro-drugs, the oxazaphosphorines, rendering them inert.[62] Cyclophosphamide, one of the most widely used oxazaphosphorines, is bio-activated by hepatic cytochrome P450 to produce the 4-HC metabolite, which releases the alkylating agent that drives anti-cancer activity.[63] The role of ALDH in cyclophosphamide resistance was reported by Hilton (1984) who described a uniquely high expression of ALDH in cyclophosphamide-resistant L1210 leukaemia cells *in vitro* and *in vivo*.[53] And as such, the ability for ALDH1A1 and ALDH3A1 to metabolise this cytotoxic 4-HC metabolite into a non-toxic carboxyl derivative in breast carcinomas,[61] presents a functional role for ALDH in specifically mediating chemo-resistance to this class of pro-drugs. Further, when cells transfected to overexpress ALDH3A1 were exposed to cyclophosphamide, it was found they were highly resistant to treatment.[63,64] This presents a functional role for ALDH enzymes in directly metabolising chemotherapeutic compounds. Although the mechanisms of chemo-resistance to other drug classes have yet to be established, for instance with Paxitaxel,[56] it could be likely that metabolism by ALDH is a primary cause for resistance in many cancer types.

Retinoic acid pathways are also likely to play an important role in mediating CSC drug tolerance. Formelli and Claris (1993) first described the use of a synthetic retinoic acid to increase cisplatin anticancer capacity in ovarian carcinoma xenografted mice.[65] Since then, the use of retinoic acid for chemo-sensitising cancers has been widely explored,[44] however the exact mechanism in which retinoic acid mediates this resistance is not fully understood. It is likely that interplay between ALDH1 expression and retinoic acid levels are at the foundation, where only the $ALDH^{high}$ breast cancer cells, and not $ALDH^{low}$ cells, displayed increased sensitivity to paclitaxel after retinoic acid pre-treatment.[56] It is suggested that due to the function of retinoic acid as a cellular differentiation agent, chemo-sensitivity could be driven by reduction of CSC-like properties in the chemo-resistant population.[44] However, because retinoic acid treated A549 lung cancer cells exhibited increased sensitivity coupled with down-regulation of ALDH1A1 and 1A3,[66] it could also be plausible

that the loss of the protective effects exhibited by ALDH1 activity leads to increase chemotherapeutic susceptibility in CSCs.

1.1.4 ALDH as a CSC marker in melanoma

It is now understood that there is a stem-like sub-population of cells expressed in melanoma, which are highly tumorigenic,[67,68] chemo-resistant,[57] and can implement self-renewal as well as differentiation to give rise to heterogeneous progeny.[69] Fang *et al*. (2005) first described a stem-like subpopulation within primary metastatic melanoma cultures, possibly due to spheroid formation, self-renewal and melanocytic differentiation, where transplantation into immunosuppressed mice drove tumour formation.[67] Isolation of a small subpopulation of melanoma cells (1%) that expressed CD133, a marker for CSC in other cancers, exhibited tumour-initiated potential *in vivo*, and expressed stem-like factors associated with angiogenesis (notch 4) and lymphoangiogenic markers (VEGFR-3 & prox-1), which may lead to the aggressive behaviour of melanoma.[70] A key paper from Schatton *et al.* (2008) reported a subset of malignant melanoma cells with tumour initiating capabilities that can be identified by ABCB5 expression, a marker which in turn can mediate chemo-resistance.[30] They reported that ABCB5 expression overlapped with expression of melanotransferrin, a factor important for melanoma growth, and monoclonal antibody driven ablation of ABCB5 significantly inhibited tumour growth *in vivo*,[30] suggesting an important functional role for melanoma CSCs in initiation, growth and maintenance of melanomas. These melanoma-initiating cells, or melanoma stem cells, have now been widely described, with characterised markers including: ABCB5, CD271 and CD10.[30,67,71,72]

The ALDH1A sub-family is primarily expressed in adult epitheliums of many organs, and may be involved in both foetal development and retinoic acid synthesis,[2] but somewhat unsurprisingly is shown to have a key role in certain chemo-resistance pathways in a variety of cancers.[73-75] Melanoma is no exception to this trend of ALDH as a biomarker for CSCs, where Aldefluor™ flow-sorted $ALDH^+$ primary melanoma cells xenographed into NOD/SCID mice were found to have significantly more rapid and efficacious tumour formation, compared to the parental and $ALDH^-$ counterparts.[35,76] Serial xenographs of flow sorted ALDH metastatic melanoma cells found that the $ALDH^+$ cells displayed self-renewal, where $ALDH^+$ enriched xenographs gave rise to melanoma cell populations similar to the parental,

whereas ALDH$^-$ xenographs were not able to replenish an ALDH$^+$ population.[35,76] ALDH$^+$ melanoma flow-sorted cells were able to give rise to a heterogeneous cancer cell population and had increased sphere formation, which again was not seen in ALDH$^-$ cells.[34,35] ALDH^{high} subpopulations have shown localisation to the tumour/host interface,[34] suggesting a functional role for ALDH in both tumour proliferation and invasion. Although, another study found no difference in tumorigenic potential between ALDH$^+$ and ALDH$^-$ melanoma cells when transplanted into NSG mice.[77] However, this study suffered from discrepancies in comparison to previous studies, in both cellular samples and methodology i.e. the 'gold standard' of serial transplantation in order to reveal the capacity of both these populations to self-renew and drive continued tumorigenicity, was not investigated.[78]

Microarray analysis of human melanoma cells, subcutaneously xenographed into immunosuppressed mice, found >15 fold increase in the ALDH1A1 and ALDH1A3 isoforms, while siRNA induced knock-down of ALDH1A3 inhibited xenograph tumour formation in mice, promoted cell cycle arrest, and reduced cell viability and sphere formation.[35,76] They concluded that ALDH1A1 and ALDH1A3 specifically are the key ALDH markers for CSC 'stem-like' potential in melanoma. Aldefluor™ flow sorting of cancer cells has been shown to correlate with cellular expression of ALDH1A1 and 1A3.[46,79,80] In melanoma, Aldefluor™ flow-sorted cells showed increased resistance to the chemotherapeutics; temozolomide, paclitaxel and doxorubicin as well as being the driver of melanoma cancer cell growth in xenographed mice.[35] This highlights the requirement of ALDH1A1 and 1A3 in melanoma to maintain cancer cell 'stemness'. Further, microarray data showed upregulation of downstream retinoic acid associated genes, many associated with stem cell behaviour, anti-apoptosis or cell cycle arrest.[31] ALDH1A1 specifically is required to modulate CSC behaviour, with specific knock-down in melanoma cells reducing cell migration, but interestingly did not inhibit tumorigenesis in this study.[81] The overlap of ALDH1A1^{high} cell populations with other melanoma CSC markers (CD133$^+$/CD29$^+$/CD44$^+$), also decreased upon ALDH1A1 knock-down, highlighting the role of ALDH1A1 in maintaining melanoma CSC potential.[81]

Questions have been raised regarding the frequency of ALDH driven CSCs present in melanoma, with reported ratios ranging from 2%,[69] to <0.1%,[35,76] and as high as 25%.[68] It

makes it incredibly difficult to establish and describe a distinct CSC niche with conflicting data, however it has been suggested these discrepancies may arise from factors such as the set ALDH expression limitation, the model and assay in which these cells are subjected to, as well as heterogeneity within the cancer cell populations themselves.[82] This may also provide some insight between the conflicting data of the presence of a distinct $ALDH^+$ tumorigenic population detailed earlier in this chapter.[35,76,83]

1.1.5 Regulation of ALDH in CSCs in melanoma

The role of ALDH in melanoma CSCs is largely unknown, however, considering the involvement of ALDH1A enzymes in melanoma CSCs, it seems logical to conclude their role in retinoic acid signalling. Luo *et al*. (2012) did show that the stem cell gene, CDC42, associated with retinoic acid pathways, was regulated by ALDH1A3 expression, however another stem cell gene, USH1C, with no involvement with retinoic acid signalling, was also regulated by ALDH1A3. This suggests that, although ALDH1A is expected to have a crucial role in retinoic acid signalling in melanoma CSCs, this is likely not the only nor primary role it serves. Certainly, there are indications ALDH is required for cell cycle arrest, reduction of apoptosis,[35] additional retinoic acid signalling[66] and protection against oxidative stress.[84] Recently, ALDH1A3 has been associated with the transcription factor, signal transducer and activator of transcription 3 (STAT3), in CSCs of melanoma[85] and non-small cell lung cancer.[86] STAT3 is a transcription factor central in mediating tumour pathogenesis, however it is not essential for functionality in normal cells. STAT3 is thought to be involved in progression and regulation in several cancers,[87] where STAT3 upregulation is associated with poor prognosis in melanoma patients.[88] STAT3 activation, and consequent signalling pathways, are associated with senescence of CSC-like cells in melanoma, where this STAT3 expression is also coupled with an increase in ALDH1A3 expression.[85] As ALDH1A3 has been highlighted as a melanoma stem cell marker,[79] this suggests interplay between ALDH1A3 expression and STAT3 activation in mediating and regulating CSC potential in melanoma.

Hedgehog-GLI (HH) signalling has also been linked to cancer cell 'stemness' in melanoma. HH expression is elevated in melanoma, compared to normal melanocytes, where pharmacological inhibition as well as genetic knock-down of the HH-pathway reduced melanoma proliferation, both *in vitro* and *in vivo*, induced apoptosis and decreased the

tumorigenic capability of CSCs.[89,90] Knock-down of the HH-pathway also significantly reduced the number of ALDH^{high} cells within the melanoma population.[90] ALDH^{high} melanoma cells had increased expression of GLI1, a downstream transcription factor of HH, not shared in the ALDH^{low} cells, where it was only the ALDH^{high} cells that were tumorigenic and could induce sphere formation.[76] This suggests a functional role of HH to regulate ALDH expression and promote melanoma CSC potential, leading to the association of expression of HH-signalling factors with increased melanoma metastasis and poor prognosis.[89] HH is a regulator of Sox2, which also been shown to reduce CSC self-renewal, plus it induces both DNA damage and apoptosis upon knock-down.[91] Similarly to HH, Sox2 expression was significantly higher in ALDH^{high} melanoma cells, compared to ALDH^{low}, and Sox2 knock-down decreased the tumorigenic capacity of ALDH^{high} cells, as well as the total number of ALDH^{high} cells within the melanoma population. Interestingly, Sox2 expression has been shown to directly affect ALDH1A1 expression in melanoma[81] in a study where the dioxin receptor (AhR), responsible for integrating pathways in metabolism and tissue homeostasis, inversely regulates ALDH1A1 expression in melanoma cells. AhR depletion drives melanoma tumorigenesis, metastatic potential, cell migration and invasion, where increased ALDH1A1 expression is also observed upon AhR knock-down.[81] Further to this, interplay between AhR, ALDH1A1 and Sox2 is suggested as a regulator of stem-like potential in melanoma, where AhR can mediate ALDH1A1/Sox2 expression to induce differentiation potential.[81] This suggests a possible mechanism for the expression and function of ALDH in maintaining a CSC subpopulation in melanoma and pathway for which ALDH expression can regulate melanoma CSC behaviour.

1.1.6 ALDH1L2 and circulating melanoma cells

ALDH1L2 is the enzyme responsible for mitochondrial folate metabolism in normal tissue.[92] Although the correlation between folate levels and cancer risk is currently unclear,[93-97] a recent study looking at frequency of circulating melanoma cells in xenographed NSG mice found that knock-down of ALDH1L2 significantly reduced the number of circulating melanoma cells in the blood.[98] However, this goes against meta-analytic data that links folic acid intake with protection against melanoma.[97] It has been suggested that folate acid plays a role in NADPH production in response to oxidative stress,[99] and inhibition of this pathway significantly reduces the incidence of metastasis in NSG mice; a pathway which is otherwise

amplified in melanoma cells.[98] It is suggested that because circulating tumour cells are rare, and the efficiency at which they can cause metastasis is even lower,[100] these circulating melanoma cells essentially fail to survive long enough in the blood to cause metastases due to oxidative stress.[98] This suggests an important role for ALDH1L2 in metastasis through regulation of pathways to suppress oxidative stress in these circulating melanoma cells. Although there is some evidence that suggests ALDH1L2 may contribute to Aldefluor™ activity in rhabdomyosarcoma cells,[101] where these ALDH^{high} cells (by Aldefluor™) were also associated with an increased self-renewal, tumorigenicity and chemo-resistance, characterisation, the Aldefluor™ contribution and indeed functionality in cancer has yet to be established.[2]

1.2 Targeting ALDH in Cancer

1.2.1 Conventional therapies and cancer relapse

Considering the CSC model, it is reasonable to assume that tumour growth and cancer development is driven by CSCs.[24,26,102] Normal chemotherapeutics (for instance platinum compounds that cause DNA damage in rapidly diving cells) will only target the highly-proliferative, non-tumorigenic cell majority. However the dormant CSC population remain unscathed.[26,102] This is supported by reports that subpopulations of cancer cells, i.e. CSCs, have much greater potential for chemo-resistance through various defence mechanisms.[26-29] As such, these dormant CSCs are regarded as the primary culprit in mediating cancer relapse, considering their characteristically high tumorigenicity.[26] Chen *et al.* (2012) showed in glioblastoma that a subset of dormant cells in the cell population remained after treatment with temozolomide (TMZ), where TMZ was only shown to target the highly proliferative glioblastoma cell bulk. Genetic ablation of these dormant cells was performed using a nestin-Cre system in mouse, where tumour relapse was consequently delayed following treatment of the glioblastoma xenographs with TMZ.[103] Resistance in CSCs can also include increased DNA damage repair agents, protective mechanisms for oxidative stress, impairment of normal apoptotic pathways, or increased ABC transporter expression that can simply efflux the cytotoxic drug out of the cell.[104]

The use of retinoic acid in the treatment of cancer is widely used against some blood cancers, where the promotion of differentiation through retinoic acid signalling pathways plays an apparent role in reducing the 'stem-like' potential and resistance in CSCs, providing an effective and lasting anti-cancer treatment.[44] The use of retinoic acid to sensitise tumours to conventional chemotherapeutics is now becoming more favourable in a wide range of cancers.[44,65] Although this treatment does prove effective, it is one of very few examples that are seeking to affect the CSCs specifically within the tumour bulk in order to promote lasting anti-cancer activity. A clinical trial using retinoic acid in head and neck cancer did result in tumour regression in the majority of patients, however the incidence of relapse was also a common problem, only months after treatment.[105]

Most oncological drug discovery is focused towards compounds that exhibit potent cytotoxicity against whole cancer cell populations.[27,104] While most treatments, including targeted therapies, now common place in melanoma treatment, will only target the tumour bulk unambiguously, it is becoming increasingly clear that designing therapeutics that can target these CSC subpopulations will be highly desirable, especially in developing treatments that will deliver long lasting cancer remission.[44,45,104] In melanoma there has been a lot of progress in developing new compounds with potent anti-cancer activity, with the new class of BRAF inhibitors now being in the front line treatment for malignant melanoma.[106,107] However, resistance is a hard fought battle in melanoma drug discovery, and targeting the CSC population has been proposed as potential option to combat this ever-growing need for new, lasting melanoma therapeutics (**Figure 1.4**).[78] This is supported by a report that treatment of melanoma with sub-lethal doses of BRAF inhibitor induced a resistant subpopulation with increased CSC-like characteristics *in vitro* and *in vivo*, including increased ALDH activity, which was then sustained to invoke chemo-resistance.[107] Recently, Tirosh *et al*. (2016) discovered a subpopulation of cells, through single cell sequencing, within malignant melanomas that have an altered cell state and are key to mediating resistance of these tumours to MAPK inhibitors.[108] This subpopulation of $AXL^{high}MITF^{low}$ melanoma cells, within the tumour bulk, had significant alterations in cellular state, which increased upon treatment with debrafenib and trametinib.[108] This highlights the cellular heterogeneity that exists within malignant melanoma, and how changes to the cellular ecosystem can alter cell state, mediate resistance and ultimately, provides evidence of a dormant, CSC-like, subpopulation within malignant melanoma, governed by cell state

changes. Schatton *et al*. (2008) explored targeting the melanoma stem cell marker, ABCB5, an efflux pump highly expressed in melanoma CSCs that directly contributes to chemo-resistance.[30] They found that the ABCB5^{+} subpopulation is highly tumorigenic through *in vivo* xenotransplantation in mice, confirming their use as a functional melanoma CSC selection marker. Treatment of xenographed mice with anti-ABCB5 monoclonal antibodies inhibited tumour growth, where antibody mediated cell toxicity specifically targeted the ABCB5^{+} tumorigenic CSC population.[30] Yue *et al*. (2015) put forward ALDH1 as a potential target against melanoma, where they found that inhibition of ALDH1 with DEAB or disulfiram in combination with the conventional therapeutic, dacarbazine, lead to reduction in tumour proliferation, but also depletion of CSCs in the tumour population.[106] As such, they suggested that inhibiting ALDH1 enzymes offers a novel treatment option in the progression of melanoma treatment.

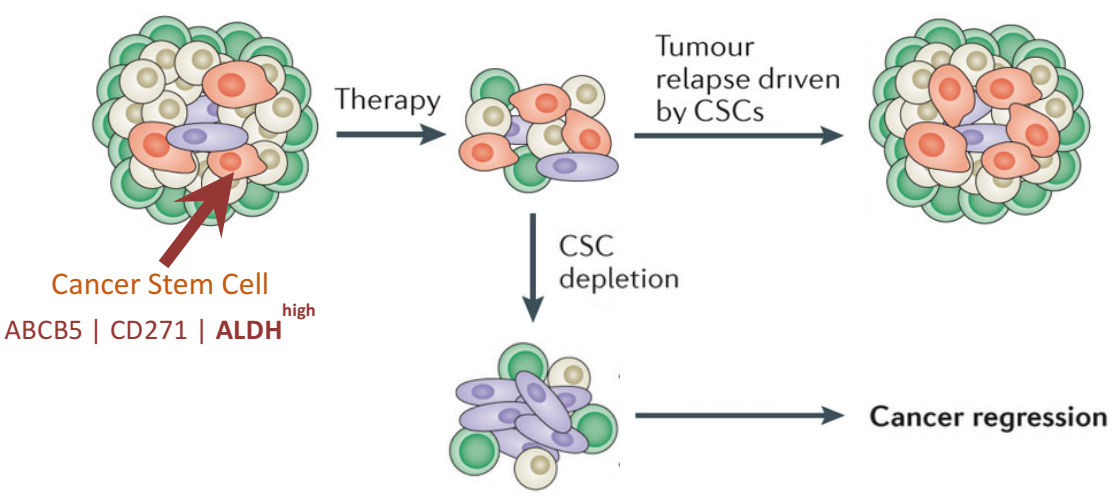

Figure 1.4: Cancer relapse is driven by CSC repopulation, upon failure of conventional chemotherapy. Heterogonous tumours contain CSCs, with notable high expression of certain markers, for example, ABCB5, CD271 and ALDH expression are associated markers for melanoma CSCs. Conventional chemotherapy will target and reduce the cancer cell population unequivocally, however CSCs, which are typically resistant to these therapies, will drive cancer repopulation upon chemo-failure or relapse. Designing therapies that can specifically target, kill and ablate these CSC subpopulations will help conventional chemo-therapeutics achieve cancer regression. Figure adapted from Beck & Cedric (2013).[26]

1.2.2 ALDH inhibitors

There are several ALDH inhibitors that have been developed and widely used, however only one is available clinically.[60] The ALDH2 inhibitor, daidzin (**Figure 1.5A**), derived from the Chinese vine, *Puearia lobata*, is a potent competitive inhibitor for ALDH2 (IC_{50} = 80nM).[109] The mechanism of daidzin mediated ALDH inhibition works through a strong van der waals contribution within the catalytic pocket, forming interactions with the catalytic Cys302 and Glu268 residues, essential for activity. Disulfiram (**Figure 1.5B**) in currently the only clinically available ALDH inhibitor. Used since the 1940's as an alcohol-abuse deterrent, disulfiram is a covalent inhibitor of ALDH2. Patients treated with disulfiram will accumulate acetaldehyde on the action of drinking alcohol (ethanol), developing undesirable symptoms such as nausea, face flushing and vertigo,[60] similar to that seen in those with the ALDH2*2 mutation.[10] The mechanism of covalent inhibition by disulfiram is driven by the formation of its metabolites promoting the carbamylation of the catalytic Cys302 residue. Upon treatment with disulfiram, the active metabolites are produced biologically through the cleavage of the disulphide bond via sulphide exchange with Cys302 on ALDH2.[60] N,N-diethylaminobenzaldehyde (DEAB) (**Figure 1.5C**), although labelled as an ALDH inhibitor, is more accurately described as a competitive substrate for ALDH, where the catalytic conversion of the tightly bound benzaldehyde derivative to its benzoic acid conjugate by ALDH occurs so exceptionally slowly that ALDH activity is essentially inhibited.[110] DEAB is commonly used as a negative control in the Aldefluor™ assay,[13] where the inhibition of Aldelfuor™ expression is through its specificity as a substrate for both ALDH1A1 and 1A3.[110] Although ALDH activity will begin to recover over time after DEAB treatment, as the DEAB carboxylate is produced, it is interesting to note that a covalent inhibition is seen between DEAB and ALDH7A1 on the catalytic Cys302,[111] and some evidence of a covalent modification with ALDH2 has also been reported.[110]

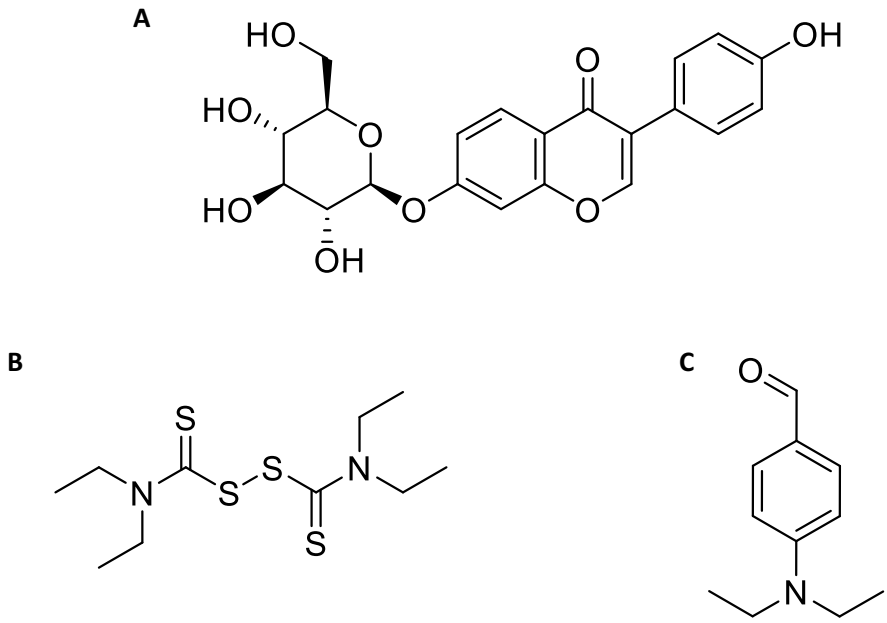

Figure 1.5: Molecular structures of ALDH inhibitors. **A**) Molecular structure of daidzin. The triple aromatic ring structure is critical for ALDH inhibition, where the phenol hydroxyl plays a key role in Cys302 interaction and the glycosyl has a strong interaction with the hydrophobic cleft opposite NAD^+ binding pocket. **B**) Molecular structure of disulfiram. Cleavage of the disulphide bond by ALDH Cys302 sulphide exchange mediates inhibitory activity, where the metabolites of disulfiram upon cleavage become highly electrophilic to promote carbamylation of the catalytic ALDH cysteine. **C**) Molecular structure of DEAB. The benzyl aldehyde moiety is vital for ALDH activity, where the bulky amide drives a tight binding in the catalytic pocket, as the slow conversation to the benzoate derivative essentially inhibits ALDH activity.

ALDH inhibitors have also been detailed for their anti-cancer potential. First used in ancient Chinese medicine, daidzin in its crude form was a common ailment to prevent cancer.[112] In more recent times, after ALDH1A1 knock-down in leukemia and lung cancer cell lines were reported to counteract chemo-resistance,[54] the use of ALDH inhibitors has been reported in the reduction of tumour relapse in xenographed mice,[43] and shown to increase sensitivity to chemo-therapeutics in breast and lung cancers[43,55,56] Classically, disulfiram has been described as an inhibitor for ALDH2, however, it is a much more potent inhibitor of ALDH1A1.[113] Its anti-cancer effectiveness as an ALDH1 inhibitor was reported by Raha *et al*. (2014), who demonstrated that treatment with disulfiram promotes

chemo-sensitivity and increase of intercellular ROS in the $ALDH^{high}$ subpopulation of breast cancer cells.[43] However, in melanoma, Cen *et al*. (2004) attributes the anti-cancer activity of disulfiram treatment to Cu^{2+} accumulation, to promote ROS formation.[114,115] It is most likely that the Cu-chelating potential of disulfiram drives cancer toxicity, whereas the additional ALDH-inhibition will further promote cancer sensitivity and intercellular ROS production.[116] DEAB is also commonly used for its anti-cancer potential. The inhibition of ALDH1 by DEAB drove the differentiation of $ALDH^{high}$ breast CSCs, through disruption of retinoic acid signalling,[56] but also reduced melanoma tumour growth in xenographed mice, and reduced melanoma CSC tumorigenic potential.[106] As ALDH plays a vital role in the metabolising of cyclophosphamide chemotherapeutics to invoke resistance in cancers,[61] inhibiting ALDH therefore presents itself as a favourable target to promote chemo-sensitivity. Novel ketone-based covalent ALDH inhibitors have recently been synthesised by Mochley-Rosen, Hurley and their team,[117] in a bid to combat this. These ALDH1A1 and 3A1 inhibitors are reported as non-toxic yet increased sensitivity of cancer cell lines to cyclophosphamide-based therapeutics, paving the way for a new series of ALDH inhibitors as potential therapeutic option for chemo-resistant cancers. Last year (April 2016), a clinical trial was initiated looking at the effect the ALDH inhibitor, dimethylampalthiolester (DIMATE) has on both leukaemia and normal haematopoietic stem cells, and whether DIMATE treatment can effectively reduce cellular proliferation and induce apoptosis in leukaemia (ClinicalTrials.gov, Identifier: NCT02748850).

1.2.3 Targeting $ALDH^{+}$ cells

Designing therapeutics targeting ALDH has previously been offered up as a favourable target to hit CSCs in tumour cell populations.[35,45,118] The association between ALDH expression and chemo-resistance in melanoma presents a favourable therapeutic target to combat highly aggressive, chemo-resistant melanoma and development of drugs that can inhibit ALDH enzymes to sensitise cells to therapy, or better yet, to selectively target $ALDH^{high}$ cancer cell populations, are increasingly desirable.

During a small molecule screen, 5-nitrofurans (5-NFNs) (**Figure 1.6A**) were shown to be substrates for ALDH2 *in vitro* and *in vivo*.[115] Zhou *et al*. (2012) reported that bio-activation of these 5-NFN compounds is initiated by an Aldh2b-dependent reduction of the $5\text{-}NO_2$

functional group to generate free radical oxygen species, that can cause melanocyte specific cell death in zebrafish. Bio-activation of 5-NFNs by ALDH2 is seen across multiple species, where pre-treatment with the ALDH2 inhibitor, daidzin, offers protection from 5-NFN toxicity, however loss of the 5-NO_2 moiety (**Figure 1.6B**) confers the compounds inactive. This suggests 5-NFN toxicity is mediated by reduction of the NO_2 moiety to drive ROS production; in similarity to the action of 5-NFNs at NTRs.[119] Patton and her team discovered their synthetic 5-NFNs, and the clinical 5-NFN nifurtimox (**NFX** – **Figure 1.6C**), were substrates for human ALDH2 *in vitro*, and were cytotoxic in human melanoma cells.[115] This suggests the potential to use 5-NFNs to target $ALDH^+$ cells, where ALDH activity can bio-activate 5-NFNs to drive cell toxicity through ROS production.

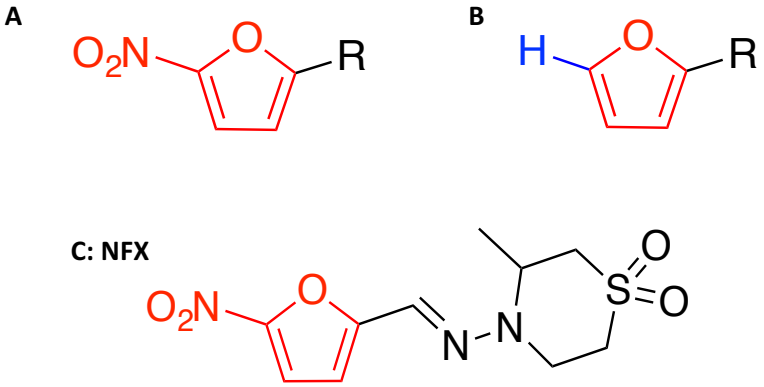

Figure 1.6: 5-nitrofuran moiety. **A**) Generic molecular structure of 5-NFNs, where the 5-nitrofuran moiety is highlighted in red. The 5-NO2 is important in activity of 5-NFNs, where the R-group will dictate specificity towards NTRs, ALDH and ultimately treatment of specific disease. **B**) Generic molecular structure of no-nitro 5-NFN controls. Replacement of the 5-NO_2 group with 5-H will ablate biological activity of 5-NFNs against both NTRs and ALDH enzymes. **C**) Molecular structure of clinical 5-NFN, nifurtimox (**NFX**).

1.3 5-Nitrofurans: old drugs as new treatments for cancer

1.3.1 5-Nitrofurans

5-Nitrofurans (5-NFN) are a class of anti-biotic and anti-parasitic pro-drugs in both human and veterinary medicine. **NFX** is one of the most widely used 5-nitrofuran drugs as a front-line treatment for Chagas Disease (*Trypanosoma cruzi*), endemic in Latin America affecting around 16-18million people worldwide.[120] The mode of 5-NFN action is through reduction of the NO_2-moiety by nitroreductases (NTRs), not common to eukaryotic cells, thereby inducing cytotoxicity (**Figure 1.7**).[119] Although **NFX** is on the WHO list of essential medicines,[121] treatment often leads to many undesirable side effects including gastrointestinal distress, neuronal problems and alcohol intolerance; in many cases, patients will have to cease treatment as a direct result (approximately 1 in 3).[122] Although some 5-NFNs are used to treat mild human infectious diseases, such as nitrofurantoin (**NFT**) for the treatment of urinary tract infections or nifuroxazide (**NAZ**) as a treatment for colitis, the primary use of 5-NFNs was originally as an antibiotic additive to animal feeds.[123] The practise of bulk treating livestock with 5-NFNs was consequentially banned in 1993 by the European Commission due to safety concerns towards human health after findings that 5-NFNs and their metabolites are potentially carcinogenic,[123-125] however the veterinary and human treatment with 5-NFNs, such as **NFX** and **NFT**, still continues. Although, while **NAZ** is still in human prescription in the majority of countries worldwide, it is not approved for use in the USA. 5-NFNs are also plagued by their poor pharmacokinetics. 5-NFNs are orally bioavailable and almost completely absorbed, however the total serum concentrations are relatively low.[126-128] Upon treatment with **NFT**, nearly 70% of the total dose was lost almost immediately, presumably through high first-pass metabolism in the liver;[127] where it was reported to be greater than 90% for **NFX**.[126,129] Sholler *et al*. (2011) reported better bioavailability in patients under 21, with a mean of 4.80µg/mL max serum concentration 6-hours after a single 30mg/kg dose, compared to a mean of 0.751µg/mL serum concentration 2.2-hours after a single 15mg/kg dose in healthy human males.[126] Although the minimum inhibitory IC_{50} for NFX in the treatment of Chagas disease is relatively low, more than 10-times this concentration is administered to counteract such poor bioavailability.[129]

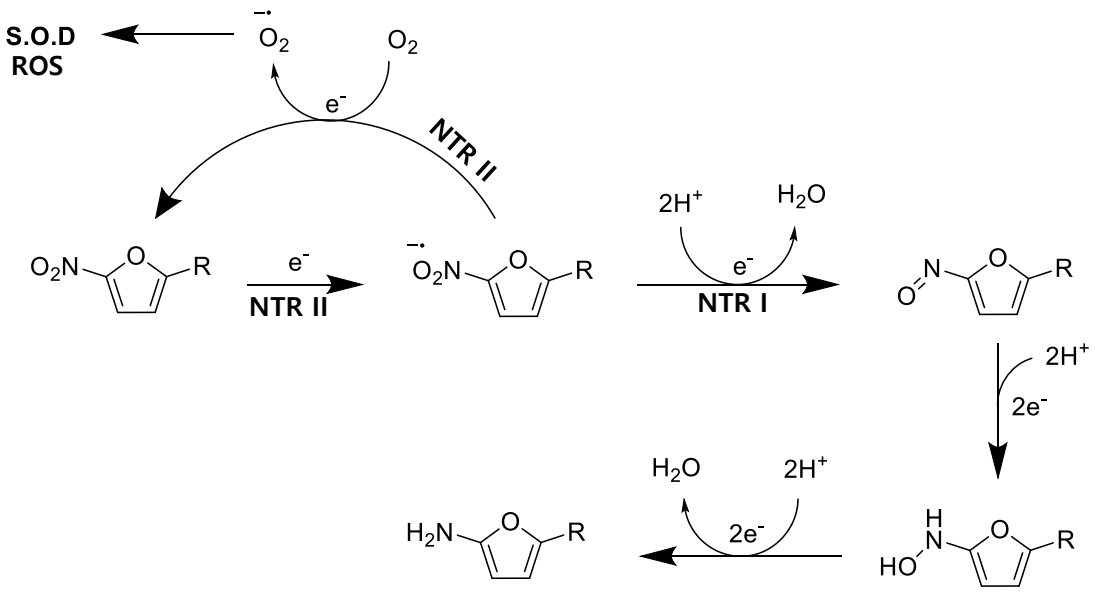

Figure 1.7: Mechanism of action of 5-NFNs against NTRs. 5-NFNs are one electron reduced to a 5-NFN radical species in an initial reaction by NTR II. The consequent 5-NFN radical can reduce oxygen to a radical species, which in turn, can cascade through super oxide dismutase redox-cycling, inducing ROS formation and promoting cytotoxicity. The 5-NFN NO_2 moiety is then reduced to a primary amide through a 3-step, $5e^-$ mechanism by NTR I, where N=O species is a good scavenger of parasitic thiols. Figure adapted from Boiani *et al*. (2010).[130]

1.3.2 5-Nitrofurans and Cancer

The anti-cancer activity of 5-NFNs has recently been described. When treating a 5-year-old girl with chemo-resistant neuroblastoma who also contracted Chagas disease, Sholler *et al.* (2006) reported that treatment with **NFX** induced tumour regression.[131] This finding led Sholler and her team to discover the anticancer potential of **NFX** in neuroblastoma.[132] They reported **NFX** treatment induced apoptosis in childhood neuroblastoma cell lines and was paralleled with inhibition of tumour growth in xenographed mice. Further, they suggested that **NFX** interferes with the TrkB signalling pathways, another mediator of chemo-resistance in neuroblastoma, where downstream phosphorylation of Akt, vital for cell survival, is ablated upon **NFX** treatment.[132] Similar findings have also been reported in the **NFX** treatment of meduloblastoma,[112] and a successful phase I clinical trial in the treatment of relapsed, chemo-resistant neuroblastomas with **NFX** was completed in 2011.[126] Similar actions of **NFX** have been

described in other neuronal tumour cell lines, such as glioblastoma, where the synthetic lethal action of buthionine sulfoximine (BOS), a γ-glutamylcysteine synthetase inhibitor, is also described.[133] γ-Glutamylcysteine synthetase regulates glutathione (GSH) production, an intercellular tri-peptide with crucial antioxidant action, further alluding to direct ROS production via **NFX** and explaining the observed **NFX**-BOS synergy. As Phase 2 clinical trials for the treatment of neuroblastoma and medulloblastoma with **NFX** in patients under 21 continue (ClinicalTrials.gov, Identifier: NCT00601003), the underlying mechanism for this anticancer activity remains unknown. NFX treatment of neuroblastoma cells reduced viability and promoted cell cycle arrest through the formation of ROS.[132,134] Further, the levels of N-Myc, a proto-oncogene amplified in malignant and chemo-resistant childhood neuroblastomas,[132] is downregulated upon NFX treatment of neuroblastoma cells, where tumour glucose metabolism is also reduced.[134]

This is not the only reported case of 5-NFNs as anticancer therapeutics, with a recent report detailing **NAZ** (**Figure 1.8A**) in promoting cell death in myeloma driven by STAT3 inhibition, however normal HSCs remained unaffected.[135] STAT3 inhibition by **NAZ** led to inhibition of phosphorylation in upstream kinases, JAK2 and Tyk2, where the STAT3 target gene, *Mcl-1*, important in mediating myeloma metastatic survival, was also downregulated. Similar findings were found following the treatment of breast cancer cell lines with **NAZ**, which led to inhibition of cell migration and invasion, induction of apoptosis, and slowing of tumour growth and lung metastases *in vivo*.[136] The activity of **NAZ** against melanoma has recently been published, where inhibition of cell proliferation, promotion of apoptosis and accumulation of intercellular ROS in melanoma cells, coupled with the suppression of metastasis in melanoma xenographs have been observed post-**NAZ** treatment.[137] Interestingly, **NFT** (**Figure 1.8B**) has been demonstrated to be effective at killing bladder cancer cell lines,[138] however, no further reports of the anti-cancer potential of **NFT** have been reported.

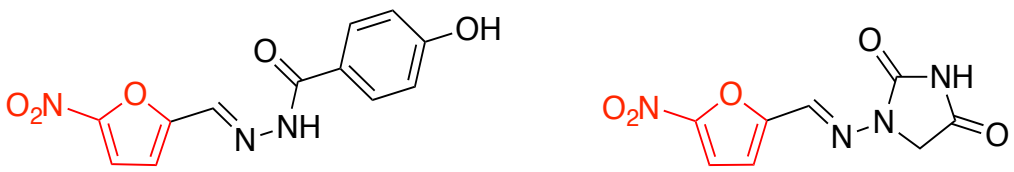

Figure 1.8: **A**,**B**) Molecular structures of clinical 5-NFNs: nifuroxazide (**NAZ**) and nitrofurantoin (**NFT**), respectively.

1.3.3 Can 5-nitrofurans target ALDH^{+} cancer cell subpopulations?

The anti-cancer potential of **NFX** has been described in neuroblastoma and medulloblastoma, however the mechanism of this anti-cancer activity is unknown. Considering the findings that 5-NFNs, including **NFX**, are competitive substrates for ALDH2 *in vitro* and *in vivo*, coupled with Sholler *et al.* (2011) reporting that treatment with **NFX** increased intercellular ROS in cancer cells, it is likely that **NFX** driven cancer cell toxicity is mediated by ALDH-driven bio-activation. Zhou *et al.* (2012) showed that the toxicity of 5-NFN pro-drugs is initiated by an ALDH-dependent reduction of the 5-NO_2 functional group to generate free radical oxygen species, that then causes cell death in zebrafish melanocytes and in melanoma cells,[115] which would explain why **NFX** was so active in neuroblastoma, considering dopaminergic rich neuroblastoma need increased levels of ALDH for dopamine metabolism. Further, Stanchi *et al.* (2015) reported **NFX** treatment reducing lactate production in neuroblastoma cells, where the activity of lactate dehydrogenases can be inhibited by **NFX** *in vitro*.[134] The production of ROS they observed upon **NFX** treatment could be produced through bio-activation from other dehydrogenases, such as ALDH. Similarly, **NAZ** treatment of melanoma cells induced apoptosis mediated by ROS accumulation and, although inhibiting STAT3 is known to be cytotoxic, ROS production may again be as a direct result from NO_2 reduction of **NAZ** by ALDH enzymes. This would also help to explain the severe side effects associated with 5-NFN treatment, such as gastrointestinal distress, neuronal problems and alcohol intolerance,[122] where bio-activation of 5-NFNs by ALDH enzymes offers a likely source. This is not the first case where antibiotics have been known to have ALDH enzymes side targeting, where cephalosporin antibiotics have been shown to covalently inhibit ALDH1A1 enzymes, in a similar mechanism to that of disulfiram.[139]

I hypothesise that 5-NFNs can be bio-activated by ALDH enzymes to promote cancer cell death. Similar to the mechanism between 5-NFNs and NTRs in anti-microbial action, ALDH enzymes can bio-activate 5-NFNs, through 5-NO_2 reduction/cleavage, promoting ROS formation and driving cancer cell death (**Figure 1.9**). ALDH^{high} subpopulations, especially ALDH1, are thought to be associated with increased tumorigenicity, promoting metastasis and driving chemo-resistance, now commonly described as CSCs. If 5-NFNs can be bio-activated by ALDH1 enzymes both *in vitro* and *in vivo*, the potential use of 5-NFNs to

selectively target ALDH^{high} CSCs within the tumour bulk offers a novel therapeutic pathway that can reduce tumorigenesis, inhibit metastasis and ultimately, prevent cancer relapse. This new approach to ALDH targeting offers a pro-drug that can selective target and kill ALDH^{high} cells, i.e. those cell most associated as CSCs, rather than reducing their stem like capability through ALDH-inhibition.[60]

Our idea is that we can use 5-NFN pro-drugs as a novel approach to target ALDH^{high} cancer cell populations and the development of new compounds that can specifically utilize the activity of these enzymes, specifically ALDH1, is therefore highly desirable.

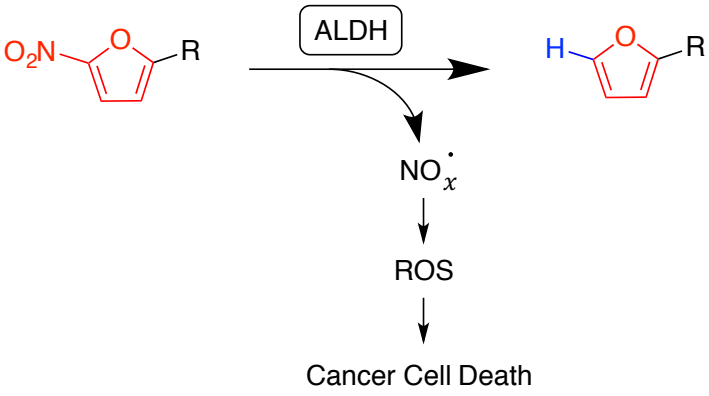

Figure 1.9: Hypothesised mechanism of 5-NFN bio-activation by ALDH enzymes. Cleavage of the 5-NO_2 moiety promotes ROS formation which can ultimately drive cancer cell death. This process reduces 5-NFN, rendering a 5-H substituted 5-NFN product.

1.4 Hypothesis

5-Nitrofurans (5-NFNs) are pro-drugs commonly used for parasitic and bacterial infection. We have recently shown that ALDH2 enzymes can bio-activate 5-NFNs in yeast, zebrafish and *in vitro*. This is significant for cancer because ALDH enzymes are enriched in cancer stem cells in many cancer types. My hypothesis is that 5-Nitrofuran pro-drugs have the potential for use in cancer treatment by targeting $ALDH^{+}$ cancer stem cell populations through bio-activation by ALDH enzymes, promoting cancer cell death.

1.5 Aims

The overall Aim of my work is to understand the molecular mechanism of 5-NFN-ALDH interactions and to establish if they have the potential to target $ALDH^{high}$ subpopulations within a tumour. My thesis will contain four data chapters, each aligned with a specific Aim:

Aim 1. To establish the anti-cancer activity of currently available 5-NFNs in melanoma, and other cancer cell lines. I will test if 5-NFNs are substrates for ALDH enzymes in human cancers using Aldefluor™, the gold standard for $ALDH^{high}$ activity in cells, and through *in vitro* enzymatic assays.

Aim 2. Assess whether 5-NFN toxicity in melanoma is mediated by the melanoma CSC markers, ALDH1A1 and ALDH1A3. Through genetic knock-down and overexpression, I will scope a functional role of ALDH1A enzymes in driving 5-NFN toxicity and ultimately, I will assess 5-NFN activity in a range of melanoma cell lines that have been fully sequenced for ALDH RNA expression to determine the molecular phenotype most sensitive to 5-NFNs.

Aim 3. Identify clinical 5-NFN compounds for potential use as anti-cancer therapeutics. There are around a dozen 5-NFNs used clinically for infection. Importantly, nifurtimox is in clinical trial for treating neuroblastoma and medulloblastoma (ClinicalTrials.gov Identifier: NCT00601003),[131] but the mechanism of action remains unknown. I will test a range of clinically available 5-NFN drugs for

specific and relevant interactions with ALDH, and determine if some 5-NFNs may have previously unknown anti-cancer activity. Further, I will also synthesise a small library of novel synthetic 5-NFNs, and analyse whether 5-NFN anti-cancer activity, and indeed ALDH efficacy, can be improved.

Aim 4. Determine the mechanism and structure of ALDH enzymes with 5-NFNs. Working in collaboration with Dr Alex von Kriegsheim at the Edinburgh Cancer Research UK Centre (University of Edinburgh), Dr Martin Weir and Dr Douglas Houston at the Institute of Structural and Molecular Biology (University of Edinburgh). This is important because it will enable us determine the how 5-NFNs engage with ALDH enzymes, provide a platform for how to develop potent and specific 5-NFNs, and provide new insight into the pharmacological potential of 5-NFNs with different ALDH enzymes.

Chapter 2

Materials and Methods

2.1 Materials

Standard laboratory procedures were used throughout this project. All reagents were used in accordance to manufacturers guidelines where available.

2.1.1 Materials and Reagents

Abcam	Anti-ALDH1A1 antibody (ab23375) (rabbit) Anti-ALDH2 antibody (EPR4493) (rabbit) Nifuroxazide (**NAZ**)
Acros Organics	Tris(hydroxymethyl)aminomethane (Tris-base)
BioLabs	1kB DNA Ladder 6x Gel loading dye (purple)
BioLegend	DRAQ7™ Far-Red Fluorescent Flow Cytometry DNA Dye Kit
Bio-Rad	Mini-PROTEAN® TGX™ Gels (4-15%) Mini-PROTEAN® TGX™ Stain Free Gels (4-15%)
Biotium	NucView™ 488 caspase-3 assay kit
BioVision	Disulfiram Human recombinant ALDH2
Cell Signalling	Anti-ALDH1A1 antibody (D4R9V) (Rabbit)
Essen BioScience	Incucyte™ BacmMan 2.0 NucLight™ Green
Expedeon	InstantBlue™ Gel Stain
Fischer	Acetaldehyde Ethylenediaminetetraacetic acid (EDTA) Glycerin Glycerol Imidazole
GE Healthcare Life Sciences	Amersham™ Protion™ supported 0-2mm Nitrocullulose blotting membrane
Gibco, Life Technologies	Opti-MEM® reduced serum medium Phosphate Buffer Saline (PBS)

Invitrogen	Deoxynucleotide triphosphate (dNTP)
	Lipofectamine 3000
	Lipofectamine RNiMAX
	Magnesium Chloride
	PCR Rxn Buffer
	SYBR® Safe gel stain
	Taq DNA Polymerase
	Ultra Pure™ Agarose
LI-COR Biosciences	IRDye® 680RD Donkey anti-Mouse IgG
	IRDye® 800CW Donkey anti-Rabbit IgG
LifeTechnologies	ALDH1A3 Silencer® Validated siRNA s30 & s32
	ALDH2 Silencer® Validated siRNA 8884
	SYPRO® Orange protein gel stain
Marvel	Original dried skimmed milk
Merck Millipore	OmniPur® Sodium Dodecyl Sulfate (SDS)
OriGene	ALDH1A3 Human cDNA Clone pCMV6-XL4 vector (NM_000693)
	ALDH2 Human cDNA Clone pCMV6-XL5 vector (NM_000690)
	pCMV6-XL4 TrueClone empty vector
Promega	Tween® 20
QIAGEN	QIAprep spin miniprep kit
Roche	cOmplete ULTRA Tablets protease inhibitor cocktail tablets
Sigma Aldrich	Dimethyl Sulfoxide (DMSO)
	Dulbecco's Modified Eagle's Medium
	Furazolidone (**FURA**)
	HEPES
	Isopropyl alcohol
	Isopropyl β-D-1-thiogalactopyranoside (IPTG)
	L-Glutamine
	MISSION® siRNA Universal negative control #1
	Nifurtimox (**NFX**)

Sigma Aldrich (cont.)	Nickel Sulphate
	Nitrofurantoin (**NFT**)
	Penicilin/Streptavidin
	RPMI-1640 Medium
	Sodium Chloride
	Sodium Hydroxide
	Sodium Phosphate mono-/di-basic
	Tricaine mesylate (MS222)
	Trypsin
Stem Cell	Aldefluor™ kit (DEAB inc.)
Thermo	Pierce™ Anti-ALDH1A3 antibody (rabbit)

2.1.2 Buffers

HEPES Buffer	50mM HEPES
	250mM NaCl
	pH 7.5
	Filtered & degassed
Elution Buffer	HEPES Buffer
	1M Imidozole
	pH 7.5
	Filtered & degassed
Phosphate Buffer	50mM Na_2HPO_4
	50mM NaH_2PO_4
	pH 7.4
	Filtered & degassed
Sample Buffer	4% SDS
	10% 2-mercaptoethanol
	20% glycerol
	0.0004% bromophenol blue
	0.125M Tris-Base
	pH 6.8

Running Buffer	25mM Tris-Base
	192mM Glycine
	0.1% SDS
	pH 8.3
Transfer Buffer	25mM Tris-Base
	190mM Glycine
	20% Methanol
	pH 8.3
Lysis Buffer	150mM NaCl
	50mM Tris-Base
	0.5% NP-40
	1x cOmplete ULTRA Protease inhibitor cocktail tablet
Trypsin	10% Trypsin
	PBS
	EDTA
PCR Master Mix	PCR Rxn Buffer
	$MgCl_2$
	dNTP
	Taq Polymerase

2.1.3 Equipment

Amersham Biosciences	Ultrospec® 10 Cell Density Meter
BD Bioscience	LSR II Flow Cytometer
	LSRFortessa™ Flow Cytometer
BIO-RAD	ChemiDoc™ MP Imaging system
	Gel Doc™ EZ Imager
	iQ™5 Multicolor Real-Time PCR detection system iCycler
	SmartSpec™ Plus Spectrophotometer
Bruker	Avance system III 500MHz NMR spectrometer
Constant Systems Ltd.	ONE SHOT cell disruptor
Essen BioScience	IncuCyte ZOOM® Live Cell Analysis System

G-Storm	GS2 Thermocycler PCR System
GE Healthcare Life Sciences	ÄKTApurifier™ UPC 100 HiPrep™ 26/10 Desalting column HiLoad™ 16/600 Superdex™ 200 pg size exclusion column HiTrap™ IMAC Fast Flow (FF) 1mL column
LI-COR Biosciences	Odyssey® CLx Imaging System
Merck Millipore	Muse® Cell Analyzer
Microsaic	Midas 4000 MiD ESI ionchip® quadrupole mass spectrometer
Molecular Devices	Spectramax M5 plate reader
MSE	SoniPrep 150 prep Sonicator
NanoDrop	NanoDrop™ 2000 UV-Vis Spectrophotometer
Nikon	COOLPIX MxA 5400 Digital Camera Eclipse Ti-E Inverted Microscope SMZ1500 Stereomicroscope
PerkinElmer	EnVision 2101 Multilabel Reader
Sortorius Biotech	VivaSpin 20 centrifugal concentrator
Thermo Scientific	Nanodrop Lite Spectrophotometer
Zeiss	SteREO Discovery.V12 Stereomicroscope

2.2 ALDH activity

2.2.1 His-tagged ALDH expression trials

Plasmids for His-tagged human ALDH2 and ALDH2*2 in the pTrcHis-TOPO® vector were kindly provided by Dr Che-Hong Chen and Professor Daria Mochley-Rosen (Stanford University, CA, USA).[140] Expression trials were conducted by transformation into *E.coli* strains BL21, BL21* and C41. Target plasmids (1µL) were incubated with 50mL *E.coli* cultures on ice (20mins), heat shocked (42^{o}C, 2mins) and put back on ice (3mins). Super optimal broth (250µL) was added and resultant cultures placed in shaking incubator (37^{o}C, 1hr, 250rpm). Cultured suspensions (15µL) were streaked onto carbenicillin-lased agar

plates and incubated (37°C) overnight. Single colonies picked and inoculated in 5mL LB broth and carbenicillin (100µg/mL). Cultures were incubated (37°C, 250rpm) until Absorbance = 0.6, measured by Ultrospec® 10 Cell Density Meter against blank LB, where expression induced with 1mM isopropyl β-D-1-thiogalactopyranoside (IPTG) and grown overnight (37°C or 30°C, 250rpm). Samples (1mL) were taken pre-inoculation, centrifuged (5500g, 5mins, 4°C) and frozen (-20°C) for non-induction controls. Overnight cultures (1mL) were centrifuged (5500g, 5mins, 4°C) suspended in 2M NaCl solution (333.3µL) and lysed via sonication (Amplitude 4.2, 10secs) on SoniPrep 150 prep sonicator. Whole cell samples and aqueous samples - taken from supernatant after centrifuging (14,000g, 5mins, 4°C), were mixed with sample buffer (5:1) and assessed for ALDH2 or ALDH2*2 expression using gel chromatography. Non-induction controls were also resuspended in 2M NaCl (100µL) and sonicated, where only whole cell samples were used as non-expressing controls.

Gel chromatography was performed by the following protocol throughout: Sample (5µL) was added to sample buffer (1µL) and boiled (100°C, 3mins). The samples were loaded onto Mini-PROTEAN® TGX™ Precast Gel or Stain Free Gel and proteins separated by electrophoresis (240V, 26mins) in running buffer. The gel was either stained with InstaBlue™ (50mL, 30mins) or activated by Gel Doc™ EZ Gel Documentation System (Stain-free only). Gels were imaged and bands were detected using Gel Doc™ EZ Gel Documentation System and Image Lab software.

Plasmids for His-tagged human ALDH1A3 in the pTrcHis-TOPO® vector were kindly created by a senior research assistant in our group, Dr Zhiqiang Zeng (University of Edinburgh, UK). The same expression trial protocol was followed for ALDH1A3-His, except C43 *E.coli* strains trials were also tested.

2.2.2 His-tagged ALDH expression

From previous cultured plates, single colonies picked from BL21* streaked plates for ALDH2-His or ALDH2*2-His and inoculated in 5mL LB broth and carbenicillin (100µg/mL), and grown overnight (37°C, 250rpm). Inoculation cultures added to LB broth (500mL + 100µg/mL carbenicillin) and cultured (37°C, 250rpm) until Absorbance = 0.5, and further cultured (30°C, 250rpm) until Absorbance = 0.6 when inoculated with IPTG (1mM) and

cultured overnight (30°C, 250rpm). ALDH2-His or ALDH2*2-His expression was assessed, against non-induction, using gel electrophoresis as before. Cultures were centrifuged (5000g, 30mins, 4°C) and resuspended in HEPES buffer. Suspension were homogenised and lysed using Constant ONESHOT Cell Disruption System. Lysates centrifuged (50,000g, 45mins, 4°C) and supernatant filtered.

The same expression protocol was followed for ALDH1A3-His, except all incubations were performed at 37°C throughout. Single colonies were picked from BL21* streaked plates for both plasmids.

2.2.3 His-tagged ALDH purification

All purification work on the ÄKTApurifier™ UPC 100 was performed at 4°C.

HiTrap IMAC FF 1mL column was charged and prepared with 5mL $NiSO_4$ (100mM) then 5mL Imidazole buffer, staggered with 5mL dH_2O washes. Centrifuged and filtered protein lysate, containing His-tagged ALDH, was run over charged HiTrap IMAC FF 1mL column on ÄKTApurifier™ UPC 100. Column washed with 20mL HEPES buffer and His-tagged protein was eluted over a gradient of 1M NaCl HEPES buffer (0%-100% over 30mL buffer). Fractions collected (500µL) were assessed for ALDH expression by gel chromatography. Fractions with high ALDH expression were pooled and concentrated to <5mL using Vivaspin 20 concentrator spin column (4000g, 10+mins, 4°C)

HiLoad™ 16/600 Superdex™ 200 pg size exclusion column was equilibrated on ÄKTApurifier™ UPC 100 with HEPES buffer (180mL). Pooled ALDH-His fractions were injected onto the size exclusion column and eluted with HEPES Buffer (180mL). Fractions collected (1mL) were assessed for ALDH expression by gel chromatography and purified ALDH fractions pooled.

ALDH was equilibrated into phosphate buffer using HiPrep™ 26/10 Desalting column equilibrated on ÄKTApurifier™ UPC 100 with phosphate buffer (50mL). Fractions pooled and protein concentrated using VivaSpin20 centrifugal concentrator (4000rpm, 4°C, 10mins). ALDH concentration assessed using a NanoDrop Lite Spectrophotometer and

blanked against phosphate buffer. ALDH-His protein stored at 4^{o}C in phosphate buffer with 1mM DTT for no longer than 7days.

2.2.4 His-tagged ALDH Characterisation

His-tagged ALDH2 and ALDH2*2 were characterised using thermal denaturation. Serial dilutions of ALDH2 or ALDH2*2 (8µM, 4µM, 2µM …) were mixed with SYPRO orange (25µL, 1:1) in 96-well PCR plate. Thermal denaturation was performed on the iQ™5 Multicolor Real-Time iCycler in 1^{o}C increments (20^{o}C – 90^{o}C, 30sec hold).

2.2.5 His-tagged ALDH Activity

ALDH *in vitro* activity was determined based on previous method.[115] Purified His-tagged ALDH2, ALDH2*2 ALDH1A1 or ALDH1A3 (5µg) was pre-incubated at 25^{o}C in 50mM sodium phosphate buffer (pH7.4) and 2.5mM NAD^+ for 10mins. The assay was initiated with 2.5mM NAD^+ acetaldehyde, totalling a reaction volume of 100µL. NADH turnover was measured using Spectramax M5 plate reader at 340nm (ε = 6.22mM/cm) for a total of 30mins to determine ALDH activity. The enzymatic rate (V) was determined using the initial linear change of absorbance between 60 – 300secs. This was repeated over a series of protein concentrations (10µg – 1.25µg).

Purified His-tagged ALDH enzymes were subject to characterisation by Michaelis-Menten kinetics. To determine K_m values for NAD^+, the assay was conducted as before against a serial dilution of NAD^+ (10µM, 5µM …). Similarly, the same was repeated to determine K_m values for acetaldehyde (10µM, 5µM …). ALDH enzyme was kept constant throughout (5µg).

2.2.6 His-tagged ALDH2 in vitro *drug assay*

Purified His-tagged ALDH2 or ALDH2*2 (5µg) was pre-incubated at 25^{o}C in 50mM sodium phosphate buffer (pH7.4), 2.5mM NAD^{+} and logarithmic dilution of 5-NFN (**NFN1**, **NFX**, **NAZ**) dose (10µM, 3µM, 1µM … 0.3nM) or vehicle (final DMSO concentration at 1%) for 10mins. The assay was initiated by the addition of 2.5mM acetaldehyde, totalling a reaction volume of 100µL. NADH turnover was measured using Spectramax M5 plate reader at 340nm ($\varepsilon = 6.22mM^{-1}cm^{-1}$) for a total of 30mins to determine ALDH activity. The enzymatic rate (V) and IC_{50} values determined were determined using the initial linear change of absorbance between 60 – 300secs. Daidzin (10µM) was used as a positive control and **NFN1.1** (10µM) was also tested. Normalised t-tests were used for statistics.

The *in vitro* activity assay to assess for **RC-NFN5** ALDH2 activity was conducted using commercially bought ALDH2 (BioVision) rather than synthesised His-tagged protein as before. ALDH2 (5µg) was pre-incubated at 25^{o}C in 50mM sodium phosphate buffer (pH7.4), 0.4mM NAD^{+} and 1µM **RC-NFN5**, or vehicle (1% DMSO), for 10mins. Daidzin (10µM) was used as a positive control. The assay was initiated by the addition of 0.4mM acetaldehyde, totalling a reaction volume of 100µL. NADH turnover was measured using NanoDrop™ 2000 UV-Vis spectrophotometer at 340 nm ($\varepsilon = 6.22mM/cm$) after 10mins to determine ALDH activity against DMSO. Normalised t-tests were used for statistics.

2.2.7 ALDH1A3 in vitro *drug assay*

The *in vitro* activity assay to assess for ALDH1A3 was conducted using commercially bought ALDH1A3, rather than synthesised His-tagged protein as before. ALDH1A3 (5ug) was pre-incubated at 25^{o}C in 50mM sodium phosphate buffer (pH7.4), 0.4mM NAD^{+} and drug (1µM **NFN1**, **RC-NFN5**, **NFN1.1**; 10µM **NAZ**) or vehicle (1% DMSO) for 10mins. Disulfiram (10µM) when was used as a positive control. The assay was initiated by the addition of 0.4mM acetaldehyde, totalling a reaction volume of 100µL. NADH turnover was measured using NanoDrop™ 2000 UV-Vis spectrophotometer at 340nm ($\varepsilon = 6.22mM/cm$) after 10mins to determine ALDH activity against DMSO. Normalised t-tests were used for statistics.

2.3 Cell Culture

Unless otherwise stated, all cell lines were grown in T75 Flasks in Dulbecco's Modified Eagle Medium (DMEM) with 10% foetal bovine serum, 1% L-Glutamine and 1% Pen-Strep, and incubated at 37°C under 5% CO_2.

2.3.1 Cell Lines

The cell lines below were kindly gifted from colleagues within the Edinburgh Cancer Research UK Centre, IGMM (University of Edinburgh, UK). A375 is a malignant melanoma cancer cell line with a $BRAF^{V600E}$ mutation from a 54-year-old female. A2780 is a human ovarian carcinoma cell line, established from an untreated patient. HCT116 is a malignant colonic carcinoma cell line with a RAS mutation in codon 13 from an adult male.

Cell lines in the melanoma cell panel kindly provided by Dr Marco Ranzani and Dr David Adams (Wellcome Trust Sanger Institute, Cambridge, UK). Information for cell growth, cell splitting and cell seeding for cell lines in the melanoma cell panel can be found in **Appendix I**. ALDH characterisation by RNA_{seq}, performed by Dr Marco Ranzani, can be found in **Appendix II**.

2.3.2 Cell Splitting

Cell cultures were split at 60%-80% confluence. Adhered cells were washed with PBS (T25 – 5mL; T75- 10mL) and trypsonised (Trypsin: T25 – 500µL; T75 - 1mL, 5mins, 37^{o}C). Trypsin was inactivated with DMEM growth media (9mL) and centrifuged (1000g, 5mins). Cell pellets were resuspended in DMEM growth media, seeded at dilution factor 1:10, unless otherwise stated, in same media (T25 – 6mL; T75 - 15mL) and incubated until 60%-80% confluence was achieved. Where other media is stated for particular cell line growth, that media will replace DMEM growth media throughout this protocol.

2.3.3 Cell Freezing

Cell cultures were split as previous; however, pellet was resuspended in 20% DMSO in DMEM growth media. Cell suspensions were aliquotted (1.5mL) and frozen (-80^{o}C). For cell seeding from frozen stocks, cell inoculations defrosted (37^{o}C), seeded with DMEM growth media (T25 – 6mL; T75 – 15mL) and incubated. Where other media is stated for particular cell line growth, that media will replace DMEM growth media throughout this protocol.

2.3.4 Cell viability seeding trials

Optimisation of cell growth needed for cell viability was performed by serial dilution. Cells were seeded (A375, A2780 and HCT116 on a 96-well plate under a serial cell density dilution (10,000cell/well, 5,000cell/well … 625cells/well) in DMEM growth media, totalling 100µL per well. Cells were grown for 7days, and cell growth was assessed by the addition 10µL PrestoBlue™ and incubated for 1hr. Fluorescence emission was detected using a PerkinElmer EnVision 2101 multilabel reader (Ex: 540nm and Em: 590nm).

2.3.5 Cell Viability

Cells were seeded on a 96-well plate and incubated 48hrs prior to treatment. A375 cells were seeded at 1000cells/well, A2780 cells were seeded at 1000cells/well, HCT116 cells were seeded at 1000cells/well.[141] Cells were treated at 48hrs with a 0.1% logarithmic drug dose (10µM, 3µM … 1nM, vehicle only) in DMSO and incubated for 96hrs. Cell viability was assessed by the addition 10µL PrestoBlue™ and incubated for 1hr. Fluorescence emission was detected using a PerkinElmer EnVision 2101 multilabel reader (Ex: 540nm and Em: 590nm).

The protocol for the melanoma cell line panel has a small variation. Cells seeded according to **Appendix I** and A375 cells seeded at 2500cells/well. Cell viability performed as previous, with exception that drug treatment was added after 24hrs as opposed to 48hrs. Cell viability was assessed by the addition 10µL PrestoBlue™ on Day 7 as before and analysed with PerkinElmer EnVision 2101 multilabel reader.

All drugs were serially diluted in DMSO for 1000-fold desired concentration. Dilution for assay was done in 2-step in DMEM growth media at 1:50 followed by 1:20 dilutions (total 1:1000). Where other media is stated for particular cell line growth, that media will replace DMEM growth media throughout this protocol.

2.3.6 Aldefluor™ Assay

Cell cultures were split as before, and the resultant cell resuspension diluted to cell density of 1 x 10^5 cells/mL. Cells were put through the Aldefluor™ assay, followed according manufacturer instructions. Cell suspensions were washed with PBS (2x 2mL) and resuspended in Aldefluor Buffer (1mL). Cell suspensions were incubated with Aldefluor™ Reagent (5µL/mL) for 45mins. DEAB (10µL/mL) was used as a negative control. Fluorescence analysed on the BD LSR II™ (Ex: 488nm & Em: 525nm) where 25,000 events were recorded for each sample.

2.3.7 Aldefluor™ Assay Drugs

A375 melanoma cells were seeded on a 6-well plate at 5 x 10^4 cells/well and incubated for 24hrs. The subsequent cultures were treated with drug (1µM **NFN1**, **NFN1.1**, **RC-NFN5** or 10µM **NAZ**, **NFX**) against vehicle (1% DMSO) and incubated a further 24hrs. Cells were put through the Aldefluor™ assay, followed according manufacturer instructions. Cell cultures were trypsonised (500µL), washed with PBS (2x 2mL) and resuspended in Aldefluor Buffer (1mL). Cell suspensions were incubated with Aldefluor™ Reagent (5µL/mL) for 45mins. DEAB (10µL/mL) was used as a negative control. Fluorescence analysed on the BD LSR II™ or LSRFortessa™ (Ex: 488nm & Em: 525nm) where 25,000 events were recorded for each sample.

2.3.8 Aldefluor™ Assay Time Course

A375 melanoma cells were seeded on a 6-well plate at 5 x 10^4 cells/well and incubated. 2hrs, 24hrs, 48hrs, 72hrs and 96hrs prior to Aldefluor™ analysis, cell cultures were treated with **NFN1** (1µM) or vehicle (1% DMSO) and incubated. Cells were put through the Aldefluor™ assay, followed according manufacturer instructions. Cell cultures were

trypsonised (500µL), washed with PBS (2x 2mL) and resuspended in Aldefluor™ Buffer (1mL). Cell suspensions were incubated with Aldefluor™ Reagent (5µL/mL) for 45mins. DEAB (10µL/mL) was used as a negative control. Fluorescence analysed on the BD LSR II™ (Ex: 488nm & Em: 525nm) where 25,000 events were recorded for each sample.

2.3.9 Aldefluor™ Imaging cells only

A375 melanoma cells were seeded in a T25 flask (1:5 split dilution) and incubated for 24hrs. The adhered cells were PBS washed (2x 5mL), treated with Aldefluor reagent (10µL in 2mL Aldefluor™ buffer) and incubated for 45mins. A375 cells were imaged using Nikon Eclipse Ti-E Inverted Microscope under GFP fluorescent excitation (Ex: 488nm & Em: 525nm), and captured using ImageJ software.

2.3.10 Aldefluor™ imaging drug treatment

A375 melanoma cells were seeded on a 6-well plate at 5 x 10^4 cells/well and incubated for 24hrs. The subsequent cultures were treated with drug (1µM **NFN1**, 10µM **NAZ**) or vehicle (1% DMSO) and incubated a further 24hrs. Cells were put through the Aldefluor™ assay, followed according manufacturer instructions. Cell cultures were trypsonised (500µL), washed with PBS (2x 2mL) and resuspended in Aldefluor Buffer (1mL). Cell suspensions were incubated with Aldefluor™ Reagent (5µL/mL) for 45mins. DEAB (10µL/mL) was used as a negative control. Cell suspensions (500µL) were placed on a glass slide and imaged using Nikon Eclipse Ti-E Inverted Microscope, under GFP fluorescent excitation (Ex: 488nm & Em: 525nm).

2.4 siRNA

Protocol for siRNA transfection was followed according to Lipofectamine RANiMAX manual instructions. siRNA used were selected according to previous.[79,142]

2.4.1 siRNA confluence assay

A375 cells were seeded on a 96-well plate at 2.5 x 10^3 cells/well and incubated for 24hrs. The subsequent cultures were treated with 5pmol siRNA (ALDH1A1 (QIAGEN), ALDH1A3 (LifeTechnologies) or ALDH2 (LifeTechnologies) vs scrambled control (Sigma)) in Opti-MEM™ media with Lipofectamine RNAiMAX (1.5µL/well) and incubated for 96hrs. Cell growth was monitored using an IncuCyte ZOOM® (10x magnification, 4 photos/well every 30-60mins). Cellular confluence was analysed using IncuCyte ZOOM® in-built artificial intelligence software. Normalised t-tests were used for statistics.

For analysis of response of siRNA treated cells to drug treatment, the same procedure was repeated as previous however, cultures were treated with 3µM **NFN1** or vehicle (1% DMSO), 24hrs after siRNA transfection and incubated for a further 72hrs. Apoptosis was monitored using the Caspase-3 marker, NucView™ 488 Caspase 3 Substrate (1µL/mL), by fluorescence at 488nm or cell death was monitored using Draq7 (5µL/mL) by fluorescence at 599nm. Normalised t-tests were used for statistics.

2.4.2 siRNA flow cytometry

ALDH activity of siRNA treated A375 melanoma cells was analysed using Aldefluor™ kit. A375 cells were seeded on a 6-well plate at 5 x 10^4 cells/well and incubated for 24hrs. The subsequent cultures were treated with 30pmol siRNA (ALDH1A3 vs scrambled control) in OptiMEM media with Lipofectamine RNAiMAX (9µL/well) and incubated for 96hrs. Cells were put through the Aldefluor™ assay, followed according manufacturer instructions. Cell cultures were trypsinised (500µL), washed with PBS (2x 2mL) and resuspended in Aldefluor Buffer (1mL). Cell suspensions were incubated with Aldefluor™ Reagent (5µL/mL) for 45mins. DEAB (10µL/mL) was used as a negative control. ALDH activity analysed by fluorescence on the LSRFortessa™ (Ex: 488nm & Em: 525nm).

Detection of early apoptosis of siRNA treated A375 melanoma cells was analysed by flow cytometry using AnnexinV (Exitation: 495nm, Emission: 519nm). A375 cells were seeded on a 6-well plate between 5 x 10^4 cells/well and incubated for 24hrs. The subsequent cultures were treated with 30pmol siRNA (ALDH1A3 vs scrambled control) in OptiMEM media with Lipofectamine RNAiMAX (9µL/well) and incubated for 24hrs. Cultures were treated with 1mM NFN1 or vehicle (1% DMSO) and incubated for a further 72hrs. Consequent cultures were trypsonised centrifuged (1000g, 5mins) and washed 2x with PBS. Resuspended cultures (1mL PBS) were treated with AnnexinV staining and counter stained with PI (5µL/mL for both). AnnexinV expression was monitored Fluorescence analysed on the BD LSR II™ (Ex: 495nm & Em: 519nm) where 25,000 events were recorded for each sample.

2.5 Overexpression

Protocol for cDNA transfection for overexpression was followed according to Lipofectamine 3000 manual instructions.

2.5.1 Plasmid expression

ALDH1A3/pCMV6-XL4 cDNA plasmids (1µL/mL) were incubated with 50mL *E.coli* cultures on ice (20mins), heat shocked (42oC, 2mins) and put back on ice (3mins). LB broth (250µL) was added and resultant culture placed in shaking incubator (37^{o}C, 1hr, 250rpm). Cultured suspensions (15µL) were streaked onto ampicillin lased agar plates. Plates and incubated (37^{o}C) overnight. From the resultant plate cultures, single colonies were picked to inoculate LB Broth (10mL with 1µL/mL Ampicillin) and incubated overnight (37^{o}C, 250rpm). The cell cultures were centrifuged (4000g, 4^{o}C, 15mins) and cDNA extracted from pellet using QIAprep spin miniprep kit according to manufacturer's instructions. cDNA concentration was measured using NanoDrop™ 2000 UV-Vis spectrophotometer.

2.5.2 Plasmid confirmation by PCR

Purified ALDH cDNA plasmids were assessed for purity and expression by PCR. cDNA (1µL) was added to PCR Master Mix (49µL) and PCR performed on G-Storm GS2 Thermocycler PCR system. PCR conditions as table below. cDNA purity was analysed using gel electrophoresis. PCR samples (1µL) were combined with sample buffer (5µL) and gel electrophoresis ran on 1.5% agar (+SYBRSafe 1µl/mL – 180V, 1hr) in running buffer. Gel imaged by the ChemiDoc™ MP Imaging system and analysed using ImageJ software.

PCR protocol conditions

Event	**Temperature (°C)**	**Time**
Heated Lid	110	-
Hold	95	3mins
Cycle x30	95	10secs
	58	20secs
	72	50secs
Hold	72	5mins
Hold	4	-

2.5.3 Overexpression cellular proliferation

A375 cells were seeded on a 96-well plate at 2500 cells/well and incubated for 24hrs. The subsequent cultures were treated with 0.1µg cDNA (ALDH1A3/pCMV6-XL4 vs pCMV6-XL4 empty vector control) in Opti-MEM™ media with Lipofectamine 3000 (0.3µL/well) and P3000™ Reagent (0.2µL/well), and incubated for 72hrs. IncuCyte™ NucLight™ Red BacMam 3.0 Reagent was also added to detect cellular proliferation. Cell growth was monitored using an IncuCyte ZOOM® (10x magnification, 4 photos/well every 30-60mins). Cellular proliferation was analysed using IncuCyte ZOOM® in-built artificial intelligence software. Proliferation was determined by GFP-expressing nuclei count (Ex: 400nm, Em: 509nm) through IncuCyte™ NucLight™ Red BacMam 3.0 Reagent treatment.

2.5.4 Overexpression cell viability

A375 cells were seeded on a 6-well plate at 5 x 10^4 cells/well and incubated for 24hrs. The subsequent cultures were treated with 2.5µg cDNA (ALDH1A3/pCMV6-XL4 vs pCMV6-XL4 empty vector control) in OptiMEM media with Lipofectamine 3000 (7.5µL/well) and P3000™ Reagent (5µL/well), and incubated for 24hrs. Cultures were treated with 3µM **NFN1** or vehicle (1% DMSO) and incubated for a further 24hrs. Cell viability was assessed by Muse™ Cell Analyzer. Normalised t-tests were used for statistics.

2.5.5 Overexpression flow cytometry

ALDH activity of transient ALDH1A3 overexpressing A375 melanoma cells was analysed using Aldefluor kit. A375 cells were seeded on a 6-well plate at 5 x 10^4 cells/well and incubated for 24hrs. The subsequent cultures were treated with 2.5µg cDNA (ALDH1A3/pCMV6-XL4 vs pCMV6-XL4 empty vector control) in OptiMEM media with Lipofectamine 3000 (7.5µL/well) and P3000™ Reagent (5µL/well), and incubated for 48hrs. Cells were put through the Aldefluor™ assay, followed according manufacturer instructions. Cell cultures were trypsonised (500µL), washed with PBS (2x 2mL) and resuspended in Aldefluor™ Buffer (1mL). Cell suspensions were incubated with Aldefluor™ Reagent (5µL/mL) for 45mins. DEAB (10µL/mL) was used as a negative control. ALDH activity analysed by fluorescence on the LSRFortessa™.

2.6 Western Blotting

Antibodies were diluted and used according to manufacturer's guidelines.

Cell cultures on 6-well plates were washed with cold PBS (2x 2mL) and lysed with lysis buffer (100µL). Cell cultured were scraped and incubated on ice for 20mins prior to centrifuging (10mins, 4^{o}C, 13,000g). Protein concentrations were analysed using NanoDrop™ 2000 UV-Vis Spectrophotometer. Protein solution (45 or 20µg protein) was added to sample buffer (1:1) and made up to 40µL with lysis buffer. Samples were loaded onto Mini-PROTEAN® TGX™ Precast Gel and separated by gel chromatography (180V, 1hr)

in running buffer. The resultant gel was placed in a transfer dock with nitrocullulose blotting membrane and transferred (400mA, 1hr) in transfer buffer. The membrane was blocked in 5% milk in PBS/T solution (1hr) and treated with primary antibody overnight (ALDH1A1 1:10,000; ALDH1A3 1:10,000; ALDH2 1:2000; GAPDH 1:10,000 in 5% milk/PBS/T solution, 4^{o}C). Membrane washed (3x PBS/T, 5mins each) and LI-COR fluorescent secondary antibodies added (1:10,000 in 5% milk/PBS/T solution, 1hr). Membrane washed again (3x PBS/T, 5mins each) and imaged using Odyssey® CLx Imaging System. Image analysis were performed by ImageJ software.

2.7 Zebrafish Models

Zebrafish work was done at the Ganga Zebrafish Facility, MRC HGU, IGMM, University of Edinburgh, UK. All zebrafish work below was performed using AB WT zebrafish. Zebrafish embryos were grown only until 5dpf, where they were culled in accordance to Home Office Regulations.

2.7.1 Breeding

Individual adult male and female zebrafish were placed in personal breeding tanks and allowed to breed overnight. Embryos were collected, washed and placed in E3 media.

2.7.2 Drug treatment

Zebrafish embryos were placed in a 24-well plate (5 embryos/well) in E3 media (1mL) and treated with drug (1µM **NFN1**, 3µM **RC-NFN-WP1**, 10µM **NAZ**) vs vehicle (1% DMSO) control, for 48hrs. Drug was washed out with fresh E3 media (1mL), zebrafish decoreonated and grown for 72hrs. At 5dpf, zebrafish embryos were culled with MS222 (1:10,000) and imaged using Nikon COOLPIX MxA 5400 digital camera under the Nikon SMZ1500 Stereomicroscope. Melanocyte cell number on the head and tail of each embryo was counted manually using Nikon SMZ1500 Stereomicroscope. Normalised t-tests were used for statistics.

2.8 Chemical Synthesis

2.8.1 General Information

All experiments were conducted under an inert N_2 atmosphere throughout using commercially available anhydrous solvents. Unless stated otherwise, all reagents were purchased from Sigma-Aldrich, UK or Fisher Scientific, UK and used without purification.

^{1}H-nuclear magnetic resonance (NMR) spectra of all synthesised compounds dissolved in deuterated DMSO were obtained on a 500MHz Bruker Avance III spectrometer. Chemical shifts are reported in parts per million (ppm) and multiplicity denoted as: s = singlet, d = doublet, t = triplet, q= quartet, m = multiplet.

Mass spectroscopy data was obtained using Microsaic Systems 4000 MiD Electrospray ionisation (ESI) system and recorded as *m/z*.

2.8.2 RC-NFN-WP1

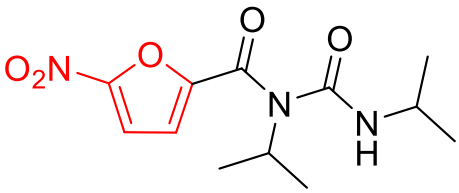

Synthesis of **RC-NFN-WP1** was produced following **Scheme 1**, originally designed to produce **RC-NFN5**. N,N'-diisopropylcarbodiimide (DIC – 554mg, 4.4mmol, 2.2eq) was added to 5-nitro-2-furoic acid (690mg, 4.4mmol, 2.2eq) and 1,4-phenylene diamide (216mg, 2mmol, 1eq) in DCM (10mL) under reflux (12hrs, 60^{o}C). DCM was used as it has a low-dielectric constant, and therefore should promote amide formation. The reaction was confirmed using thin layer chromatography (TLC). Reaction solution was washed (3x dH_2O brine), dried with $MgSO_4$ and filtered. Side-product, **RC-NFN-WP1** was purified by flash chromatography (EtOAc:Hexane) and dried under rotary evaporation to produce a yellow powder (513mg, 1.81mmol, 45.3% yield). **^{1}H NMR** (500MHz, $DCCl_3$): δ 0.96 (d, 6H); δ 1.29

(d, 6H); δ 3.70 (m, 1H); δ 4.51 (m, 1H); δ 7.19 (d, 1H); δ 7.73 (d, 1H); δ 8.31 (dd, 1H). **MS** (ES +ve) - Mass found: [M+Na$^+$] = 306.12Da. No **RC-NFN5**, or indeed any 5-NFN including the benzene linker, was synthesised through this mechanism.

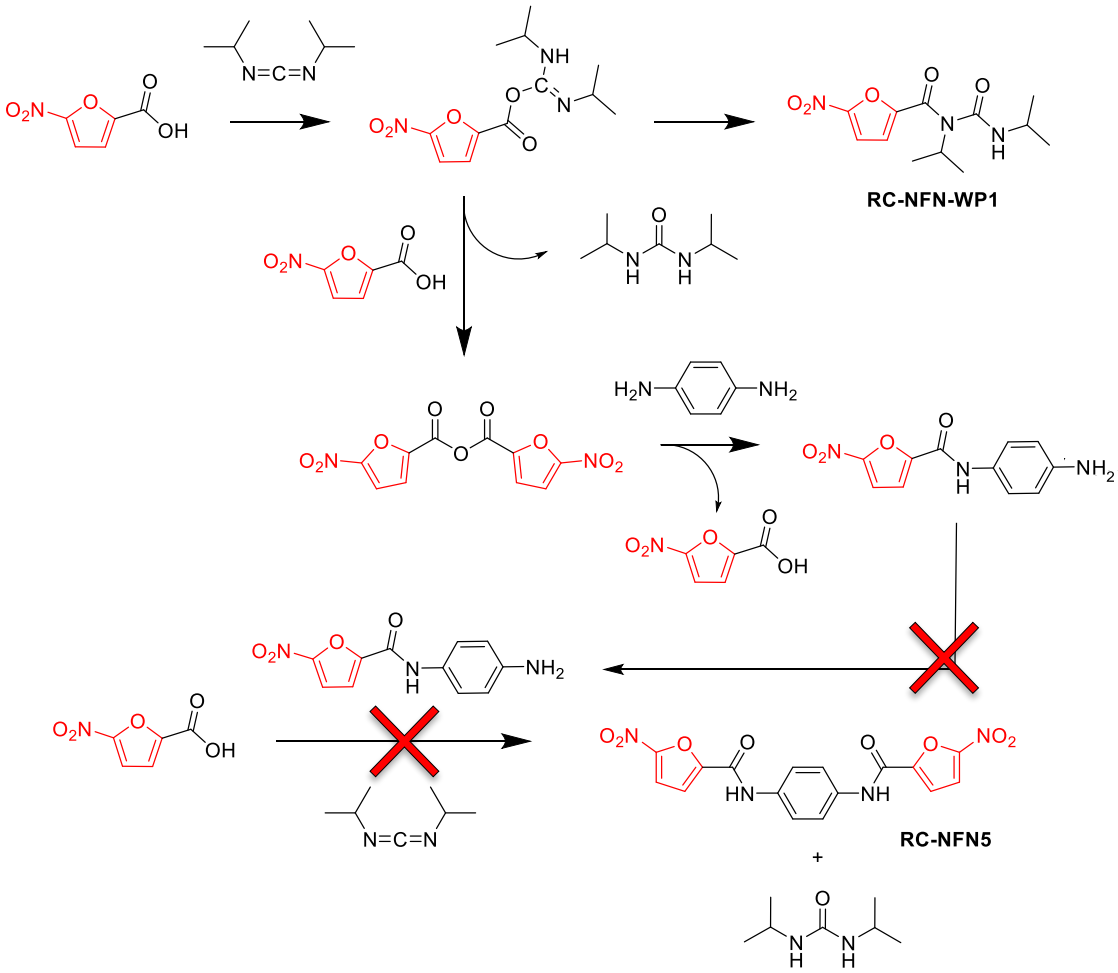

Scheme 2.1: Synthesis of **RC-NFN-WP1**. Single step reaction using carbodiimide, N,N'-diisopropylcarbodiimide (DIC) to promote peptide bond formation between diamide and furoic acid. Dual peptide bond formation to create *bis*-5-NFN expected end product. The reaction was carried out in DCM, at 60^{o}C over 12hrs. **RC-NFN-WP1** was created as an unavoidable side product to the reaction. Although some of the single substituted 5-NFN was synthesised, the *bis*-1,4-transformation was not successful.

2.8.3 RC-NFN5

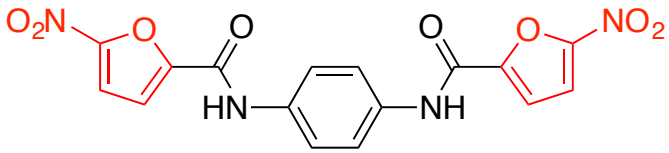

Synthesis of **RC-NFN5** was produced following **Scheme 2**. **i**: The reaction between 5-nitro-2-furoic acid (690mg, 4.4mmol) in thionyl chloride (5mL, xs) was initiated with DMF (0.1mL) added dropwise and refluxed (75°C, 24hrs). The reaction was confirmed using TLC. Thionyl chloride was removed via rotary evaporation and washed with diethyl ether (2x 10mL), forming an oil. **ii**: Trethylamine (0.5mL, xs) was added dropwise to the reaction oil and 1,4-phenylene diamide (216mg, 2mmol) in DCM (10mL) and stirred (48hrs, rt). The reaction was confirmed using TLC. Reaction solution was washed (3x dH_2O brine), dried with $MgSO_4$ and filtered. Product, **RC-NFN5** was purified by flash chromatography (EtOAc:Hexane) and dried under rotary evaporation to produce a dark orange/brown powder (89mg, 11.1% yield). **^{1}H NMR** (500MHz, $DCCl_3$): δ 6.73 (d, 2H); δ 7.40 (d, 2H); δ 7.42 (d, 4H); δ 7.89 (s, 2H). **MS** (ES +ve) - Mass found: [M+Na^+] = 409.02Da.

2.8.4 RC-NFN5.1

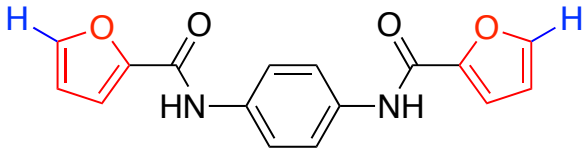

The same synthetic mechanism for **RC-NFN5** (**Scheme 2**) was followed using 2-furoic acid (493mg, 4.4mmol) instead of 5-nitro-2-furoic acid, to synthesise **RC-NFN5.1**. The reaction was confirmed using TLC and produced an off-white powder (207mg, 33.7% yield). **^{1}H NMR** (500MHz, $DCCl_3$): δ 6.71 (dd, 2H); δ 7.32 (dd, 2H); δ 7.71 (d, 4H); δ 7.93 (dd, 2H); δ 10.16 (s, 2H). **MS** (ES +ve) - Mass found: [M+H^+] = 270.53Da.

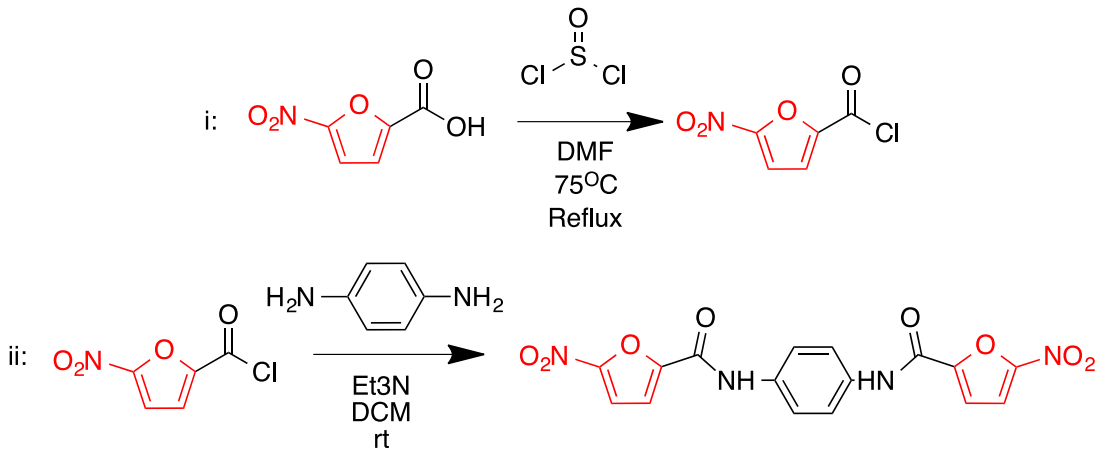

Scheme 2.2: Synthesis of **RC-NFN5** – *bis*-nitrofuran molecule with a 1,4-phenylene diamide bridge (*para*). **i:** Conversion of carboxylic acid to acid chloride via thionyl dichloride under reflux. **ii:** Synthesis of *bis*-molecule with the addition of *para*-phenylene diamide. **N/B: RC-NFN5.1** (no-nitro derivative) is synthesised using 2-furoic acid instead of 5-nitro-2-furoic acid.

2.9 Graphs and Statistics

All experiments were replicated at least in triplicate, unless stated otherwise. All graphs were created using GraphPad Prism 6.0. All cell viability EC_{50} data was extrapolated by a fitted sigmoidal variable slope curve, where the data was normalized to the untreated cells (100%) and no cell (0%). All enzyme kinetic data was extrapolated by a fitted Michaelis-Menten kinetics, drug IC_{50} values were extrapolated by fitted Log(inhibitor) curves against DMSO. All statistics were extrapolated computationally by GraphPad Prism 6.0 also. Unless stated otherwise, all error bars represent the standard error of the mean (SEM) as calculated by GraphPad prism 6.0.

2.10 ALDH1 Melanoma Staining – Performed by Sonia Wojciechowska (Edinburgh Cancer Research UK Centre, IGMM, University of Edinburgh, UK)

Staining performed according to previous method,[143,144] where melanoma and healthy skin tissue sections (mounted 4µM thick) obtained from US Biomax, were used rather than zebrafish sections. Sections were first Hematoxylin and eosin stained: Mayer's hematoxylin

(4mins) and eosin counterstain (2mins), wash with water and dehydrate with ethanol and xylene. Immunostaining against ALDH1 was achieved using the Abcam anti-ALDH1A1 antibody (ab23375). Slides were bleached from pigment with 3% H2O2 (15mins) and subjected to antigen retrieval in pressure cooker and microwave (1.8mM citric acid, 8.2mM sodium citrate, distilled water, pH 6 – 7mins). Sections were incubating in 3% hydrogen peroxidase (10min) and washed with TBS. Sections were then treated with serum-free protein blocking solution (DAKO – 30mins) and washed. Sections were further incubated with primary anti-ALDH1A1 antibody diluted in DAKO (1:1000, overnight, 4^{o}C). Sections washed with TBS and treated with HRP anti-rabbit secondary antibody (30mins). Washed sections were then treated with 1:50 DAB chromogen:DAB substrate (30mins) and counter stained with Mayer's hematoxylin (4mins). Sections were then imaged using Nikon SMZ1500 Stereomicroscope.

2.11 Molecular Docking – Performed by Dr Douglas R. Houston (Institute of Structural & Molecular Biology, University of Edinburgh, UK).

Molecular docking studies were performed on ALDH1A1 with **NFN1**, **NFX**, **NAX** and **NFN1.1**, on Autodock 4.2.3 and Autodock Viva. Water molecules and other hetero atoms were removed from the structures of ALDH1A1 (PDB 4XL4)[145] and the program PDB2PQR 1.8 used to assigned position-optimised hydrogen atoms,[146] utilising the additional PropKa algorithm with a pH of 7.4 to predict protonation states.[147] The MGLTools 1.5.4 utility prepare_receptor4.py was used to assign Gasteiger charges to atoms. Hydrogen atoms were assigned to compound structures using OpenBabel 2.3.2,[148] utilising the -p option to predict the protonation states of functional groups at pH 7.4. The MGLTools utility prepare_ligand4.py was used to assign Gasteiger charges and rotatable bonds.[149] Autodock 4.2.3 was used to automatically dock the compounds into the NADH binding pocket of the crystal structures.[150] A grid box that encompassed the maximum dimensions of the cognate NADH ligand plus 12Å in each direction was used. The starting translation and orientation of the ligand and the torsion angles of all rotatable bonds were set to random. The Autogrid grid point spacing was set at 0.2Å. The Autodock parameter file specified 10 Lamarckian genetic algorithm runs, 15,000,000 energy evaluations and a population size of 300. PyMol was used to develop theoretically 5-NFN docked protein structures.

2.12 Proteomic Mass Spectrometry

2.12.1 ALDH1A1 and ALDH2 Quadrupole-Time of Flight Mass Spectrometry – Performed by Professor Thomas D. Hurley (Center for Structural Biology, University of Indiana, USA)

Un-tagged ALDH2 and ALDH1A1 were used throughout, kindly synthesised and purified by Thomas D. Hurley. ALDH samples were set up using 10µM ALDH isoenzyme with 100µM drug (**NFN1**, **NFX**, **NAZ**, **NFN1.1** or vehicle – 2% final DMSO concentration) ±NAD^+ (500µM) and incubated (1hr, rt) in HEPES buffer (10mM, pH 7.5). Samples (2µL) were injected using an Agilent 1200SL HPLC with a low rate of 0.3 mL/min consisting of 70% H_2O and 30% acetonitrile with 0.1% formic acid into an Agilent 6520 quadrupole-time of flight (Q-TOF) mass spectrometer operating in TOF mode. The spectra were extracted and deconvoluted using MassHunter and Bioconfirm software.

*2.12.1 His-tagged ALDH2 and ALDH2*2 Proteomics* – Performed by Dr Alex von Kriegsheim and Dr Jimi Wills (Edinburgh Cancer Research UK Centre – Proteomics Facility, IGMM, University of Edinburgh, UK)

Purified ALDH2-His and ALDH2*2-His from earlier enzymatic experiments were used throughout. ALDH samples were set up using 5µg ALDH isoenzyme with 100µM drug (**NFN1**, **NAZ**, **NFN1.1** or vehicle – 1% final DMSO concentration) ±NAD^+ (500µM) and incubated (1hr, rt) in HEPES buffer. Samples were trypsin digested, cysteine alkylated (iodoacetamide) and subjected to reverse phase HPLC. Fragmented protein samples were injected onto Q Exactive™ Plus Hybrid Quadrupole-Orbitrap™ mass spectrometer the presence of reducing agent (DTT). Spectra extracted and analysed by MaxQuant 1.5 software.

2.13 RT-qPCR ALDH Expression – Performed by OakLabs (Berlin, Germany)

Samples were prepared in house according to procedures described above. All samples taken contained $1x10^5$ – $1x10^7$ cells (>5ng), spun down (1000rpm, 5mins) and pellets were flash frozen. Samples were shipped to OakLabs (Berlin, Germany) where ALDH expression was characterised using RT-qPCR. Primers used are described in **Appendix III**. GAPDH, 18S and TBP were used for reference genes.

Chapter 3

5-Nitrofurans and ALDH

3.1 Introduction

5-NFN mediated melanocyte cell death in zebrafish is driven via bio-activation by Aldh2b, and 5-NFNs have been demonstrated to be competitive substrates for human ALDH2 *in vitro*.[115] Interestingly, 8% of the human population have a non-active ALDH2*2 mutation,[10] and it would be also interesting to explore how 5-NFNs may interact with this mutant ALDH enzyme *in vitro*. Many cancers, including melanoma,[79,151] have a subpopulation of tumour-initiating, chemo-resistant cells with characteristically high ALDH expression. ALDH1A1 and ALDH1A3 are highly expressed in melanoma (specifically ALDH1A3 in the A375 melanoma cell line),[79] where their role is associated with cancer stem cell-like behaviour and are considered functional CSC markers. Recently, ALDH1 has been offered up as a favourable target in the treatment of many cancers, including melanoma.[35,45,118] Inhibition of ALDH enzymes has been reported as a new approach in treating and chemo-sensitising cancers,[43,55,56,116] and development of novel ALDH inhibitors is beginning to cultivate interest.[60,117,152] Development of compounds that can both inhibit ALDH as well as drive cytotoxicity, will therefore offer a novel approach in exploiting high ALDH expression in melanoma. I hypothesize that 5-NFNs can be bio-activated by ALDH enzymes, where 5-NFNs are competitive substrates for ALDH1 *in vitro*. Through *in vitro* enzymatic activity assays of ALDH1 and ALDH2 enzymes coupled with utility of the flow cytometry Aldefluor™ assay to analyse ALDH activity in cancer cells, I was able to explore whether 5-NFNs are competitive substrates for human ALDH enzymes *in vitro* and in cancer cells.

Here I demonstrate that 5-NFNs are substrates for human ALDH2 *in vitro*, which is lost in the human ALDH2*2 mutation. I also demonstrate that 5-NFNs are competitive substrates for the A375 functional CSC marker, ALDH1A3, highly expressed in this cell line.[79] I also describe 5-NFNs as competitive substrates for ALDH activity in A375 cells, where 5-NFN treatment also gave rise to a prolonged reduction in ALDH activity assessed through Aldefluor™ activity, providing some indication that 5-NFNs may strongly inhibit ALDH activity after bio-activation.

3.2 5-NFNs are competitive substrates for ALDH enzymes

As 5-NFNs are competitive substrates for Aldh2b in zebrafish,[115] and are toxic in human cancer cells,[115,132,153] I hypothesise that human ALDH enzymes are bio-activating 5-NFNs, in these cancer cell lines, to drive toxicity. ALDH2 was the obvious candidate to explore first, to further characterise the effect of **NFN1** on human ALDH2, and whether the non-active ALDH2*2 mutant, present in 8% of the human population,[10] can still bio-activate 5-NFNs *in vitro* also. ALDH1 enzymes are highly expressed in melanoma,[79] and other cancers,[2,14,44,80] so if 5-NFNs are competitive substrates for ALDH1 enzymes also, it is hypothesised that 5-NFNs may also be toxic to human cancer cells.

The following work was done with purified His-tagged ALDH2 and ALDH2*2. The His-tagged ALDH2 and ALDH2*2 plasmids were kindly provided by Dr Che-Hong Chen and Professor Daria Mochley-Rosen (Stanford University, CA, USA). The following work with ALDH1A3 was performed using commercially purchased His-tagged protein from Life Technologies.

*3.2.1 His-tagged ALDH2 & ALDH2*2 synthesis and purification*

Expression trials were set up to determine optimum conditions for ALDH expression. Both plasmids were transformed into *E.coli* strains: BL21, BL21* and CD43, and induced cultures grown at either 37^{o}C or 30^{o}C overnight. Gels were ran to determine ALDH2 and ALDH2*2 expression (Both 55kDa). ALDH2-His had the best expression at 30^{o}C, with minimal expression seen at 37^{o}C (**Figure 3.1A**). BL21* cells had the best expression of ALDH2-His, so were selected. ALDH2*2-His appeared to have better expression, however there was more obvious expression at 30^{o}C (**Figure 3.1B**). As all 3 strains showed similar expression, BL21* was also selected, as with ALDH2, as it appeared to have the best out of the range. Final growing conditions were *E.coli* BL21* grown overnight at 30^{o}C after induction.

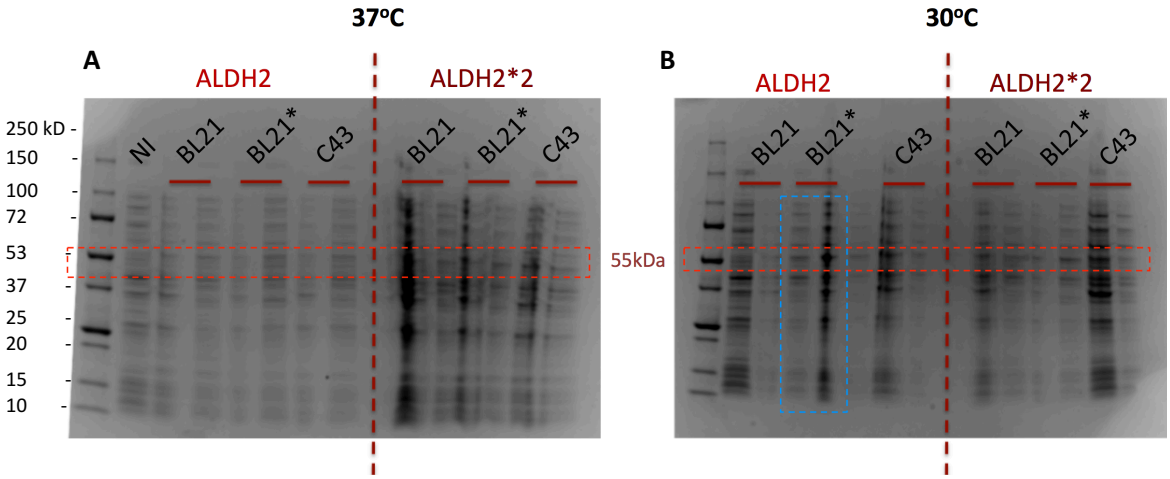

Figure 3.1: Gels for His-tagged ALDH2 (left) and ALDH2*2 (right) expression (55kDa, red box) trials stained with InstaBlue. Expression trials were performed at 30°C and 37°C in E.clo strains: BL21, BL21* and C43. Expression of ALDH2-His was much stronger in BL21* at 30°C (blue box). Expression was strongest for ALDH2*2-His at all 3 strains grown at 30°C. Minimal expression was seen in all samples grown at 37°C. **A**) 37°C. **B**) 30°C.

Growth of induced *E.coli* was consequently scaled up to produce higher quantities of protein. Bacterial cells from these large scale cultures were lysed, protein extracted and assessed for ALDH-His expression. Purification of ALDH-His proteins occurred over 2 steps, firstly through His-trapping with the HiTrap IMAC FF 1mL column and then gel filtration size exclusion column, using a Superdex 200 column. The His-tagged protein can be purified using a His-trap, by running sample over the column and eluting over a gradient of NaCl buffer to cleave the His-Tag interaction in the column. This provided a quick method to effectively remove the majority of the *E.coli* proteins against an increasing salt gradient to allow distinction between non-specific binding proteins and his-tagged ALDH (**Figure 3.2A**,**B**). As ALDH2 exists as a tetramer (212kDa),[9,10] the his-tagged protein can be purified due to its weight using the size exclusion column; Superdex 200 (10kDa – 600kDa). The resulting fractions were substantially cleaner (**Figure 3.2C,D**) and were pooled, assessed for overall purity and used for *in vitro* studies. These steps were completed for both ALDH2-His and ALDH2*2-His.

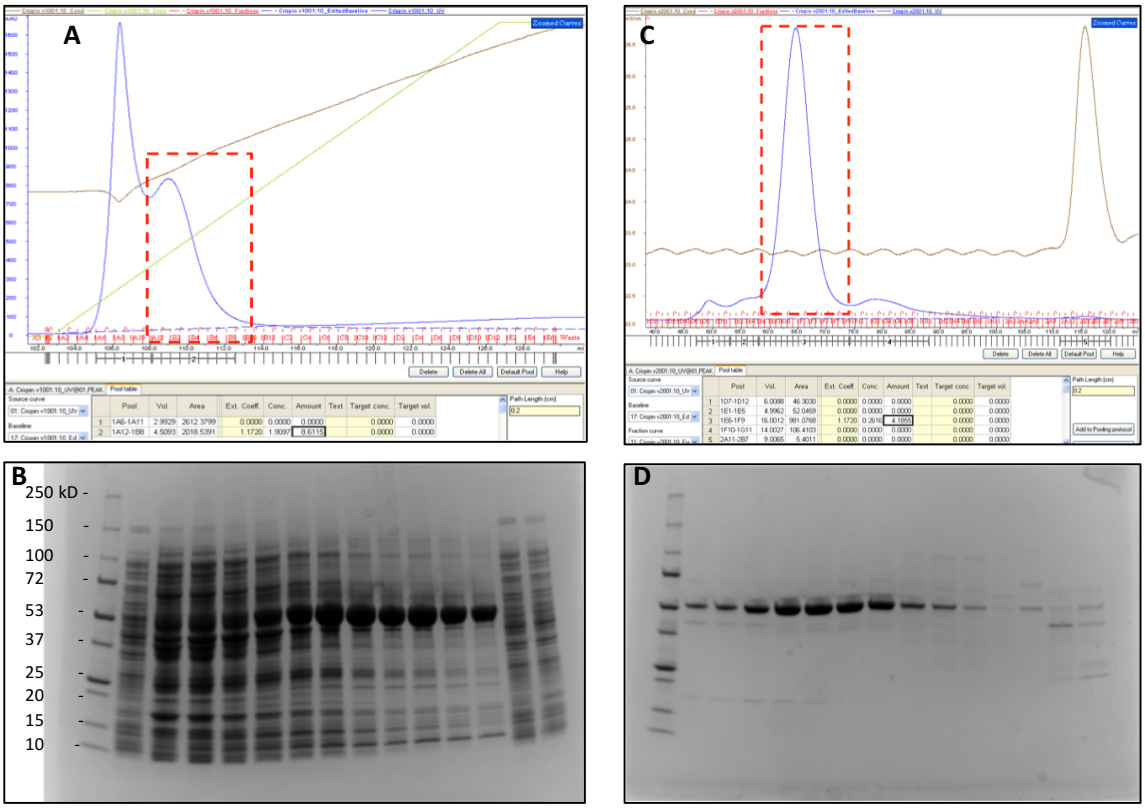

Figure 3.2: Purification of ALDH2-His by His-trap and size exclusion columns. **A**) UV trace of crude ALDH2-His protein samples after loading onto HiTrap column from ÄKTAPurifier 100. 1M imidazole buffer was used to elute over 30-step gradient (green line). ALDH2-His likely found is later protein peak as His-tag is eluted off the column (red box). **B**) Gel to check purity of His-trap elution fractions. ALDH2-His expression is much higher and cleaner in later wells corresponding with red box fractions. **C**) UV trace of crude ALDH2-His protein samples after loading onto Superdex 200 size exclusion column from ÄKTAPurifier 100. ALDH2-His likely found is later protein peak as His-tag is eluted off the column (red box). **D**) Gel to check purity of size exclusion fractions. ALDH2-His expression appeared universally pure in wells corresponding to red box fractions. These fractions were pooled.

*3.2.2 His-tagged ALDH2 & ALDH2*2 thermal denaturation*

His-tagged ALDH2 and ALDH2*2 were assessed for thermal denaturation using SYPRO orange over increasing temperature (1°C increments, 20°C-90°C) and analysed using iQ™5 Multicolor Real-Time iCycler. ALDH2-His had a denaturation temperature of 51.57°C (**Figures 3.3A**) and ALDH2*2 has a denaturation temperature of 54.89°C (**Figure 3.3B**). The increased denaturation temperature for ALDH2*2-His suggests that the mutant

ALDH2*2-His tetramer is bound more strongly than the native ALDH2-His tetramer. This may be indicative of the structural alteration inferred by the single amino acid substitution of ALDH2*2, where disorder of the alpha-helix important in dimer formation, will lead to much tighter binding, and as such, lose the plasticity needed for native ALDH activity.

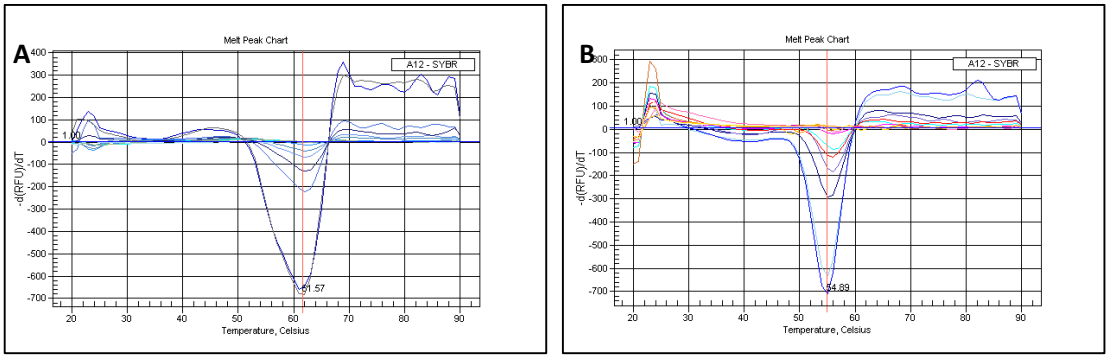

Figure 3.3: Thermal denaturation traces for ALDH2-His and ALDH2*2-His over a range of concentrations. Denaturation indicating by a sudden change in fluroescnece, as SYPRO orange binds to the hydrophobic surfaces of un-folded protein (n=3). **A**) ALDH2-His denaturation curve, indicating ALDH2-His has a denaturation temperature of 51.57^{o}C. **B**) ALDH2*2-His had a higher denaturation temperature of 54.89^{o}C.

3.2.3 Enzyme characterisation

To determine the enzymatic activity of ALDH2-His, an *in vitro* assay was set up similar as previously described.[115] ALDH2-His and ALDH2*2-His were pre-incubated with NAD^+ and enzymatic activity initiated with acetaldehyde addition. ALDH activity was monitored through NADH production at λ = 340nm (ε = 6220$M^{-1}cm^{-1}$). ALDH2*2-His activity was 200-fold lower than ALDH2-His activity (**Figure 3.4A**), reflecting previous reports.[154] ALDH2-His was further subjected to Michaelis-Menten kinetic studies against NAD^+ and acetaldehyde (AcAld), the natural substrates for ALDH2. Systematic concentrations of NAD^+ were measured against constant acetaldehyde concentration to determine K_m^{NAD+}, and the reverse was done to determine K_m^{AcAld}. ALDH2-His kinetics[155] were determined (**Figure 3.4B,C**) where K_m^{NAD+} = 325µM and K_m^{AcAld} = 114µM. Peak enzymatic activity was seen at 2.5µM NAD^+. At concentrations above 2.5mM acetaldehyde, substrate inhibition of ALDH2-His activity was observed, reflecting previous work,[156] however K_m^{AcAld} was markedly higher, which may reflect the lower activity seen with ALDH2-His (k_{cat} = 9.2min^{-1}) compared to previous.[154]

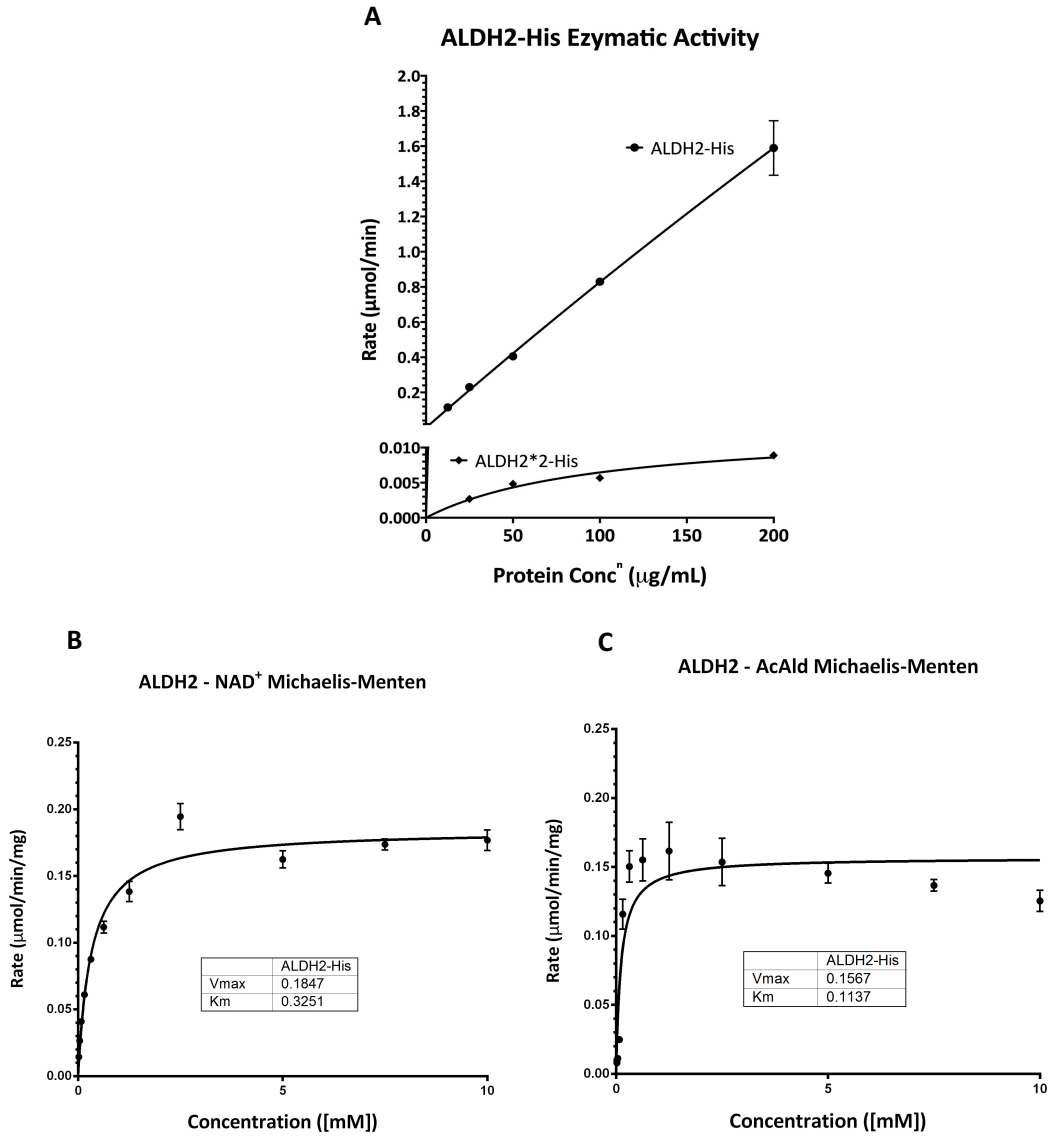

Figure 3.4: His-tagged ALDH2 protein enzyme characteristics. **A**) Activity of His-tagged ALDH2 and ALDH2*2 measured over a range of protein concentrations. Enzymatic rate determined using initial linear rate of NAD^+ to NADH turnover at λ = 340nm (ε = 6220$M^{-1}cm^{-1}$), upon acetaldehyde initiation. ALDH2-His is 200-fold more active than ALDH2*2-His. **B**) NAD^+ Michaelis-Menten curve for ALDH2-His. K_m = 325.1µM and V_{max} = 0185µmol/min/mg. **C**) Acetaldehyde Michaelis-Menten curve for ALDH2-His. K_m = 1113.7µM and V_{max} = 0.157µmol/min/mg. Acetaldehyde driven substrate inhibition is seen above 2.5mM.

3.2.4 5-Nitrofurans can inhibit ALDH enzymatic activity in vitro

To determine the potency of 5-NFNs *in vitro*, His-tagged ALDH2 was subjected to the *in vitro* activity assay as described above, where ALDH2-His was pre-incubated with NAD^+ against a varying doses of **NFN1** prior to acetaldehyde initiation. Present controls were vehicle (1% DMSO), no-nitro control **NFN1.1** and ALDH2 inhibitor, daidzin. DEAB could not be used as a control, as emission of DEAB at 360nm bleeds into the band at 340nm at which NADH production is monitored.[110] **NFN1** exhibited potent reduction in ALDH2-His activity (**Figure 3.5A**); IC_{50} = 69.3nM, where ALDH2-His activity was significantly reduced at concentrations >100nM ($P < 0.0001$). As expected, the ALDH2 inhibitor, daidzin, had significant reduction of ALDH2-His activity *in vitro* ($P < 0.0001$) and the no-nitro control, **NFN1.1**, showed no reduction in ALDH2-His activity, further evidence for the need of the NO_2 moiety for 5-NFN activity towards ALDH enzymes.

The ALDH2*2 mutation is present in 8% of the human population, primarily in persons of Eastern Asian descent.[10] As the mutant ALDH2*2-His still has some *in vitro* activity, it was expected that 5-NFNs could also be competitive substrates for ALDH2*2-His *in vitro*. The same experiment was set up as described above, where ALDH2*2-His activity was assessed. Although reduction in ALDH2*2-His activity is seen (**Figure 3.5B**) with significant reduction in activity at much higher **NFN1** doses ($P = 0.023$, IC_{50} = 8.31μM), the accuracy of these findings were limited to the sensitivity of the SpectraMax® M5 Multimode Plate Reader. As ALDH2*2-His activity is 200-fold less than ALDH2-His and, as previously mentioned, ALDH2-His activity is slower than expected, the degree of accuracy of measuring the changes in the rate of ALDH2*2-His upon **NFN1** treatment had a standard error ±1.47μM, compared to ALDH2-His at ±5.2nM. Although there was a significant reduction in ALDH2*2-His activity, the actual interpretation of behaviour is therefore limited. It is still expected that ALDH2*2-His activity will be attenuated, as shown, however, it will be a reduction in activity which was otherwise negligible to begin with. The ALDH2*2 mutation results in ablation ALDH2 activity *in vivo*,[10] and although it exhibited some affinity for **NFN1**, its rate of turnover was trivial. As such, it would be interesting to explore whether those with the ALDH2*2 mutation may have better tolerance towards 5-NFNs, such as **NFX**.

ALDH1 is the predominant marker for CSCs,[44] where ALDH1A3 is the stem cell marker for A375 melanoma cells.[79,151] If 5-NFNs are competitive substrates for ALDH2 *in vitro*, I hypothesised that 5-NFNs will also be competitive substrates for ALDH1 isoforms. To test for this, I set up an ALDH1A3 *in vitro* assay along the same lines as with ALDH2 and previous work.[157] ALDH1A3 was pre-incubated with NAD^+ and **NFN1**, prior to acetaldehyde initiation. Activity was monitored against vehicle (1% DMSO) control, no-nitro control, **NFN1.1** and ALDH1 inhibitor, disulfiram. **NFN1** treatment significantly reduced ALDH1A3 activity ($P = 0.03$, **Figure 3.5C**) where NADH turnover was reduced by 78%. As expected, the ALDH1 inhibitor, disulfiram, had significant reduction of ALDH1 activity *in vitro* ($P = 0.017$) and in correlation with ALDH2, the no-nitro control, **NFN1.1**, showed no reduction in ALDH1A3 activity, further evidence for the need of the NO_2 moiety for 5-NFN activity towards ALDH1 enzymes also.

It was originally hoped to determine an IC_{50} value for ALDH1A1 and 1A3 against **NFN1**, using a similar set up as for ALDH2-His. His-tagged ALDH1A1 and 1A3 had been produced, through plasmids kindly created by a senior research assistant in our group, Dr Zhiqiang Zeng (University of Edinburgh, UK), and purified through the same His-tagged protocol as for ALDH2-His. However, the activity of his-tagged ALDH1 enzymes couldn't be verified, so commercially purchased ALDH1A3 was used instead. As this limited the amount of protein available, only single concentrations of drug were tested. It was hypothesised that due to the placing of the His-tag or through the actual purification method itself resulted in unstable protein, ablating activity, and further work would be needed to optimise condition in order to produce stable, active His-tagged ALDH1 enzymes.

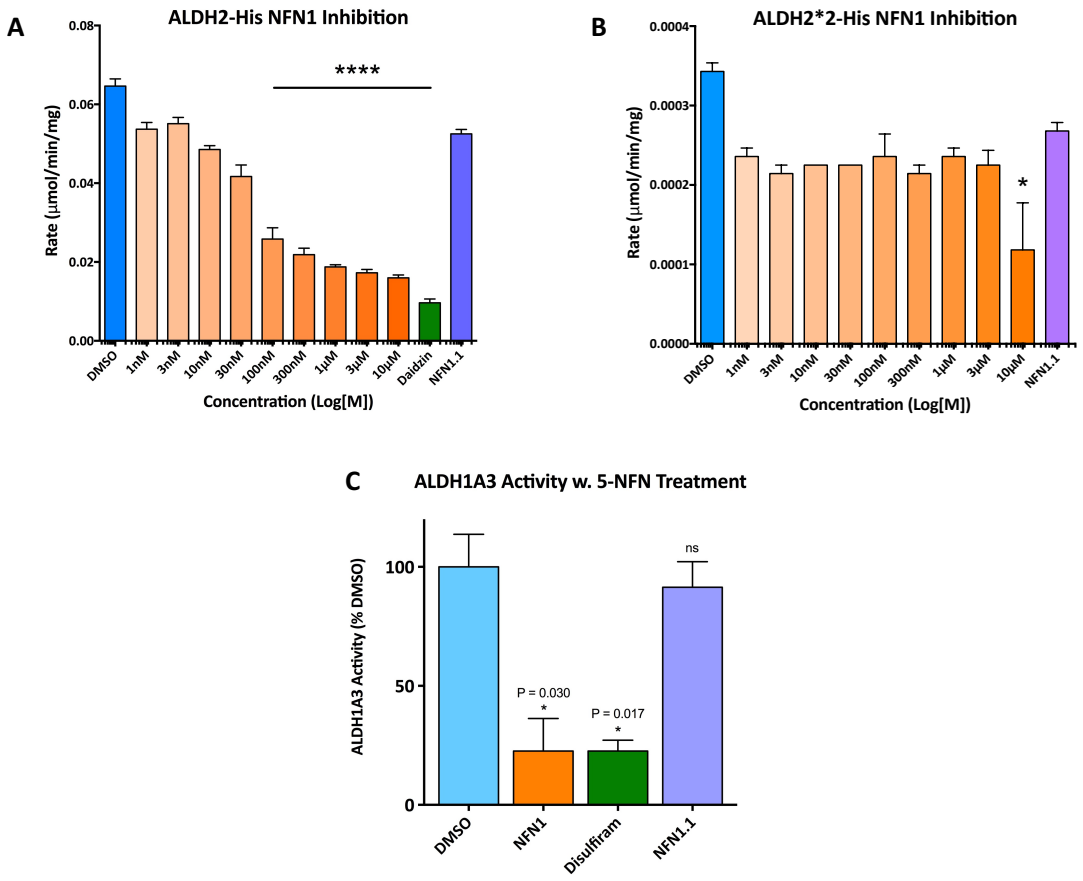

Figure 3.5: **NFN1** is a competitive inhibitor for ALDH enzymes. **A**) ALDH2-His activity against **NFN1** (orange) treated over a logarithmic dose range, against **NFN1.1** (purple), DMSO (blue) and daidzin (green). Enzymatic rate determined using initial linear rate of NAD^+ to NADH turnover at λ = 340nm (ε = 6220$M^{-1}cm^{-1}$), upon acetaldehyde initiation. ALDH2-His activity significantly reduced ($P < 0.0001$) upon **NFN1** treatment higher than 100nM. **NFN1** IC_{50} = 63.9nM. The ALDH2 inhibitor, daidzin (10µM), had significant reduction in ALDH2-His activity (87%, $P < 0.0001$: ANOVA) and **NFN1.1** had no significant effect of ALDH2-His activity (n=3). **B**) ALDH2*2-His activity **NFN1** (orange) treated over a logarithmic dose range, against **NFN1.1** (purple), and DMSO (blue). Enzymatic rate determined using initial linear rate of NAD^+ to NADH turnover at λ = 340nm (ε = 6220$M^{-1}cm^{-1}$), upon acetaldehyde initiation. ALDH2*2-His activity significantly reduced ($P < 0.05$: ANOVA) upon **NFN1** treatment only at 10µM. **NFN1** IC_{50} = 8.31µM. **NFN1.1** had no significant effect of ALDH2*2-His activity. ALDH2*2-His activity remained 200-fold less active than ALDH2-His (n=2). **C**) ALDH1A3 *in vitro* enzymatic activity upon **NFN1** (1µM, orange), **NFN1.1** (10µM, purple), DMSO (blue) and disulfiram (10µM, green) treatment was determined using NADH turnover at λ = 340nm (ε = 6220$M^{-1}cm^{-1}$) after 10mins. ALDH1A3 activity represented at %DMSO activity. ALDH1A3 activity was significantly reduced after **NFN1** treatment ($P = 0.03$: t-test) and **NFN1.1** had no change to ALDH1A3 activity. The known ALDH1 inhibitor, disulfiram, had a significant reduction ($P = 0.017$) in ALDH1A3 activity (n=3).

3.3 Analysis of ALDH activity using the Aldefluor™ assay

The Aldefluor™ assay indicates cellular ALDH activity through the fluorescent Aldefluor™ reagent being negatively charged by ALDH enzymes and retained in the cell (**Figure 3.6A**). The higher the ALDH activity results in more cellular Aldefluor™ accumulation, fluorescing the cell with a higher intensity (Ex: 488nm, Em: 525nm). DEAB, an ALDH inhibitor provided in the Aldefluor™ kit, is used as a positive control, preventing the ALDH-driven cellular oxidation of Aldefluor™, so passes through the cell leading to no accumulation and a non-fluorescing cell. It has been reported that Aldefluor™ is only active in ALDH1 specifically,[32] and this report is also shared by the manufacturers description, however, there has been some evidence that other ALDH enzymes, such as ALDH2, can also have a major impact on Aldefluor™ activity also,[4,32,45] so the exact ALDH isoforms contributing to Aldefluor™ activity in the cell lines tested is largely unknown. Cells were incubated with Aldefluor™ reagent and subjected to cell counting by flow cytometry. Alive cells were gated, and assessed for Aldefluor™ activity (represented by FITC). DEAB was used a positive control, where Aldefluor™ activity is downshifted upon DEAB treatment. The overall Aldefluor™ activity is represented as a histogram, where the mean fluorescence is taken throughout (**Figures 3.6B-E**). FITC parameters were used (and consequently axis-labelled) as they are identical to those needed for Aldefluor™ activity. Thus, throughout this section, FITC intensity directly correlates to Aldefluor™ fluorescence.

3.3.1 5-Nitrofuran treatment leads to sustained inhibition of cellular ALDH activity

If 5-NFNs are competitive substrates for ALDH *in vitro*, it was expected that a shift in Aldefluor™ activity should be seen upon 5-NFN treatment. A375 melanoma cells pre-treated with **NFN1** were subjected to the Aldefluor™ assay as before, and ALDH activity assessed. DEAB used again as a positive control, and assumed to give 100% ALDH inhibition; the no-nitro control, **NFN1.1**, was also assessed. After 2hrs of treatment, ALDH activity was approximately 80% reduced in the **NFN1** treated cells, compared to vehicle (1% DMSO) control (**Figure 3.6F**). After the reagents are left on for 24hrs, DEAB treated cells began to recover their ALDH activity, as DEAB is a reversible inhibitor of ALDH,[110] however this is not seen with **NFN1** (**Figure 3.6G**). At 24hrs post treatment, **NFN1** seems to inhibit ALDH activity even more potently, with an inhibition that of the assumed 100% seen with DEAB

after 2hrs. This unexpected result gave some clue into the mechanism in which 5-NFNs interact with ALDH, and there may be some form of potent inhibition, irreversible or otherwise, of the ALDH enzymes coupled with the bio-activation of 5-NFNs. This correlates with previous work, where other synthetic irreversible ALDH1 & 3 inhibitors also sustained inhibition of ALDH activity until 72hrs post treatment.[158] **NFN1.1** showed no reduction in ALDH activity, as expected (**Figure 3.6H**).

3.3.2 5-Nitrofuran mediated inhibition of ALDH activity is sustained over 48hours

To further probe the magnitude of ALDH inhibition by 5-NFNs, A375 melanoma cells were treated with **NFN1** over a time course to assess recovery of ALDH activity (if at all) after 5-NFN treatment; and whether there is any indication of irreversible inhibition of ALDH upon 5-NFN treatment. A375 melanoma cells were treated with **NFN1** at systematic time intervals prior to Aldefluor™ treatment and ALDH activity analysed. ALDH inhibition by **NFN1** lasted at least 48hrs, with recovery of ALDH activity not detectable until 72hrs after treatment (**Figure 3.7A**). After 72hrs, the ALDH activity begins to recover, with full recovery seen by 96 hours post treatment – however, side peaks from cell debris are present, most likely due to 5-NFN driven cell death (**Figure 3.7B,C**). This is a good indication that ALDH activity is being directly inhibited by 5-NFN treatment and its lasting affect (upwards of 48hrs) hinting as an irreversible mechanism in doing so. A possible explanation for why the ALDH activity recovers after 72hrs may be due to the cells replenishing their ALDH activity by synthesising more ALDH enzymes. However, it is clear that 5-NFNs are in some way inhibiting ALDH to a greater extent to that of a reversible inhibitor, possibly indicative of an irreversible interaction.

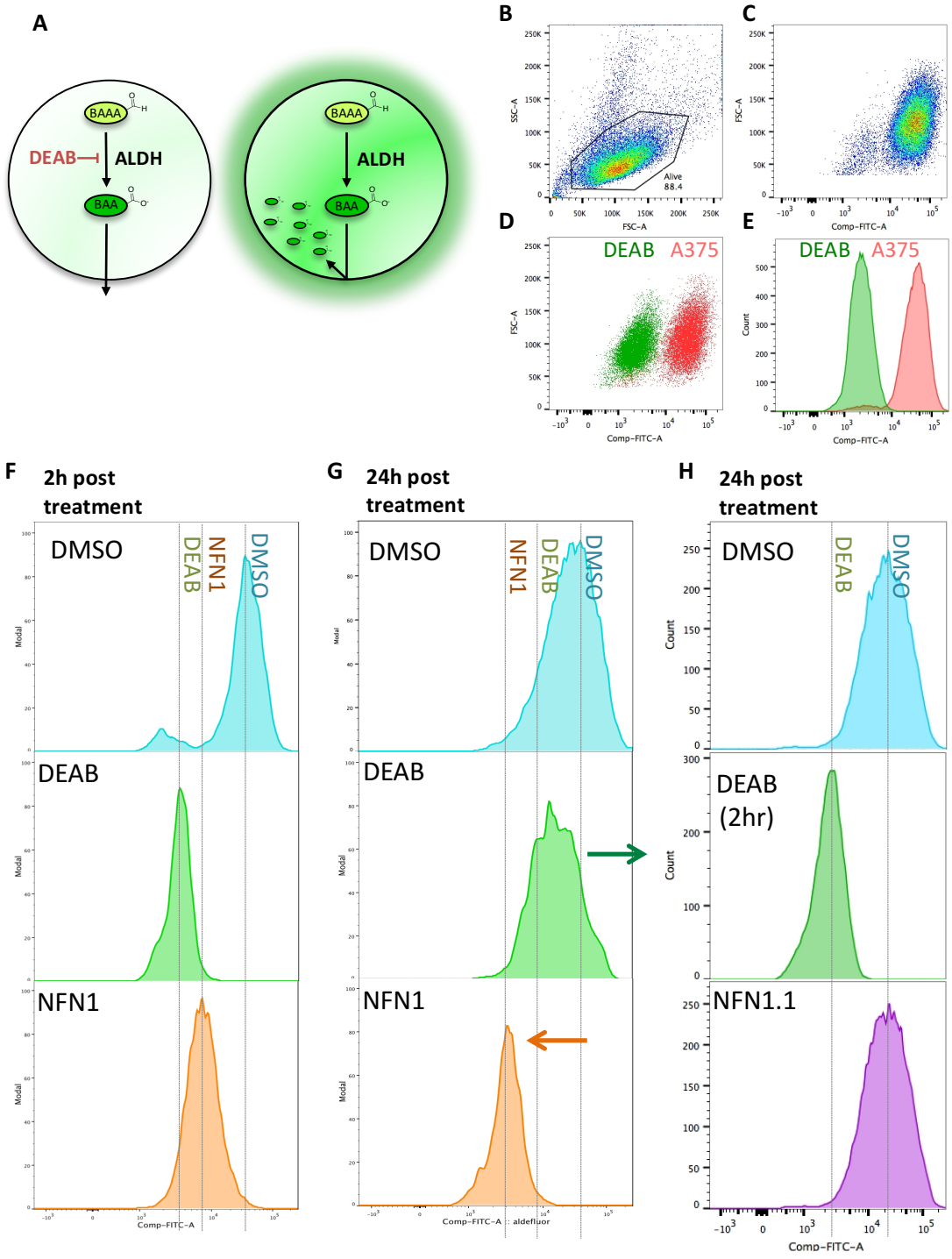

Figure 3.6: **NFN1** treatment leads to a prolonged reduction in A375 melanoma Aldefluor™ activity (n=3). Aldefluor™ activity (FITC) represented as histogram counts of A375 melanoma cells treated with **NFN1** and **NFN1.1** (1µM and 10µM respectively). DMSO and DEAB treated A375 cells after 2hrs assumed 100% and 0% Aldefluor™ activity respectively. **A**) Mechanism of Aldefluor™ activity in cells. Fluorescent BAAA Aldefluor™ reagent is negatively charged by cellular ALDH enzymes, is retained within the cell and accumulates, causing the cell to fluoresce. DEAB, an ALDH inhibitor, prevents

BAAA Aldefluor™ reagent activation, and will pass through the cell, resulting in a non-fluorescent cell. Figure adapted from Luo, Y. *et al*. (2012).[79] **B**) Flow cytometry plot of A375 melanoma cells plotted as forward scatter (FSC) against side scatter (SSC), gated around the Alive cell population (88.4%). **C**) Flow cytometry plot of 488/525nm (FITC) expression in A375 melanoma cells against FSC. FITC parameters were used (and consequently axis-labelled) as they are identical to those needed for Aldefluor™ activity. Thus, FITC intensity correlates to Aldefluor™ activity. A375 cells have high expression on Aldefluor™, with the majority cell population with an intensity $>10^4$. **D**) Flow cytometry plot of FITC intensity in A375 melanoma cells only against FSC (red) and DEAB treated A375 melanoma cell (green). DEAB has a clear downshift in FITC intensity. **E**) Histogram representation of FITC intensity count of A375 melanoma cells only (red) vs DEAB treated A375 melanoma cells (green). DEAB treatment noticeably downshifts A375 melanoma FITC intensity. **F**) Aldefluor™ activity of A375 cells after 2hrs **NFN1** (orange) treatment. DMSO (blue) vehicle and DEAB (green) negative controls treated for 2hrs also. **NFN1** reduces Aldefluor™ activity in A375 cells by 72.2% after 2hour of treatment (Mean intensity: 1.94×10^4 DMSO vs 5.40×10^3 **NFN1**). Ablation of Aldefluor™ activity by DEAB treatment and full Aldefluor™ activity by DMSO treatment also highlighted. **G**) Aldefluor™ activity of A375 cells after 24hrs **NFN1** (orange) treatment. DMSO (blue) vehicle and DEAB (green) negative controls treated for 24hrs also. **NFN1** reduces Aldefluor™ activity even further in A375 cells, to 100% after 24hour of treatment. Cell treated with DEAB, a reversible ALDH inhibitor, begin to recover their Aldefluor™ activity after 24hrs post treatment. **H**) Aldefluor™ activity of A375 cells after 24hrs **NFN1.1** (purple) treatment. DMSO (blue) vehicle and DEAB (green) negative controls treated for 24hrs and 2hrs respectively. **NFN1.1** has no effect on Aldefluor™ activity in A375 cells, with a sustained FITC intensity to that of DMSO.

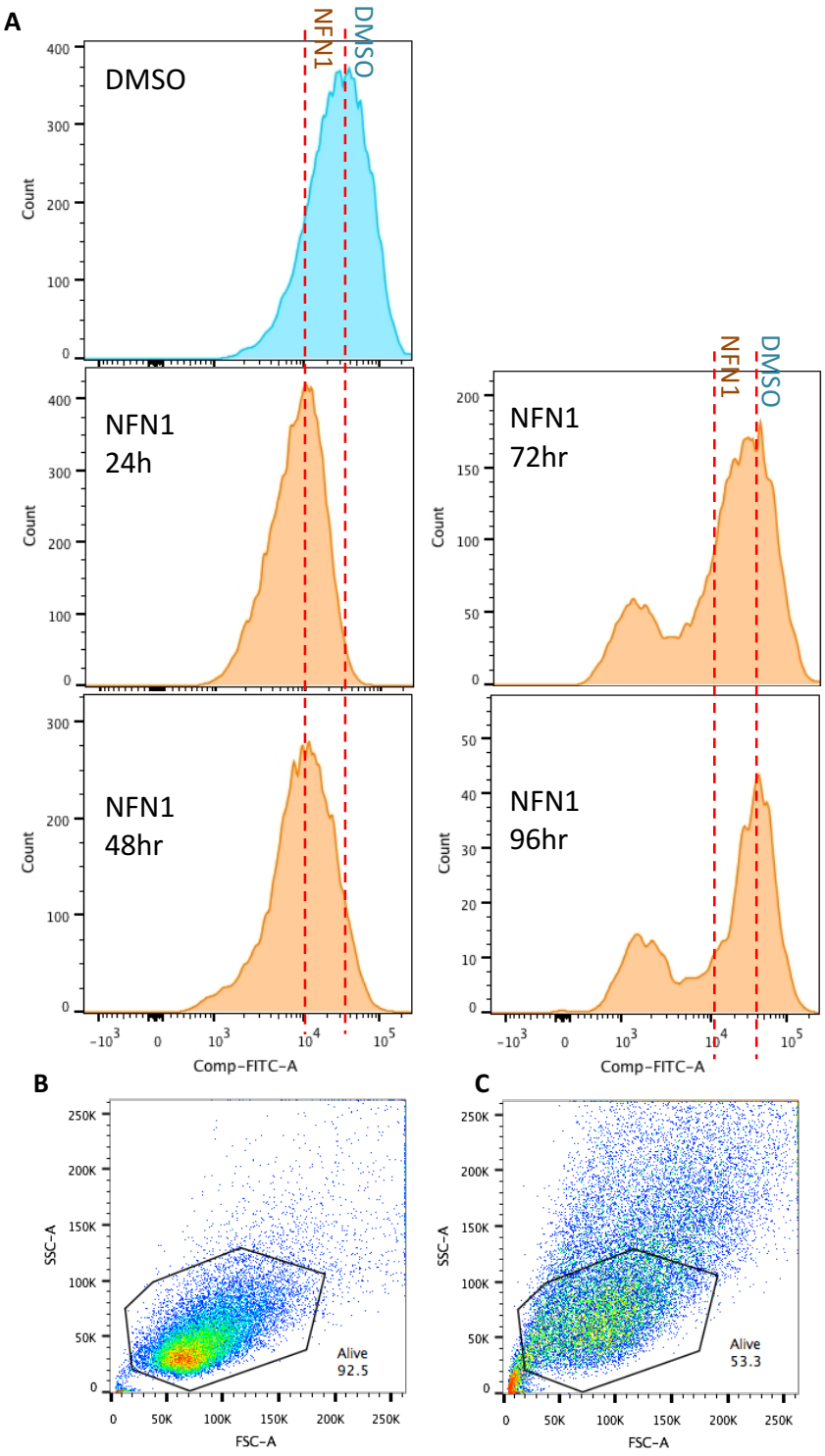

Figure 3.7: **NFN1** mediated inhibition of Aldefluor™ activity is sustained up to 48hrs post **NFN1** treatment (1µM, n=2). **A**) Aldefluor™ activity (FITC) of A375 melanoma cells treated with **NFN1** (orange) over 96 hours compared to vehicle (1% DMSO, blue) control. **NFN1** mediated reduction in Aldefluor™ activity is seen at both 24hrs and 48hrs post **NFN1** treatment. After 72hrs post **NFN1** treatment, A375 cells begin to recover Aldefluor™ activity, however with a clear low Aldefluor™

activity peak, likely due debris from **NFN1** mediated A375 cell death. Full recovery of Aldefluor™ activity is seen after 96hours, again with debris peak from **NFN1** driven cell death. **B**) Pseudocolour flow cytometry plot of A375 melanoma cells, upon DMSO treatment, plotted as forward scatter (FSC) against side scatter (SSC), gated around the Alive cell population (92.5%). **C**) Pseudocolour flow cytometry plot of A375 melanoma cells, 72hours post-**NFN1** treatment, plotted as forward scatter (FSC) against side scatter (SSC), gated around the Alive cell population (53.3%), however it is clear cellular debris is present through **NFN1**-mediated cell death.

3.4 Conclusion

Here I demonstrate 5-NFNs are targets for human ALDH2 and ALDH1A3 *in vitro*. By utility of the Aldefluor™ assay, I also validate that 5-NFNs are inhibitors for ALDH enzymes in melanoma cells. Further, I report that 5-NFNs can also potently inhibit ALDH enzymes for up to 72hrs, suggesting a new mechanism for 5-NFN-ALDH activity (**Figure 3.8**). Finally, I demonstrate that the human ALDH2*2 mutation has limited normal functionality, to which, 5-NFNs had minimal activity. As such, it would be interesting to explore if those patients with ALDH2*2 mutations are protected from the toxic side effects of clinical 5-NFNs, such as **NFX**. I therefore hypothesise that 5-NFNs have the potential to exhibit potent toxicity in cancer cells lines with known ALDH^{high} expression

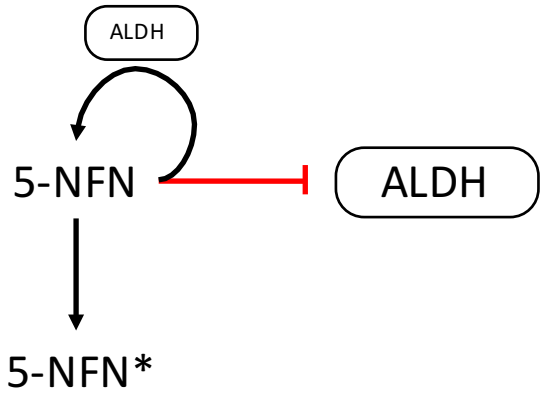

Figure 3.8: Schematic for the mechanism 5-NFN-ALDH activity. 5-NFNs are pro-drugs, bio-activated by ALDH enzymes to their active metabolite. This consequently results in inhibition of ALDH activity, sustained for up to 72hrs.

Chapter 4

ALDH1A3 activity mediates 5-NFN toxicity in melanoma cells

4.1 Introduction

ALDH1A1 and ALDH1A3 have been reported as CSC markers for melanoma,[79,151] where ALDH1A3 appears to be the major ALDH enzyme for marking CSCs in the A375 melanoma line.[79] These ALDH^{high} melanoma cells are highly tumorigenic[67,68] and exhibit increased resistance to conventional chemo-therapeutics,[57] that in many cases, will lead to cancer relapse, usually more aggressive and chemo-resistant than the original tumour. As such, being able to target these ALDH^{high} cells in melanoma could be therapeutically favourable. From the previous chapter, I have demonstrated that 5-NFNs are inhibitors of ALDH1A3, and following previous work reporting ALDH mediated-toxicity in zebrafish,[115] I hypothesise that 5-NFNs should present potent toxicity in the A375 melanoma cell lines. If ALDH1 enzymes play a key role in mediating 5-NFN toxicity in A375 cells, then knock-down of ALDH1 should invoke cellular resistance to 5-NFNs, and in a mirror experiment, overexpressing ALDH1 enzymes should also hypersensitise these cells to 5-NFNs. Considering current literature,[45,79,80,151] siRNA knock-down of ALDH enzymes in A375 cells should be able to provide some insight into whether ALDH1 enzymes contribute to Aldefluor™ activity in this cell line, and to what extent do the levels of individual isoforms correlate with Aldefluor™. Further, it would be interesting to explore how all 19-ALDH isoforms can influence 5-NFN sensitivity, as it is likely that other ALDH enzymes will contribute to activity also, such as ALDH2.

Here I demonstrate that 5-NFNs display potent cytotoxicity in the A375 melanoma cell line, as well as a small panel of other cancer cell lines. Although sensitivity of melanoma cells to **NFN1** did not correlate to ALDH1A3 expression, I hypothesise that ALDH1A3 activity contributes to sensitivity for a small subpopulation of cells, where I display that A375 melanoma cells and human melanoma sections are heterogeneous for ALDH^{+} subpopulations, in keeping with literature reports[79,151] I describe a functional role for ALDH1A3 in driving 5-NFN mediated toxicity in A375 melanoma cells. Knock-down of ALDH1A3 by siRNA renders A375 cells resistant to **NFN1**, and overexpression of the enzyme induces in A375 hypersensitivity. Further, I show that ALDH1A3 is the key ALDH isoform responsible for Aldefluor™ activity in A375 cells, where there is some indication of a small ALDH1A1 expression that shows synergistic expression with ALDH1A3. Looking more broadly, it was difficult to pick out specific isoforms that offered significant contribution in

ALDH-driven 5-NFN mediated cell toxicity, especially in my findings that there was not a significant correlation between ALDH1A3 expression and 5-NFN sensitivity on a panel of melanoma cell lines.

4.2 5-Nitrofurans are cytotoxic in cancer cell lines

High ALDH expression is a marker CSCs in melanoma,[79,151] and other cancers.[7,14,44] As 5-NFNs are competitive substrates for Aldh2b in zebrafish,[115] and with Aldefluor™ in A375 melanoma cells, I hypothesised that human ALDH enzymes can bio-activate 5-NFNs in cancer cell lines to promote cytotoxicity.

4.2.1 5-Nitrofurans are cytotoxic in melanoma cells

To test the potential for 5-NFNs to target cancer cells, the cytotoxicity of four 5-NFN compounds, identified through a previous small molecule screen,[115] were tested against the A375 melanoma cell line. A375 is a malignant melanoma cancer cell line with a $BRAF^{V600E}$ mutation established from a 54-year-old female. A375 cells were incubated with **NFN1-4 (Figure 4.1A-D**) over a logarithmic concentration range, where cell viability was determined by PrestoBlue™ treatment and EC_{50} concentrations were obtained (**Figure 4.1E**). All 5-NFNs tested exhibited toxicity in the A375 melanoma cell line, EC_{50} = 1.77µM (**NFN1**); 7.52µM (**NFN2**); 4.50µM (**NFN3**); 8.77µM (**NFN4**). **NFN1** was the most potent 5-NFN tested in this cell line, however all four compounds exhibited A375 cell toxicity with EC_{50} values ranging from 1-10µM. This provides evidence that 5-NFNs are cytotoxic against melanoma cells. **NFN1** was the most potent against the A375 cell line and as such, was selected as a tool compound throughout.

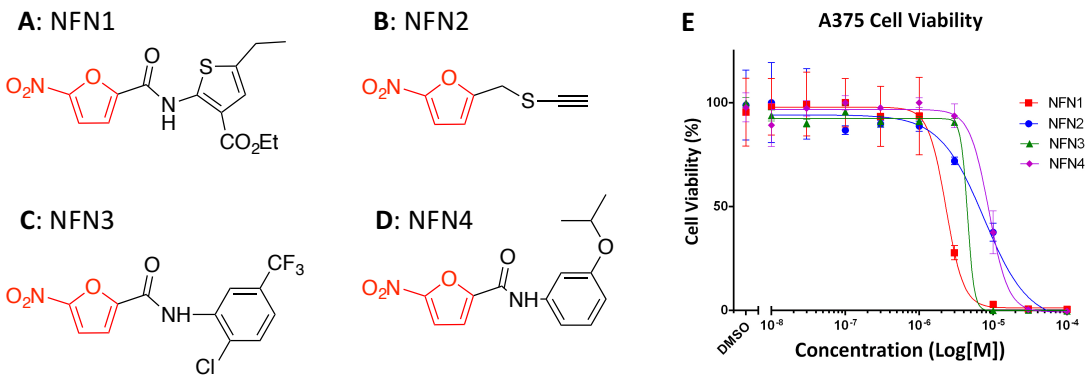

Figure 4.1: 5-NFN activity on A375 melanoma cells. **A**-**D**) Molecular structures of **NFN1**-**4** respectively. The 5-nitrofuran moiety is highlighted in red. **E**) Cell viability assay of A375 melanoma cell treated with **NFN1** (red), **NFN2** (blue), **NFN3** (green), and **NFN4** (purple) over 96hrs. EC_{50} values determined by PrestoBlue™ treatment normalised to vehicle (1% DMSO) control. EC_{50} = 1.77µM (**NFN1**); 7.52µM (**NFN2**); 4.50µM (**NFN3**); 8.77µM (**NFN4**).

4.2.2 5-Nitrofurans are cytotoxic in other cancer cell lines

NFN1 toxicity in cancer cells was further explored on two other cancer cell lines known to have CSC ALDH expression: A2780 (ovarian) and HCT116 (colorectal);[36,79,159] compared to A375 melanoma cells. A2780 is a human ovarian carcinoma cell line, established from an untreated patient and HCT116 is a malignant colonic carcinoma cell line with a RAS mutation in codon 13 established from an adult male.

Cell viability assays were set up for each cell line as before and treated with a logarithmic doses of **NFN1**. The no-nitro compound, **NFN1.1**, was used as a control to see if the NO_2 moiety is important for 5-NFN activity and tested at the same logarithmic concentrations on each cell line. All cell lines were sensitive to **NFN1** (**Figure 4.2**); HCT116 EC_{50} = 1.85µM, A2780 EC_{50} = 45.8nM, A375 EC_{50} = 867nM. This provides evidence that 5-NFNs are active in a range of cancers and not limited to melanoma. The variation in EC_{50} values could reflect ALDH activity within the cell lines themselves, where the 20-fold increase in sensitivity seen in A2780 ovarian cells could reflect a much higher ALDH activity status. The no-nitro compound, **NFN1.1**, showed no activity at any concentration in any cancer cell line,

providing a link between the requirement of the NO_2 moiety to be present and 5-NFN anti-cancer activity; mirroring that seen previously.[115]

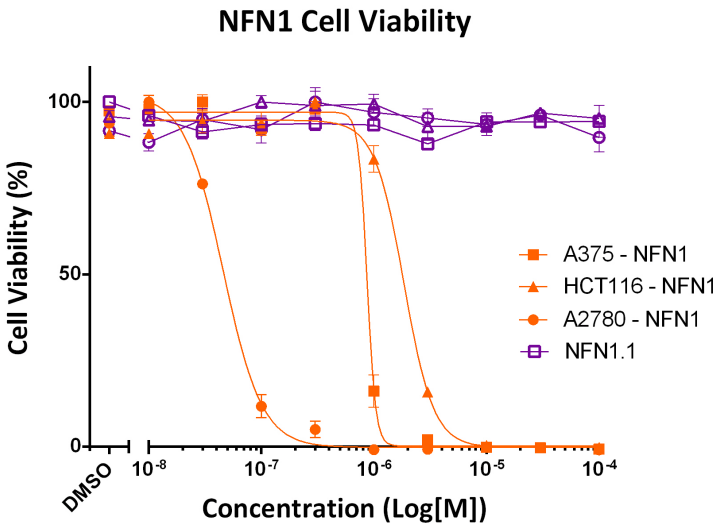

Figure 4.2: Cell viability assays upon **NFN1** or **NFN1.1** treatment over 96hrs, EC_{50} values determined by PrestoBlue™ treatment and normalised to vehicle (1% DMSO) control. A375 melanoma (squares), A2780 ovarian (circles) and HCT116 colorectal (triangles) cell viability against **NFN1** (orange) and **NFN1.1** (purple). For **NFN1**, A2780 EC_{50} = 45.8nM, A375 EC_{50} = 867nM and HCT116 EC_{50} = 1.85µM. **NFN1.1** treatment had no effect of cell viability in all 3 cell lines.

4.2.3 Aldefluor™ activity does not correlate with 5-nitrofuran sensitivity in cancer cell lines

To analyse if the ALDH activity in cancer cell lines correlated with their sensitivity to **NFN1**, the cells were subjected to the flow cytometry based Aldefluor™ assay. A375 melanoma cells, A2780 ovarian cells and HCT116 colorectal cells cells were subjected to the Aldefluor™ assay, where Aldefluor™ activity was measured using BD LSR II Flow Cytometer. DEAB was used as a negative control, and represented mean shown as green dashed line. A375 melanoma cells had high Aldefluor™ activity, with HCT116 colorectal cells having more of a broad, heterogeneous expression (**Figure 4.3**). It was unusual to see that A2780 ovarian cells had low Aldefluor™ activity, considering their high sensitivity to **NFN1**, however, this correlated with previous studies.[39] If **NFN1** sensitivity was based purely on Aldefluor™

activity alone, it would suggest A375 melanoma cells would be most sensitive and A2780 ovarian cells would be resistant, which is not consistent with my results. This is suggestive that Aldefluor™ reagent could be selective for the activity of a subset of ALDH isoforms, as mentioned previously,[32] and not truly represent the activity of all 19-ALDH isoforms present in human cells that can potentially contribute to 5-NFN activity.

	Sample Name	Count	Mean : Comp-FITC-A
	Specimen_001_HCT116.fcs	17671	14793
	Specimen_001_A2780.fcs	21893	5138
	Specimen_001_A375.fcs	22554	46410

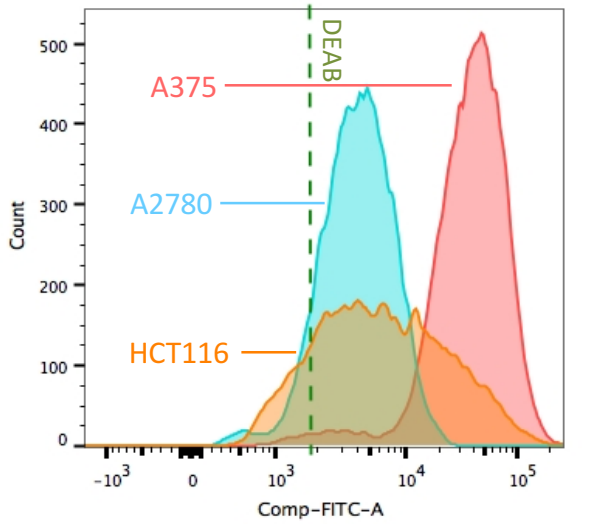

Figure 4.3: Aldefluor™ flow cytometry assay on cancer cell lines (n=2). Aldefluor™ (FITC) expression of A375 melanoma (red), A2780 ovarian (blue) and HCT116 colorectal (orange) cells represented as histogram counts. A375 cells have high Aldefluor™ activity (Mean: 4.64×10^4), HCT116 cells have more broad Aldefluor™ activity (Mean intensity: 1.48×10^4) and A2780 cells have markedly lower Aldefluor™ activity (Mean intensity: 5.14×10^3). Mean DEAB Aldefluor™ activity is represented by the green dashed line (Mean intensity: 1.87×10^3).

4.2.4 No correlation between ALDH1A3 expression and 5-NFN sensitivity in melanoma cell lines

The following work was done in collaboration with Dr Marco Ranzani and Dr David Adams (Wellcome Trust Sanger Institute, Cambridge, UK), who kindly provided the panel of melanoma cell lines, growth conditions and cellular characteristics (**Appendix I**). All RNA_{seq} data was completed by Dr Marco Ranzani (**Appendix II**).

To understand whether there was a correlation between ALDH1A3 expression and 5-NFN sensitivity, EC_{50} values were obtained for **NFN1** on a panel of melanoma cell lines with previously characterised ALDH RNA expression levels. It was expected that melanoma cell lines with high expression of ALDH1A3 should be more sensitive to **NFN1**. Cell viability assays were set up as before and in accordance to **Appendix I**, treated with **NFN1**. Cell lines were also treated with **NFN1.1** as a control. Sensitivity to **NFN1** (EC_{50} value) was correlated against the RNA_{seq} expression for ALDH1A3 in each individual cell line. Of the 21 cell lines provided, after only half were recorded, it was clear to see there was no correlation between ALDH1A3 expression and 5-NFN sensitivity (**Figure 4.4**). Although a trend towards lower EC_{50} values is matched with higher ALDH1A3 sensitivity, there is a weak correlation ($R^2 = 0.0246$) and it is visually obvious when examining the raw points themselves. This lack of correlation was surprising considering work from **Chapter 3**, demonstrating 5-NFNs can inhibit ALDH1A3 activity *in vitro*. As ALDH1A3 is a previously described functional CSC marker for A375 melanoma cells, it is likely that only a subpopulation of cells are more highly sensitive to 5-NFNs, and this is why no correlation is observed when probing whole cell populations. As such, knock-down of ALDH1A3 should invoke resistance in this subpopulation of A375 cells to 5-NFNs and this should be reflected when monitoring the cellular response to 5-NFN treatment.

ALDH1A3 may still contribute to 5-NFN toxicity in these cancer cell lines, however looking at a single ALDH isoform from a family of 19 may not be representative of which ALDH isoforms are driving 5-NFN toxicity in each individual cell line. Most likely, it will be a differing series of ALDH expression in each cell line that contributes to 5-NFN toxicity, and will not be mediated by just one isoform. It would be interesting to discover the affinity (IC_{50}) 5-NFNs have to each of the 19 ALDH isoforms, and how this correlates with their

sensitivity over a series of expression patterns. There is likely valuable information within this dataset, however, it almost becomes obsolete when trying to consider single ALDH isoforms only rather than digging for statistical correlations for the whole ALDH expression pattern and protein levels. Ideally, the ALDH expression would be characterised for each cell line after every cell viability assay, to give a true representation of ALDH expression at that specific time, for that particular EC_{50}. Further, it would also be possible to explore how fluctuations in both EC_{50} and ALDH expression in the same cell line over time/serial passages are correlated. However, although this panel does give a good foundation for exploring fluctuations in ALDH expression between melanoma cell lines, it became difficult to successfully extract correlations between these expression and sensitivity to 5-NFNs.

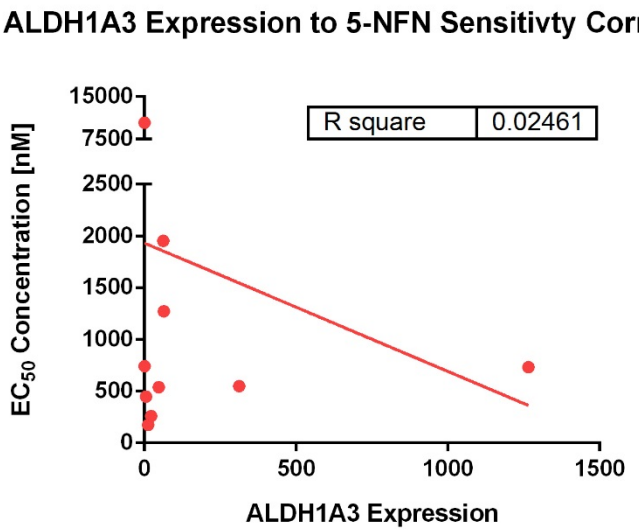

Figure 4.4: Scatter plot correlating **NFN1** sensitivity to ALDH1A3 expression in a panel of 11 melanoma cells. **NFN1** sensitivity is represented by EC_{50} values determined by cell viability, where the lower the EC_{50} the more sensitive the cell line is to **NFN1**. ALDH1A3 is determined through RNA_{seq} and directly proportional to expression. Although some correlation that **NFN1** sensitivity increases as ALDH1A3 expression is higher, this is very weak (R^2 = 0.0246). Looking at the raw data points, it is clear that most melanoma cells have low ALDH1A3 and those with much higher levels were not more sensitive to **NFN1**, where the most sensitive cells lines appear to have effectively no ALDH1A3 expression.

4.3 Melanoma cells appear to have heterogeneous ALDH1 subpopulation

A375 cells are reported to have heterogeneous ALDH expression, with a sub-population having a much higher expression of ALDH1 enzymes.[79] This heterogeneity may be reflected in Aldefluor™, where the broadness of the Aldefluor™ histogram seen may be as a direct result of ALDH heterogeneity within the A375 population. To visualise this, adhered A375 melanoma cells treated with Aldefluor™ reagent were imaged using Nikon SMZ1500 stereomicroscope (Ex: 488nm, Em: 525nm). The A375 cells appear have a clear heterogeneous expression of Aldefluor™ activity seen visually (**Figure 4.5A**). This is in keeping with literature reports that there is a heterogeneous population in regards to ALDH activity in A375 melanoma cells and that A375 melanoma CSCs have significantly higher ALDH1 expression.[79] So if 5-NFNs are cytotoxic to cells with higher Aldefluor™ expression, then they may specifically be able to target CSCs in A375 melanoma cells.

To visualise ALDH heterogeneity seen in A375 melanoma cells reported previously,[79,151] malignant melanoma and healthy skin sections were purchased from US Biomax and stained for ALDH1 through 3,3'-diaminobenzidine (DAB) immunohistochemistry (IHC) by a Ph.D. student in our group, Sonia Wojciechowska (University of Edinburgh, UK). The IHC staining reveals that melanoma sections have clear subpopulations with high ALDH1 expression and other cells that have no detectable ALDH1 expression at all (**Figure 4.5B**). This mirrors the characteristics seen in the Aldefluor™ treated A375 melanoma cells and in previous literature.[79,151] The healthy skin showed almost no ALDH1 activity (**Figure 4.5C**) suggesting that high ALDH1 cellular subpopulations are unique to cancer of the skin, and not healthy skin tissue, in agreement with a previous study[90] and work from the Human Atlas Project, where only very low expression of ALDH1 is seen in skin tissue.[160] It is notable that ALDH1 expression in the melanoma sections was surprisingly higher than expected for the CSC population percentage,[30] although this may be explained by reports stating CSCs may have a higher incidence in melanoma than previously reported.[68,71] One other explanation could be down to specificity of the antibody staining, where low ALDH1 activity may be detected by IHC, but is not detected by Aldefluor™. Thus, while the IHC may not be quantitative compared with Aldefluor™, this staining has shown a clear heterogeneous ALDH1 population within human melanoma sections. Although, it is also likely that high expression of melanin present in melanoma, and not in human normal human skin tissue,

may also interfere with the ALDH1 DAB staining, and could also be presenting false positive data. As such, another melanin rich tissue sample, such as a mole, could be used to better asses this staining and quantify ALDH1 heterogeneity.

If there are heterogeneous ALDH1 subpopulations, this may also explain why no correlation between 5-NFN sensitivity and ALDH expression was reported, however further quantitative analysis would be needed to verify this hypothesis. While treatment of cells with 5-NFNs through cell viability explores the sensitivity of the whole cell population, the expression of ALDH1, specifically ALDH1A3 in this instance, may only correlate to sensitivity of the subpopulation of melanoma cells. As such, considering the likely heterogeneity of ALDH1A3 expression in the A375 melanoma cells, knock-down of ALDH1A3 expression should invoke resistance in the sensitivity of this cell line to 5-NFN treatment. This would provide an explanation for why whole cell ALDH1A3 expression did not correlate with 5-NFN sensitivity, as expression was localised to only a subpopulation, while trying to describe behaviour of cells as a whole population.

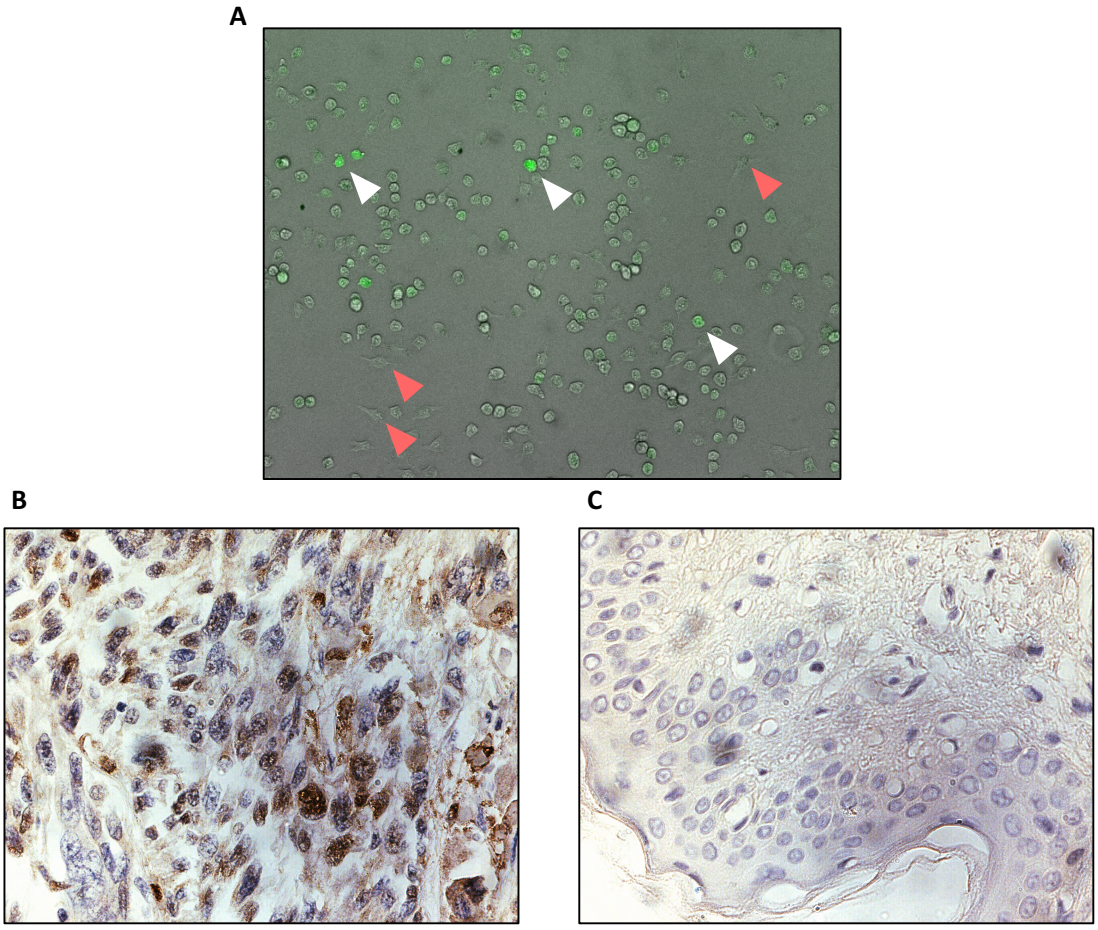

Figure 4.5: Visual images showing ALDH heterogeneity in melanoma cells. **A**) Adhered A375 melanoma cells stained with Aldefluor™ imaged 10x magnification (Ex: 488nm, Em: 525nm). Heterogeneity within the A375 cell population is seen, both high Aldefluor™ expressing cells (white arrows) and low Aldefluor™ expressing cells appear are present in the whole A375 cell population. Cells with high Aldefluor™ activity appear more rounded, whereas low Aldefluor™ expressing cells show elongation. **B**) Section of a human malignant melanoma from the right thumb of a 62-year old patient. The section was DAB-stained for ALDH1 and counter stained with hematoxylin and eosin (H&E). A heterogeneous $ALDH1^{+}$ subpopulation of cells (brown) is present in the whole melanoma cell population, where $ALDH1^{-}$ cells (purple) are readily abundant also. **C**) Section of healthy skin tissue adjacent to melanoma from a 50-year old female patient. The section was DAB-stained for ALDH1 against H&E background counterstain. In the whole cell population, minimal ALDH1 expression is seen in any of the healthy skin tissue.

4.4 Knock-down of ALDH1A3 expression protects melanoma cells from 5-NFN toxicity

As shown in the previous section, A375 melanoma cells have a heterogeneous population for ALDH1 expression. It has also been reported previously that ALDH1A1 and ALDH1A3 are CSC markers in melanoma, with ALDH1A1 being largely found as the key CSC marker in primary melanoma tissue and ALDH1A3 as the major ALDH CSC marker in A375 melanoma cells.[79] Although there was no correlation between ALDH1 expression in melanoma and 5-NFN sensitivity, it is likely that it is only a subpopulation of the whole cell population which is highly sensitivity to 5-NFNs. As such, if 5-NFN toxicity is driven by ALDH in A375 cells, knock-down of ALDH expression through siRNA treatment should offer some protection from 5-NFN treatment, specifically those ALDH isoforms considered as CSC markers, as their expression is much higher compared to other ALDH enzymes.

4.4.1 Effect of siRNA knock-down on A375 cells

Knock-down of ALDH1A3 and ALDH2 by siRNA in A375 melanoma cells was confirmed by western blot (**Figure 4.6A,B**). Treatment with siRNA against ALDH1A3 and ALDH2 resulted in a 73.1% and 87.4% reduction in protein expression respectively, against GAPDH expression in all samples. No ALDH1A1 expression was detectable in the A375 melanoma cell line (**Figure 4.6C**) by western blot, compared to HepG2 and his-tagged protein positive controls. This is in agreement with a previous report from Luo *et al.* (2012) that ALDH1A3, rather than ALDH1A1, is the prominent ALDH CSC marker in the A375 cell line.[79] However, some loss of ALDH1A3 expression was seen upon treatment of A375 cells with siALDH1A1 (**Figure 4.6D**), suggesting that any phenotypes observed will likely be attributable to a reduction ALDH1A3 activity. Loss of ALDH activity was also confirmed by Aldefluor™ activity (**Figure 4.6E**). The Aldefluor™ assay analyses ALDH activity in live-cell population, where ALDH activity will negatively charge a fluorescent marker which is then retained within the cell and it will fluoresce green. DEAB is an ALDH inhibitor provided in the kit, used as a negative ALDH activity control, where ALDH activity is inhibited, not allowing the negative charging of the fluorescent molecule, so will pass through the cell and not fluoresce. Histogram plots rendered from flow cytometric analysis of Aldefluor™ expression indicates high ALDH activity in A375 cells, with a shift higher (right) in the fluorescence intensity,

whereas treatment with DEAB will shift the histogram plot lower (left), indicating lower (or no) ALDH activity. Knock-down of ALDH1A3 completely eradicated Aldefluor™ activity, and a partial reduction of Aldefluor™ activity is seen with ALDH1A1 knock-down. ALDH2 knock-down appeared to have no effect of Aldefluor™ activity in these cells. This shows that ALDH1A3 activity is the key ALDH isoform that drives Aldefluor™ activity in A375 cells. Although some loss of Aldefluor™ activity is seen with ALDH1A1 knock-down, this is in keeping with the reduction of ALDH1A3 expression observed by western blot upon treatment with siALDH1A1. Knock-down of ALDH1A1, 1A3 and ALDH2 by siRNA in A375 melanoma cells did not have any effect of cell behaviour or growth. Visually, ALDH knock-down of A375 cells appeared normal in morphology and behaviour (**Figure 4.7**), compared to control siRNA treated and WT A375 cells. Luo *et al.* (2012) reported siRNA knock-down of ALDH1A3 in $ALDH^{+}$ A375 cells induced apoptosis and led to a 55% reduction in cell viability,[79] however, this was only reported in the $ALDH^{high}$ subpopulation, and not the A375 population whole, as shown in this chapter, offering an explanation for the differences observed.[79]

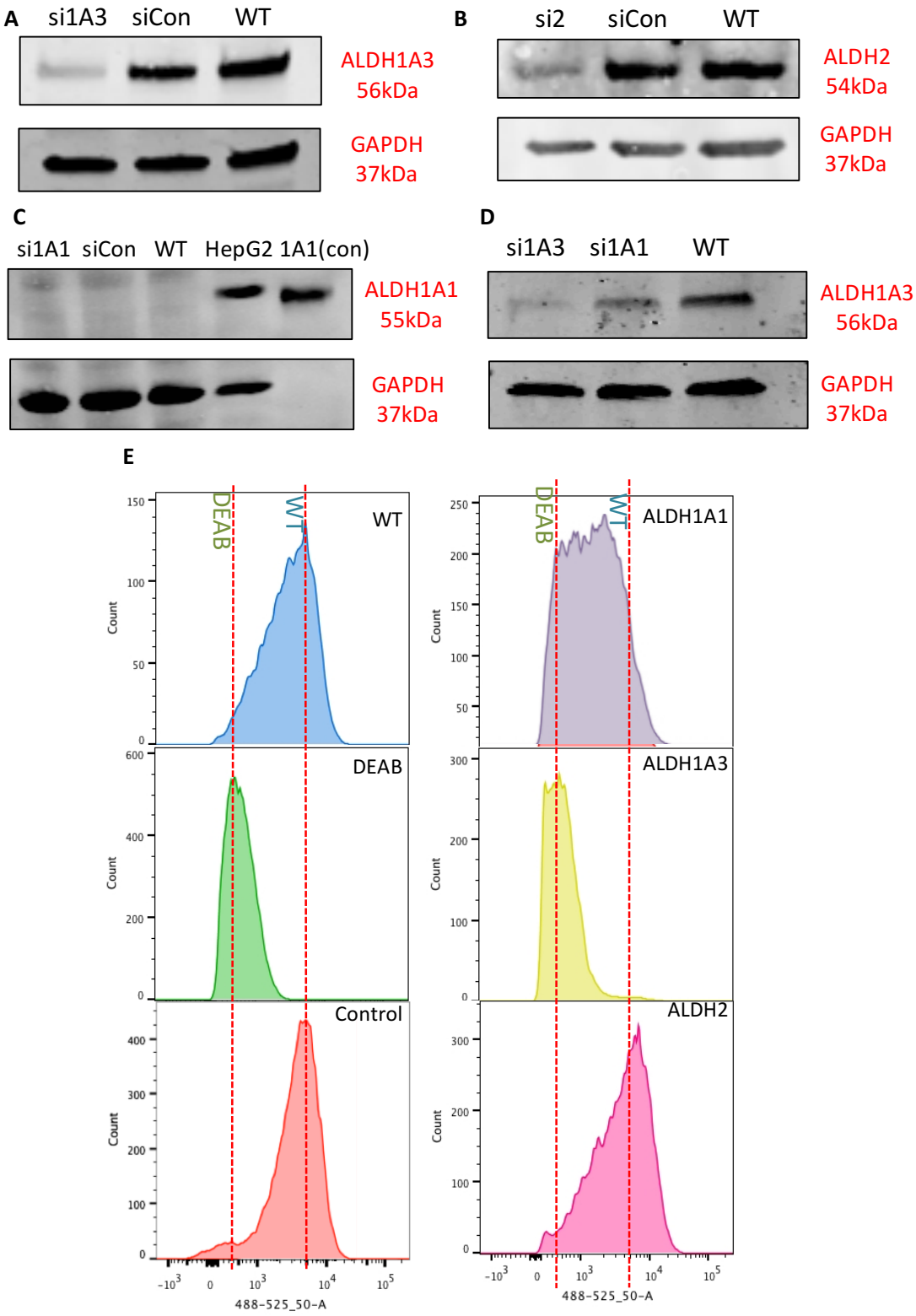

Figure 4.6: Efficiency and characterisation of knock-down of ALDH by siRNA in A375 melanoma cells. **A,B**) Western blot of ALDH1A3 and ALDH2 knock-down A375 cells respectively against scrambled siRNA control and WT A375 cells. GAPDH expression was used as a loading control. ALDH1A3 and ALDH2 siRNA treatment led to 73.1% and 87.4% respectively reduction in ALDH expression.

Treatment with scrambled control led to no alteration in ALDH expression. **C**) Western blot of ALDH1A1 knock-down A375 cells against scrambled siRNA control, WT A375 cells and positive controls: HepG2 cells and recombinant ALDH1A1 protein. There is no detectable ALDH1A1 expression in A375 cells upon western blotting with ALDH1A1 antibody. **D**) Western blot of ALDH1A1 and ALDH1A3 knock-down A375 cells against WT A375 cells stained with ALDH1A3 antibody. ALDH1A1 knock-down cells displayed a 52% reduction in ALDH1A3 expression (86% upon siALDH1A3 treatment as control) **E**) Aldefluor™ activity of ALDH1A1 (purple), 1A3 (yellow) and ALDH2 (pink) knock-down A375 cells against scrambled siRNA control (red) and WT (blue) A375 cells. DEAB (green) was used as a negative control. ALDH1A1 knock-down led to a reduction in Aldefluor™ activity, with broader expression pattern seen, indicating more heterogeneous Aldefluor™ activity in this population. ALDH1A3 knock-down completely ablated Aldefluor™ activity, so expression levels were similar to DEAB. ALDH2 knock-down had no effect of Aldefluor™ activity. As expected, control siRNA had no effect on Aldefluor™ activity also.

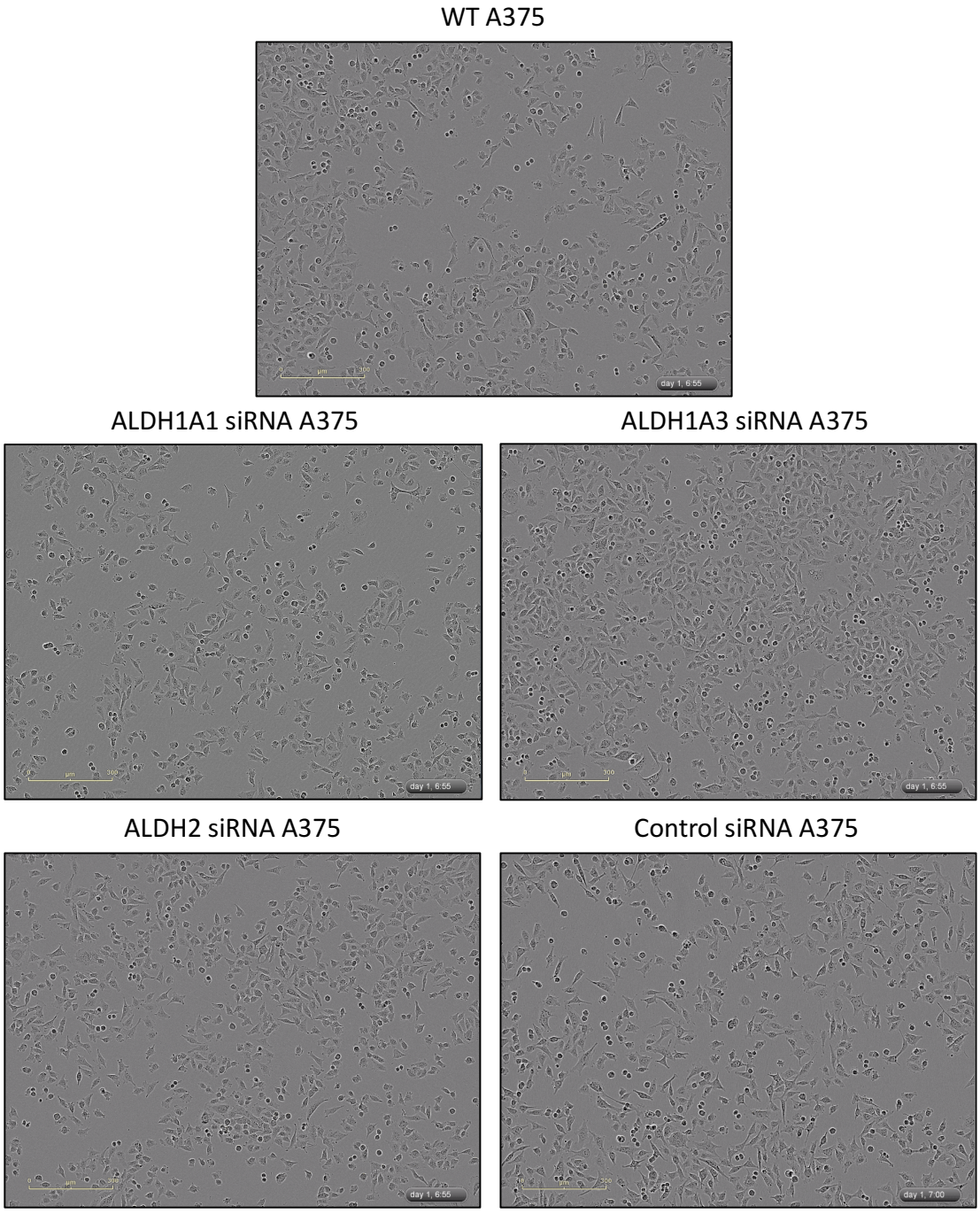

Figure 4.7: IncuCyte ZOOM® images of ALDH1A1, 1A3 and ALDH2 knock-down A375 cells against scrambled siRNA control and WT A375 cells during normal growth. Stills were taken 24hrs after siRNA treatment. siRNA treatment of both ALDH and scrambled control appeared to have no effect of cellular visual appearance or behaviour compared to WT A375 cells.

4.4.2 A375 melanoma cells are resistant to 5-nitrofurans upon ALDH1A3 knock-down

Aldh2b drives 5-NFN activity in zebrafish melanocytes,[115] so ALDH2 was the obvious candidate to explore first when looking at ALDH-driven bio-activation of 5-NFNs in human melanoma cells. ALDH2 was knocked-down in A375 melanoma cells by siRNA and treated with **NFN1** or vehicle (1% DMSO), compared to a scrambled siRNA control. ALDH2 knock-down A375 melanoma cells grew to 100% confluence, as monitored by IncuCyte ZOOM®, when treated with vehicle (1% DMSO) control (**Figure 4.8A**). The growth was also shown to be consistent with control siRNA treated A375 melanoma cells. Knock-down of ALDH2 in A375 melanoma cells did offer some protection against 5-NFN activity upon treatment with **NFN1** (**Figure 4.8B**), however, this protection was not significant ($P = 0.2672$). This indicates that, unlike in zebrafish melanocytes, ALDH2 may not be the primary ALDH isoform responsible for 5-NFN toxicity in A375 cells. ALDH1 isoforms have markedly increased expression in melanoma cells due to their function as CSC markers,[79,151] so it is likely that knock-down of these isoforms would provide more significant protection against 5-NFNs. Luo *et al.* (2012) reported that expression of ALDH1A enzymes were >15-fold greater in the $ALDH^+$ population compared to $ALDH^-$ cells, where ALDH1A3 copy number was 200-fold more abundant on average in $ALDH^+$ melanoma cell lines than ALDH1A1, leading them to conclude that ALDH1A3 expression specifically is a marker for CSC activity in A375 melanoma cells, so it is likely ALDH1A3 will have a much greater contribution to 5-NFN toxicity than ALDH1A1 in this cell line.[79]

To query whether 5-NFN toxicity is driven by ALDH1 isoforms in A375 melanoma cells, ALDH1A1 and ALDH1A3 expression was silenced through siRNA and treated with the same dose of **NFN1** or vehicle (1% DMSO), compared to a scrambled siRNA control. ALDH1A1 and 1A3 knock-down A375 melanoma cells all grew to 100% confluence, as monitored by IncuCyte ZOOM®, when treated with vehicle (1% DMSO) control (**Figure 4.8C**). The growth was also shown to be consistent with control siRNA treated and WT A375 melanoma cells. ALDH1A3 knock-down had a small yet significant ($P = 0.034$) increase in cell survival upon **NFN1** treatment against the scrambled control (**Figure 4.8D**), however ALDH1A1 knock-down did not share this characteristic ($P = 0.6302$), showing that 5-NFN toxicity can be driven by ALDH1A3 in A375 melanoma cells. This protection of ALDH1A3 is clearer when

looking at the raw IncuCyte ZOOM® footage taken before and after **NFN1** treatment (**Figure 4.9A**). Control A375 cells are more stressed with far more cells appearing to round up, and eventually rupture, compared to ALDH1A3 knocked-down A375 cells. The abundance of these rounded up cells is much clearer when artificially coloured purple (**Figure 4.9B**). It is interesting to see visually how the cells are behaving in response to 5-NFNs, where it is clear less cells are dying in ALDH1A3 knock-down A375 cells.

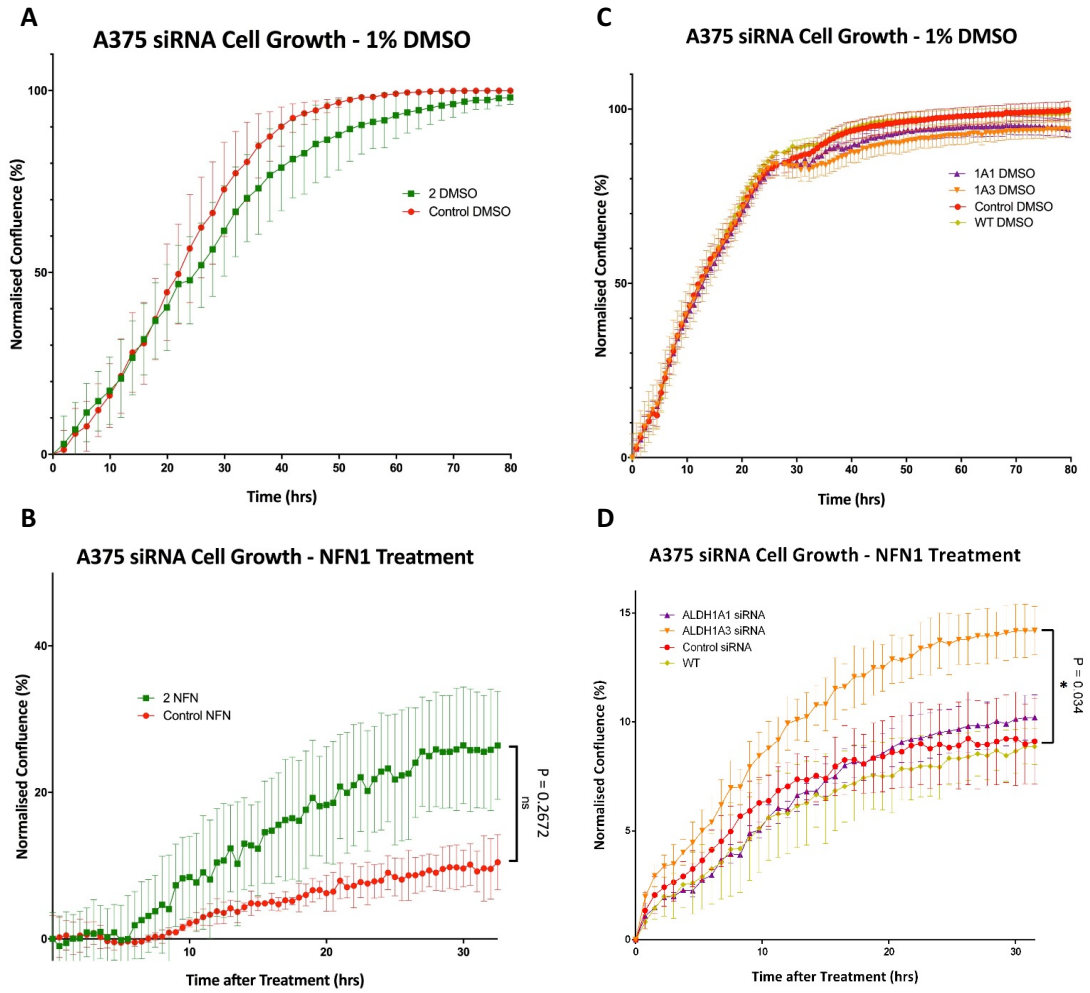

Figure 4.8: Confluence graphs of siRNA A375 melanoma cells treated with **NFN1** (1µM) or vehicle (1% DMSO). Confluence is normalised to 0% prior to treatment with drug. **A**) Growth of ALDH2 knock-down A375 cells (green) compared to scrambled control siRNA A375 cells (red) after treatment with 1% DMSO. Both grew to 100% confluence at the same rate. **B**) Growth of ALDH2 knock-down A375 cells compared to scrambled control siRNA A375 cells after treatment with **NFN1**. ALDH2 knock-down did provide some protection against **NFN1** over control siRNA cells, however this was not significant (P = 0.2672: t-test). **C**) Growth of ALDH1A1 (purple) and 1A3 (orange) knock-down

A375 cells compared to scrambled control siRNA (red) and WT (yellow) A375 cells after treatment with 1% DMSO. All cells grew to 100% confluence at the same rate (n=2). **D**) Growth of ALDH1A1 and 1A3 knock-down A375 cells compared to scrambled control siRNA and WT A375 cells after treatment with **NFN1**. ALDH1A3 knock-down was the only isoform that provided significant protection against **NFN1** toxicity over control siRNA and WT cells (P = 0.0.34: t-test; n=2).

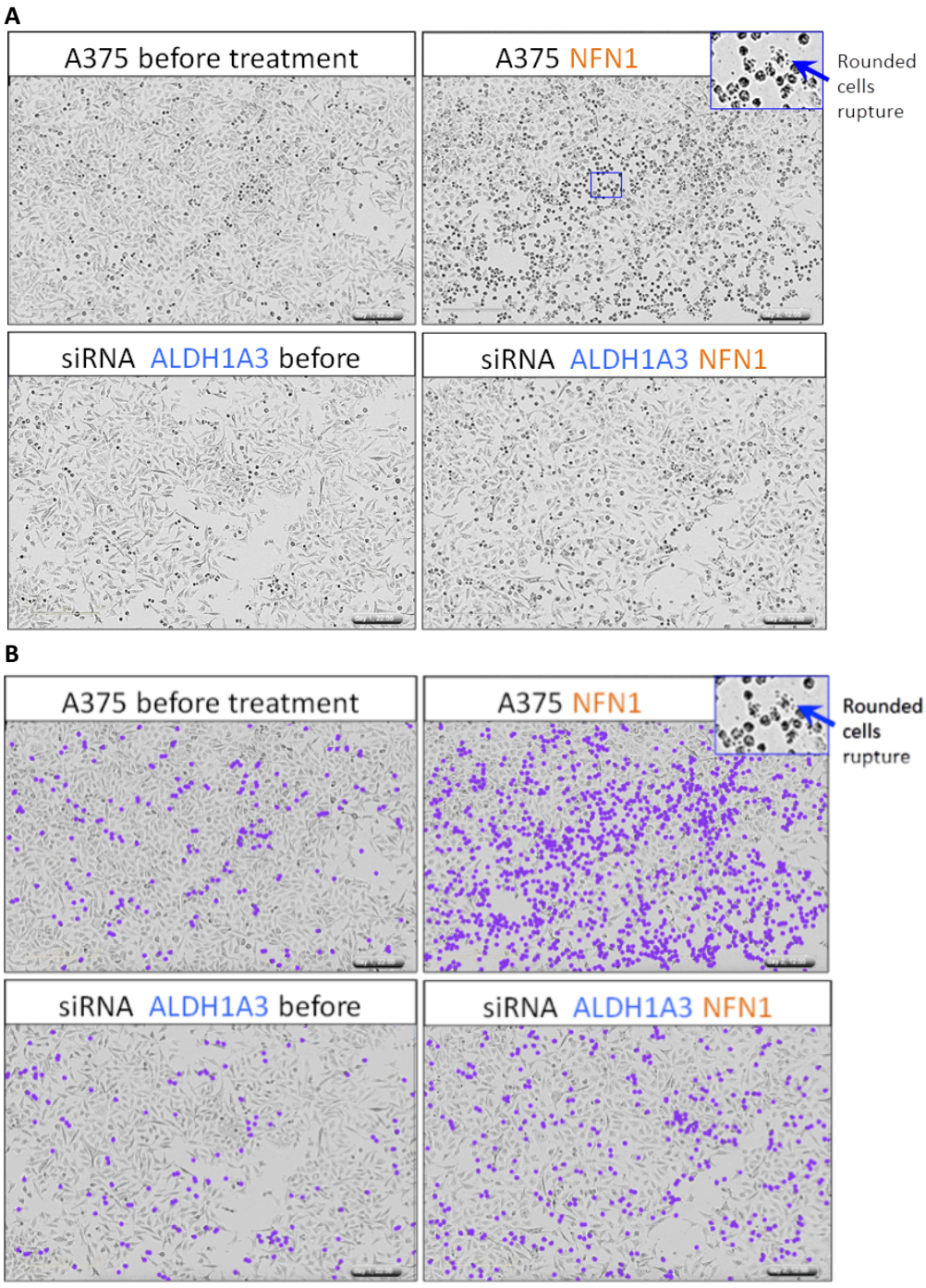

Figure 4.9: IncuCyte ZOOM® stills of ALDH1A3 knock-down A375 melanoma cells compared to control A375 cells, treated with **NFN1**. **A**) **NFN1** treatment induced cells rounding up, which would

eventually rupture. ALDH1A3 knock-down had a clear reduction in stressed/dying cells compared to A375 control cells. **B**) Upon **NFN1** treatment, cells became visually stressed, rounded up and eventually ruptured (i.e. cell death). These cells have been highlighted in purple to further show the protection provided from ALDH1A3 knock-down. Prior to **NFN1** treatment, the number of rounded up cells was low and consistent between both cells.

It was concerning that the extent to which ALDH1A3 knock-down protects A375 cells from 5-NFN toxicity is not fully reflected in the confluence curves. This may be a direct result of the accuracy of the IncuCyte ZOOM® artificial intelligence (AI) to measure cellular confluence, where dying/dead cells and cellular debris can still contribute towards cellular confluence by the in-built AI software (**Figure 4.10A,B**). As such, I wanted to refine the assay, and the way in which cellular sensitivity to **NFN1** was measured. If ALDH1A3 knock down protected A375 melanoma cells from 5-NFN activity, then a reduction in cell death should be detected. By utilising fluorescent cell death dyes, optimised for use in the IncuCyte ZOOM®, I could more accurately explore if ALDH1A3 knock down can protect A375 cells from 5-NFN mediated cell death.

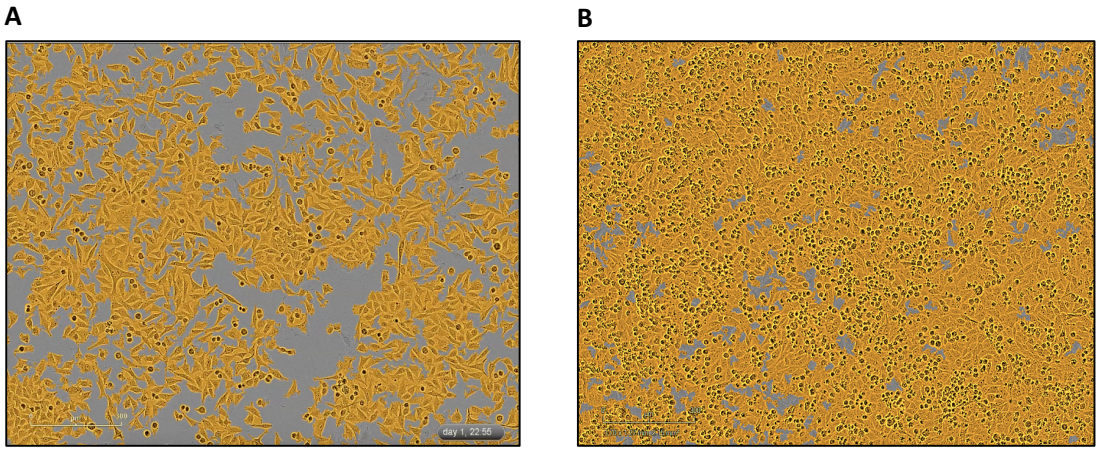

Figure 4.10: Confluence masks do not accurately discriminate A375 melanoma cells. **A**) Cell confluence on WT A375 melanoma cells during normal growth as recorded by the IncuCyte ZOOM® AI software. Confluence mask (yellow) highlights adhered A375 cells by defining the cellular boarder **B**) Cell confluence on WT A375 melanoma cells 24hrs after **NFN1** treatment as recorded by the IncuCyte ZOOM® AI software. Confluence mask (yellow) highlights both dying/dead cells as well as normal adhered A375 cells, and does not discriminate between them.

4.4.3 5-Nitrofuran mediated cell death not driven by apoptosis

To more accurately investigate the protection against 5-NFN toxicity seen in ALDH1A3 knock-down A375 melanoma cells, apoptosis was monitored fluorescently using NucView™ – a fluorescent caspase-3/7 cellular marker. ALDH1A1 or 1A3 knock-down A375 cells were **NFN1** treated in the presence of NucView™, compared to a scrambled siRNA control, and analysed using the IncyCyte ZOOM®. There was no detectable change in NucView™ expression in the ALDH1A1 or 1A3 knock-down cells compared to the scrambled siRNA control cells (**Figure 4.11**). Although there was an increase in apoptosis upon **NFN1** treatment, this only amounted to 6% of the confluent population. This may largely be due to the mechanism by which cell death is induced by 5-NFNs. Ferroptosis is a newly discovered form of regulated cell death, distinct from previously described pathways of regulated cell death, such as apoptosis.[161,162] Ferroptosis is an iron-dependant process, which results in mitochondrial membrane rupture that drives cell death and can be induced by an accumulation of intercellular ROS.[161] 5-NFN toxicity is driven by the formation of ROS within the cell to promote cell death,[115] and as such, it is likely that cell death could be driven by ferroptosis in 5-NFN treated cells, where it has been previously reported that dying melanoma cells do not undergo apoptosis upon high intercellular ROS exposure.[163] This might explain why there is no change in apoptosis in A375 cells upon 5-NFN treatment. The morphology of ferroptosis mediated cancer cell death is described by cells rounding up before rupturing, similar to what is seen after 5-NFN treatment.[164] So analysing expression of apoptotic markers, such as caspase-3/7, may not offer the best solution for monitoring cell death upon 5-NFN treatment.

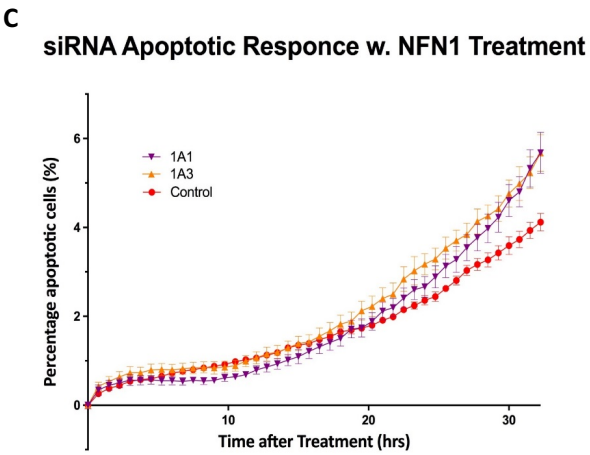

Figure 4.11: NucView™ expression in ALDH1A1 (purple) and 1A3 (orange) knock-down A375 cells compared to scrambled control cells (red) upon treatment with **NFN1** (3µM). Apoptosis is represented as percentage of total population and normalised to 0% prior to **NFN1** treatment (n=2). Although apoptosis increase upon NFN1 treatment in all cells, there was no difference in the amount of apoptosis between the ALDH knock-down and the control cells. Overall, apoptosis was unexpectedly low (<6%).

4.4.4 ALDH1A3 knock-down protects A375 melanoma cells from 5-nitrofuran mediated cell death

As it is likely that 5-NFN mediated cell death does not occur via apoptotic pathways, cell death was monitored more broadly using Draq7 (Ex: 633nm, Em: 599nm) – a membrane impermeable fluorescent dye that only stains the nuclei of dead and permeabilized cells; which is useful considering nuclei of cells that have undergone ferroptosis remain intact.[164] ALDH1A3 knock-down A375 cells were treated with **NFN1** in the presence of Draq7, and analysed using the IncyCyte ZOOM®, compared to a scrambled siRNA control. ALDH1A3 knock-down significantly reduced Draq7 labelling of in A375 cells compared to the control (**Figure 4.12A**; $P < 0.0001$) upon **NFN1** treatment. The protection ALDH1A3 knock-down provided against 5-NFN driven cell death can also be seen visually from stills taken from the IncuCyte ZOOM® footage, where there is a visible reduction in Draq7 expression in ALDH1A3 knock-down A375 cells compared to control (**Figure 4.12B**). This is clear evidence that 5-NFN mediated cell death is driven by ALDH1A3 in A375 melanoma cells.

Cell death was further analysed using AnnexinV. AnnexinV is a fluorescent flow cytometry dye which binds membrane surface-expressing phosphatidylserine in early apoptotic cells (Exitation: 495nm, Emission: 519nm). ALDH1A3 knock-down A375 cells were treated with **NFN1** in the presence of AnnexinV, and analysed using the BD LSRFortessa™, compared to a scrambled siRNA control (**Figure 4.6C**; 20% AnnexinV$^+$ ALDH1A3 vs 35.4% AnnexinV$^+$ control). This data shows that there is a distinct AnnexinV$^+$ population in the A375 cells treated with **NFN1**, which is lost upon ALDH1A3 knock-down. This population is indicative of early apoptosis induced by **NFN1** treatment, contradicting the data shown with NucView™. However, it is somewhat in agreement with data showing that oxidative stress of myoblast cells have significantly higher AnnexinV expression upon ALDH inhibition.[165]

It is clear that ALDH1A3 knock-down protects A375 melanoma cells from 5-NFN induced cell death, however it was unusual to find that this behaviour was not mirrored in apoptosis levels between the ALDH1A3 knock-down and scrambled siRNA control populations. NucView™ expression, although increasing upon 5-NFN addition, was unexpectedly low, with only approximately 6% of the confluent population expressing the apoptotic markers, caspse-3/7, after drug treatment. The detection of phosphatidylserine, by utility of the AnnexinV assay, presented a substantial increase in expression upon 5-NFN treatment. Phosphatidylserine is important in the phagocytic clearance of cells, upon regulated cell death, where phosphatidylserine is expressed as soon as cellular functions shut down.[166] Phosphatidylserine is widely considered as a surface marker in the detection of early apoptotic cells,[167] so its increase upon 5-NFN treatment appears counter-intuitive considering this was not reflected in the caspase-3/7 assay. However, a recent review highlighting how the expression of phosphatidylserine could be important in phagocytic clearance of cells in other, non-apoptotic cell death pathways,[168] provides evidence that may indicate 5-NFN mediated cell death is driven by ferroptosis. Magtanong *et al.* (2016) linked reports describing the expression of oxidised membrane lipids during ferroptosis and their function in the phosphatidylserine expression pathway, upon apoptisis.[169,170] It will be interesting to discover the exact mechanism in which 5-NFN treatment promotes regulated cell death, and whether the recently described ferroptosis pathway is a key driver of this activity.

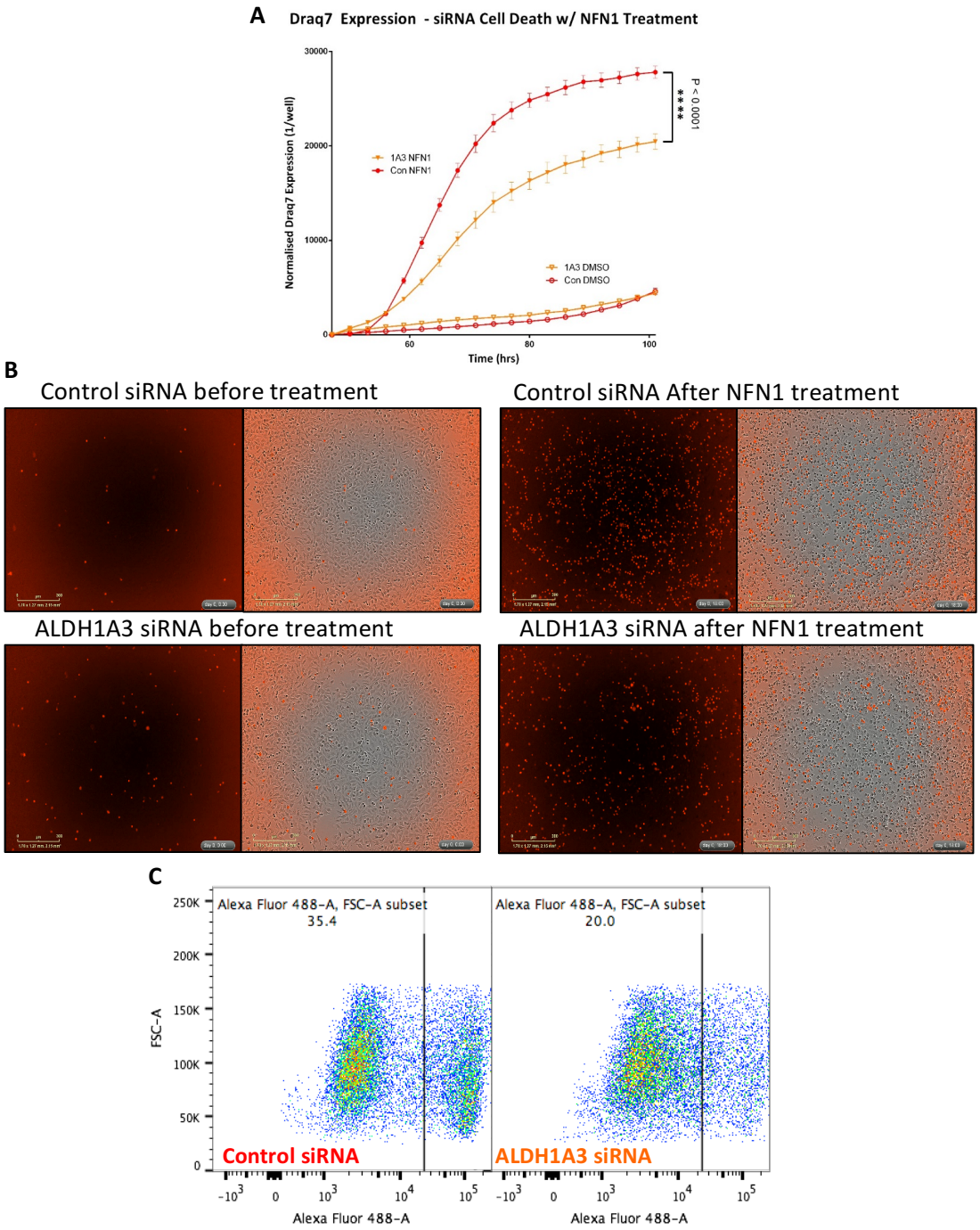

Figure 4.12: Effect of ALDH1A3 knock-down had A375 melanoma cell death upon treatment with **NFN1** (3µM). **A**) Expression of cell death stain, Draq7 (Ex: 633nm, Em: 599nm), of ALDH1A3 A375 melanoma cells (orange) compared to scrambled control siRNA A375 cells upon **NFN1** treatment or 1% DMSO (vehicle). NFN1 treatment results in sizable increase in cell death, however ALDH1A3 knock-down had significantly lower Draq7 expression compared to control siRNA cells ($P < 0.0001$: t-test). Cells treated with DMSO had low levels of Draq7 throughout (n=3). **B**) IncuCyte ZOOM® stills of ALDH1A3 knock-down and control siRNA A375 cells showing Draq7 expression and Draq7-Phase merge. Images are pre- and 12-hours post **NFN1** treatment. ALDH1A3 knock-down has

noticeably lower Draq7 protection and less cell death after **NFN1** treatment compared to control siRNA cells. Draq7 and cell death prior to treatment was low and consistent in both cells. **C**) AnnexinV, an early apoptotic marker stain, expression (Ex: 495nm, Em: 519nm) of ALDH1A3 knock-down A375 cells compared to control siRNA cells upon **NFN1** treatment. AnnexinV expression was recorded by flow cytometry and analysed using FlowJo software. ALDH1A3 knock-down had reduced AnnexinV expression upon **NFN1** Treatment (ALDH1A3 20% vs Control 35.4%) and a notable reduction of the AnnexinV$^+$ population, visibly present in control siRNA cells (n=2).

4.5 Overexpression of ALDH1A3 sensitises melanoma cells to 5-nitrofurans

If ALDH1A3 knock-down provides protection against 5-NFN toxicity in a subpopulation of A375 melanoma cells, I hypothesized that increasing (overexpressing) ALDH1A3 expression in the total cell population should hypersensitise this A375 cells to 5-NFNs.

4.5.1 Efficiency of overexpression

Overexpression of ALDH1A3 in A375 melanoma cells were produced through transient transfection of human cDNA clones. The empty vector (EV), pCMV6-XL4, was used in parallel as a control throughout. ALDH1A3 overexpression in A375 cells was confirmed by western blot (**Figure 4.13A**), leading to a 42.4% increase in ALDH1A3 expression. ALDH1A3 overexpression was also confirmed by the Aldefluor™ assay (**Figure 4.13B**) where Aldefluor™ intensity increased 3-fold from empty vector control and WT cells. Visually, both ALDH1A3 overexpressing and empty vector control A375 cells appeared normal in shape and size, compared to WT A375 cells (**Figure 4.13C-E**).

ALDH1A3 overexpression in A375 cells did have an effect on cellular proliferation. Proliferation of transiently-transfected A375 cells was monitored using IncuCyte™ NucLight™ Green BacMam 3.0 reagent, which enables expression of nuclear-restricted GFP (Excitation: 400nm, Emission: 509nm). Proliferation was recorded by nuclei count and analysed by IncuCyte ZOOM®. Proliferation was much slower in the ALDH1A3 overexpressing cells compared to empty vector control cells (**Figure 4.13F**). It appeared the process of transiently-transfecting A375 cells could directly affect proliferation, with empty vector control cells growing slower than the untreated WT control, however, ALDH1A3 overexpression exacerbated this phenotype.

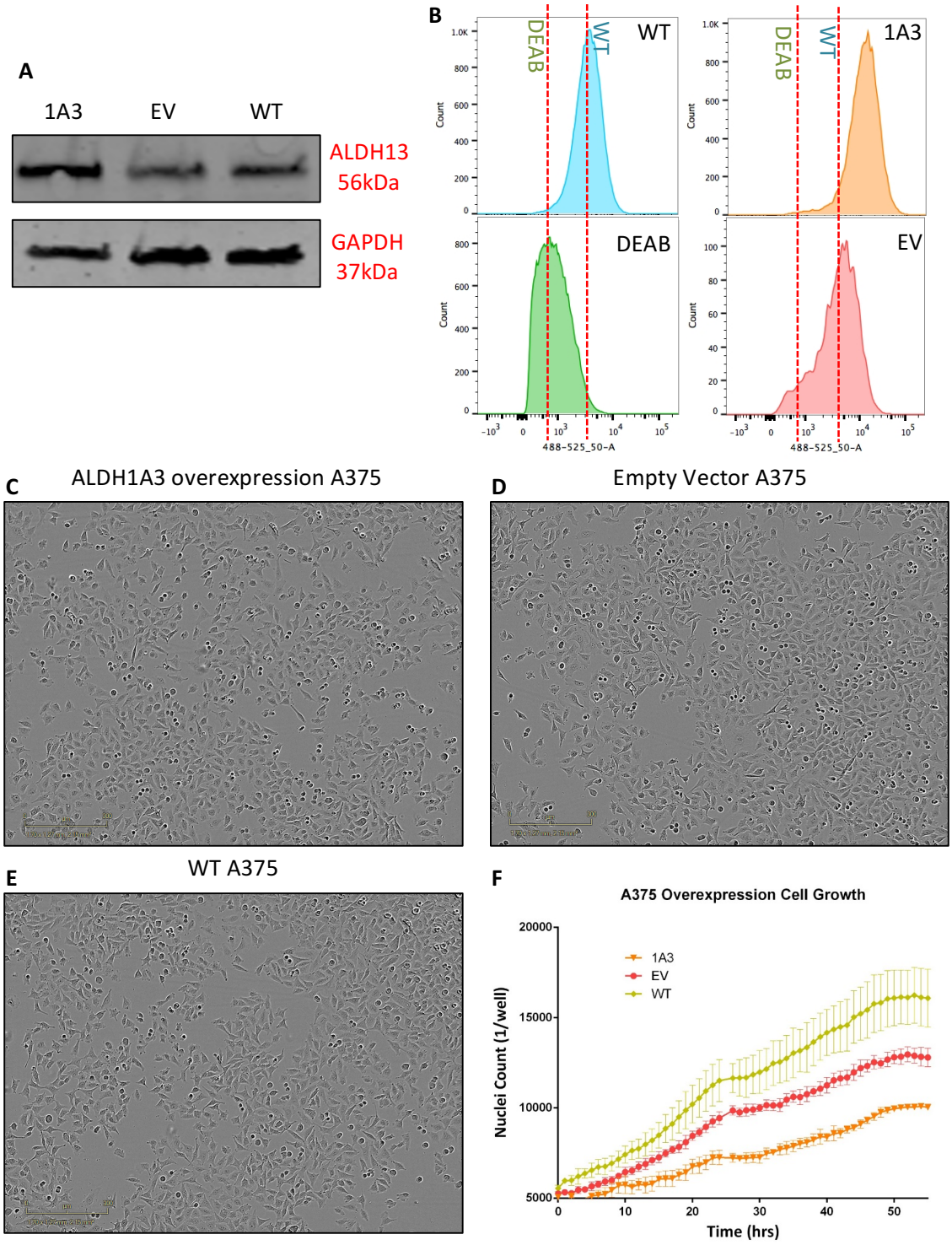

Figure 4.13: Efficiency and characterisation ALDH1A3 overexpression by transient transfections of cDNA in A375 melanoma cells. **A**) Western blot of ALDH1A3 overexpression A375 cells against empty vector (EV) control and WT A375 cells. GAPDH expression was used as a loading control. ALDH1A3 cDNA transfection led to a 42.4% increase in ALDH expression. Treatment with empty vector control led to no alteration in ALDH expression. **B**) Aldefluor™ activity of ALDH1A3 (orange) overexpression in A375 cells against empty vector control (red) and WT (blue) A375 cells. DEAB (green) was used as

a negative control. ALDH1A3 overexpression led to a 3-fold increase in Aldefluor™ activity compared to WT. As expected empty vector transient transfection control had no effect on Aldefluor™ activity, although did produce a broader Aldefluor™ activity characteristic. **C-E**) IncuCyte ZOOM® stills of ALDH1A3 overexpressing A375 cells against empty vector control and WT A375 cells respectively during normal growth. Stills were taken 12-hours after transfection. Transfection of both ALDH1A3 and empty vector control appeared to have no effect of cellular visual appearance or behaviour compared to WT A375 cells. **F**) Cell proliferation of ALDH1A3 overexpressing A375 cells (orange) compared to empty vector control (red) and WT (yellow) A375 cells during normal growth. Proliferation was determined by GFP-expressing nuclei count (Ex: 400nm, Em: 509nm). Transient-transfections appeared to slow proliferation, with empty vector control cells growing slower than WT cells. This slowing of proliferation was exacerbated in ALDH1A3 overexpressing A375 cells.

4.5.2 ALDH1A3 overexpression significantly reduces cell viability in 5-nitrofuran treated melanoma cells

It was expected that because ALDH1A3 knock-down protected A375 melanoma cells from 5-NFN sensitivity, ALDH1A3 overexpression within the same cells should result in hyper-sensitivity to **NFN1**. Unlike siRNA treated cells, which grew at the same rate, ALDH1A3 overexpressing A375 cells grew much slower compared to empty vector control cells. As such, cell viability (i.e. the ratio of live to dead cells) was assessed upon **NFN1** treatment rather than looking at changes in cell growth as before. Cell viability was assessed using Muse™ count and viability reagent, where live and dead cells are differentially stained based on their permeability to the DNA-binding dyes in the reagent. Cell viability of transiently transfected A375 cells was analysed using Muse® Cell Analyser. Cells were trypsinised and treated with the Muse® Cell viability Live/Dead marker before being subjected to Muse® Cell Viability Cell Analysis. ALDH1A3 overexpression significantly hyper-sensitised the A375 cells to **NFN1** toxicity, compared to empty vector control (**Figure 4.14A**, $P < 0.001$). ALDH1A3 overexpression led to 63.8% reduction in cell viability upon **NFN1** treatment, compared to 20.3% seen in the empty vector control. Empty vector cells also had reduced viability compared to WT cells (EV 20.3% reduction vs WT 10.0% reduction) however this was not significant ($P = 0.147$). Cell viability remained unchanged across each condition upon DMSO treatment. This was further confirmed visually, where

images of the adhered transiently transfected A375 cells (**Figure 4.14B**) show clear increase in cell death with ALDH1A3 overexpression compared to empty vector control. The ALDH1A3 overexpressing A375 cells do appear slightly altered in morphology compared to empty vector control cells, where they're slightly elongated, possibly an indication of stress. It could be argued that ALDH1A3 overexpressing A375 cells are more prone to cell death when looking at cell viability, where there is a slight decrease in vehicle (1% DMSO) treated cell viability, though this was not significant (P = 0.1271). However, this shows that increased expression of ALDH1A3 hyper-sensitises A375 cells towards 5-NFNs. This provides a clear correlation, mirroring the siRNA data, where 5-NFN toxicity in A375 melanoma cells is primarily driven by ALDH1A3 expression.

As the previous transient transfection protocol was showing signs of toxicity, through decrease of cell growth, the methodology was altered and the QIAGEN Attractene Transfection assay was used, which was less toxic to A375 melanoma cells. Cells displayed a very clean ALDH1A3 overexpression by Western (**Figure 4.15A**) and displayed significantly less toxicity, providing an ideal transfection protocol to do prolonged cell viability studies. The sensitivity of A375 cells transiently transfected to overexpress ALDH1A3 was determined using cell viability against **NFN1**, in comparison to A375 melanoma cells transiently transfected with pCMV6-XL4 empty vector (**Figure 4.15B**). ALDH1A3 overexpression hypersensitised the A375 cells to **NFN1** (EC_{50} = 584nM ttALDH1A3 vs EC_{50} = 1.15μM EV Control). This correlated to results of the Muse® cell viability assay (**Figure 4.14**), which also displayed hypersensitivity of cells at a non-lethal dose of **NFN1**. This further gives evidence that ALDH1A3 can drive 5-NFN toxicity in cells, and suggests that the $ALDH1A3^{high}$ subpopulation in A375 melanoma cells should therefore be more sensitive to 5-NFNs.

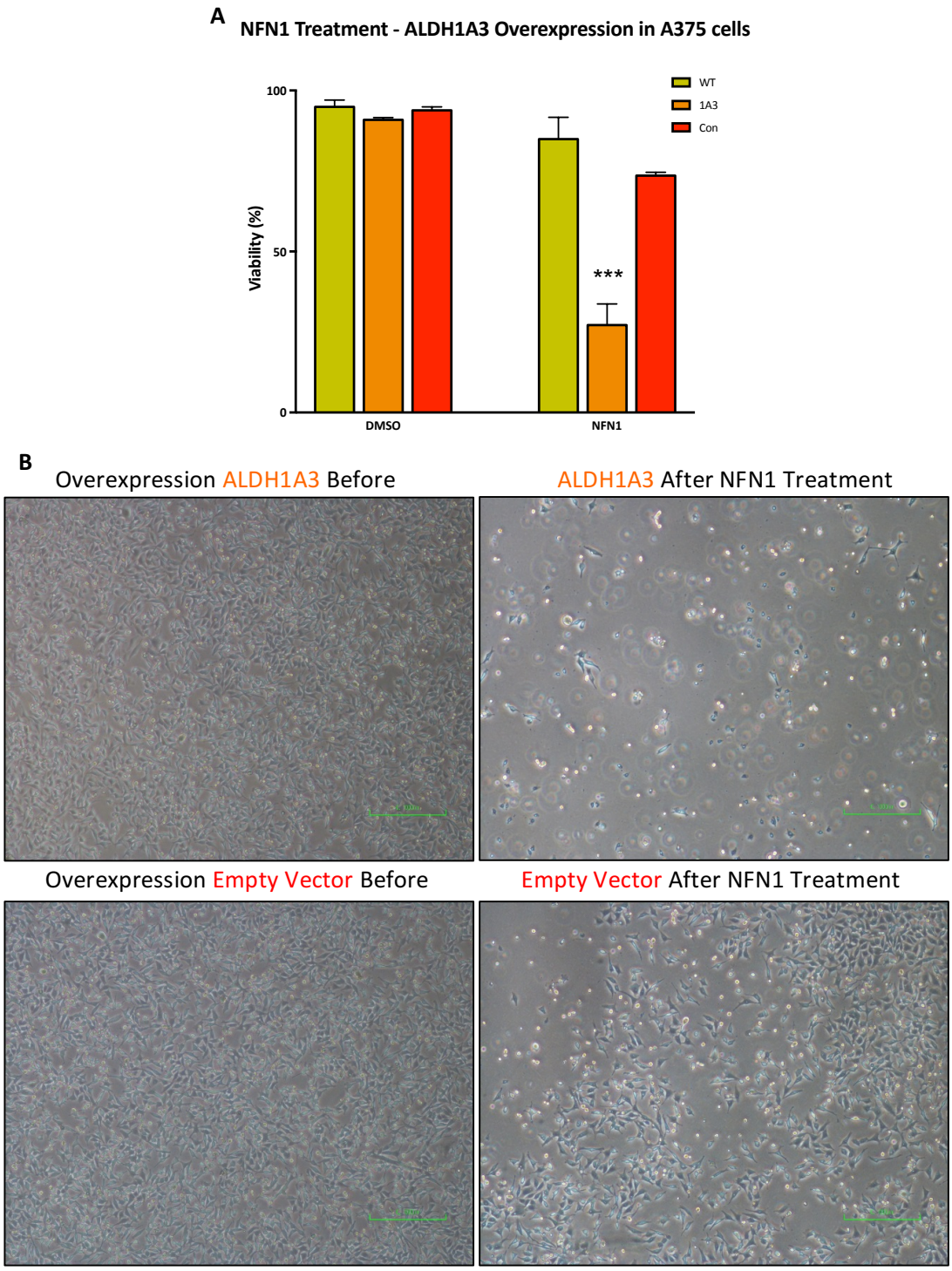

Figure 4.14: Effect of cell viability on ALDH1A3 overexpression A375 melanoma cells upon non-lethal dose (500nM) of **NFN1** (n=2). **A**) Cell viability of ALDH1A3 overexpressing A375 cells (orange) compared to empty vector (EV) control (red) and WT A375 cells (yellow) upon treatment with **NFN1** or 1% DMSO (vehicle). Cell viability is represented as percentage viable cells vs non-viable cells. **NFN1** treatment caused a significant reduction in cell viability in ALDH1A3 overexpression cells compared to empty vector and WT cells ($P < 0.001$: ANOVA), where 63.8% reduction in cell viability is

seen in the ALDH1A3 overexpressing cells compared to 20.3% in empty vector cells. Empty vector cells had reduced viability compared to WT also (EV 20.3% vs WT 10.0%) however this was not significant (P = 0.147) Cell viability remained unchanged between all 3 cells upon DMSO treatment. **B**) Photographs (10x magnification) of adhered ALDH1A3 overexpressing A375 melanoma cells compared to adhered empty vector control A375 cells pre- and 24-hours post **NFN1** treatment. ALDH1A3 overexpressing cells had drastically less adhered cells and more cell death compared to empty vector cells. Cells were of equal confluence and exhibited normal characteristics prior to treatment.

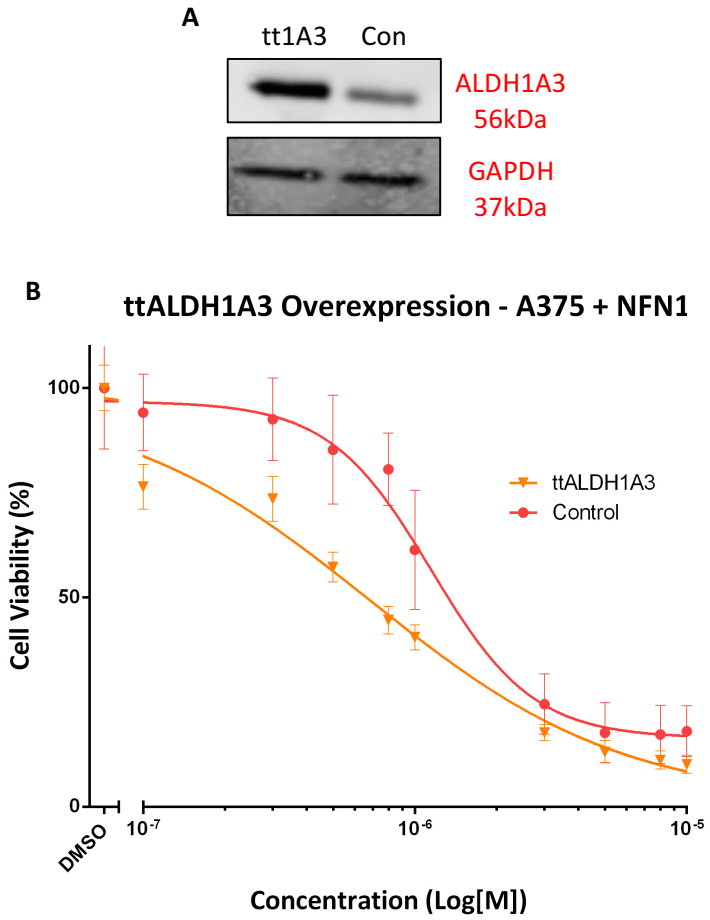

Figure 4.15: A375 melanoma cells overexpressing ALDH1A3 by transient transfection are hypersensitive to **NFN1** by cell viability. **A**) Western blot of ALDH1A3 overexpression A375 cells against empty vector (EV) control. GAPDH expression was used as a loading control. ALDH1A3 cDNA transfection led to a 136% increase in ALDH1A3 expression compared to empty vector control. **B**) Cell viability assays upon **NFN1** treatment over 24hrs, EC_{50} values determined by PrestoBlue™ treatment and normalised to vehicle (1% DMSO) control. A375 melanoma cells overexpressing ALDH1A3 by transient transfection (ttALDH1A3 – orange) were more sensitive to **NFN1** compared to A375 empty vector transfected cells (Control – red). EC_{50} = 584nM, ttALDH1A3 vs EC_{50} = 1.15μM, Control (n=3).

4.6 Conclusion

Here I demonstrate that 5-NFNs are cytotoxic in a small panel of cancer cell lines, including the A375 melanoma cell lines. The heterogeneity of ALDH1 expression in melanoma, including A375 cells, offered an explanation for why no correlation between 5-NFN sensitivity and ALDH1 expression, either by Aldefluor™ or RNA_{seq}, was observed. ALDH1A3 has previously been described as a CSC marker in the A375 melanoma cell line,[79] so I hypothesised that ALDH1A3 was driving 5-NFN sensitivity in a subpopulation of A375 cells and consequently, the sensitivity of the $ALDH1A3^{high}$ A375 melanoma subpopulation to 5-NFNs was explored. Knock-down of ALDH1A3 by siRNA invoked resistance of A375 melanoma cells to 5-NFN toxicity, and in contrast, ALDH1A3 overexpression induced hypersensitivity to 5-NFNs. Displayed in **Figure 4.16**, I highlight ALDH1A3 is driving 5-NFN toxicity in a subpopulation of A375 melanoma cells, in a total A375 cell population heterogeneous for ALDH1 expression. Finally, I describe how ALDH1A3 is the essential ALDH isoform driving Aldefluor™ activity in the A375 melanoma cell line.

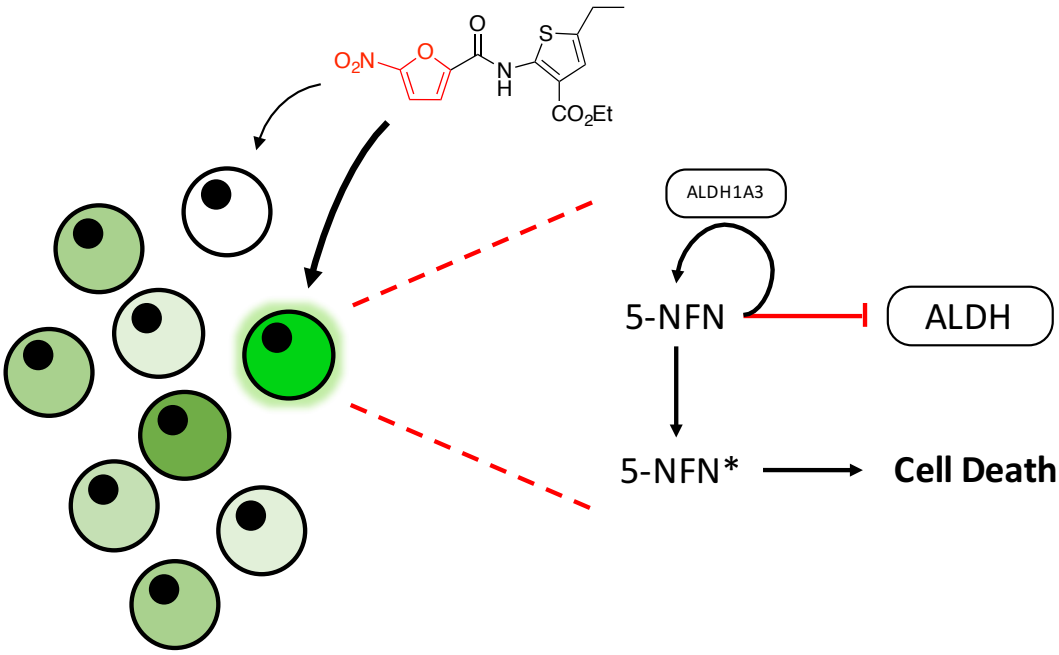

Figure 4.16: Schematic describing the mechanism of 5-NFN toxicity in the A375 melanoma cells. A375 cells are heterogeneous for ALDH1 expression, as described by Aldefluor™. 5-NFN are competitive substrates for ALDH1A3, determined *in vitro* and by Aldefluor™, where 5-NFNs are bio-activated in a subpopulation of cells by ALDH1A3 to drive melanoma cell death. Manipulating the expression of ALDH1A3 expression in A375 cells correlates with sensitivity to 5-NFN, suggesting ALDH1A3 is a key driver of 5-NFN in this subpopulation.

Chapter 5

Clinical and new synthetic 5-nitrofurans

5.1 Introduction

The anti-cancer activity of clinical 5-NFNs in patients has been previously reported,[126,131] with nifurtimox (**NFX**), an anti-parasitical 5-NFN pro-drug, currently in phase 2 clinical trials for the treatment of neuroblastoma and medulablastoma (ClinicalTrials.gov Identifier: NCT00601003). Previous to this trial, Sholler and her team demonstrated that **NFX** can induce apoptosis in neuroblastoma cells and inhibit growth of neuroblastoma xenographs *in vivo*, where an increase of ROS formation is a likely driver of this phenotype.[132] This is shared in the treatment of medulloblastoma cells with **NFX** also, where cells treated with **NFX** upregulated HMOX1, GCLM, SLC7A11 and SRXN1 - all genes associated with oxidative stress, where use of the anti-oxidant, N-acetyl-L-cysteine, rescued medulloblastoma cells from **NFX** induced apoptosis.[112] The exact target of **NFX** in cancer, and consequently the mechanism in which this can mediate ROS accumulation, is currently unclear. Considering previous work using the tool 5-NFN compound, **NFN1**, from our lab[115] and in my previous chapters, the anti-cancer activity and production of ROS species is driven by bio-activation of 5-NFNs by ALDH enzymes *in vivo* and *in vitro*. Many ALDH isoforms are expressed in the brain,[2] however ALDH1A1 is highly regulated in dopaminergic neurons, as retinoic acid (RA) plays a crucial role in development of these neurons, and decreased RA and/or ALDH1A1 is seen in patients with Parkinson's disease.[171,172] ALDH1A1 may also have a role in metabolising levels of the toxic dopaminergic aldehyde, 3,4-dihydroxyphenylacetaldehyde (DOPAL).[172] ALDH9A1 is also highly expressed in the brain, likely due to its high affinity for DOPAL, but is also essential in the alternative biosynthesis of GABA, and as such has an important role in brain development.[2] ALDH also plays an important part in the pathogenesis of brain tumours.[40] ALDH2 is essential in dopaminergic neurons, where it has been reported that cocaine-induced dopamine release can be suppressed in rats upon selective ALDH2 inhibition, suggesting an important functional role for ALDH2 in the synthesis of dopamine.[173] In neuroblastoma cells, ALDH1A2, ALDH1L1 and ALDH3B2 are highly upregulated, where ALDH1A2 specifically is shown to be essential in sphere and colony formation, tumorigenesis, and triggering resistance to RA treatment.[42] This tumorigenic potential has also been described in the $ALDH^+$ subpopulation in a variety of brain cancers, including medulloblastoma,[40] where ALDH expression has further been linked to cyclophosphamide resistance in medulloblastoma cell lines also.[174] Considering the importance for ALDH expression in the dopaminergic pathway of normal and cancerous

brain tissues, coupled with the sensitivity of neuroblastoma, medulloblastoma, and other neural cancers to **NFX**,[112,132,133] I hypothesise that the anti-cancer activity reported with **NFX** being is mediated by ALDH-driven bio-activation. This is also supported by data showing that dopamine-dependant catecholaminergic neurons are more sensitive to **NFX**,[132] which is likely due to the higher expression of ALDH needed in the dopaminergic pathway. It is thus logical to assume that other clinical 5-NFNs may also be substrates for ALDH enzymes and show prominent anti-cancer activity, considering the high ALDH expression found in melanoma CSCs.[79,151] It is an interesting area to explore both for the anti-cancer potential of current clinical 5-NFNs, but also to design new, synthetic 5-NFNs as novel lead compounds in the efforts to discover and develop new and effective cancer therapeutics.

In this chapter, my aim is to identify those clinically available 5-NFNs that are substrates for ALDH enzymes, and as such exhibit potent anti-cancer activity, and to develop new, synthetic 5-NFN molecules that are efficient ALDH substrates. Here, I compare **NFX** and **NAZ**, and demonstrate that **NAZ**, a clinical compound used primarily as a livestock antibiotic, displays promising anti-cancer activity and some selectivity for ALDH1 enzymes. Further, through the development of *bis*-5-NFN derivatives, I describe novel 5-NFNs with two active moieties per molecule, increasing drug efficiency, i.e. a 'double hit'. These benzene-linked *para-bis*-5-NFN compound have strong anti-cancer and ALDH-targeting characteristics, and provide a solid foundation when developing more bis-5-NFN compounds as anti-cancer therapeutics.

5.2 Clinical leads

Unless stated otherwise, the following work in this section was performed by a visiting Honours student to the lab, Nathalie M. Spockeli, under my direct supervision.

5.2.1 Nifurtimox anti-cancer activity is not as effective in melanoma cells

The work in the following section was conducted by myself.

The anti-cancer activity of the clinical 5-NFN, nifurtimox (**NFX**), has previously been described in neuroblastoma,[126,131,132] and phase 2 clinical trials for the treatment of neuroblastoma and medulablastoma with **NFX** in patients under 21 is showing promising results in clinical trials (ClinicalTrials.gov Identifier: NCT00601003), however the mechanism underlying this anti-cancer activity in unknown. I hypothesise that the anti-cancer properties seen in both neuroblastoma and medulloblastoma are derived from bio-activation by ALDH enzymes,[115] and as such, should also present similar properties in other cancer cell lines with ALDH expression, such as melanoma.[79,151]

To determine the anti-cancer activity of **NFX** in A375 melanoma cells, a cell viability assay was set up as before. A375 cells were treated with **NFX**, **NFN1**, **NFN1.1** and vehicle (0.1% DMSO). Although **NFX** has proven effective against neuroblastoma in clinic, this was not represented in A375 cells (**Figure 5.1A**). **NFX** did not converge to determine an exact EC_{50} value, however was approximated at 103.1µM, 100-fold less potent that **NFN1** (EC_{50} = 1.01µM). Although the potency of the anti-cancer activity of **NFX** was low, I wanted to test if **NFX** was still effective at inhibiting ALDH activity in cells. To assess this, A375 cells treated with **NFX** were subjected to the Aldefluor™ assay. Cells treated with DEAB for 2hrs were used as a negative control and samples compared against vehicle (1% DMSO) control. **NFX** treatment led to a minor reduction in Aldefluor™ activity (18.3% reduction) 24hrs post treatment (**Figure 5.1B**). This indicates that ALDH enzymes are a target for **NFX**, however the affinity is low. This was further shown by determining the affinity of **NFX** towards ALDH2-His. ALDH2-His *in vitro* activity assay was set up as before, treated with a logarithmic dose of **NFX**. Daidzin and vehicle (1% DMSO) were used as controls. **NFX** treatment has quite a low affinity for ALDH2-His (IC_{50} = 80.9µM, **Figure 5.1C**) where only at the highest

dose (100µM) was any notable reduction of ALDH activity seen, although this was not significant (P = 0.0506). The PK of **NFX** is considerably poor (C_{max} = 4.8µg/ml in serum) and as such it is administered in much higher doses for treatment of neuroblastoma (30mg/kg/day),[126] which may also help overcome its low affinity towards ALDH2.

Although **NFX** does present some anti-cancer activity, which is likely driven by its weak interaction with ALDH enzymes in the A375 melanoma cell line, it is still considerably less active than the tool compound, **NFN1**. As the use of 5-NFNs as anti-cancer therapeutics continues, it will become increasingly important to discover and development new 5-NFNs with improved anti-cancer activity, ALDH affinity and PK. As such, there is potential for other 5-NFNs, both clinically available and newly synthetic, to be identified as potential treatments for cancer, with improved efficacy compared to the promising results already reported with **NFX**.[126,131]

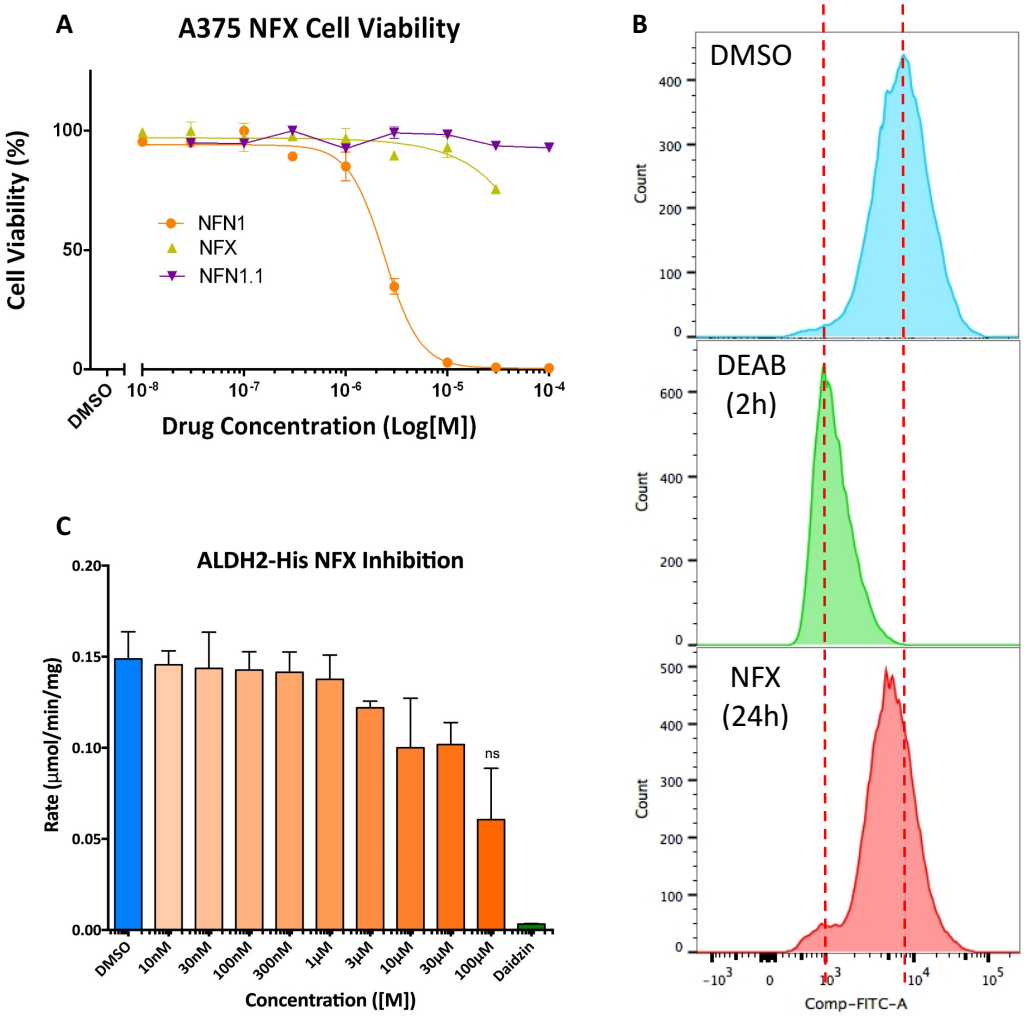

Figure 5.1: Lack of efficacy of **NFX** in melanoma is likely due to reduced efficiency in targeting ALDH (n=2). **A**) A375 melanoma cell viability assay upon **NFX** (yellow), **NFN1** (orange**)** or **NFN1.1** (purple) treatment over 96hours, EC_{50} values determined by PrestoBlue™ treatment and normalised to vehicle (1% DMSO) control. **NFX** did not converge past 50%, so an estimated EC_{50} = 103.1µM was determined. **NFN1** EC_{50} = 1.01µM. **B**) Aldefluor™ activity of A375 cells treated with **NFX** (red) for 24hours. Vehicle (1% DMSO, blue) and 2hrs DEAB (green) was used as positive and negative controls. **NFX** treatment led to a 18.3% reduction in Aldefluor activity in A375 cells. **C**) ALDH2-His activity against **NFX** (orange) treated over a logarithmic dose range against DMSO (blue) and daidzin (green). Enzymatic rate determined using initial linear rate of NAD^+ to NADH turnover at λ = 340nm (ε = 6220$M^{-1}cm^{-1}$), upon acetaldehyde initiation. ALDH2-His activity was reduced upon 100µM **NFX** treatment, however this was not significant (p = 0.0506). **NFX** IC_{50} = 88.1µM.

5.2.2 Nifuoxazide highlighted for promising anti-cancer activity from a screen of clinical 5-nitrofurans

As 5-NFNs are not novel compounds, with many already being available clinically, it was predicted that some, if not all, clinical 5-NFNs would be active against ALDH and have some degree of anti-cancer activity, such as **NFX**. As shown previously in this chapter and work from Dr Saulnier Sholler,[112,126,131,132] **NFX** is an effective anti-cancer agent, however there is much room for improvement when you compare experimental data of **NFX** to **NFN1**. To explore whether other clinical 5-NFNs may show promising anti-cancer activity, a small screen of clinical 5-NFNs was set up against the A375 melanoma cell line and potency compared against **NFN1** and **NFX**. Cell viability assays were set up as before, with a logarithmic dose of each clinical drug, Nifurtimox (**NFX**), Nifuroxazide (**NAZ**), Nitrofurantoin (**NFT**) and Furazolidone (**FURA**) (**Figure 5.2A-D**) in series with **NFN1** against a vehicle (0.1% DMSO) control. **NAZ** is used in the treatment of diarrhoea and colitis in humans administered orally at 400mg/day,[175] however **NAZ** is more commonly used as a feed additive in livestock, and the only 5-NFNs still approved by the FDA to do so. However, there are growing concerns over the safety **NAZ** in the bulk treatment of livestock, considering that **NAZ**, and its potentially carcinogenic metabolites, have been detected in chicken meat up to 7days post-treatment.[176] **NFT** is a WHO essential medicine as a basic health medicine for the treatment of UTIs.[121] **NFT** is one of the most widely prescribed 5-NFNs, along with **NFX**, typically given in doses at 5-7mg/kg/day, however is also plagued with several adverse and toxic side effects, with hospitalization and fatalities from treatment also reported.[177] **FURA** is broad spectrum anti-biotic and anti-parasitical, used in both veterinary and human medicine, however amid safety concerns that **FURA** may be carcinogenic to humans, through cross-contamination of residues in livestock,[178] it is consequently banned for use in the treatment of livestock (NB. The use of **FURA** is banned completely in the US, where the prescription of **FURA** as an antibiotic for both human and veterinary use was banned in 2005). **FURA**, however, is and continues to be an efficacious treatment for childhood cholera, where a dose of 7mg/kg/day is usually prescribed and only results in minor side-effects.[179] Interestingly **FURA** is reported to mediate cell death in HepG2 liver cancer cells through DNA damage and ROS production.[180]

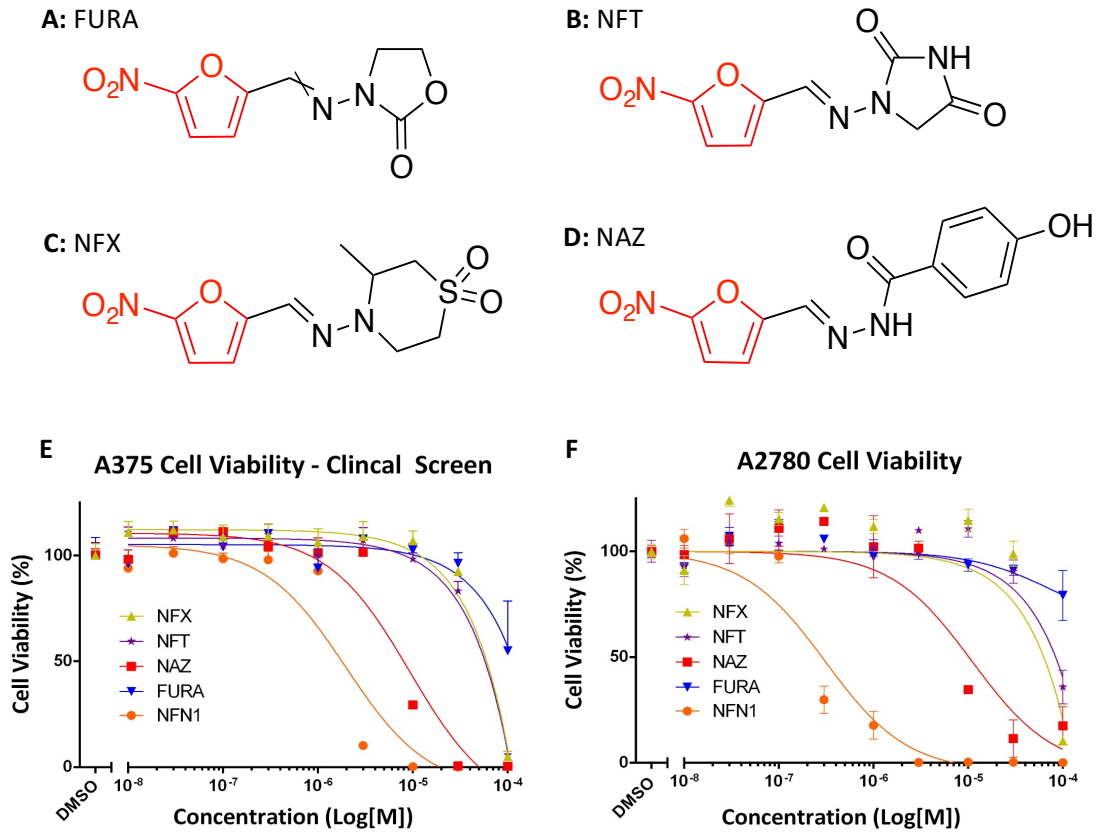

G

Drug	$EC_{(50)}$ (A375)	$EC_{(50)}$ A2780
Nifurtimox (NFX)	82.9µM	77.8µM
Nitrofurantoin (NFT)	78.2µM	97.2µM
Nifuroxazide (NAZ)	9.78µM	8.63µM
Furazolidone (FURA)	N/A	N/A
NFN1	1.03µM	241nM

Figure 5.2: Screen of clinical 5-NFNs for anti-cancer activity. **A-D**) Molecular structures of Furazolidone (**FURA**), Nitrofurantoin (**NFT**), Nifurtimox (**NFX**) and Nifuroxazide (**NAZ**) respectively. The 5-nitrofuran moiety is highlighted in red. **E**,**F**) Cell viability assay of A375 melanoma cells and A2780 ovarian cells respectively upon **NFX** (yellow), **NFT** (purple), **NAZ** (red) or **FURA** (blue) against **NFN1** (orange) treatment over 96hours, EC_{50} values determined by PrestoBlue™ treatment and normalised to vehicle (1% DMSO) control. EC_{50} values for each drug in both A375 and A2780 cells are displayed in **Table G**. All drugs showed some degree of anti-cancer activity, however **NAZ** treatment resulted in EC_{50} values approximately 10-fold less than **NFN1** however 10-fold more sensitive than **NFX**.

We tested all the stated clinical 5-NFN compounds on A375 melanoma cell growth, and found that all clinical compounds had some degree of anti-cancer activity (**Figure 5.2E**), however **NAZ** was the only compound to show substantial toxicity in A375 cells (EC_{50} = 9.78μM), approximately 10-fold less potent than **NFN1**. The other clinical compounds, although showing toxicity in A375 cells at much higher doses, did not show any notable improvement in comparison to **NFX** (**NFX** EC_{50} = 82.9μM, **NFT** EC_{50} = 78.2μM and **FURA** EC_{50} = Did not converge). Similar results were seen when the same cell viability screen was conducted on a second cell line, the A2780 ovarian cell line (**Figure 5.2F**),[39] where **NAZ** was the obvious candidate to take forward (EC_{50} = 8.63μM) with **NFX** still inadequate in comparison (EC_{50} = 88.8μM).

Although the anti-cancer activity of **NFX** has already been described,[112,126,131,132] this was not reflected in the A375 melanoma or the A2780 ovarian cell lines. ALDH1A2 is highly expressed in neuroblastoma CSCs,[42] where the affinity of ALDH1A2 towards 5-NFNs could be greater than ALDH1A3, as seen in melanoma,[79] or ALDH1A1 in ovarian cancer.[39] Perhaps the way 5-NFNs behave clinically differs from in culture also, where targeting the $ALDH^{high}$ population in solid tumours is driving regression, which is difficult to mimic in culture alone. **NAZ** was selected as a lead clinical compound going forward due to its improved potency in A375 melanoma cells compared to **NFX**. It could also be likely that **NAZ** can more readily permeate across the melanoma cell membrane than **NFX**, to drive this increased toxicity. Similarly, it could also be the opposite effect, where NFX could more readily be effluxed from the melanoma cell compared to **NAZ**, leading to why **NAZ** is more potent than **NFX**. Regardless, it is clear that **NAZ** presents major improvement in therapeutic potential for treatment of melanoma compared to **NFX**.

5.2.3 Nifuroxazide exhibits promising anti-cancer activity in cancer cell lines

The anti-cancer activity of **NAZ** was assessed in comparison to **NFN1** on the same 3 cells lines as previous: A375 melanoma cells, A2780 ovarian cells and HCT116 colorectal cells. **NAZ**, **NFN1** and **NFN1.1** was treated on a logarithmic dose curve and vehicle (1% DMSO) was used as a control. Although **NAZ** was markedly less potent than **NFN1**, **NAZ** exhibited toxicity in all 3 cell lines (**Figure 5.3A-C**). The degree of difference between **NFN1** and **NAZ** was not consistent however. Where **NAZ** is 30-fold less potent than **NFN1** in A2780 ovarian

cells (EC_{50} = 8.54µM **NAZ** vs EC_{50} = 275nM **NFN1**), it is only 10 fold less in A375 melanoma cells (EC_{50} = 9.55µM **NAZ** vs EC_{50} = 1.04µM **NFN1**) and 3-fold less potent than **NFN1** in HCT116 colorectal lines (EC_{50} = 3.91µM **NAZ** vs EC_{50} = 1.31µM **NFN1**). This gives some indication that different ALDH enzymes may bio-activate **NFN1** and **NAZ**, and the differing affinities these two 5-NFNs have for each target. This can be further explained by differing ALDH expression profile between these 3 cell lines, that may consequently influence their sensitivity to both **NFN1** and **NAZ**, and as such, allude to the variability between sensitivity differences between these 2 compounds.

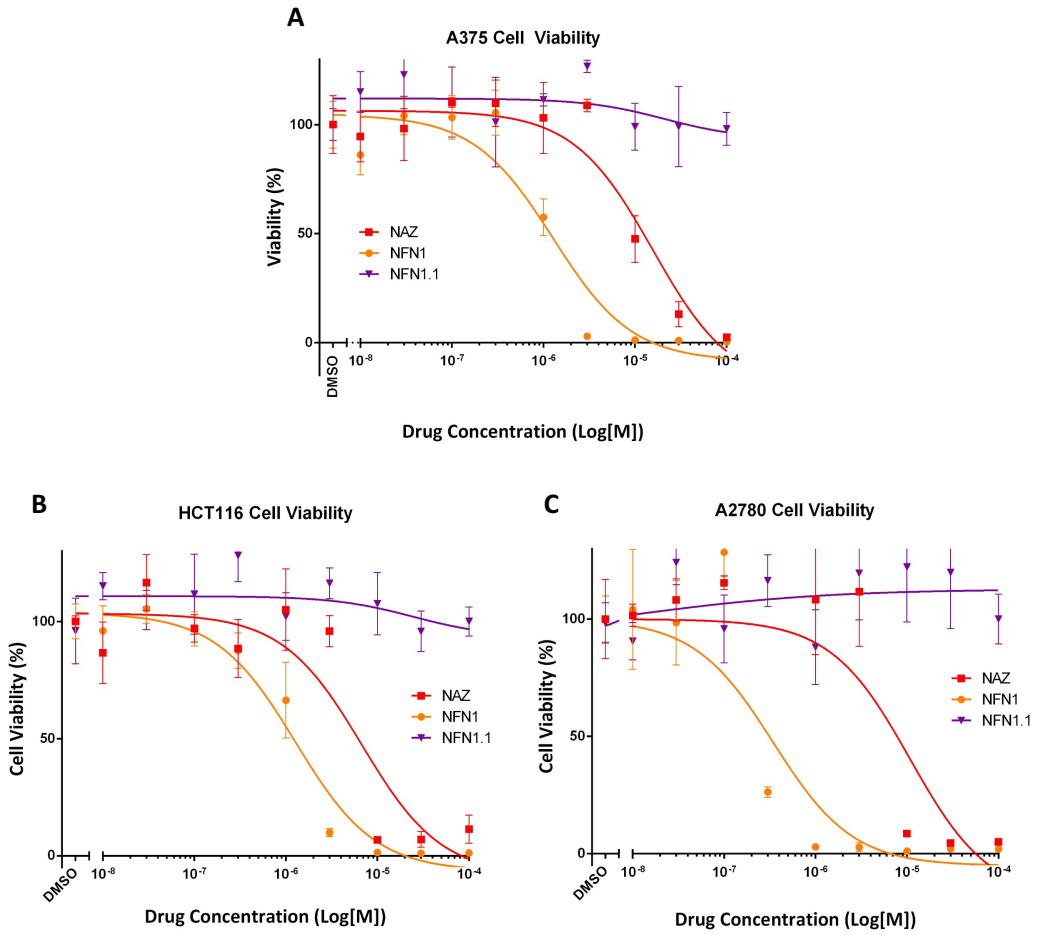

Figure 5.3: Cell viability assays upon **NAZ** (red) treatment against **NFN1** (orange) or **NFN1.1** (purple) treatment over 96hours, EC_{50} values determined by PrestoBlue™ treatment and normalised to vehicle (1% DMSO) control **A**) A375 melanoma cell viability. **NAZ** EC_{50} = 9.55µM vs **NFN1** EC_{50} = 1.04µM **B**) HCT116 colorectal cell viability. **NAZ** EC_{50} = 3.91µM vs **NFN1** EC_{50} = 1.31µM. **C**) A2780 ovarian cell viability. **NAZ** EC_{50} = 8.54µM vs **NFN1** EC_{50} = 275nM. **NFN1.1** treatment had no effect of cell viability in all 3 cell lines.

5.2.4 Nifuroxazide in a competitive substrate for ALDH in A375 melanoma cells

The treatment of A375 melanoma cells with **NFN1** led to a reduction in ALDH activity, seen through prolonged, potent reduction in Aldefluor™ activity. Should NAZ be targeting ALDH enzymes in A375 cells, a similar reduction in Aldefluor™ activity is expected to be observed. A375 cells were subjected to the Aldefluor™ assay 24hrs after treatment with **NAZ**. The dose of **NAZ** used was 10-fold more concentrated than in the **NFN1** assay to reflect the 10-fold reduction in potency seen with **NAZ** compared to **NFN1** in A375 cells. Cells treated with DEAB for 2hrs were used as a negative control and samples compared against vehicle (1% DMSO) control. **NAZ** treatment of A375 melanoma cells resulted in a 42.6% reduction of Aldefluor™ activity compared to vehicle control (**Figure 5.4A**). Although **NAZ** treatment didn't reflect the same inhibition of ALDH activity seen after treatment with **NFN1**, it still provided a good basis of a clinical 5-NFN that can target ALDH enzymes in A375 melanoma cells.

The following work below was conducted by myself.

As Aldefluor™ activity is attenuated in A375 melanoma cells by treatment with 5-NFNs during flow cytometry analysis, it should be possible to see visually on adhered cells cultures the same reduction of Aldefluor™ activity, including **NAZ**. A375 melanoma cells treated with **NFN1**, **NAZ** or vehicle (1% DMSO) control, against negative control, DEAB, were assessed for Aldefluor™ activity visually (Ex: 488nm, Em: 525nm). Vehicle treated A375 cells had high Aldefluor™ activity, compared to A375 cells treated with both **NFN1** and **NAZ**, where this expression was dramatically reduced (**Figure 5.4B**). DEAB also had similar reduction in Aldefluor™ activity as expected. This is visual confirmation that the 5-NFNs, **NFN1** and clinical **NAZ**, can both ablate Aldefluor™ activity, and consequently ALDH activity, in A375 melanoma cells. Although this is likely due to a direct inhibition of ALDH enzymes in the cells themselves leading to such a dramatic reduction in Aldefluor™ activity, it could also be possible that the 5-NFNs specifically targeted and eradicated the $ALDH^{high}$ melanoma cells, leaving only the $ALDH^{low}$ cells in the sample. Although both outcomes would be desirable, further work to explore how cells with different ALDH status respond to 5-NFNs, in a whole cell population sample, would be required to conclude the efficacy in which 5-NFNs can target $ALDH^{high}$ melanoma cells.

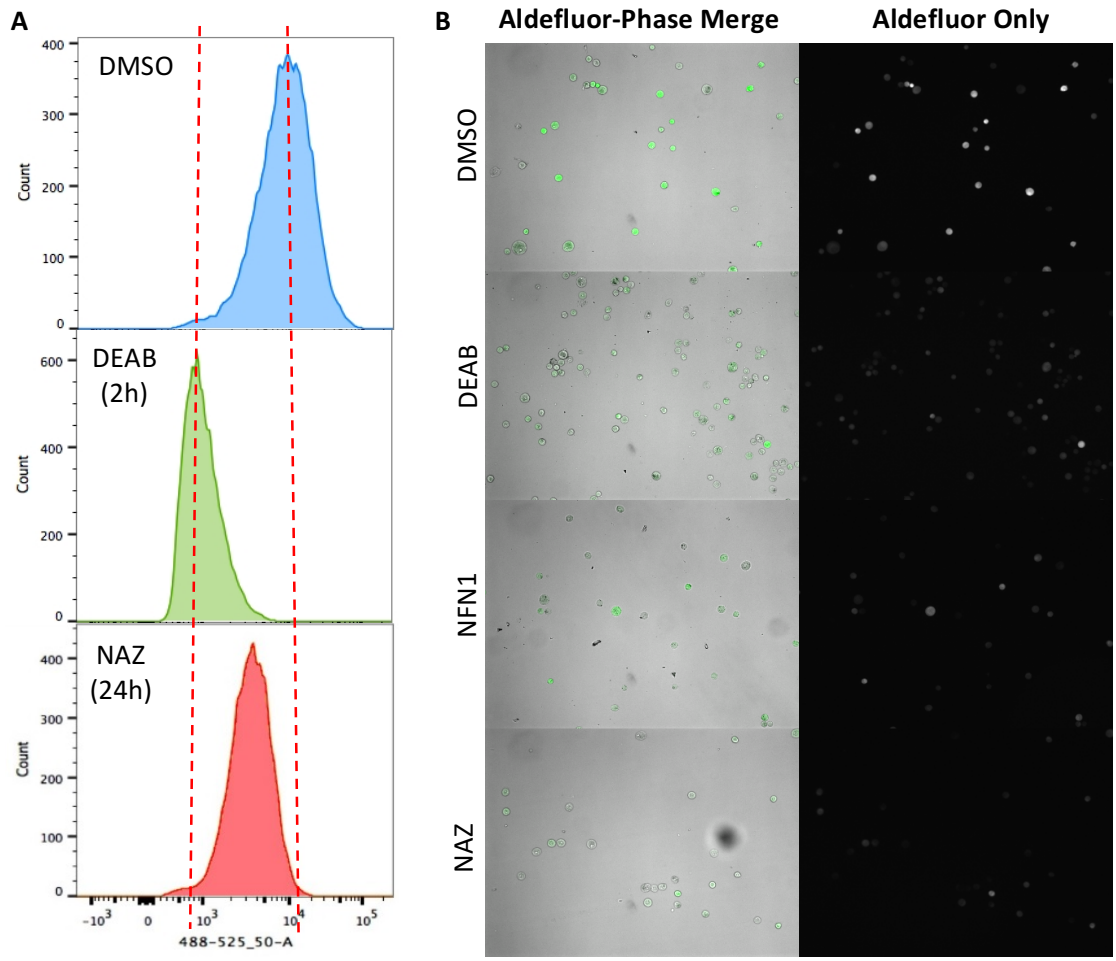

Figure 5.4: Aldefluor™ activity in A375 melanoma cells in response to **NAZ** treatment. **A**) Aldefluor™ activity in A375 cells after 24hrs **NAZ** (red) treatment. DMSO (blue) positive and DEAB (green) negative control treated for 24hrs and 2hrs respectively. **NAZ** reduced Aldefluor™ activity in A375 cells by 42.6% after 24hrs of treatment. DMSO and DEAB treated A375 cells assumed 100% and 0% Aldefluor™ activity respectively (n=2). **B**) Non-adhered A375 melanoma cells treated with **NAZ**, **NFN1** or vehicle (1% DMSO) for 24hrs; DEAB treated for 2hrs used as negative control, stained with Aldefluor™ imaged 10x magnification (Ex: 488nm, Em: 525nm). Treatment with **NAZ**, **NFN1** and DEAB displayed a dramatic reduction in Aldefluor activity in comparison to DMSO control, where high Aldefluor™ activity is seen (n=2).

5.2.5 Nifuroxazide is selective for ALDH1 enzymes over ALDH2

The work in the following section was conducted by myself.

NAZ can reduce Aldefluor™ activity, and consequently ALDH activity, in A375 melanoma cells, so it expected this reduction of ALDH activity should be mirrored *in vitro*. As with **NFN1**, His-tagged ALDH2 was subjected to the *in vitro* activity assay as before, where ALDH2-His was pre-incubated with NAD^+ against a logarithmic dose of **NAZ** prior to acetaldehyde initiation. Present controls were vehicle (1% DMSO) and ALDH2 inhibitor, daidzin. ALDH2-His activity was unaffected by **NAZ** treatment (**Figure 5.5A**), where no reduction of activity was seen at any dose of **NAZ**. This was in contrast to **NFN1**, which saw a high affinity for ALDH2-His (IC_{50} = 63.9nM). However, considering **NAZ** treatment reduced Aldefluor™ activity in A375 cells, this led me to ask whether **NAZ** exhibits some specificity towards ALDH1 over ALDH2.

As shown before, ALDH1A3 activity drives Aldefluor™ activity in A375 cells. Because **NAZ** was able to attenuate Aldefluor™ activity in these cells, this should also be reflected by a reduction in ALDH1A3 activity *in vitro* upon **NAZ** treatment. As before, ALDH1A3 was pre-incubated with NAD^+ and **NAZ** or **NFN1**, prior to acetaldehyde initiation. Activity was monitored against vehicle (1% DMSO) control. **NAZ** and **NFN1** treatment significantly reduced ALDH1A3 activity (**NAZ**: P = 0.017, **NFN1**: P = 0.016; **Figure 5.5B**) where NADH turnover was reduced by 73.9% and 65.5% respectively. Considering this data that **NAZ** is not a competitive substrate for ALDH2, but can reduce ALDH1A3 activity *in vitro*, it provides evidence that **NAZ** has some selectivity towards ALDH1 over other ALDH isoforms. As ALDH1 has been described as a desirable target in recent reports,[35,45,118] it would be a promising discovery to find a potent, clinically approved, anti-cancer therapeutic that is driven by ALDH1 activity.

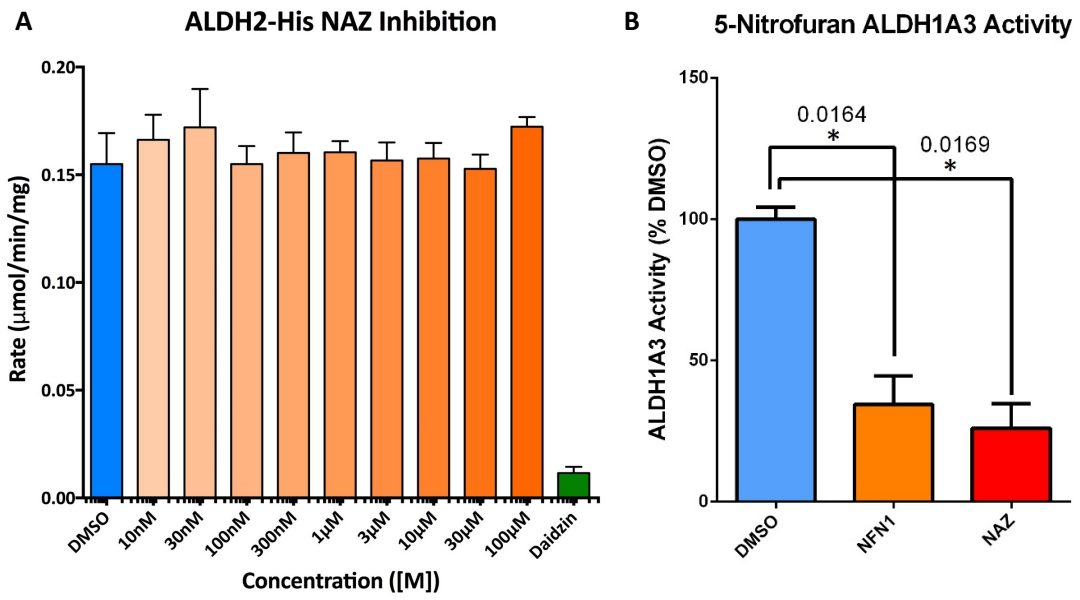

Figure 5.5: **NAZ** exhibits specificity towards ALDH1 enzymes *in vitro*. **A**) ALDH2-His *in vitro* enzymatic assay against **NAZ** (orange) treated over a logarithmic dose range, against DMSO (blue) and ALDH2 inhibitor, daidzin (green). Enzymatic rate determined using initial linear rate of NAD^+ to NADH turnover at λ = 340nm (ε = 6220$M^{-1}cm^{-1}$), upon acetaldehyde initiation. ALDH2-His activity was unaffected by **NAZ** treatment (ANOVA), even at highest doses. Daidzin resulted in a 92% reduction in ALDH2-His activity as expected (n=2). **B**) ALDH1A3 *in vitro* enzymatic activity upon **NAZ** (10μM, red), **NFN1** (1μM, orange) and vehicle (1% DMSO, blue) treatment was determined using NADH turnover at λ = 340nm (ε = 6220$M^{-1}cm^{-1}$) after 10mins. ALDH1A3 activity represented at %DMSO activity. ALDH1A3 activity was significantly reduced after **NAZ** treatment (P = 0.017) with a 73.9% reduction in ALDH1A3 activity. **NFN1** treatment has a significant reduction in ALDH1A3 activity (P = 0.016: t-test) as expected (n=3).

5.2.6 Nifuroxazide is not bio-activated by Aldh2b in zebrafish melanocytes

As shown previously,[115] 5-NFN mediated melanocyte cell death in zebrafish is driven via bio-activation by Aldh2b. If **NAZ** is indeed not being bio-activated by ALDH2, melanocytes should be unaffected in zebrafish treated with **NAZ**. AB WT zebrafish embryos were treated with **NAZ**, **NFN1** of vehicle (1% DMSO) control at 48hpf. Drug was washed off at 3dpf and embryos were allowed to grow until 5dpf where melanocyte numbers were analysed. It was immediately visible that **NAZ** treatment had no effect on melanocytes in the zebrafish,

with similar melanocytes compared to vehicle treated fish (**Figure 5.6A**). As expected, **NFN1** treatment resulted in a dramatic reduction in melanocytes, with numbers noticeably depleted and the melanocytes remaining on the **NFN1** zebrafish appearing smaller and more rounded. The lack of activity of **NAZ** on zebrafish melanocytes was confirmed by counting melanocyte cell numbers on the zebrafish. Melanocyte cell number of **NAZ** treated fish was not significantly decreased compared to vehicle treated fish (P = 0.650, **Figure 5.6B**) however, **NFN1** treatment had a significant ablation of melanocyte cell number compared to vehicle treatment (P > 0.0001). This is consistent that **NAZ** has no activity towards ALDH2 *in vivo*, confirming the results seen *in vitro*.

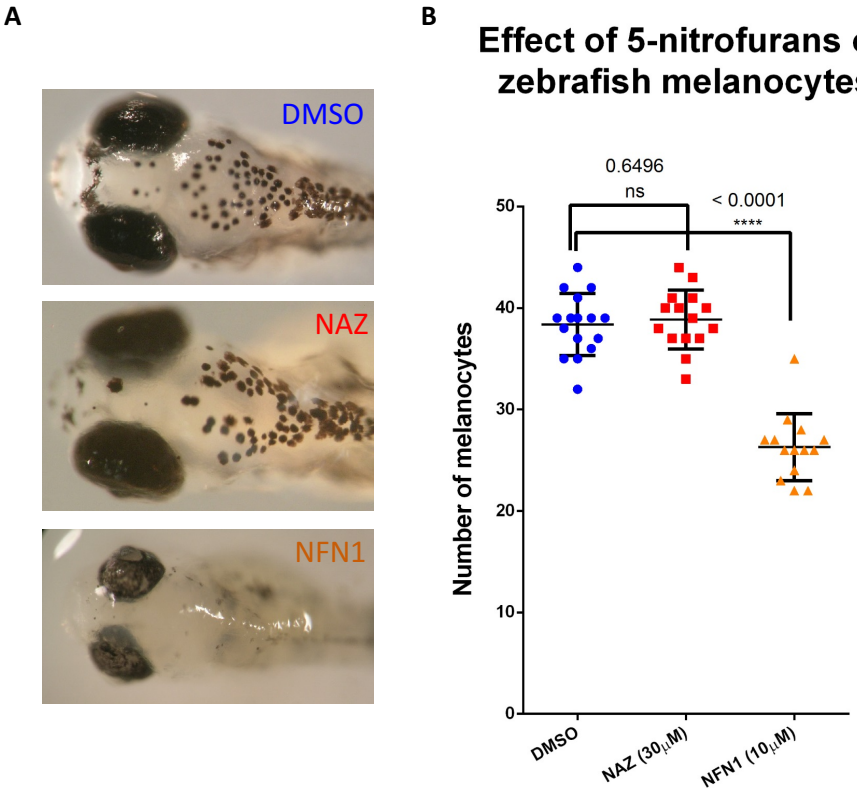

Figure 5.6: **NAZ** does not mediate melanocyte cell death in zebrafish embryos (n=15). **A**) Photographs of zebrafish embryos (5dpf) treated with **NAZ**, **NFN1** or vehicle (1% DMSO) for 48hrs. **NAZ** treatment led to no change in zebrafish melanocytes, with fish looking similar to that of DMSO treated fish. As expected, **NFN1** treatment resulted in a near-white fish, with all melanocytes ablated. **B**) Graph depicted melanocyte cell number of treated zebrafish embryos (5dpf) 48hrs post **NAZ**, **NFN1** or vehicle (1% DMSO) treatment (n = 15). **NAZ** did not cause any change in melanocyte cell number (P = 0.650: t-test) whereas **NFN1** has a significant reduction in melanocyte cell number (P < 0.0001: t-test), compared to DMSO treated embryos.

5.2.7 No strong correlation between ALDH1A3 expression and sensitivity of melanoma cells to nifuroxazide

As **NAZ** exhibits some specificity towards ALDH1A3, it is probable that there is a correlation between ALDH1A3 expression in melanoma cells and sensitivity to **NAZ** treatment. To assess this, cell viability assays were set up on the same 11 cell lines kindly provided by Dr Marco Ranzani and Dr David Adams (Wellcome Trust Sanger Institute, Cambridge, UK) as before in accordance to **Appendix I**, where the expression of all 19 isoforms has been previously determined by RNA_{seq} (**Appendix II**). Sensitivity to **NAZ** (EC_{50} value) was correlated against the RNA_{seq} expression for ALDH1A3 in each individual cell line (**Figure 5.7**). Although there was a trend that increasing ALDH1A3 expression correlated with sensitivity to **NAZ**, this was particularly weak (R^2 = 0.0944). As with **NFN1**, which has a far weaker correlation (**Figure 4.4**, R^2 = 0.0246), this gives an indication that far more than just the expression of ALDH1A3 plays a role in mediating 5-NFN driven toxicity, and most likely the full ALDH environment within each cell line will play a role in **NAZ** sensitivity. However, this is also indicative of anti-cancer effects being driven by other targets. For instance, **NAZ** has been previously reported as a STAT3 inhibitor, in turn promoting death in myeloma and breast cancer cell lines.[135,136] The activity of **NAZ** against melanoma has recently been published, where inhibition of cell proliferation, promotion of apoptosis, accumulation of intercellular ROS, and suppression of metastasis in melanoma xenographs have been observed post-**NAZ** treatment.[137] Although the study suggests these effects are attributable to STAT3 inhibition, it is likely that bio-activation by ALDH plays an important factor in driving these phenotypes also. As such, it is important to characterise all the targets for **NAZ**, and indeed all the 5-NFNs, where it is likely that some, if not all, 5-NFNs have dual target effects promoting anti-cancer activity. However, it has been reported that STAT3 regulated CSC behaviour in melanoma cells also regulates the expression of ALDH1A3.[85] It is therefore possible that **NAZ** treatment may affect this STAT3-ALDH1A3 pathway in melanoma, and be possible to target a more specific $STAT3^{high}ALDH1A3^{high}$ CSC subpopulation. Within the last few years, novel derivatives of **NAZ** have been synthesised, showing marked improvement in anti-microbial activity compared with **NAZ**.[181-183] Considering this improvement in anti-microbial activity, it would be interesting to explore whether these compound also have improved anti-cancer activity, especially in regards to their efficiency and specificity in targeting ALDH in melanoma.

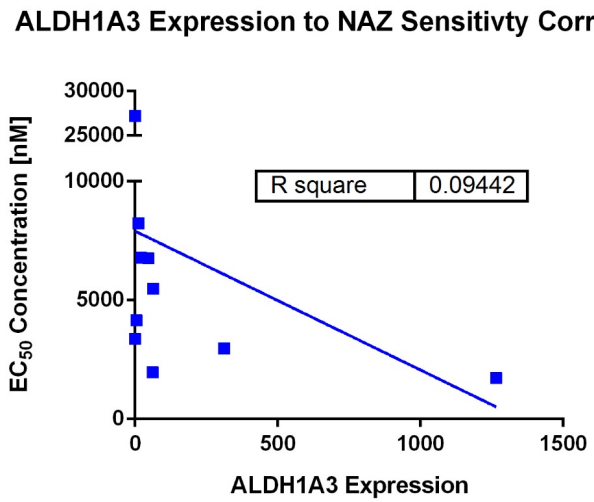

Figure 5.7: Scatter plot correlating **NAZ** sensitivity to ALDH1A3 expression in a panel of 11 melanoma cells. **NAZ** sensitivity is represented by EC_{50} values determined by cell viability, where the lower the EC_{50} the more sensitive the cell line is to **NAZ**. ALDH1A3 expression is determined through RNA_{seq} and directly proportional to expression. Although there is some correlation that **NAZ** sensitivity increases as ALDH1A3 expression is higher, this is very weak (R^2 = 0.0944). It does appear like there may be a slight trend in favour of ALDH1A3 expression correlating with sensitivity to **NAZ**, although this is not consistent.

5.3 Synthetic compounds

Clinical 5-NFNs are available, however their potency in cancer cells is still 10-fold less than **NFN1**. The activity seen with **NFN1** shows there is still a lot of room for improvement with the 5-NFNs drugs, and creating novel 5-NFN compounds with a much higher affinity for ALDH and efficacy in cancer, specifically any selectivity for ALDH1, would be greatly desired.

NFN1 is a previously published compound,[115] so although it possesses favourable characteristics against cancer and ALDH, it is unable to be patented and brought forward as a hit compound in drug development. Other drawbacks to **NFN1** also include both its solubility and stability. **NFN1** is insoluble in aqueous solution at concentrations of 10μM or higher. Although **NFN1** is much more soluble in DMSO, precipitation over time is a common problem, in which **NFN1** activity will dissipate over time.

Developing new 5-NFNs that could mimic the potency seen with **NFN1**, maintain its stability and increase its solubility, would be highly desirable when creating new hit compounds for ALDH -driven anti-cancer drug development. Creating *bis*-5-NFN molecules could lead to 5-NFNs that have a 'double-warhead', where both 5-NFN moieties on a single molecule can contribute to ALDH-driven cancer cell death.

5.3.1 RC-NFN-WP1

For the development of a *bis*-5-nitrofuran molecule I designed a strategy to bind two 5-NFNs through an amide-bound benzene linker. This compound has some structural similarities to **NFN3** (**Figure 3.1C**), which showed similar cancer cell toxicity to **NFN1**, and **NFN5**, a previously reported active 5-NFN tool compound used for biotin-linker conjugation.[115] Further, the presence of the benzene linker would also allow the alteration for *para*-, *meta*- and *ortho*- conjugates of the *bis*-5-NFN, where the variability of the relative positions of the 5-NFNs on the benzene could directly affect the potency of the compound.

The original pathway to synthesise the proposed *bis*-5-NFN involved the carbodiimide, N,N'-diisopropylcarbodiimide (DIC) to promote amide bond formation between a diaminobenzene and furoic acid. (**Scheme 2.1**) However, an abundance of an expected, undesired bi-product, **RC-NFN-WP1**, was produced (**Figure 5.8A**). The product was produced in a substantial yield (43%) and could be readily purified. As this novel compound was still a 5-NFN, there was potential for anti-cancer activity as seen with other 5-NFNs previously. To test for this, a simple cell viability assay was set up as before with A375 melanoma cells, with a logarithmic dose of **RC-NFN-WP1** and **NFN1**. **RC-NFN-WP1** had no activity in A375 cells (**Figure 5.8B**) compared against **NFN1** (EC_{50} = 1.76μM). A probable cause for the lack of activity may be through the presence of *tert*-butyl side chains on the amine. These bulky groups on the molecule may affect the way in which ALDH will interact with the 5-NFN, depleting its affinity.

To further confirm the lack of biological activity presented by **RC-NFN-WP1**, zebrafish embryos were treated with **RC-NFN-WP1** and **NFN1** and vehicle (1% DMSO) for 48hrs. At 5dpf, zebrafish embryos were examined for melanocyte cell number, to assess for any Aldh2b driven bio-activation. **RC-NFN-WP1** treated fish looked healthy and normal, with no

change in melanocyte pattern compared to DMSO treated fish (**Figure 5.8C**). As expected, **NFN1** has a severe depletion of melanocytes in the zebfrafish embryos. This confirms there is no biological activity of the newly synthesised 5-NFN**, RC-NFN-WP1**. Due to this lack of activity, no further characterisation of the compound was done.

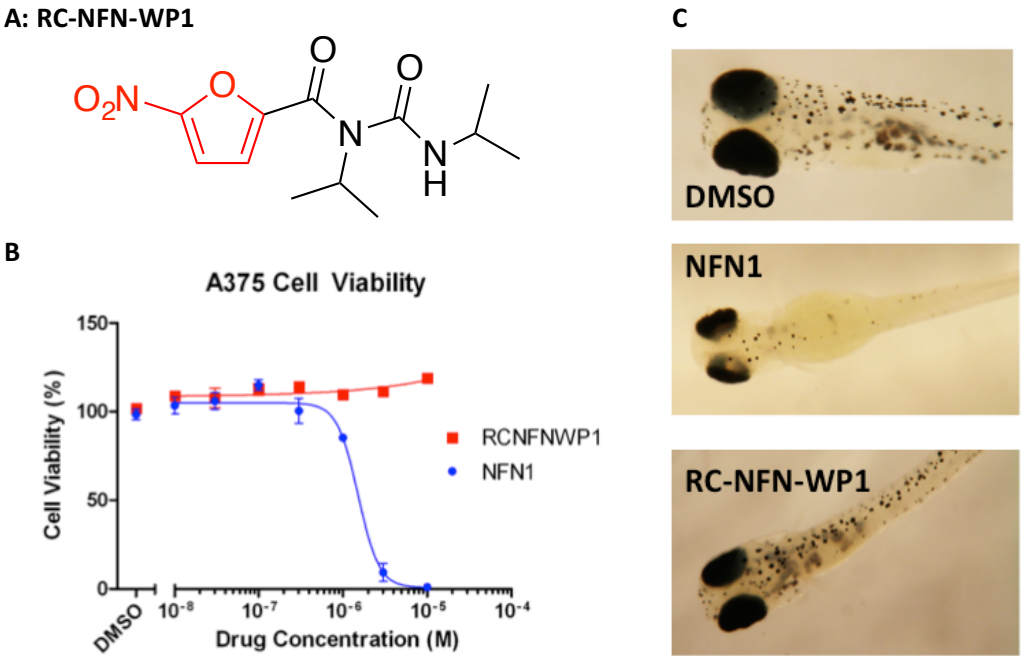

Figure 5.8: Bi-product 5-NFN, **RC-NFN-WP1**, displayed no biological activity. **A**) Molecular structure of the **RC-NFN-WP1**. The 5-nitrofuran moiety is highlighted in red. **B**) A375 melanoma cell viability upon **RC-NFN-WP1** or **NFN1** treatment. treatment over 96hours, EC_{50} values determined by PrestoBlue™ treatment and normalised to vehicle (1% DMSO) control. **RC-NFN-WP1** had no activity in A375 cells, with no change in cell viability across all concentrations. **NFN1** EC_{50} = 1.76µM **C**) Photographs of zebrafish embryos (5dpf) treated with **RC-NFN-WP1**, **NFN1** or vehicle (1% DMSO) for 48hrs (n=15). **RC-NFN-WP1** treatment led to no change in zebrafish melanocytes, with fish looking similar to that of DMSO treated fish. As expected, **NFN1** treatment resulted in a near-white fish, with almost all melanocytes ablated (n=15).

5.3.2 RC-NFN5

The original synthetic pathway using DIC to synthesise a *bis*-5-NFN derivative was not promising. The synthetic pathway was therefore altered, where the conversion of 5-nitro-furoic acid to the acyl chloride using thionyl dichloride was implemented prior to reaction with the daminobenzene (**Scheme 2.2**) Following a method adapted from the literature.[115]

The *para-bis*-5-NFN derivative, **RC-NFN5**, was synthesised through this mechanism, as well as was its *para-bis*-no-nitro conjugate, **RC-NFN5.1**, as a control (**Figure 5.9A,B**). Both molecules were tested on A375 melanoma, A2780 ovarian and HCT116 colorectal cells for anti-cancer activity using a cell viability assay, set up as described before. Cells were treated with a logarithmic dose of **RC-NFN5** or **RC-NFN5.1**. **RC-NFN5** treatment displayed toxicity in all 3 cell lines (**Figure 5.9C**) where EC_{50} values were comparable to **NFN1** treatment (A375: **RC-NFN5** EC_{50} = 1.45µM vs **NFN1** EC_{50} = 867nM; HCT116: **RC-NFN5** EC_{50} = 3.08µM vs **NFN1** = 1.85µM; A2780: **RC-NFN5** EC_{50} = 285nM vs **NFN1** EC_{50} = 45.8nM). The no-nitro control compound, **RC-NFN5.1**, displayed no cell toxicity in all 3 cell lines.

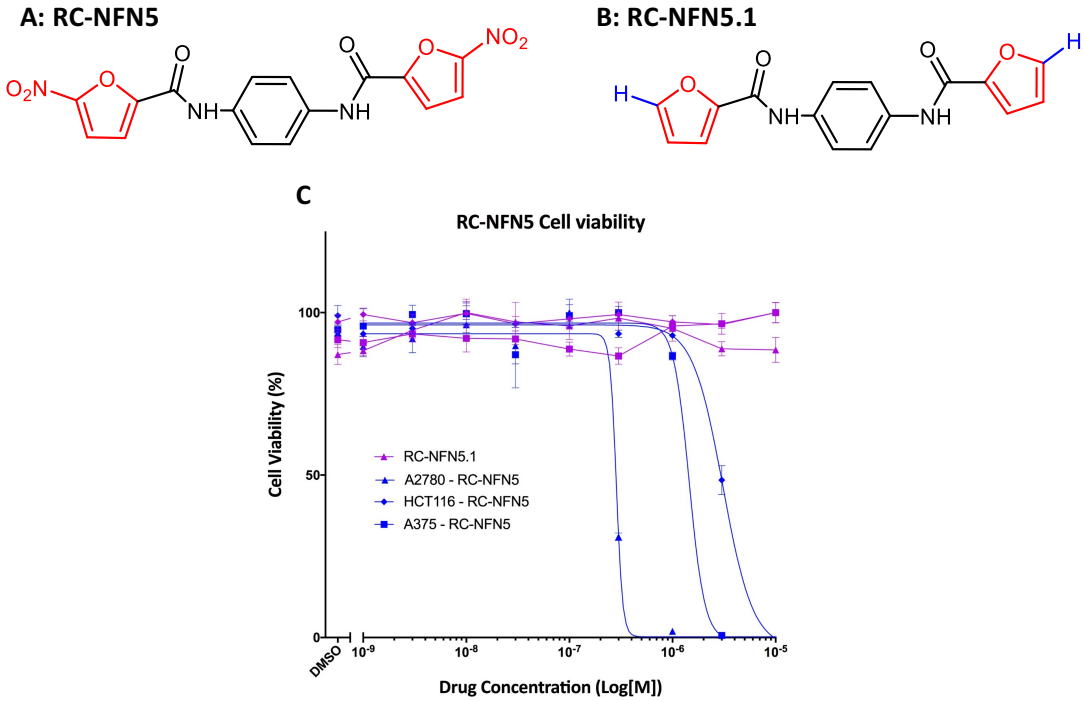

Figure 5.9: RC-NFN5 exhibits promising anti-cancer activity mediated by 5-NFN moiety. **A**) Molecular structure of *bis*-5-NFN, **RC-NFN-WP1**. The 5-nitrofuran moiety is highlighted in red. **B**) Molecular structure of the no-nitro *bis*-control, **RC-NFN5.1**. The furan moiety is highlighted red and the 5-H replacing the NO_2 highlighted blue. **C**) A375 melanoma (squares), A2780 ovarian (triangles) and HCT116 colorectal (diamond) cell viability against **RC-NFN5** (blue) and **RC-NFN5.1** (purple) treatment over 96hours, EC_{50} values determined by PrestoBlue™ treatment and normalised to vehicle (0.1% DMSO) control. For **RC-NFN5**, A2780: EC_{50} = 285nM, A375: EC_{50} = 1.45µM and HCT116: EC_{50} = 3.08µM. **RC-NFN5.1** treatment had no effect of cell viability in all 3 cell lines.

If the cellular toxicity of **RC-NFN5** is attributable to bio-activation by ALDH enzymes, a comparative reduction in ALDH activity should be observed through Aldefluor™ analysis. A375 cells treated with **RC-NFN5** were subjected to the Aldefluor™ assay, against DEAB and vehicle (1% DMSO), to analyse intercellular ALDH activity. After 24hrs of treatment with **RC-NFN5**, A375 cells had a dramatic reduction in Aldefluor™ activity (**Figure 5.10A**) where approximately 100% of Aldefluor™ activity was ablated, comparable to that seen with 24hrs of **NFN1** treatment (**Figure 3.6**). To reaffirm this finding, *in vitro* assays were set up to analyse whether **RC-NFN5** was a substrate for both ALDH2 and ALDH1A3. As before, ALDH enzymes were pre-incubated with NAD^+ and **RC-NFN5**, where enzymatic activity was determined using NADH turnover at λ = 340nm ($\varepsilon = 6220 M^{-1}cm^{-1}$) after 10mins. For ALDH2 assay, **RC-NFN5** treatment was compared against **NFN1**, **NFN1.1**, known ALDH2 inhibitor daidzin and vehicle (1% DMSO). **RC-NFN5** treatment resulted in a significant reduction in ALDH2 activity (**Figure 5.10B**, P = 0.005) where 76.2% reduction in ALDH1A3 activity in observed. Treatment with **NFN1** and daidzin also resulted in a significant reduction in ALDH2 activity (P = 0.005 & P = 0.014 respectively) as expected. For the ALDH1A3 assay, **RC-NFN5** treatment was compared against **NFN1** and vehicle (1% DMSO) only. Both **RC-NFN5** and **NFN1** treatment also led a significant reduction in ALDH1A3 (**Figure 5.10C**, P = 0.024 and P = 0.030 respectively) where **RC-NFN5** caused a 74.2% reduction in ALDH1A3 activity.

RC-NFN5 displayed potent cellular toxicity, similar to that of **NFN1**, where it is a substrate for ALDH enzymes both *in vivo* and *in vitro*. Although **RC-NFN5** does not have the ALDH1 selectivity as seen with **NAZ**, it still proves to be an effective novel 5-NFN compound in cancer cells. **RC-NFN5** provides the building blocks for developing new synthetic 5-NFN *bis*-derivatives, including the *meta*- and *ortho*- conjugates, and offers a platform to develop further 'double-warhead' 5-NFN compounds. Developing further compounds, based on the *bis*-backbone developed in **RC-NFN5**, offers a novel route in 5-NFN drug discovery with the potential both in increasing potency against cancer cells and ALDH1 selectivity. Another factor in which **RC-NFN5** highlights the need for new 5-NFN compounds is through problems experienced when working with **NFN1**. **RC-NFN5** combats some of these problems, with improved solubility and appeared to have far greater stability during use.

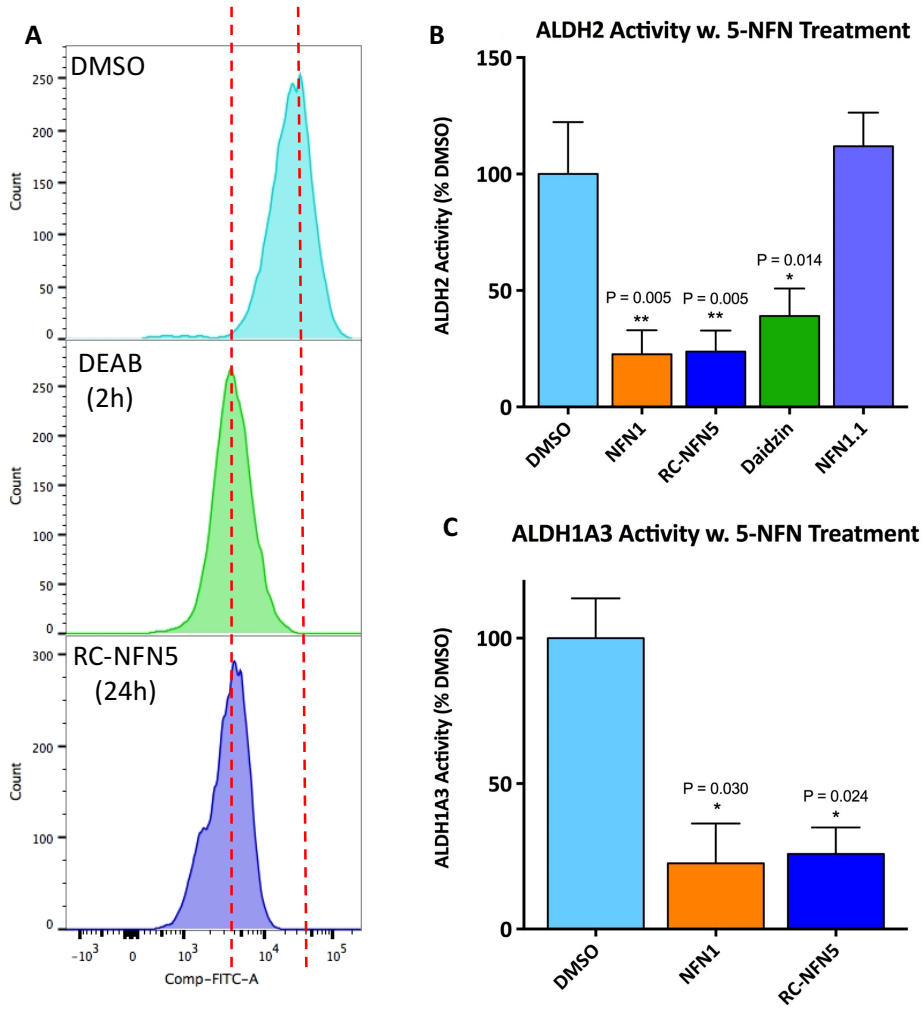

Figure 5.10: **RC-NFN5** is a substrate for ALDH enzymes. **A**) Aldefluor™ activity (FITC) represented as histogram counts of A375 melanoma cells treated with **RC-NFN5**. DMSO (light blue) positive and DEAB (green) negative controls. DMSO and DEAB treated A375 cells assumed 100% and 0% Aldefluor™ activity respectively. Aldefluor™ activity of A375 cells after 2hrs **RC-NFN5** (dark blue) treatment. **RC-NFN5** treatment reduces Aldefluor™ activity in A375 cells by approximately 100% after 24hrs of treatment (n=2). **B**) ALDH2 *in vitro* enzymatic activity upon **RC-NFN5** (dark blue), **NFN1** (orange), ALDH2 inhibtor, **NFN1.1** (purple), Daidzin (green) and vehicle (1% DMSO, blue) treatment was determined using NADH turnover at λ = 340nm (ε = 6220$M^{-1}cm^{-1}$) after 10mins. ALDH2 activity represented at %DMSO activity. ALDH2 activity was significantly reduced after **RC-NFN5** treatment (P = 0.005) with a 76.2% reduction in ALDH1A3 activity. **NFN1** and daidzin treatment had a significant reduction in ALDH2 activity (P = 0.005 & P = 0.014 respectively: t-test) as expected (n=3). **C**) ALDH1A3 *in vitro* enzymatic activity upon **RC-NFN5** (dark blue), **NFN1** (orange) and vehicle (1% DMSO, light blue) treatment was determined using NADH turnover at λ = 340nm (ε = 6220$M^{-1}cm^{-1}$) after 10mins. ALDH1A3 activity represented at %DMSO activity. ALDH1A3 activity was significantly reduced after **RC-NFN5** treatment (P = 0.024: t-test) with a 74.2% reduction in ALDH1A3 activity. **NFN1** treatment has a significant reduction in ALDH1A3 activity (P = 0.030) as expected (n=2).

5.4 Conclusion

Here I demonstrate that the clinical 5-NFNs, **NFX** and **NAZ**, display anti-cancer activity against A375 melanoma cells. Although **NFX** exhibits potent anti-cancer activity in patients with neuroblastoma and medulloblastoma,[126,131] the anti-cancer activity of NFX in the A375 melanoma cell lines was much poorer than anticipated, 80-fold less potent than **NFN1**. This was also coupled with weak Aldefluor™ activity and *in vitro* evidence that **NFX** could also potently inhibit ALDH enzymes in the same regard as **NFN1**. Through a small screen of clinical 5-NFNs, **NAZ** was discovered to have similar anti-cancer properties to NFN1, with evidence through Aldefluor™ that ALDH inhibition upon bio-activation of the drug is seen. Importantly, **NAZ** was not a substrate for ALDH2, and as such exhibited selectivity for the ALDH isoform most associated with CSC-characteristic in melanoma, ALDH1. Finally, I synthesised a novel bis-5-NFN compound, **RC-NFN5**, displaying potent anti-cancer activity and can strongly inhibit ALDH, by Aldefluor™, similarly to **NFN1**. These findings describe a clinical compound that has the potential to be repurposed for use as an anti-cancer therapeutic, which is not only improved from **NFX**, the 5-NFN currently in clinical trial for neuroblastoma and medulloblastoma, but also shows selectivity for the ALDH isoforms most relevant to cancer. I also describe a novel bis-5-NFN compound with greater stability to the tool compound, **NFN1**, but with similar biological properties, providing a platform for future 5-NFN drug discovery as anti-cancer therapeutics.

Chapter 6

Mechanism of 5-NFN-ALDH activity

6.1 Introduction

ALDH enzymes catalyse the oxidation of toxic aldehydes to their carboxylic acid derivatives through hydride-transfer to reduction of $NAD(P)^+$ to NAD(P)H.[2,11,12] The reduction of NAD^+ occurs by addition of a hydrogen on the 2-amido-pyridine ring terminus, at the *para*-position to the nitrogen (**Figure 6.1**). This mechanism is somewhat similar to the chemistry expected in the bio-activation of 5-NFNs by ALDH; where 5-NO_2 reduction is likely driven by hydrogen addition (or substitution) on the heterocyclic aromatic ring. I hypothesise that 5-NFNs will be bio-activated by the catalytic cysteine present in the ALDH active site, where bio-activation of 5-NFNs by ALDH enzymes is driven by 5-NFNs 'mimicking' the chemistry of NAD^+ reduction, to facilitate reduction of the active 5-NO_2 moiety. Inhibition of ALDH by 5-NFNs (covalent or otherwise) will occur as a direct result of bio-activation, rendering the enzyme non-functional.

Here I probe the mechanism of 5-NFN-ALDH activity through use of *in silico* computational modelling, preliminary enzymatic trials and mass spectrometry; working in collaboration with both the Institute of Structural and Molecular Biology (University of Edinburgh, UK) and Center for Structural Biology (University of Indiana, USA). I report 5-NFNs can tightly bind in the ALDH binding pocket, through computational simulations, with the potential for these compounds to interact with the active cysteine residue. I show that NAD^+ is vital for 5-NFN activity, mediating an oxidation on the catalytic cysteine, as determined by mass spectrometry. This oxidation suggests that 5-NFN bio-activation can promote a covalent modification on ALDH enzymes, that is the potential mechanism for ALDH inhibition, post 5-NFN bio-activation.

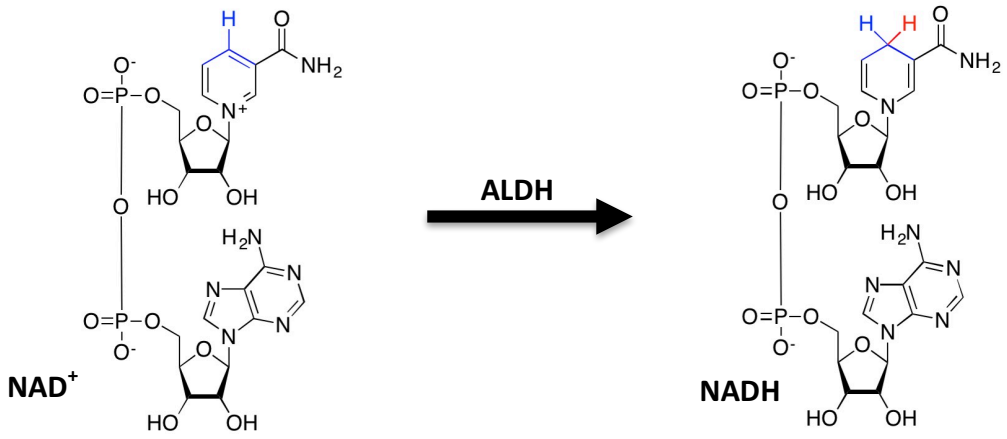

Figure 6.1: Structural mechanism of NAD^+ reduction by ALDH activity. Reduction of NAD^+ to NADH by ALDH is mediated by H-substitution on the pyridine ring.

6.2 Theoretical docking studies suggests ALDH enzymes potentially bind 5-nitrofurans at the NAD^+ binding pocket.

I wanted to explore whether 5-NFNs had the potential to bind efficiently in the NAD^+ binding pocket (or indeed, the acetaldehyde pocket) to understand whether ALDH enzymes have the potential to bio-activate 5-NFNs through a similar chemistry in which they reduce NAD^+.

Molecular docking experiments were kindly performed by our collaborator, Dr Douglas R. Houston (Institute of Structural & Molecular Biology, University of Edinburgh, UK). Modelling was performed using the structure of ALDH1A1, solved previously.[145] ALDH1A3 could not be modelled, as its structure has yet to be determined and published. ALDH1A1 was used as a suitable substitute model, considering the similarities in substrate, cellular function and evolutionary conservation between ALDH1A1 and ALDH1A3.[1,2] Docking studies were performed using AutoDock 4.2.3 or AutoDock Vina, on both the NAD^+ (co-factor) and acetaldehyde (catalytic) binding pockets, for four 5-NFN compounds (**NFN1**, **NFX**, **NAX** and **NFN1.1**). Theoretical dissociation constants (Tk_d) were determined and expressed in kcal/mol, where a shift of 1kcal/mol translates to a 10-fold reduction in Tk_d. It appears the Tk_d is universal across the 5-NFNs in the substrate-binding pocket, from both docking programs, where a slight loss of affinity is seen with **NFN1.1** (**Table 6.1A**), likely due to loss

of the 5-NO_2 moiety being able to couple to residues in the pockets. The docking of the 5-NFNs in the NAD^+ binding pocket using AutoDock 4.2.3 (**Table 6.1B**) displayed a significant loss of affinity in **NFN1.1**, in comparison to the other three 5-NFNs. This supports data observed experimentally, where **NFN1.1** has no effect of ALDH activity (**Chapter 3**), and the slight loss of affinity displayed by **NFX**, also couples with the reduction in **NFX** activity reported in **Chapter 5**. Although AutoDock quotes an approximate error margin of 2.5kcal/mol (AutoDock4.2.3 UserGuide), the loss of affinity observed theoretically upon removal of the 5-NO_2 moiety (**NFN1** -8.19kcal/mol vs **NFN1.1** -6.37kcal/mol - ΔTk_d = 1.89kcal/mol) is a large enough margin to confidently predict what is expected practically. Upon rendering how the 5-NFNs interact with the structure of ALDH1A1 (**Figures 6.2A-D**) it is clear that interactions between asparagine and lysine residues in the ALDH binding pocket, and the NO_2 moiety is crucial for the high affinity of 5-NFNs towards ALDH enzymes. Considering the structural similarities of NFN1.1 to **NFN1**, it could be expected that **NFN1.1** would show some degree of reduction in ALDH activity. However, as this interaction between NO_2 and ALDH is lost with **NFN1.1** and offers an explanation as to why no reduction in ALDH activity is seen upon **NFN1.1** treatment. This highlights the importance of the 5-NO_2 moiety for activity towards ALDH, where interactions between ALDH residues and the 5-NO_2 group are essential for the high affinity 5-NFNs have towards ALDH, and indeed, in mediating bio-activation and reduction of ALDH activity.

This data suggests that 5-NFNs have the potential to strongly interact at the NAD^+ binding pocket, where interactions between ALDH residues and NO_2 may contribute to the reduction in ALDH activity observed through both *in vitro* enzymatic assays and cellular Aldefluor™ activity. As such, I hypothesise that the chemistry required for ALDH to reduce NAD^+ to NADH is similar to the mechanism in which ALDH will bio-activate 5-NFNs, via NO_2 reduction.

A: Substrate Binding Site

	AutoDock 4.2.3	AutoDock Vina
NFN1	-7.20kcal/mol	-7.8kcal/mol
NAZ	-7.35kcal/mol	-8.2kcal/mol
NFX	-6.97kcal/mol	-7.3kcal/mol
NFN1.1	-6.84kcal/mol	-7.1kcal/mol

B: NAD^+ Binding Site

	AutoDock 4.2.3	AutoDock Vina
NFN1	-8.19kcal/mol	-7.5kcal/mol
NAZ	-8.74kcal/mol	-7.9kcal/mol
NFX	-7.29kcal/mol	-7.4kcal/mol
NFN1.1	-6.37kcal/mol	-6.9kcal/mol

Table 6.1: Theoretical dissociation constants (Tk_d) of binding between 5-NFNs and ALDH1A1. Both AutoDock 4.2.3 ad AutoDock Vina were used for all computational simulations. 5-NFNs (**NFN1**, **NAZ**, **NFX** and **NFN1.1**) were docked against both catalytic and co-factor binding pockets. **A**) 'Docking' studies of 5-NFNs in the substrate binding pocket of ALDH1A1. AutoDock Vina presents the strongest theoretical dissociation constants for 5-NFNs binding in this pocket. **B**) 'Docking' studies of 5-NFNs in the co-factor binding pocket of ALDH1A1. AutoDock 4.2.3 presents the strongest theoretical dissociation constants for 5-NFNs binding in this pocket, however there is a large reduction in Tk_d upon loss of the 5-NO_2 moiety (**NFN1.1**), in keeping with experimental data.

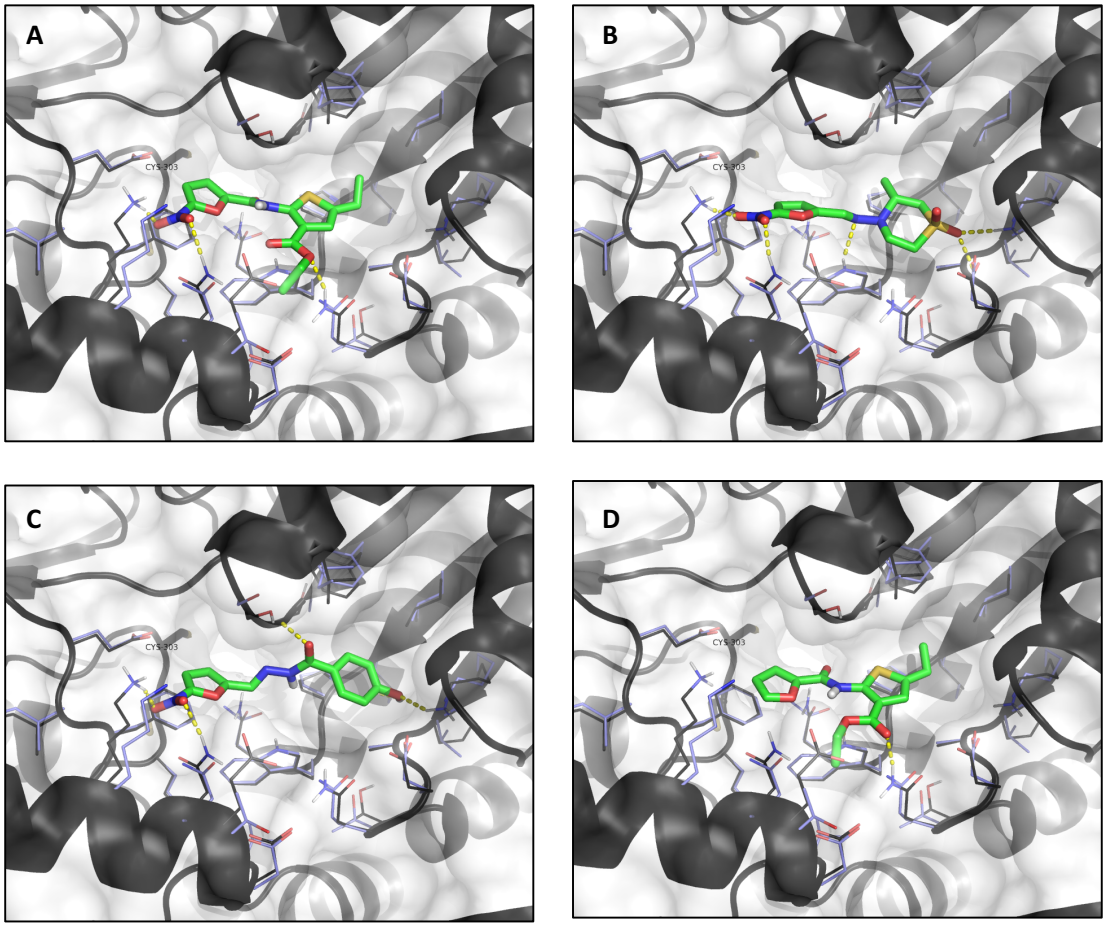

Figure 6.2: Theoretical molecular docking of 5-NFNs in the NAD^+ binding pocket of ALDH1A1, rendered by PyMol. Docking studies highlight important interaction between 5-NO2 moiety and Asparagine and Lysine ALDH residues in the co-factor pocket. Molecules also sit close in space to active Cys303 residue. Side chains of 5-NFns molecule also present other interactions within the pocket, likely contributing to affinity of compounds to ALDH1A1. **A**) **NFN1**. An additional interaction is predicted with the ester bound oxygen. **B**) **NFX**. Further interactions are predicted with sulfoxide oxygen and azo nitrogen. **C**) **NAZ**. Further interactions are predicted with amide oxygen and phenol oxygen also. **D**) **NFN1.1**. The key interactions between 5-NO_2 moiety and Asparagine and Lysine ALDH residues is lost upon substitution of NO_2. Predicted interaction relies on ester carbonyl oxygen interaction with second Asparagine residue.

6.3 Co-factor (NAD^+) required for 5-NFN-ALDH activity

The *in vitro* enzymatic ALDH assays rely on the conversion of NAD^+ to NADH, where NADH production can be monitored using absorbance (λ=340nm) to determine ALDH activity. Upon pre-incubation with 5-NFNs, ALDH activity is lost. If 5-NFNs are binding into the NAD^+ cofactor binding pocket, and 5-NO_2 reduction is being driven by hydride-transfer from the aldehyde, this suggest NAD^+ will not be required for 5-NFN bio-activation. To preliminary probe the mechanism in which 5-NFNs interact with ALDH, the *in vitro* enzymatic assay with ALDH2-His was repeated, however, different combinations of acetaldehyde (substrate), NAD^+ (co-factor) and drug (**NFN1** or vehicle (1% DMSO)), were used to initiate the assay. This allowed the understanding on the order in which 5-NFNs interact with ALDH, and what natural ligands need to be present in order for the 5-NFNs to compete for ALDH activity. As shown previously in **Chapter 3**, ALDH2-His activity can be initiated after pre-incubation with either NAD^+ or acetaldehyde, so as such, if these 2 ligands were reversed in their addition with 5-NFNs to ALDH2-His, the same reduction of ALDH2-His activity should be expected.

6.3.1 NAD^+ pre-incubation is required to mediate 5-nitrofuran bio-activation by ALDH

Enzymatic ALDH2-His assays were set up similar to previous, however ALDH2-His was pre-incubated with either NAD^+, acetaldehyde, drug (**NFN1** or 1% DMSO) or a combination of these substrates, according to **Table 6.1**.

Pre-incubated with ALDH2	Added after 10mins (Initiator)
NAD^+ + Drug	AcAld
AcAld + Drug	NAD^+
AcAld + NAD^+	Drug
NAD^+	AcAld + Drug
AcAld	NAD^+ + Drug
Drug	AcAld + NAD^+
None	AcAld + NAD^+ + Drug (All 3)

Table 6.1: ALDH2-His enzymatic order assay setup conditions.

Catalytic activity was initiated after 10mins upon addition of the remaining substrates. Enzymatic activity was monitored via NADH production (λ = 340nm, ε = 6220$M^{-1}cm^{-1}$) and enzymatic rate determined by initial linear turnover. ALDH2-His activity is significantly reduced by **NFN1** treatment in the majority of activity conditions (**Figure 6.3**: $P < 0.0001$ – $P = 0.08$), highlighting 5-NFNs as competitive substrates for ALDH2-His *in vitro*. However, the reduction of ALDH2-His activity observed upon treatment with **NFN1**, where both **NFN1** and NAD^+ have been pre-incubated with enzyme ($P < 0.0001$), was significantly greater than the corresponding reductions ($P < 0.0001$ by ANOVA). Indeed, the data suggests that pre-incubation with both NAD^+ and **NFN1**, i.e. initiated with AcAld, is essential for mediating 5-NFN activity towards ALDH2-His (Δ = 88.1% AcAld initiate vs Δ = 41.3% - AcAld + NAD^+ initiate, next best). NAD^+ is needed to bind preliminarily to ALDH in the co-factor binding pocket, in order to mitigate a conformational change and activate the catalytic cysteine.[2,11,12] As it is clear ALDH enzymes need pre-incubation with NAD^+ and **NFN1** to mediate 5-NFN bio-activation, it is likely that co-factor binding is required in order to activate the ALDH enzyme, for 5-NFN bio-activation to occur, as during its natural functionality. Although this contradicts predictions drawn from the previous *in silico* docking studies, where it was expected that 5-NFNs would be competing with NAD^+ for ALDH activity, it is unsurprising that the activation of the catalytic cysteine (Cys302) by NAD^+ binding would be required in order to mediate 5-NFN activity.

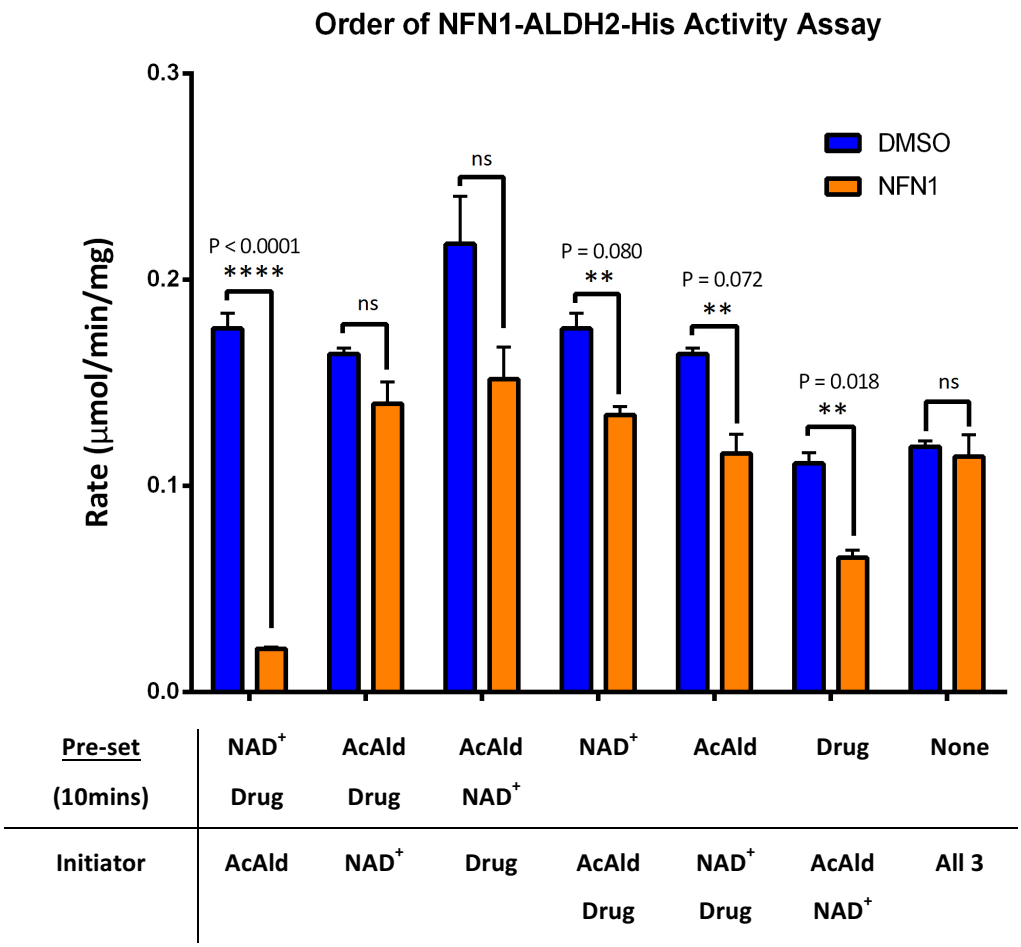

Figure 6.3: ALDH2-His activity assay, exploring the mechanistic order of 5-NFN action. ALDH2-His activity is initiated by differing combinations of substrate (AcAld), co-factor (NAD^+) and drug (**NFN1** (orange) vs DMSO (blue)). The substrates used to initiate ALDH activity are represented as the *x*-axis variable, with a direct comparison between DMSO and **NFN1**. Enzymatic rate determined using initial linear rate of NAD^+ to NADH turnover at λ = 340nm (ε = 6220$M^{-1}cm^{-1}$), upon assay initiation. **NFN1** treatment displayed significant reduction in ALDH2-His activity in the majority of assay order systems, compared to DMSO. Notably, the largest reduction of activity was observed upon initiation of ALDH2-His activity using acetaldehyde only (i.e. NAD^+ and **NFN1** were already pre-incubated with ALDH2-His, prior to initiation – P < 0.0001). Stats shown are all t-test (n=3).

6.3.2 NAD^+ not reduced by ALDH upon 5-nitrofuran addition

If NAD^+ binding is required to mediate 5-NFN bio-activation by ALDH enzymes, it could be likely that reduction of the co-factor to NADH is also required for activity. To probe this, the

in vitro ALDH2-His enzymatic assay was set up as before, however, the catalytic activity of ALDH2-His was not initiated by acetaldehyde addition. Instead, NADH production was monitored (λ = 340nm, ε = 6220$M^{-1}cm^{-1}$) with only NAD^+ and **NFN1** present, to assess whether reduction of NAD^+ by ALDH2 is required for 5-NFN activity. Traces of NADH production over time exhibited no production of NADH after treatment with **NFN1** (**Figure 6.4**). As NADH production is driven by hydride transfer from acetaldehyde in ALDH2 normal functionality,[2,11,12] it suggests that NAD^+ is required only for ALDH structural conformational changes and cysteine activation, in order to drive 5-NFN activity. This however, does not take into consideration that acetaldehyde may be required for 5-NFN bio-activation as well, where hydride transfer from the substrate could be vital for 5-NO_2 reduction. Thus, further probing whether acetaldehyde is necessary for bio-activation, to accurately determine the mode of 5-NFN action.

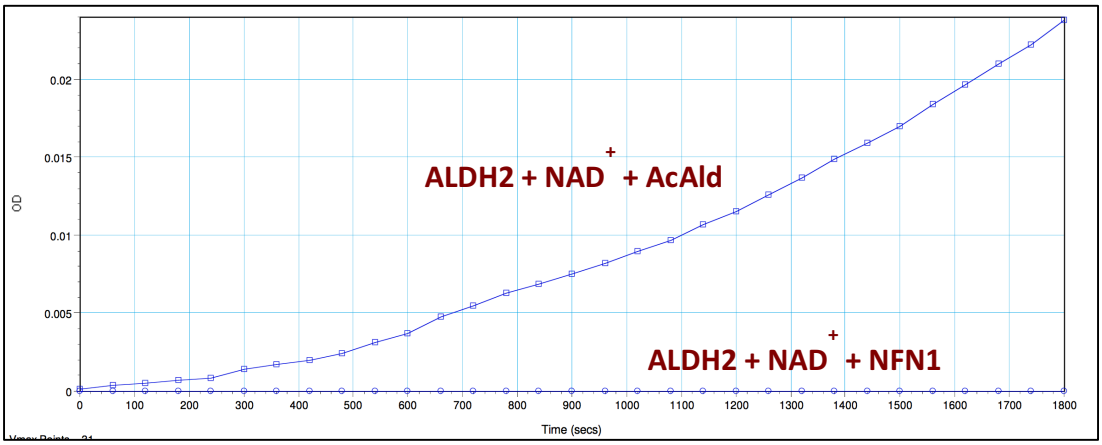

Figure 6.4: ALDH2-His activity as measured by fluorescence due to NADH production (λ = 340nm, ε = 6220$M^{-1}cm^{-1}$), over time. Normal ALDH2-His functionality (NAD^+ + AcAld) drives NADH production over time, however function of ALDH2-His with 5-NFNs (NAD+ + **NFN1**) does not produce any NADH as a result of 5-NFN bio-activation, as no increase in fluorescence at λ = 340nm is observed.

6.4 5-Nitrofuran bio-activation leads to covalent oxidation on catalytic ALDH cysteine

Insights from the Aldefluor™ assay suggest that 5-NFNs have the potential to potently inhibit ALDH activity in A375 melanoma cells. Such potent inhibition, in comparison to a known reversible inhibitor DEAB (**Figure 3.6**), could arise from a covalent interaction with ALDH enzymes, denaturing functional activity. This hypothesis is supported by the extent in which ALDH activity is inhibited by 5-NFNs, where recovery of activity was not observed until after 72hrs post-treatment (**Figure 3.7**). To explore whether 5-NFNs inhibit ALDH enzymes by a covalent interaction following bio-activation, mass spectrometry was used to detect any modification on the protein following 5-NFN treatment *in vitro*.

6.4.1 ALDH enzymes are oxidized by 5-nitrofuran treatment, only when NAD^+ is present.

The following work was performed by our collaborator, Professor Thomas D. Hurley (Indiana University School of Medicine, Indianapolis, IN, USA).

To determine whether treatment with 5-NFNs generates a covalent modification in ALDH enzymes, *in vitro* enzymatic assays were subjected to whole protein mass spectrometry analysis, using electrospray ionising (ESI) quadrupole-time of flight (Q-TOF) mass spectrometry (MS). This detection method is able to distinguish between mass differences that can be associated with small molecule binding, and as such, provide an accurate insight in to the modifications 5-NFNs can potentially yield. Similar *in vitro* enzymatic assays were setup as before (without AcAld), where ALDH2 was incubated with 5-NFNs (**NFN1**, **NFX**, **NAZ**, **NFN1.1**) with NAD^+. The samples were then subjected to ESI Q-TOS MS and analysed for changes in protein mass compared to native enzyme (1% DMSO). Only treatment with **NFN1** resulted in alteration in the mass profile of ALDH2 (**Figure 6.5**). No differences were seen in ALDH2 mass profile upon treatment with **NAZ**, **NFX** and **NFN1.1** compared to native (1% DMSO). ALDH2 treated with **NFN1** resulted in the production of 2 new products with mass increase of 31amu and 338.02amu. The increase of 31amu is likely as a result of a double oxidation substituted on an active hydrogen [ALDH2+O_2-H], likely the active cysteine residue. It was interesting to observe a mass increase of 338.02amu, which is the exact mass of **NFN1** [ALDH2+**NFN1**]. As **NFN1** is expected to be bio-activated through reduction

of the 5-nitro moiety, any increase in mass would be expected to have some loss from the whole **NFN1** molecule. Although it could be argued that this shows the potential for **NFN1** to act solely as a tightly bound inhibitor of ALDH2, it would not describe why a double oxidation adduct is also produced. As ESI is a 'soft' ionisation technique, which is employed due to the reduction in fragmentation to study whole protein mass shifts, it can also detect masses of small molecules that are tightly bound to proteins through non-covalent interactions.[184] Considering the results from theoretical binding studies previously in this chapter, describing 5-NFNs having the potential to tightly bind in both the catalytic and co-factor binding pockets of ALDH, it is likely this mass shift is associated with a tight, non-covalent interaction between **NFN1** and ALDH2, which, in turn, is required for activity. It was surprising to observe that **NFX** did not cause any variation in the mass profile of ALDH2. As shown in **Chapter 5**, **NFX** is a competitive substrate for ALDH2 *in vitro*, and has a similar theoretical affinity to ALDH2 compared to **NFN1**, so it would have been expected that some trace of this interaction would have been detected by MS. Although, as the affinity of **NFX** to ALDH2 was 1000-fold weaker than **NFN1** (**NFX**: IC_{50} = 88.1µM vs **NFN1**: IC_{50} = 63.9nM), it could be sufficiently small enough that it would be undetectable at this resolution.

To assess whether similar mass shifts are observed when the reported melanoma stem cell marker, ALDH1A1,[79] is treated with 5-NFNs, the experiment was repeated with ALDH1A1 upon pre-incubation with 5-NFNs (**NFN1**, **NFX**, **NAZ**, **NFN1.1**) and NAD^+ (**Figure 6.6**). In correlation with observations from ALDH2, ALDH1A1 also showed a double oxidation shift [ALDH1A1+O_2] = 54762.32amu (Δ = 32.16amu). It was also interesting to observe the lack of native enzyme detected after **NFN1** treatment, indicating that almost all ALDH1A1 enzyme is double oxidized by treatment with **NFN1**. In comparison to ALDH2, displaying far less efficiency in double oxidizing, this indicates that **NFN1** is much more efficacious towards ALDH1A1. Interestingly, **NAZ** and **NFX** also appeared to exhibit a similar yet subtle mass shift upon treatment on ALDH1A1. This gives an indication that **NAZ** and **NFX** can also interact with ALDH1A1, and facilitate ALDH1A1 enzymes to undergo double oxidation. The ability for **NAZ** to oxidise ALDH1A1 over ALDH2 is supported by what was observed *in vitro* (**Chapter 5**), where **NAZ** appears to exhibit some specificity towards ALDh1 enzymes. As **NFX** could also oxidise ALDH1A1, it also suggests that **NFX** has a greater affinity for ALDH1 enzymes than ALDH2, and may be indicative of the mechanism underlying anti-cancer activity *in vivo*.[132] As expected and in co-ordinance with ALDH2, treatment with **NFN1.1** did not result in any mass variation from native enzyme (1% DMSO).

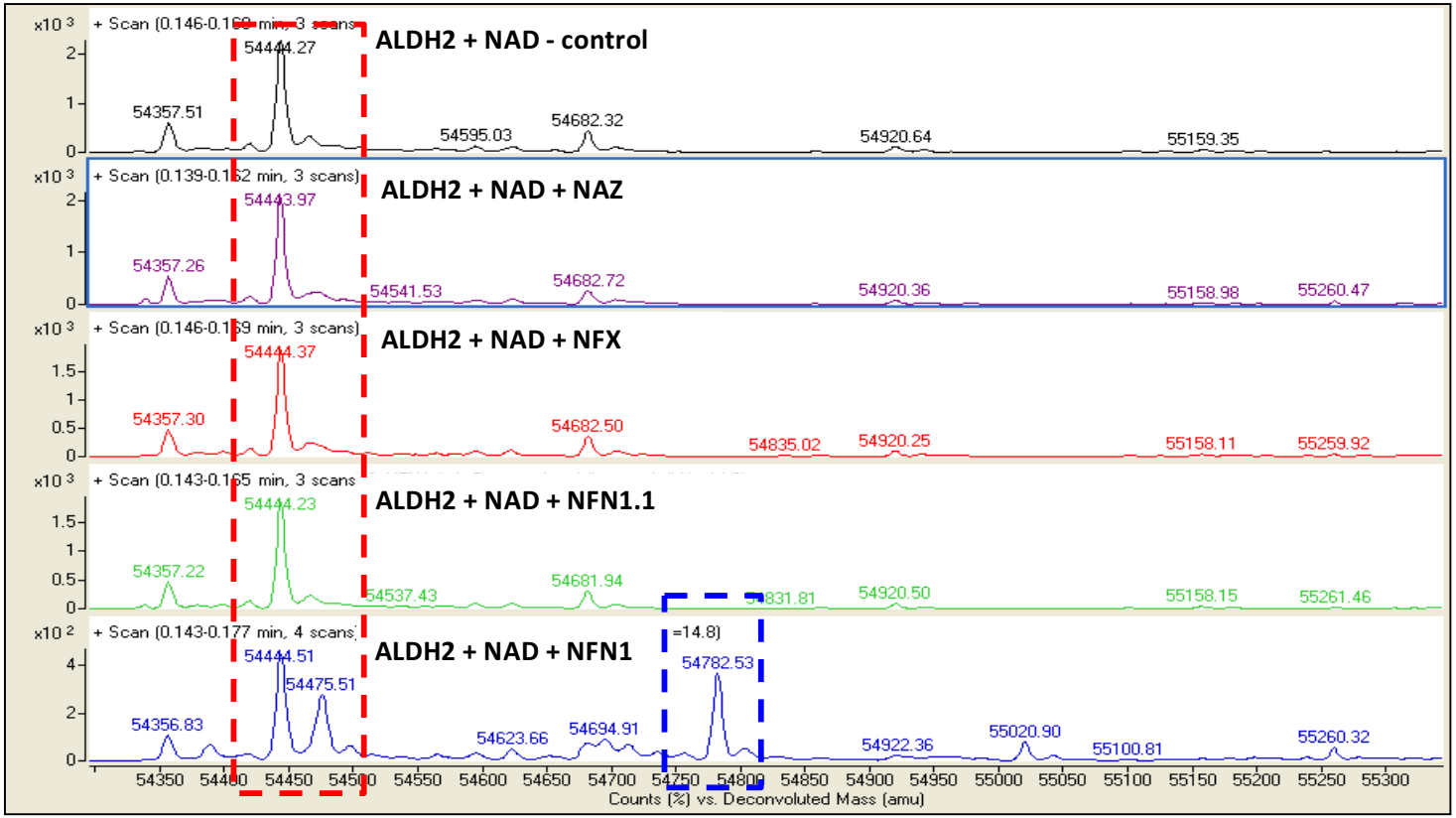

Figure 6.5: ESI-QTOF-MS spectra of ALDH2 treated with 5-NFNs (**NAZ**, **NFX**, **NFN1.1** and **NFN1** vs control), in the presence of NAD^+. Treatment of ALDH2 with **NFN1** displays a spectral shift of 31amu (red box) from native enzymes (Native: m/z = 54444amu vs **NFN1** treated: m/z = 544475amu), where approximately half of the native enzyme has been converted to [Native+31] species – suggesting the addition of O_2 moiety (or double oxidation). A spectral shift of 338amu (blue box) from native enzymes (Native: m/z = 54444amu vs **NFN1** treated: m/z = 54782amu), also suggests a strong interaction (covalent or otherwise) between ALDH2 and **NFN1** (338Da). Treatment with **NFX**, **NAZ** and **NFN1.1** appeared to have no effect of ALDH1A1 MS spectra compared to control.

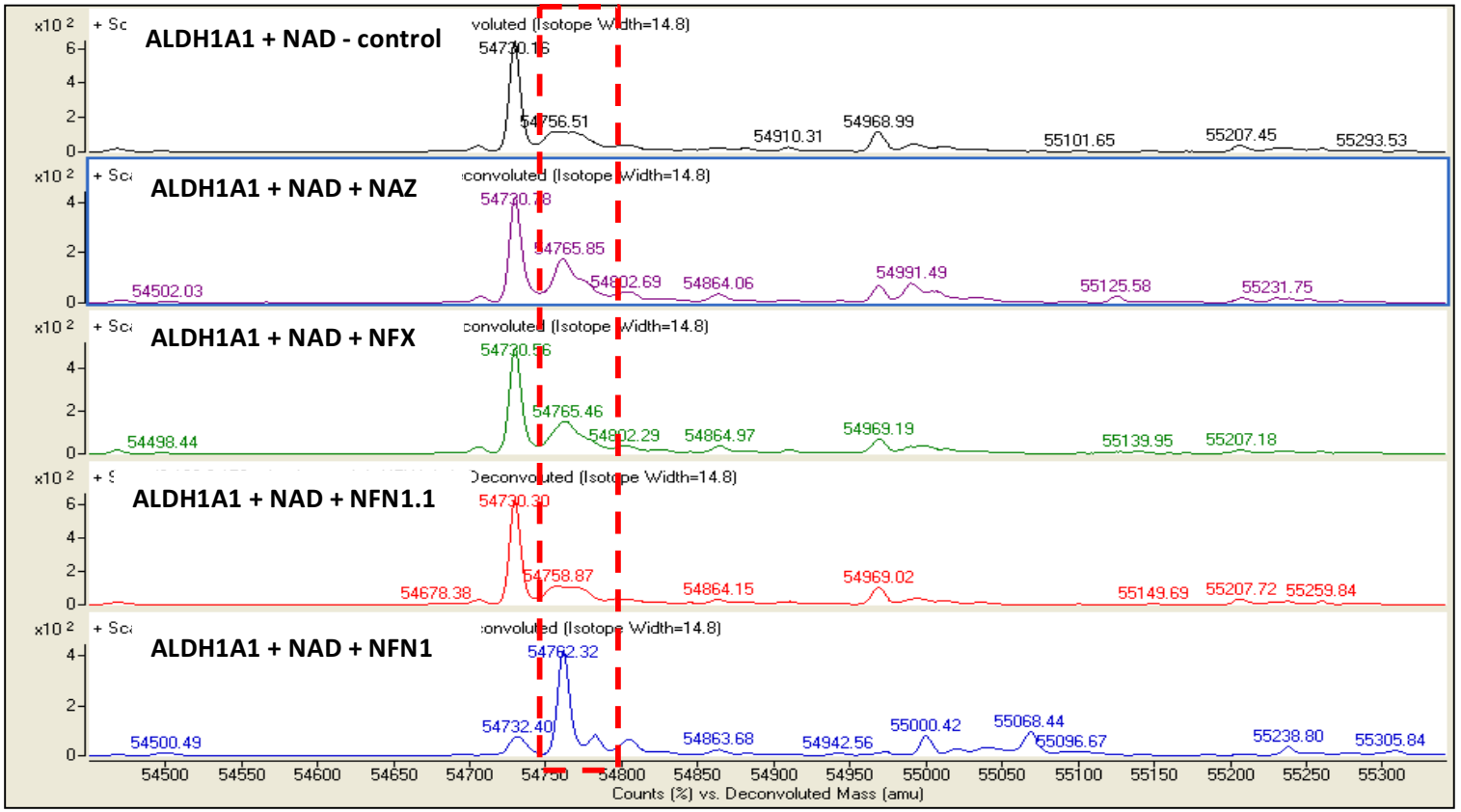

Figure 6.6: ESI-QTOF-MS spectra of ALDH1A1 treated with 5-NFNs (**NAZ**, **NFX**, **NFN1.1** and **NFN1** vs control), in the presence of NAD^+. Treatment of ALDH1A1 with **NFN1** displays a spectral shift of 32amu (red box) from native enzymes (Native: m/z = 54730amu vs **NFN1** treated: m/z = 54762amu), where a small fraction of native enzyme is detectable, with the majority existing as a [Native+32] species – in keeping with an addition of O_2 moiety (or double oxidation). Treatment with **NFX** and **NAZ** led to some double oxidised ALDH1A1 species to arise, although, to a much less extent, with the majority of native enzyme still present. **NFN1.1** appeared to have no effect of ALDH1A1 MS spectra compared to control.

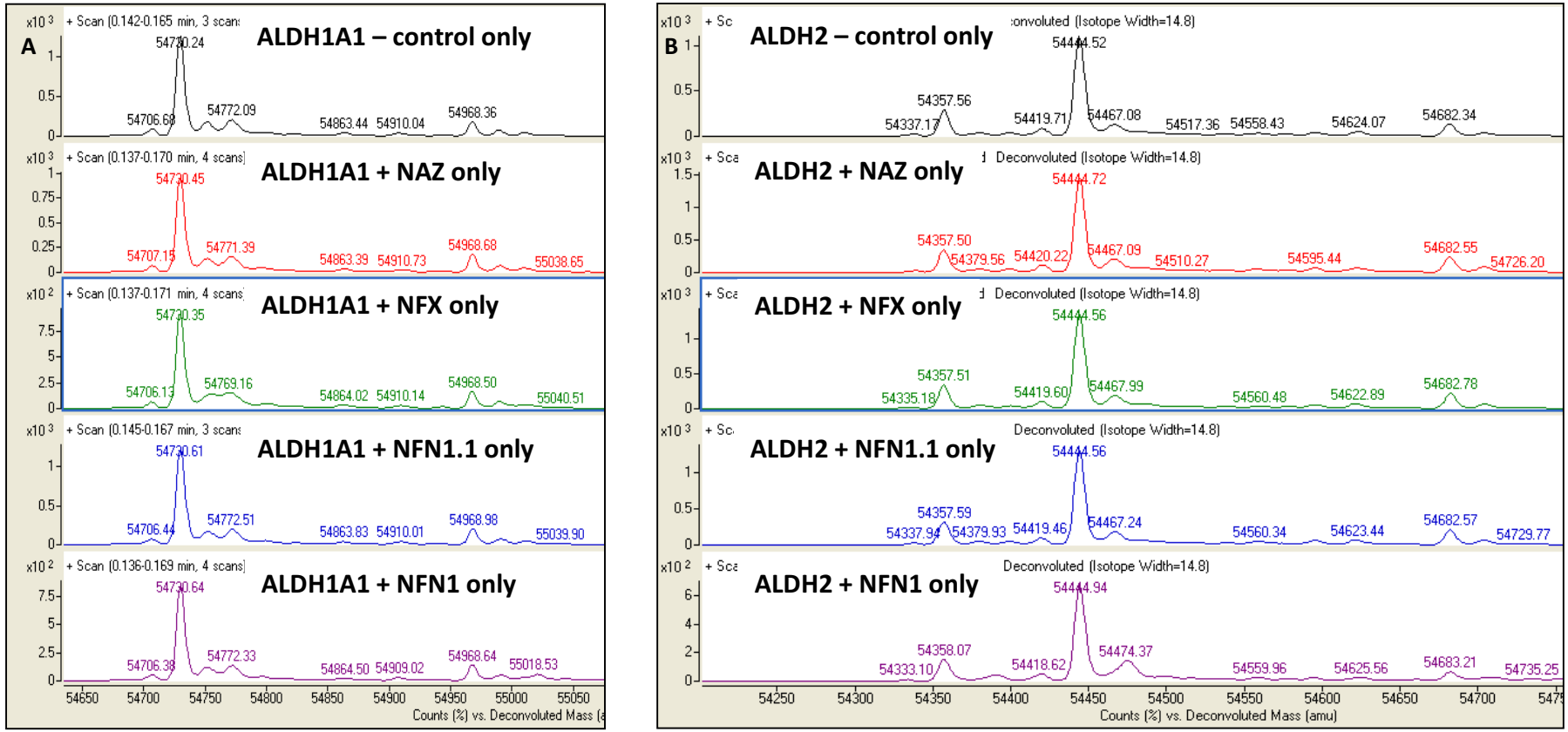

Figure 6.7: ESI-QTOF-MS spectra of ALDH enzymes treated with 5-NFNs (**NAZ**, **NFX**, **NFN1.1** and **NFN1** vs control), without the presence of NAD^+. Treatment of ALDH enzymes with 5-NFNs without NAD^+ present in the system conferred no spectral change of ALDH enzymes upon treatment, compared to control. Only native enzyme was detectable in all samples. **A**) ALDH1A1. **B**) ALDH2.

The order activity assay suggested that NAD^+ is required for ALDH enzymes to bio-activate 5-NFNs. As such, it would be appropriate to assume that modifications in protein mass associated with 5-NFN treatment will also depend on NAD^+ being present. To confirm whether NAD^+ is important for these modifications, in concurrence with the *in vitro* reaction order analysis, the ESI Q-TOF MS assay was repeated with both ALDH2 and ALDH1A1 in the absence of NAD^+. Neither ALDH2 nor ALDH1A1 (**Figure 6.7**) resulted in any alteration in protein mass upon treatment with all 5-NFNs compared to native enzyme (1% DMSO). This indicates that the double oxidation on ALDH2 and ALDH1A1 by 5-NFN treatment is dependent on the presence of NAD^+, where the whole compound interaction between **NFN1** and ALDH2 was also not observed without NAD^+. This suggests that NAD^+ is essential to mediate conformational change and cysteine activation, in order to facilitate 5-NFN-ALDH activity.

6.4.2 ALDH2 catalytic cysteine is triple oxidised by 5-nitrofuran bio-activation

Considering NAD^+ is required for 5-NFN activity, it is likely the conformational change upon NAD^+ binding in the ALDH co-factor binding pocket, in turn activating the catalytic cysteine, is also essential for 5-NFN bio-activation. Comparatively, *in silico* data performed by Dr Douglas R. Houston, also suggested 5-NFNs will 'fit' close in space to this catalytic cysteine also. As such, I hypothesised that the observed oxidation of ALDH by 5-NFNs, performed Professor Thomas D. Hurley, will likely be mediated by modification on this residue (Cys302). In order to determine the mechanism by which ALDH enzymes are oxidised by 5-NFN treatment, i.e. which amino acid residues arte modified by 5-NFN treatment; trypsinised samples were prepared and subjected to quadrupole-orbitrap mass spectrometer analysis, probing around the amino acid chain (Q290 – R308) containing the catalytic cysteine (Cys302). Working together in collaboration with Dr Alex von Kriegsheim and Dr Jimi Wills (Edinburgh cancer Research UK Centre - Proteomics facility, University of Edinburgh, UK), purified ALDH2-His samples were prepared upon treatment with 5-NFNs (**NFN1**, **NFN1.1**, **RC-NFN5**, **RC-NFN5.1** and **NFX**) and incubated in the presence of NAD^+. Samples were then digested and subjected to quadrupole-orbitrap mass spectrometer analysis. Probing the amino acid sequence containing the catalytic cysteine (Cys302) found a triple oxidisation on the Cys302 (**Figure 6.8** – y6 $\rightarrow$ y7: Δ = 151amu (Cys+$3O_2$-H_2O)). Treatment of ALDH2-His with 5-NFNs, in the presence of NAD^+, resulted in significant

production of triple oxidised (TripOx) ALDH2-His species ($P < 0.0001$ by ANOVA), compared to baseline (ALDH2+NAD^+ only - **Figure 6.9**). Importantly, however, there was no significant increase in TripOx species upon treatment with no-nitro controls (**NFN1.1** & **RC-NFN5.1**), which were also significantly less than their nitro counterparts ($P = 0.004$ & $P < 0.0001$ respectively). It was interesting to observe the increase in TripOx species upon treatment with **NFN1**, without NAD^+ present, in contrast to both the 5-NFN-ALDH order activity assay and mass spectrometry work by Professor Thomas D. Hurley, that conclude presence of NAD^+ is essential for both 5-NFN activity and ALDH oxidation. However, the increase of TripOx species upon **NFN1** treatment, without NAD^+ present, is still significantly less than when both NAD^+ and **NFN1** were present ($P = 0.016$). This suggests that, while NAD^+ is required for cysteine activation, there may be some residual ALDH activity that can potentially bio-activate 5-NFNs, leading to this small increase in TripOx species observed. Although, as treatment of ALDH2-His with **NAZ**, shown in **Chapter 5** not to be a substrate for ALDH2, also resulted in an increase of TripOx production, this suggests that treatment of ALDH2-His with any 5-NFN (or indeed any small molecule) could promote some minor TripOx species promotion. However, it is clear that, in the presence of NAD^+, 5-NFN treatment significantly increased TripOx species formation (with nearly all ALDH2-His triple oxidised upon **NFN1** treatment). This provides evidence that 5-NFN treatment will ultimately result in a covalent modification of the ALDH enzymes, which could be the likely cause of ALDH inhibition by 5-NFN bio-activation. Importantly, preliminary results with the mutant, ALDH2*2-His, appeared to show no increase in TripOx species upon treatment with **NFN1** (**Figure 6.10**), with and without NAD^+, proving that normal ALDH2 functionality is required in order to interact with 5-NFNs.

This triple oxidised cysteine, suggests an additional oxidation of the cysteine, in contrast to Professor Thomas D. Hurley's work previous. The discrepancy between the two mass spectroscopy data could be as a result of differing methodologies and ionisations, owing to the resultant cysteine oxidative state. However, both data sets suggest a covalent, oxidative modification on the catalytic cysteine of ALDH2 upon 5-NFN treatment. Structural confirmation using protein crystallography will be required in order to confirm cysteine oxidation, and also conclude which oxidative state is present. Although inhibition of ALDH by 5-NFNs required presence of co-factor NAD^+, it does not answer whether acetaldehyde is also essential to mediate its bio-activation. It will important going forward to determine exactly how 5-NFNs driven ROS production is achieved by ALDH enzymes.

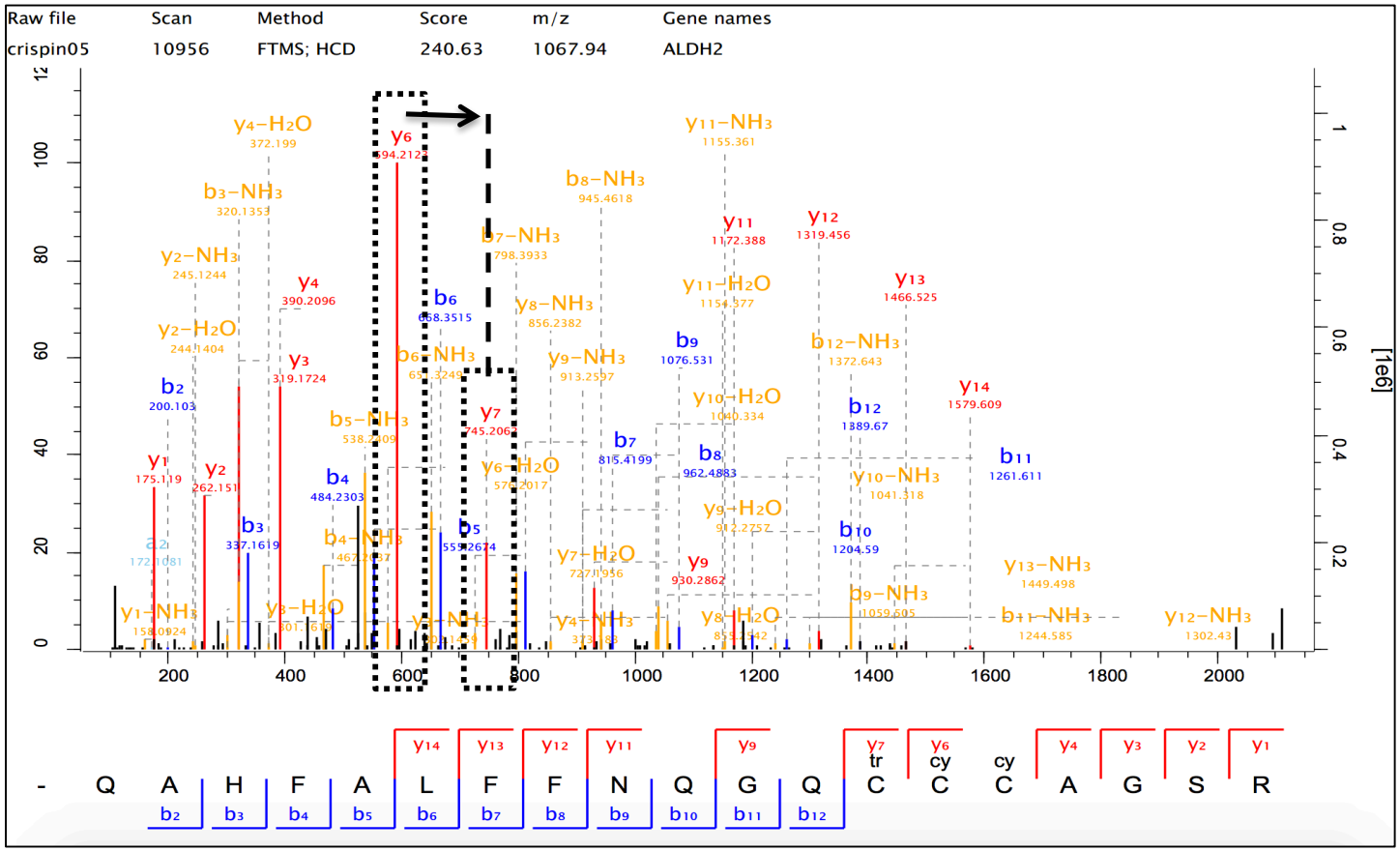

Figure 6.8: Quadrupole-Orbitrap mass spectrometer analysis of ALDH2-His amino acid chain, Q290 – R308 (inc. catalytic cysteine, Cys302), treated with **NFN1**. The shift from Cys (y6) → Cys (y7) is highlighted by the blue boxes, where the Cys302 is represented as y7. The shift (Δy6→y7 = 151amu) represents [Cys+30]. This suggests a triple oxidation on the catalytic cysteine, where the spectral shift represents Cys302 (121amu) + $3O_2$ (48amu) – H_2O (18amu), suggesting a triple oxidation on this cysteine residue upon **NFN1** treatment.

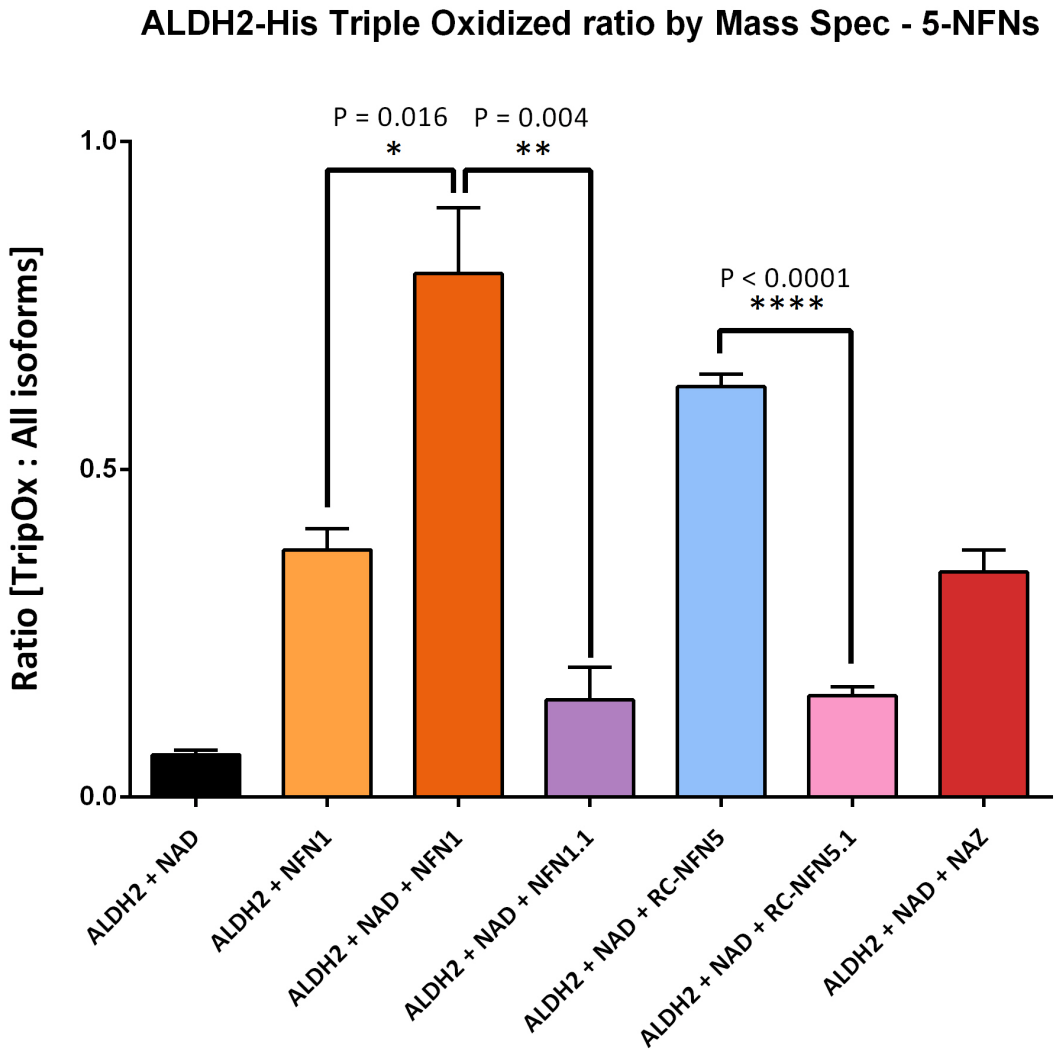

Figure 6.9: Ratio of triple oxidised (TripOx) ALDH2-His species comparable to total ALDH2-His isoforms present in mass spectrometry spectral analysis. Control, NAD^+ only (black), has little TripOx species present. Addition of 5-NFNs significantly increased TripOx species production compared to control ($P < 0.0001$ by ANOVA, not shown), with **NFN1**+NAD^+ (dark orange) showing the largest increase of average 78% total population. **NFN1** only (light orange) also showed a significant increase in TrpOx species production, however this was significantly lower than **NFN1**+NAD^+ samples ($P = 0.016$). No-nitro controls were also significantly lower than their 5-NFN derivatives (**NFN1.1** (purple): $P = 0.004$; **RC-NFN5.1** (pink): $P < 0.0001$) and were also not significantly changed compared to control (ANOVA, not shown). **NAZ** (red) also had a significant increase in TripOx species production, comparable to **NFN1** only samples.

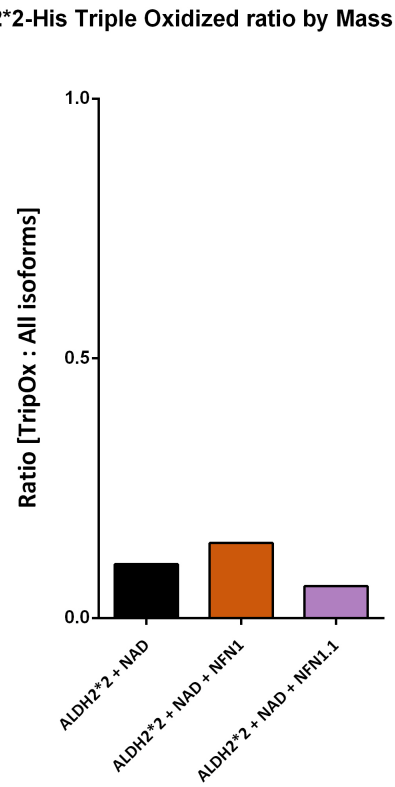

Figure 6.10: Preliminary data of ratio of triple oxidised (TripOx) ALDH2*2-His species comparable to total ALDH2*2-His isoforms present in mass spectrometry spectral analysis. Addition of **NFN1** (dark orange) or **NFN1.1** (purple) had little increase in TripOx species production compared to control (NAD^+ only, black).

6.5 Conclusion

Here I demonstrate that NAD is required for 5-NFN-ALDH activity, where NAD is likely needed as a structural co-factor in order to drive activity of ALDH enzymes towards 5-NFNs. Although this was surprising considering computational docking studies suggest that 5-NFNs would bind tightly in the NAD co-factor binding pocket, where theoretical dissociation constants were in keeping with experimental data. Through utility of mass spectrometry, I show in collaboration that 5-NFNs are substrates for ALDH enzymes, and upon bio-activation, can covalently modify ALDH enzymes through oxidation at the catalytic cysteine (**Figure 6.11**). Although the exact mechanism of the oxidation has yet to be determined, these findings provide evidence for the mechanism in which 5-NFns interact with ALDH enzymes, and suggests that 5-NFN can covalently modify ALDH enzymes in order to drive irreversible inhibition, as predicted in **Chapter 3**.

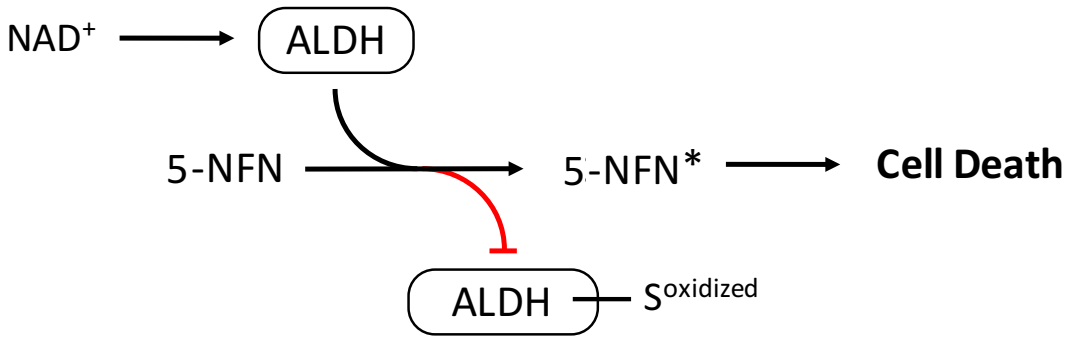

Figure 6.11: Schematic of the mechanism of 5-NFN-ALDH activity. NAD+ is required as a structural co-factor, binding to ALDH prior to 5-NFN bio-activation. 5-NFN are bio-activated to drive cell toxicity, in turn covalently modifying the active cysteine through oxidation, likely promoting the irreversible inhibition of ALDH enzymes by 5-NFN action.

Chapter 7

Future Directions and Discussion

7.1 Preliminary Data

7.1.1 Mapping all 19 ALDH isoforms in cancer cells

One of the major difficulties with working with ALDH is taking into considering all 19 human isoforms present within cells, all of which potentially contribute to 5-NFN bio-activation. Assessing the ALDH expression of all 19 isoforms in a panel of cell lines and conditions can potentially provide an idea of the cellular ALDH environment and how this varies due to such factors as Aldefluor™ sorting or 5-NFN treatment, as well as to understand how varying ALDH levels directly influences 5-NFN sensitivity.

To assess for this, cellular samples were set up in-house and sent away to be analysed for ALDH expression through RT-qPCR by OakLabs (Berlin, Germany). The 26 samples included A375 cells after treatment with drug stimuli; 5-NFNs (**NFN1**, **NAZ**, **NFN1.1** and **NFX**), natural substrate acetaldehyde (AcAld) or vehicle (1% DMSO), 2hrs and 24hrs post treatment and sorted high vs low Aldefluor™ treated cells (A375, A2780 and HCT116) against the non-treated equivalents. GAPDH, 18S and TBP were used for reference genes. Expressed as heatmaps, Δct (difference in cycle threshold) values were calculated through exponential expression comparable to reference gene expression. Δct values were determined by:

$$\Delta ct(gene) = ct(sample) - ct(reference)$$

Where a lower Δct value (red) indicates higher gene expression and a higher Δct value (blue) indicates lower gene expression.

To explore whether expression of specific ALDH isoforms in the cancer cell lines used correlated with their sensitivity to 5-NFNs, as well as to determine which ALDH isoforms played a major role in Aldefluor™ activity, the ALDH environment for these samples were characterised. As expected, ALDH1A3 was one of the dominant ALDH isoforms in the A375 melanoma cancer cell line (**Figure 7.1A**), especially considering its upregulation in melanoma CSCs.[79] Other isoforms, including ALDH3A2, ALDH18A1, ALDH7A1 and ALDH9A1, were more highly expressed in cancer cells compared to ALDH1A3, indicating that there are

other, more highly expressed ALDH isoforms in the cell environment that could be contributing to 5-NFN toxicity.

It was surprising to observe the low levels of ALDH1A1 expression across all cell samples, especially considering its supposed high expression in CSCs across nearly all tumour types.[31,75] A partial explanation lies in that because only a small subpopulation will have high ALDH1A1 expression, i.e. the CSC niche, owing to such low total expression. However, it could also be indicative that not all cancer cell populations follow this trait of ALDH1A1 as a CSC marker as so previously universally coined,[44] reflecting the more realistic view that cancer phenotypes vary between patients. This is also further supported by cross-examination with the Sanger melanoma cell line panel, where ALDH1A1 expression varies quite widely between all 22 samples. Moreover, in the A375 melanoma cell line, it has been reported that ALDH1A3, not ALDH1A1, is the predominant ALDH CSC marker. This also helps to explain why ALDH1A1 expression was not detectable by western blot in A375 cells.

Considering A2780 cells especially, which were highly sensitive to 5-NFNs, it is difficult to extract which ALDH enzymes are contributing more extensively to 5-NFN sensitivity than others; and perhaps this also suggests that 5-NFNs may have non-ALDH targets that may also contribute to 5-NFN toxicity. It may also indicate that there may be other, non-ALDH targets, contributing to the anti-cancer activity of 5-NFNs, that have yet to be characterised.

To understand how the expression of ALDH enzymes in A375 melanoma cells respond upon treatment with ALDH inhibitors, 5-NFNs or natural substrate, AcAld, cells were set up 2hrs and 24hrs post treatment and submitted for RT-qPCR analysis. When A375 cells were treated with 5-NFNs, known ALDH inhibitors, the natural substrate acetaldehyde or DMSO alone, there is no change in the ALDH expression pattern – both 2hrs and 24hrs post treatment (**Figure 7.1B**). After 2hrs of treatment with **NFN1**, a sharp increase in ALDH5A1 (succinate semialdehyde dehydrogenase) expression is seen, however is not prolonged after 24hrs. This may be indicative of an initial cellular response to ROS-induced stress, however, there is no evidence that ALDH5A1 plays a role in cellular response to oxidative stress.[84] It was also noteworthy to see that expression levels of ALDH overall seemed to decrease slightly upon treatment with all stimuli, including vehicle (1% DMSO) control, compared to the untreated A375 cell sample. This may be as a direct result to conditions in

which both samples were prepared, i.e., the act of treating A375 cells may influence their ALDH expression pattern, or be indicative of changing ALDH expression patterns as a result of time (A375 untreated vs Aldefluor™ is distinctly different from drug treated samples). This may also help to explain the slight discrepancies between minor changes in EC_{50} values against **NFN1**, where ALDH expression fluctuates depending on growth conditions or as a result of continued passaging.

One of the main problems when drawing definitive conclusion from this data comes down to its reliability. Due to the nature of the experiment, the samples provided only represent a single point in time for each condition (n=1). Although replicate values were taken in triplicate for each sample, thus improving the overall accuracy of the ALDH expression data, the samples themselves still only represent a single point in time and as such, it could be possible to be drawing a conclusion from an anomaly. The sharp but acute increase of ALDH5A1 expression in A375 melanoma cells, 2hrs after **NFN1** treatment, may not truly reflect the normal response of A375 cells to **NFN1** treatment, and ALDH5A1 is irregularly upregulated in this sample. Therefore, although this data does gives good indication of the ALDH expression behaviour for these samples and conditions, it is impossible to draw any significant conclusions without further probing whether ALDH expression is consistent upon replication. Further analysis using replicate samples would be required to confirm all the findings above, however, this data has already provided some indication about the expression of ALDH enzymes in the A375 melanoma cell lines, and would be incredibly interesting to probe whether certain behaviours, such as an increase in ALDH5A1 upon 5-NFN treatment, can be validated.

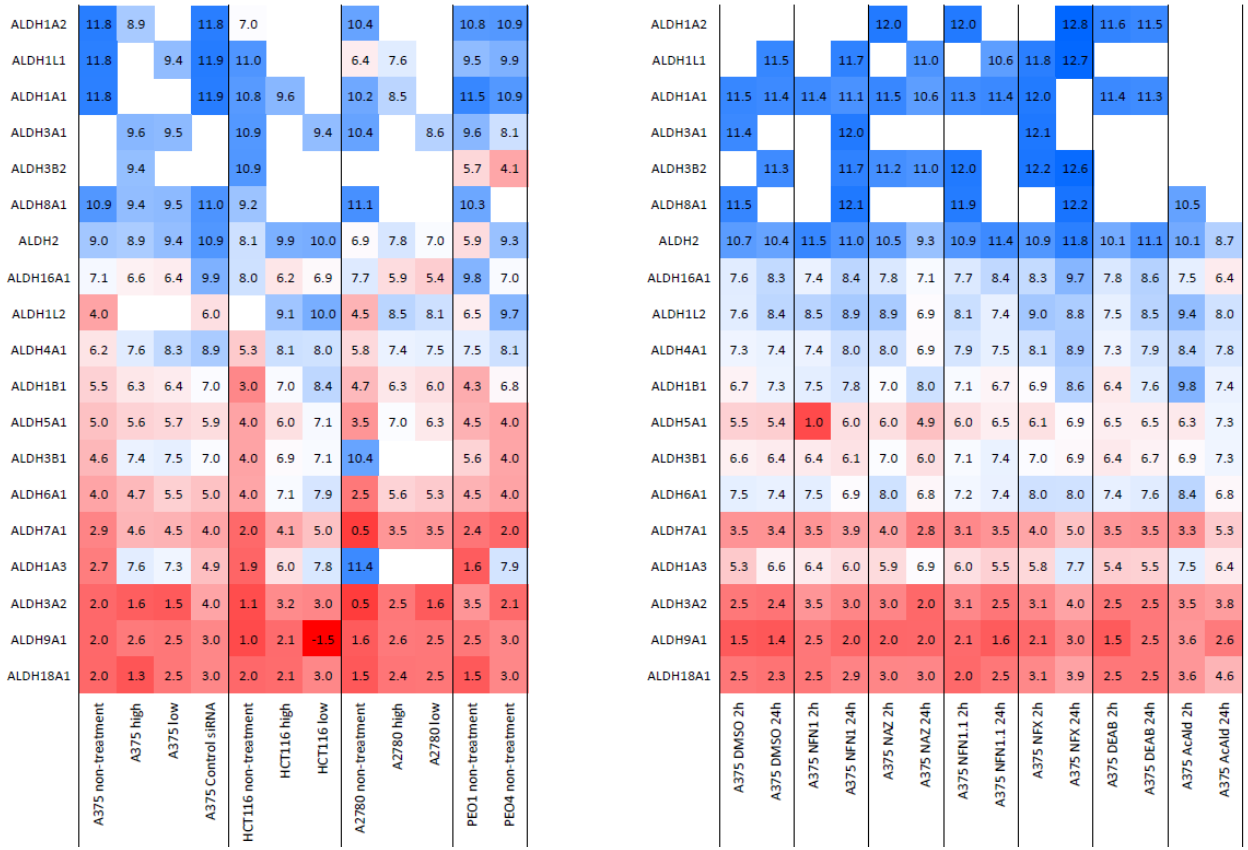

Figure 7.1: Heatmap of ALDH expression levels of all 19 ALDH isoforms in 26 cell samples. Expression measured by RT-qPCR on RNA and expressed as Δct compared to GAPDH, 18S and TBP expression. Red indicates high ALDH expression, blue indicates low ALDH expression and white indicates no detectable ALDH expression. **A**) Samples are A375 melanoma cells, HCT116 colorectal cells and A2780 ovarian cells which have also been sorted for low vs high Aldefluor™ activity. Sister PEO1 and PEO4 ovarian cells were also included. **B**) Expression in A375 cells after treatment with 5-NFNs (**NFN1**, **NAZ**, **NFN1.1** and **NFX**), natural substrate acetaldehyde (AcAld) or vehicle (1% DMSO) 2hours and 24hours post treatment.

This data reflects the ALDH profile of the cancer cell line population whole. While it may prove a useful in determining which ALDH enzymes are potentially contributing towards overall 5-NFN cancer cell toxicity, it provides little evidence towards whether 5-NFNs can specially target the $ALDH^+$ subpopulation. This may help explain why it is difficult to extract which ALDH isoforms directly contribute to 5-NFN sensitivity. As described in **Chapter 4**, 5-NFN toxicity can differ within subpopulations of a heterogeneous tumour, so while this screen provides an insight into the whole cell population ALDH expression, it does not reflect how subpopulations of cancer cells will differ in both their ALDH expression and consequent 5-NFN sensitivity. It will be thus incredibly useful to characterise these ALDH environments, however, experiments whereby the $ALDH^+$ is isolated, analysed for CSC-like behaviour and assessed for 5-NFN sensitivity, would prove more useful. As such, ALDH characterisation between these $ALDH^+$ and $ALDH^-$ counter population will provide a much more in depth characterisation to the exact ALDH isoforms contributing more readily to both CSC-potential and 5-NFN toxicity.

7.2 Future Studies

7.2.1 What are the substrates for 5-nitrofurans in A375 melanoma cells?

Zhuo *et al*. (2012) previously reported that Aldhb is the primary substrate for 5-NFNs in zebrafish melanocytes, using a biotinylated-based pulled down assay. In melanoma cells, I have already shown that 5-NFNs are competitive substrates for ALDH1A3 and ALDH2. However, there are 19 ALDH isoforms in human cells, all with the potential to bio-activate 5-NFNs. Following the results from the Sanger melanoma cell line panel, where it was increasingly difficult to extract exactly which ALDH isoforms contributed to 5-NFN toxicity, it is worth using a similar pull-down method in order to characterise the targets of 5-NFNs in melanoma cells. Working in collaboration with Promega (Madison, WI, USA) to employ their HaloTag system,[185] where a chloroalkane PEG-linker is attached to the 5-NFN compound of interest and validated by proteomic MS, the full target spectrum for 5-NFNs can be characterised. This will not only provide full identification of all ALDH targets for 5-NFNs, but also other side-targets potentially contributing to the anti-cancer activity of these compounds. Determination of all ALDH isoforms that can bio-activate 5-NFNs in

cancer cells will give a much clearer indication of which ALDH isoforms contribute to 5-NFN toxicity and can shed light on differing sensitivities observed in the Sanger melanoma cell line panel.

When considering which ALDH enzymes can bio-activate 5-NFN and contribute to 5-NFN toxicity, it is possible to detail which cancers may also benefit from 5-NFN treatment. As previously reported,[44] cancers have differing expression of specific ALDH isoforms that contribute to CSC activity. Determining which ALDH enzymes may bio-activate 5-NFNs would give some indication which cancers may also benefit from 5-NFN treatment. I have already shown in previous chapters that 5-NFN compounds, both clinical and synthetic, have potent anti-cancer activity in other tumour types. Considering ALDH activity is associated with a wide range of different cancers,[2,80] particularly ALDH1A1;[44] which I have already described as a target for **NFN1**, it is likely that as research into the use of 5-NFNs as potential anti-cancer therapeutics continues, their application of numerous tumour types will develop, determined by ALDH status. If the mode of binding can be determined for each 5-NFN (either computationally or more favourably through crystallography) tagged 5-NFNs can be designed that can potential lessen the interferences the tag may have to normal 5-NFN functionality, and give a realistic picture of the target profile for individual 5-NFNs. Which is important, as the structural differences between **NAZ** and **NFX** are only minor, yet contribute to a very differing activities and selectivity.

This technique would also allow for the characterisation of other targets for 5-NFN, beyond ALDH. Considering recent reports concluding **NAZ** as a STAT3 inhibitor,[135-137] understanding all targets for 5-NFNs in cancers will be important, in both characterising fully how 5-NFNs can drive cancer cell toxicity, and whether these side-targets can also be exploited to develop more potent 5-NFN compounds. In the case of **NAZ**, tumours with both high ALDH1A and STAT3 status should be much more sensitive to treatment. As such, designing of new 5-NFNs compounds that can exploit both bio-activation by ALDH and efficacious side-targets, presents a useful drug discovery platform when designing potent, anti-cancer compounds.

7.2.2 Determining the mechanism of the 5-NFN-ALDH interaction

Considering the mass spectroscopy data, 5-NFN driven inhibition of ALDH is mediated by oxidation on the catalytic cysteine. Crystal trials between purified native ALDH2 and 5-NFNs have been initiated, and crystals have been produced (**Figure 7.2A**), however the diffraction resolution was low (6-15Å – **Figure 7.2B**) and as such, conclusive structural definition could not be determined. Crystal trials are on-going, trying to improve diffraction resolution and ultimately determine the mechanism of 5-NFN-ALDH2 activity. It is expected that oxidation on the catalytic cysteine (Cys302) will be observed, however it will be interesting to conclude exactly which oxidised sulphur species is present, after 5-NFN treatment.

A **B**

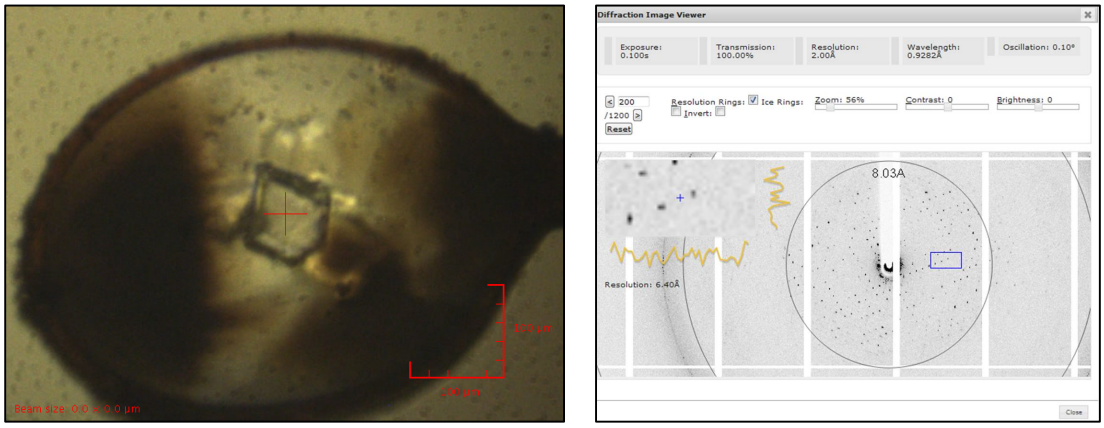

Figure 7.2: Resolution of ALDH2 crystals diffracted too low for conclusive structure solution. **A**) Photograph of purified, untagged ALDH2 crystal mounted prior to diffraction by synchrotron. Crystals were left to soak in 5-NFNs for 1hr in preparation, where it was noted the drug concentrated within the crystal. **B**) Diffraction pattern from diffracted ALDH2 crystal. Resolution was too low for significant determination of structure (8.03Å). Diffraction did suggest that the unit cell had a very large cell edge, with an expected 16 copies in the asymmetric unit.

Importantly, our attention will turn to the mechanism between 5-NFNs and ALDH1A3, the main driver of 5-NFN toxicity in A375 melanoma cells. We hypothesise that ALDH1A3 should interact with 5-NFNs in a similar mechanism that is expected with ALDH2. Mass spectrometry (ESI QTOF MS) data from Professor Thomas D. Hurley highlighted a much stronger double oxidation of ALDH1A1 upon 5-NFN bio-activation, where almost no native ALDH1A1 was observed after treatment. Further, my work from **Chapter 4** described

ALDH1A3 as the primary contributor to Aldefluor™ activity in A375 cells, where Aldefluor™ activity can be potently inhibited, for up to 72hrs, after treatment with 5-NFNs. Considering this, it is likely to assume that 5-NFN bio-activation can cause inhibition of ALDH1A3 (and indeed ALDH1A1 also) through oxidation of a catalytic cysteine. To assess for this, solving the structure of ALDH1A3 upon treatment with 5-NFNs will give the likely modification (covalent or otherwise) that renders this potent inhibition of ALDH1A3 by 5-NFNs. It is also hypothesised that the structural data will also give key indication to how ALDH1A3 can bio-activate 5-NFNs and perhaps it may be likely that the 5-NFN conjugate, post bio-activation, may still be present in the binding pocket.

One challenge when trying to solve the structure of ALDH1A3, even before treatment with 5-NFNs, is that crystallisation conditions have yet to be published. Although it may be possible to use the crystal conditions for ALDH1A1 as a template, considering their structural similarities,[11,152] it will still present a lot of optimisation and there is no guarantee that ALDH1A3 can form crystals to begin with. Although determining the exact 5-NFN-ALDH1A3 mechanism through solving of the structure is a favourable experiment, it may be the case that ALDH1A1 will have to be determined solely, and used as a guideline when interpreting the implied mechanism for ALDH1A3. Working in collaboration with the Institute of Structural and Molecular Biology at The University of Edinburgh further, these experiments can be designed and performed, and are currently on-going.

7.2.3 Can 5-nitrofurans target melanoma stem cells?

5-NFNs can be bio-activated by ALDH enzymes in melanoma cells, where high expression of ALDH, specifically ALDH1A1 and 1A3, is associated with melanoma CSCs[79,151] If 5-NFNs can target the $ALDH^+$ melanoma subpopulation, it is expected that these cells will also exhibit CSC-like properties. To assess whether or not the cells being targeted by 5-NFNs in melanoma are associated with CSC-like behaviour, it is possible to sort melanoma cells into $ALDH^+$ and $ALDH^-$ subpopulation by Aldefluor™ fluorescence-activated cell sorting. As ALDH1A3 activity is the major contributor to Aldefluor™ activity in the A375 melanoma cell line and also the key enzyme in driving toxicity of 5-NFNs in these cells also, it is expected that A375 cells with high Aldefluor™ ($ALDH^+$) will be more sensitive to 5-NFNs. Considering work by Luo *et al*. (2012),[79] it is expected that the $ALDH^+$ subpopulation should also exhibit

CSC-like properties also. Clonogenic assays should be able to distinguish whether or not the $ALDH^+$ subpopulation is more 'stem-like' than its $ALDH^-$ counterpart, where the $ALDH^+$ subpopulation is expected to have significantly increased colony and sphere formation. From this, the sensitivity of the two populations to 5-NFNs can be assessed, where it is likely that $ALDH^+$ melanoma cells will be more sensitivity to 5-NFN treatment. This will thus represent whether or not $ALDH^+$ cells, sorted by Aldefluor™, are likely to contain the melanoma CSC subpopulation and if these cells are more sensitive to 5-NFNs. This can then be confirmed through validation of a second melanoma CSC marker, CD271.[71] Sorting melanoma cells by their CD271 expression should also exhibit stem like properties, such as more clonogenic, increased sphere formation and tumorigenicity.[71,72] As $CD271^+$ melanoma cells are assumed to contain the CSC subpopulation, it would be interesting to determine whether sorted $CD271^+$ melanoma also correlated with ALDH expression, and if so, I then hypothesise the $CD271^+$ subpopulation of melanoma cells should therefore be more sensitive to 5-NFN treatment. This would help determine and characterise the CSC-nice more precisely within melanoma cells, while also serving to conclusively describe how 5-NFNs can target this CSC subpopulation.

The gold standard assay for detection of CSCs is through transplantation into immunosuppressed mice.[27] By transplanting both $ALDH^+$ and $ALDH^-$ melanoma cells into NOD/SCID mice, and monitoring tumour formation, it will be possible to determine whether the $ALDH^+$ cells are more tumorigenic, as thus, contain the melanoma CSC subpopulation. This can be determined if $ALDH^+$ xenographs, in comparison to $ALDH^-$, have a higher frequency of tumour formation upon transplantation, faster and larger tumour growth, and tumour population could also be driven using fewer cells. It would then be interesting to explore whether these $ALDH^+$ populated tumours are more sensitive to 5-NFNs, in comparison to any tumours formed by $ALDH^-$ transplantation. Characterisation of ALDH expression of these populated tumours prior to 5-NFN treatment will be essential to both determine ALDH status and predict sensitivity, especially considering reports $ALDH^+$ melanoma populations will give rise to $ALDH^-$ progeny over time.[79] However, if the $ALDH^+$ cells are found to be more tumorigenic in immunosuppressed mice, coupled with increased sensitivity to 5-NFNs *in vitro* and *in vivo*, this would give a powerful indication that 5-NFNs can target the melanoma CSC niche.

Unpublished preliminary work performed by a post-doctoral research fellow in our lab, Dr Sana Sarvi (University of Edinburgh, UK) describes how clonogensisis of $ALDH^{high}$ A375 melanoma cells is inhibited by **NFN1** treatment, where $ALDH^{low}$ cells, while exhibiting low clonogenic efficiency, were not affected by **NFN1** treatment. This highlight both the importance of ALDH in maintaining A375 CSC behaviour, but importantly, the ability for 5-NFNs to disrupt, and even target this niche. She has also described how $ALDH^{high}$ A375 melanoma cells develop much larger tumours transplanted cells in immunosuppressed mice, comparable to $ALDH^{low}$ transplantation, and begins now to investigate the effect the clinical 5-NFN, **NAZ**, has on these tumours. It is hypothesised that, when treated in combination with other chemotherapeutics (e.g. $BRAF^{v600E}$ inhibitors), $ALDH^{high}$-driven tumours will be highly responsive and drive overall tumour regression.

7.3 Discussion and Concluding Remarks

ALDH1 has been offered up as a favourable target in the treatment of many cancers.[35,45,118] Although most work in targeting ALDH enzymes focuses only on their inhibition,[60,117,152] here I describe a class of compounds, 5-NFNs, which target ALDH1A3, a known melanoma CSC marker,[79] with dual action – ALDH enzymes can bio-activate these compounds in order to drive cell death and ALDH1A3 activity is also consequently inhibited as a direct result. Bio-activation of 5-NFNs is essential in mediating cancer cell death, where ALDH enzymes can generate ROS through reduction of 5-NO_2 moiety.[115] In turn, this is likely to render the ALDH enzyme non-functional, through a double or triple oxidation at the active cysteine (**Figure 7.4**). The exact reaction mechanism for this effect has yet to be established, however it is likely to share similarities to the mechanism in which 5-NFNs are bio-activated by NTRs.[119] 5-NFN bio-activation generates oxygen radicals which cascades through redox cycling to drive ROS accumulation and in turn, oxidize the catalytic cysteine. It is also likely that the 5-NO_2 moiety is lost from the 5-NFN compound, considering zebrafish capillaries are reported to vasodilate upon 5-NFN treatment, attributable to NO formation (Patton 2012, unpublished). Further metabolomic studies in determining the 5-NFN derivatives post-ALDH bio-activation will be required in order to determine the fate of 5-NFNs.

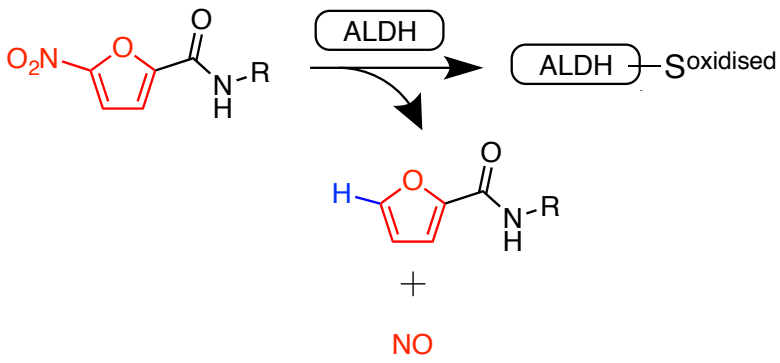

Figure 7.4: Proposed mechanism of interaction between 5-NFNs and ALDH enzymes. 5-NFNs are bio-activated by ALDH enzymes, in turn, promoting the oxidation of the catalytic cysteine on ALDH, rendering the enzyme non-functional, inhibiting activity. NO is consequently produced, and a no-nitro 5-NFN derivative is a likely metabolite.

Inhibition of ALDH1 in cancers has been reported to increase sensitivity to chemotherapeutics, such as cyclophosphamide, reduce CSC-like behaviour and increase oxidative stress.[43,55,56,116] While this is proving an effective way to chemo-sensitise cancers, the ability for 5-NFNs to kill cancer cells as well as inhibit ALDH1, offers a new approach in targeting ALDH in cancers. Up-regulation of ALDH expression in melanoma has been linked to increased chemo-resistance, metastasis and poor clinical outcome,[79,106] where it is now widely hypothesised that there exists an $ALDH^{high}$ CSC subpopulation, that promotes this phenotype and can also drive relapse.[26,43] The ability for 5-NFNs to target and kill the $ALDH^{high}$ CSC niche through ALDH-driven bio-activation offers a new approach in targeting melanoma. Since the discovery of oncogenic driver BRAF-mutations, present in the majority of melanoma cases, in particular $BRAF^{V600E}$, the introduction of targeted therapies (BRAF inhibitors), offered a new and effective treatment for melanoma.[186] Although many patients saw remarkable improvement upon BRAF-inhibitor treatment, it still not a cure, with relapse and resistance seen more often than not.[187] As research into developing new therapeutics targeting the MAPK pathway continues to show promise,[188,189] it is still weathered by prevailing resistance pathways and lack of increase in overall survival.[190-192] As such, discovering new targets for the treatment of melanoma is becoming increasingly important.[193] By using 5-NFNs to target ALDH and treating those patients with melanomas expressing high ALDH profiles, and as such, predicted poor clinical outcomes, should offer a novel therapeutic option that will not only chemo-sensitise their tumours, but also target

and kill those melanoma cells associated with CSC potential and chemo-resistance. This in turn, should help drive tumour regression and delay or even prevent cancer relapse, when treated in combination with current chemotherapeutic options. Although there have been no published reports that the melanoma cells central to mediating relapse upon resistance to MAPK inhibitors are also $ALDH^+$, it will be incredibly interesting to explore whether this is indeed the phenotype observed. If those tumours that are more metastatic, highly chemo-resistant and persistently relapsing are consistent in having higher ALDH expression profiles, it is expected that these tumours should be more sensitive to 5-NFNs. If is the case, then 5-NFNs offer a new therapeutic option that can exploit a biomarker of those tumours that have previously been extremely difficult to treat.

The anti-cancer activity of 5-NFNs has previously been described,[112,126,131,132,135-137] with on-going clinical trials using **NFX** in the treatment of neuroblastoma and medulloblastoma showing promising results.[126] Although the underlying mechanism remains unclear, here I describe the ability for 5-NFNs to target and kill melanoma cells through bio-activation by ALDH1A enzymes. In neuroblastoma, ALDH1A2 has been reported as a predominant CSC marker,[42] and overall ALDH expression is also likely to be higher in these tumours, due the functionality of dopaminergic pathway in neuronal cells. Considering the results I report highlighting the ability for ALDH1A enzymes, but also ALDH2, to bio-activate 5-NFNs and drive cancer cell death, it has become reasonable to assume the anti-cancer activity of **NFX** against neuroblastoma is likely driven by bio-activation by ALDH enzymes. Bio-activation by ALDH2 would also help to explain why **NFX** has such toxic side effects, where alcohol intolerance, gastrointestinal problems and neuronal stress,[122] can be implicated to ALDH2 driven bio-activation as a side target. One of the encouraging results from this project was the potential for the clinical 5-NFN, **NAZ**, to kill melanoma cells, where it displayed some specificity for the melanoma stem cell marker, ALDH1A3. The anti-cancer capacity of **NAZ** has also been reported in myeloma, melanoma and breast cancer, attributing this toxicity to STAT3 inhibition.[135-137] Although these reports do not explore ALDH as a target, bio-activation by ALDH enzymes may offer an explanation to the reported increase in ROS production and oxidative stress upon treatment.[135,137] Although **NAZ** hasn't be shown to directly inhibit STAT3,[135] and with evidence STAT3 expression interplays with the expression of ALDH1A3, it could also be likely that the phenotype described upon **NAZ** treatment could be as a result of ALDH1A3-driven bio-activation only; where further experimentation with

the Promega pull down could confirm this. However, it would be fantastic to discover that **NAZ**, a clinically available 5-NFN, can target 2 separate oncogenic targets in melanoma, both associated with CSC-potential. The specificity **NAZ** displays towards ALDH1 would also help to explain why **NAZ** is much better tolerated than other 5-NFNs, such as **NFX**,[175] largely through the lack of bio-activation by ALDH2, which is likely the main cause of side-effects seen in the majority of 5-NFNs. However, importantly, **NAZ** offers a pre-approved clinical therapeutic with the potential to kill melanoma cells, via a similar mechanism to that described of **NFN1**, with specificity towards the ALDH isoforms most associated with CSC-potential and chemo-resistance in these cancers. Should the results with **NAZ** be further validated on the future experiments described above, especially *in vivo*, the prospect of being able to repurpose pre-existing antibiotics for the novel treatment of melanoma sounds extremely promising.

I further report a new class of synthetic bis-5-NFN compounds, where the lead candidate, **RC-NFN5**, presents a potent anti-cancer compound with increased stability and potential for molecular editing in order to improve potency. Additional work, in both drug development and mechanism of action, is required to fully characterise the potential for **RC-NFN5** to move forward a lead compound in 5-NFN drug discovery efforts – where a *bis*-5-NFN compound, with selectivity similar to **NAZ** while keeping or improving on potency, would be the ideal next step when taking this work forward.

One drawback to this work is the sole reliance of using cancer cell lines to model behaviours of melanoma, and indeed other cancers, in their ALDH status and in response to 5-NFNs treatment. Although cancer cell lines offer a useful tool is characterising drug responses and validating mechanisms of action, their use is truncated when trying to model solid tumour behaviour, for instance the lack of hypoxia found in the majority of tumours isn't well defined in cancer cell lines,[194] but proves an important factor when considering drug responses.[195] *in vivo* modelling and transplantation is always the gold standard for assess how solid tumours will respond to drug treatments, and how this relates back to predictive patient responses.[194] Although the work reported here describes promising sensitivity of melanoma to 5-NFN compounds, the differences between the characteristics of solid tumours and cancer cell lines may actually help to explain why **NFX** is so effect in treating neuroblastomas in patient, but is poorly reflected by their toxicity in both cancer

cells lines reported here, and neuroblastoma cell lines reported previously.[132,153] Considering this increase of sensitivity to **NFX** *in vivo* compared to *in vitro*, it is with great anticipation that we begin *in vivo* studies with melanoma xenographed immunosuppressed mice and the treatment with 5-NFNs, where we hope to discover melanoma xenographs are highly sensitive to our 5-NFN compounds, especially as they are much more potent than **NFX**. It will be interesting also, to see if our clinically available compound, **NAZ**, performs better to **NFX**.

One of the limitations with working with ALDH is being able to precisely take into account the expression of all isoforms within the cellular environment, all of which may contribute to 5-NFN toxicity. Although the preliminary data above conducted through OakLabs did provide a good basis to draw some preliminary conclusions from, the expense needed to outsource this experiment made it unviable to validate through repetition. Although the work with the panel of melanoma cell lines, kindly donated from the Sanger Institute (Cambridge, UK), did offer one potential solution for this, it still proved difficult to extract any meaningful data; also considering the RNA_{seq} of these samples were also not statistically validated. One other revealing problem with ALDH expression also appeared to be fluctuations in the levels of ALDH within cell lines over serial passaging. In **Figure 7.1**, there are apparent differences in the ALDH environment between the A375 samples used for Aldefluor™ sorting and drug treatments. Although it could be argued that treatment in itself was the protagonist of this effect, it is also likely that ALDH levels fluctuate within the cell population as a response to both time and minor changes in the cellular microenvironment. This also explains why the 5-NFN EC_{50} values drift from experiment to experiment, where it is indeed highly possible that the fluctuations in ALDH expression is proportionally represented by changes in 5-NFN sensitivity. In an ideal setting, monitoring the ALDH environment with each experiment would be highly desirable, and could potentially help to indicate other ALDH enzymes that are also primary drivers of 5-NFN toxicity. Through designing a cheap, high-throughput and rapid assay that can analyse the expression pattern of all ALDH isoforms in cells would prove invaluable in counteracting these problems.

In conclusion, here I report a class of compounds, 5-NFNs, that are cytotoxic to cancer cells, including melanoma. Through bio-activation by ALDH enzymes, which are characteristically high in cancers due to their prevalence as a CSC marker, 5-NFN can both inhibit ALDH activity and drive cell death. I report 5-NFN can be bio-activated by ALDH1A3, a key melanoma stem cell marker, in turn driving toxicity in a subpopulation A375 melanoma cell lines. The sensitivity of this subpopulation can consequently be reqed upon knock-down of ALDH1A3, while transient overexpression of ALDH1A3 in turn promotes hypersneisivity, providing further evidence that 5-NFN can target melanoma cells with high ALDH1A3 expression. I describe, in collaboration, the ability for 5-NFNs to potently inhibit ALDH activity, where inhibition is likely caused by a covalent medication on the enzyme itself through oxidation of the active cysteine, rendering the enzyme non-functional. This dual action of 5-NFN offers a novel therapeutic approach, where 5-NFN can both drive cancer cell death and inhibit ALDH activity in cancer cells, a now favourable target shown to hinder CSC-properties and increase chemo-sensitivity. I report both newly synthesised *bis*-5-NFNs are also potent in killing cancer cells and targeting ALDH, and provide a new platform for the generation and development of novel, potent 5-NFN therapeutics for the treatment of cancer. Finally, I importantly describe how the clinically available 5-NFN, **NAZ**, while also able to potently promote cancer cell death, also presents selectivity towards ALDH1 enzymes, the isoforms most associated with CSC-potential. I hereby propose that 5-NFNs have the potential to target $ALDH^{high}$ CSCs within a tumour, to advance the repurposing of clinical 5-NFN pro-drug antibiotics as a future anti-cancer therapeutic option.

8. References

1 Vasiliou, V. & Nebert, D. W. Analysis and update of the human aldehyde dehydrogenase (ALDH) gene family. *Human genomics* **2**, 138-143 (2005).

2 Marchitti, S. A., Brocker, C., Stagos, D. & Vasiliou, V. Non-P450 aldehyde oxidizing enzymes: the aldehyde dehydrogenase superfamily. *Expert opinion on drug metabolism & toxicology* **4**, 697-720 (2008).

3 Lindahl, T. Instability and decay of the primary structure of DNA. *Nature* **362**, 709-715 (1993).

4 Garaycoechea, J. I. *et al.* Genotoxic consequences of endogenous aldehydes on mouse haematopoietic stem cell function. *Nature* **489**, 571-575 (2012).

5 Duester, G. Families of retinoid dehydrogenases regulating vitamin A function: production of visual pigment and retinoic acid. *European journal of biochemistry / FEBS* **267**, 4315-4324 (2000).

6 Seiler, N. & Eichentopf, B. 4-aminobutyrate in mammalian putrescine catabolism. *Biochem J* **152**, 201-210 (1975).

7 Vasiliou, V., Thompson, D. C., Smith, C., Fujita, M. & Chen, Y. Aldehyde dehydrogenases: from eye crystallins to metabolic disease and cancer stem cells. *Chem Biol Interact* **202**, 2-10 (2013).

8 Jackson, B. *et al.* Update on the aldehyde dehydrogenase gene (ALDH) superfamily. *Human genomics* **5**, 283-303 (2011).

9 Tanner, J. J. SAXS fingerprints of aldehyde dehydrogenase oligomers. *Data in brief* **5**, 745-751 (2015).

10 Gross, E. R. *et al.* A personalized medicine approach for Asian Americans with the aldehyde dehydrogenase 2*2 variant. *Annual review of pharmacology and toxicology* **55**, 107-127 (2015).

11 Liu, Z. J. *et al.* The first structure of an aldehyde dehydrogenase reveals novel interactions between NAD and the Rossmann fold. *Nature structural biology* **4**, 317-326 (1997).

12 Steinmetz, C. G., Xie, P., Weiner, H. & Hurley, T. D. Structure of mitochondrial aldehyde dehydrogenase: the genetic component of ethanol aversion. *Structure* **5**, 701-711 (1997).

13 Storms, R. W. *et al.* Isolation of primitive human hematopoietic progenitors on the basis of aldehyde dehydrogenase activity. *Proceedings of the National Academy of Sciences of the United States of America* **96**, 9118-9123 (1999).

14 Ma, I. & Allan, A. L. The role of human aldehyde dehydrogenase in normal and cancer stem cells. *Stem cell reviews* **7**, 292-306 (2011).

15 Ginestier, C. *et al.* ALDH1 is a marker of normal and malignant human mammary stem cells and a predictor of poor clinical outcome. *Cell Stem Cell* **1** (2007).

16 Moreb, J. S. Aldehyde dehydrogenase as a marker for stem cells. *Curr Stem Cell Res Ther* **3**, 237-246 (2008).

17 Tomita, H., Tanaka, K., Tanaka, T. & Hara, A. Aldehyde dehydrogenase 1A1 in stem cells and cancer. *Oncotarget* **7**, 11018-11032 (2016).

18 Chambon, P. A decade of molecular biology of retinoic acid receptors. *The FASEB Journal* **10**, 940-954 (1996).

19 Collins, S. J. The role of retinoids and retinoic acid receptors in normal hematopoiesis. *Leukemia* **16**, 1896-1905 (2002).
20 Chute, J. P. *et al.* Inhibition of aldehyde dehydrogenase and retinoid signaling induces the expansion of human hematopoietic stem cells. *Proc Natl Acad Sci U S A* **103**, 11707-11712 (2006).
21 Perin, E. C. *et al.* Randomized, double-blind pilot study of transendocardial injection of autologous aldehyde dehydrogenase-bright stem cells in patients with ischemic heart failure. *American heart journal* **163**, 415-421, 421.e411 (2012).
22 Langevin, F., Crossan, G. P., Rosado, I. V., Arends, M. J. & Patel, K. J. Fancd2 counteracts the toxic effects of naturally produced aldehydes in mice. *Nature* **475**, 53-58 (2011).
23 Oberbeck, N. *et al.* Maternal Aldehyde Elimination during Pregnancy Preserves the Fetal Genome. *Molecular Cell* **55**, 807-817 (2014).
24 Reya, T., Morrison, S. J., Clarke, M. F. & Weissman, I. L. Stem cells, cancer, and cancer stem cells. *Nature* **414**, 105-111 (2001).
25 Magee, J. A., Piskounova, E. & Morrison, S. J. Cancer stem cells: impact, heterogeneity, and uncertainty. *Cancer Cell* **21**, 283-296 (2012).
26 Beck, B. & Blanpain, C. Unravelling cancer stem cell potential. *Nat Rev Cancer* **13**, 727-738 (2013).
27 Clarke, M. F. *et al.* Cancer stem cells--perspectives on current status and future directions: AACR Workshop on cancer stem cells. *Cancer Res* **66**, 9339-9344 (2006).
28 Setoguchi, T., Taga, T. & Kondo, T. Cancer stem cells persist in many cancer cell lines. *Cell Cycle* **3**, 414-415 (2004).
29 Abdullah, L. N. & Chow, E. K.-H. Mechanisms of chemoresistance in cancer stem cells. *Clinical and Translational Medicine* **2**, 3-3 (2013).
30 Schatton, T. *et al.* Identification of cells initiating human melanomas. *Nature* **451**, 345-349 (2008).
31 Fleischman, A. G. *ALDH marks leukemia stem cell*. Vol. 119 (2012).
32 Marcato, P., Dean, C. A., Giacomantonio, C. A. & Lee, P. W. K. Aldehyde dehydrogenase: Its role as a cancer stem cell marker comes down to the specific isoform. *Cell Cycle* **10**, 1378-1384 (2011).
33 Boonyaratanakornkit, J. B. *et al.* Selection of tumorigenic melanoma cells using ALDH. *J Invest Dermatol* **130**, 2799-2808 (2010).
34 Santini, R. *et al.* Hedgehog-GLI signaling drives self-renewal and tumorigenicity of human melanoma-initiating cells. *Stem Cells* **30**, 1808-1818 (2012).
35 Luo, Y. *et al.* ALDH1A isozymes are markers of human melanoma stem cells and potential therapeutic targets. *Stem Cells* **30**, 2100-2113 (2012).
36 Huang, E. H. *et al.* Aldehyde dehydrogenase 1 is a marker for normal and malignant human colonic stem cells (SC) and tracks SC overpopulation during colon tumorigenesis. *Cancer Res* **69**, 3382-3389 (2009).
37 Rasheed, Z. A. *et al.* Prognostic significance of tumorigenic cells with mesenchymal features in pancreatic adenocarcinoma. *J Natl Cancer Inst* **102**, 340-351 (2010).
38 Ucar, D. *et al.* Aldehyde dehydrogenase activity as a functional marker for lung cancer. *Chem Biol Interact* **178** (2009).
39 Meng, E. *et al.* ALDH1A1 maintains ovarian cancer stem cell-like properties by altered regulation of cell cycle checkpoint and DNA repair network signaling. *PloS one* **9**, e107142 (2014).
40 Choi, S. A. *et al.* Identification of brain tumour initiating cells using the stem cell marker aldehyde dehydrogenase. *European Journal of Cancer* **50**, 137-149 (2014).

41 Foster, S. J., Winstead, L., Driscoll, T. A. & Balber, A. E. Aldehyde Dehydrogenase (ALDH) Activity Resolves Neuroblastoma (NB) Cells and Hematopoietic Stem and Progenitor Cells (HPC) in Graft Material: Potential Method for Clinical Purging. *Blood* **104**, 2869-2869 (2004).
42 Hartomo, T. B. *et al.* Involvement of aldehyde dehydrogenase 1A2 in the regulation of cancer stem cell properties in neuroblastoma. *International journal of oncology* **46**, 1089-1098 (2015).
43 Raha, D. *et al.* The cancer stem cell marker aldehyde dehydrogenase is required to maintain a drug-tolerant tumor cell subpopulation. *Cancer Res* **74**, 3579-3590 (2014).
44 Januchowski, R., Wojtowicz, K. & Zabel, M. The role of aldehyde dehydrogenase (ALDH) in cancer drug resistance. *Biomedecine & pharmacotherapie* **67**, 669-680 (2013).
45 Pors, K. & Moreb, J. S. Aldehyde dehydrogenases in cancer: an opportunity for biomarker and drug development? *Drug Discovery Today* **19**, 1953-1963 (2014).
46 Rodriguez-Torres, M. & Allan, A. L. Aldehyde dehydrogenase as a marker and functional mediator of metastasis in solid tumors. *Clinical & Experimental Metastasis* **33**, 97-113 (2016).
47 Croker, A. K. *et al.* High aldehyde dehydrogenase and expression of cancer stem cell markers selects for breast cancer cells with enhanced malignant and metastatic ability. *J Cell Mol Med* **13** (2009).
48 Ginestier, C. *et al.* ALDH1 Is a Marker of Normal and Malignant Human Mammary Stem Cells and a Predictor of Poor Clinical Outcome. *Cell Stem Cell* **1**, 555-567 (2007).
49 Qiu, Y. *et al.* ALDH(+)/CD44(+) cells in breast cancer are associated with worse prognosis and poor clinical outcome. *Experimental and molecular pathology* **100**, 145-150 (2016).
50 Yan, J., De Melo, J., Cutz, J. C., Aziz, T. & Tang, D. Aldehyde dehydrogenase 3A1 associates with prostate tumorigenesis. *Br J Cancer* **110**, 2593-2603 (2014).
51 Wu, J., Mu, Q., Thiviyanathan, V., Annapragada, A. & Vigneswaran, N. Cancer stem cells are enriched in Fanconi anemia head and neck squamous cell carcinomas. *International journal of oncology* **45**, 2365-2372 (2014).
52 Patel, K. J. Fanconi anemia and breast cancer susceptibility. *Nat Genet* **39**, 142-143 (2007).
53 Hilton, J. Role of Aldehyde Dehydrogenase in Cyclophosphamide-resistant L1210 Leukemia. *Cancer Research* **44**, 5156-5160 (1984).
54 Moreb, J. S., Maccow, C., Schweder, M. & Hecomovich, J. Expression of antisense RNA to aldehyde dehydrogenase class-1 sensitizes tumor cells to 4-hydroperoxycyclophosphamide in vitro. *The Journal of pharmacology and experimental therapeutics* **293**, 390-396 (2000).
55 Liu, J. *et al.* Lung cancer tumorigenicity and drug resistance are maintained through ALDH(hi)CD44(hi) tumor initiating cells. *Oncotarget* **4**, 1698-1711 (2013).
56 Croker, A. K. & Allan, A. L. Inhibition of aldehyde dehydrogenase (ALDH) activity reduces chemotherapy and radiation resistance of stem-like ALDHhiCD44+ human breast cancer cells. *Breast Cancer Research and Treatment* **133**, 75-87 (2011).
57 Luo, Y. *et al.* Side Population Cells from Human Melanoma Tumors Reveal Diverse Mechanisms for Chemoresistance. *Journal of Investigative Dermatology* **132**, 2440-2450 (2012).

58 Jimeno, A. *et al.* A direct pancreatic cancer xenograft model as a platform for cancer stem cell therapeutic development. *Molecular cancer therapeutics* **8**, 310-314 (2009).
59 Mao, P. *et al.* Mesenchymal glioma stem cells are maintained by activated glycolytic metabolism involving aldehyde dehydrogenase 1A3. *Proc Natl Acad Sci U S A* **110**, 8644-8649 (2013).
60 Koppaka, V. *et al.* Aldehyde Dehydrogenase Inhibitors: a Comprehensive Review of the Pharmacology, Mechanism of Action, Substrate Specificity, and Clinical Application. *Pharmacological Reviews* **64**, 520-539 (2012).
61 Sladek, N. E. Aldehyde dehydrogenase-mediated cellular relative insensitivity to the oxazaphosphorines. *Current pharmaceutical design* **5**, 607-625 (1999).
62 Zhang, J., Tian, Q., Chan, S. Y., Duan, W. & Zhou, S. Insights into oxazaphosphorine resistance and possible approaches to its circumvention. *Drug Resistance Updates* **8**, 271-297 (2005).
63 Giorgianni, F., Bridson, P. K., Sorrentino, B. P., Pohl, J. & Blakley, R. L. Inactivation of aldophosphamide by human aldehyde dehydrogenase isozyme 3. *Biochemical Pharmacology* **60**, 325-338 (2000).
64 Bunting, K. D. & Townsend, A. J. Protection by transfected rat or human class 3 aldehyde dehydrogenase against the cytotoxic effects of oxazaphosphorine alkylating agents in hamster V79 cell lines. Demonstration of aldophosphamide metabolism by the human cytosolic class 3 isozyme. *J Biol Chem* **271**, 11891-11896 (1996).
65 Formelli, F. & Cleris, L. Synthetic Retinoid Fenretinide Is Effective against a Human Ovarian Carcinoma Xenograft and Potentiates Cisplatin Activity. *Cancer Research* **53**, 5374-5376 (1993).
66 Moreb, J. S. *et al.* Retinoic Acid Down-Regulates Aldehyde Dehydrogenase and Increases Cytotoxicity of 4-Hydroperoxycyclophosphamide and Acetaldehyde. *Journal of Pharmacology and Experimental Therapeutics* **312**, 339-345 (2005).
67 Fang, D. *et al.* A Tumorigenic Subpopulation with Stem Cell Properties in Melanomas. *Cancer Research* **65**, 9328-9337 (2005).
68 Quintana, E. *et al.* Efficient tumour formation by single human melanoma cells. *Nature* **456**, 593-598 (2008).
69 Lee, N., Barthel, S. R. & Schatton, T. Melanoma Stem Cells and Metastasis: Mimicking Hematopoietic Cell Trafficking? *Laboratory investigation; a journal of technical methods and pathology* **94**, 13-30 (2014).
70 Monzani, E. *et al.* Melanoma contains CD133 and ABCG2 positive cells with enhanced tumourigenic potential. *European Journal of Cancer* **43**, 935-946 (2007).
71 Boiko, A. D. *et al.* Human melanoma-initiating cells express neural crest nerve growth factor receptor CD271. *Nature* **466**, 133-137 (2010).
72 Civenni, G. *et al.* Human CD271-Positive Melanoma Stem Cells Associated with Metastasis Establish Tumor Heterogeneity and Long-term Growth. *Cancer Research* **71**, 3098-3109 (2011).
73 Sládek, N. E., Kollander, R., Sreerama, L. & Kiang, D. T. Cellular levels of aldehyde dehydrogenases (ALDH1A1 and ALDH3A1) as predictors of therapeutic responses to cyclophosphamide-based chemotherapy of breast cancer: a retrospective study. *Cancer Chemotherapy and Pharmacology* **49**, 309-321.
74 Schnier, J. B. *et al.* Identification of cytosolic aldehyde dehydrogenase 1 from non-small cell lung carcinomas as a flavopiridol-binding protein. *FEBS Letters* **454**, 100-104 (1999).

75 Januchowski, R., Wojtowicz, K. & Zabel, M. The role of aldehyde dehydrogenase (ALDH) in cancer drug resistance. *Biomedicine & Pharmacotherapy* **67**, 669-680 (2013).
76 Boonyaratanakornkit, J. B. *et al.* Selection of Tumorigenic Melanoma Cells Using ALDH. *Journal of Investigative Dermatology* **130**, 2799-2808 (2010).
77 Prasmickaite, L. *et al.* Aldehyde Dehydrogenase (ALDH) Activity Does Not Select for Cells with Enhanced Aggressive Properties in Malignant Melanoma. *PloS one* **5**, e10731 (2010).
78 Nguyen, N., Couts, K. L., Luo, Y. & Fujita, M. Understanding melanoma stem cells. *Melanoma management* **2**, 179-188 (2015).
79 Luo, Y. *et al.* ALDH1A isozymes are markers of human melanoma stem cells and potential therapeutic targets. *Stem Cells* **30** (2012).
80 Marcato, P., Dean, C. A., Giacomantonio, C. A. & Lee, P. W. Aldehyde dehydrogenase: its role as a cancer stem cell marker comes down to the specific isoform. *Cell Cycle* **10** (2011).
81 Contador-Troca, M. *et al.* Dioxin receptor regulates aldehyde dehydrogenase to block melanoma tumorigenesis and metastasis. *Molecular Cancer* **14**, 1-14 (2015).
82 dos Santos, R. V. & da Silva, L. M. A possible explanation for the variable frequencies of cancer stem cells in tumors. *PloS one* **8**, e69131 (2013).
83 Deng, S. *et al.* Distinct expression levels and patterns of stem cell marker, aldehyde dehydrogenase isoform 1 (ALDH1), in human epithelial cancers. *PloS one* **5**, e10277 (2010).
84 Singh, S. *et al.* Aldehyde Dehydrogenases in Cellular Responses to Oxidative/electrophilic Stress. *Free radical biology & medicine* **56**, 89-101 (2013).
85 Ohanna, M. *et al.* Secretome from senescent melanoma engages the STAT3 pathway to favor reprogramming of naive melanoma towards a tumor-initiating cell phenotype. *Oncotarget* **4**, 2212-2224 (2013).
86 Shao, C. *et al.* Essential Role of Aldehyde Dehydrogenase 1A3 for the Maintenance of Non–Small Cell Lung Cancer Stem Cells Is Associated with the STAT3 Pathway. *Clinical Cancer Research* **20**, 4154-4166 (2014).
87 Johnston, P. A. & Grandis, J. R. STAT3 SIGNALING: Anticancer Strategies and Challenges. *Molecular Interventions* **11**, 18-26 (2011).
88 Wu, Z. S., Cheng, X. W., Wang, X. N. & Song, N. J. Prognostic significance of phosphorylated signal transducer and activator of transcription 3 and suppressor of cytokine signaling 3 expression in human cutaneous melanoma. *Melanoma Res* **21**, 483-490 (2011).
89 O'Reilly, K. E. *et al.* Hedgehog Pathway Blockade Inhibits Melanoma Cell Growth in Vitro and in Vivo. *Pharmaceuticals* **6**, 1429-1450 (2013).
90 Santini, R. *et al.* HEDGEHOG-GLI Signaling Drives Self-Renewal and Tumorigenicity of Human Melanoma-Initiating Cells. *STEM CELLS* **30**, 1808-1818 (2012).
91 Santini, R. *et al.* SOX2 regulates self-renewal and tumorigenicity of human melanoma-initiating cells. *Oncogene* **33**, 4697-4708 (2014).
92 Krupenko, N. I. *et al.* ALDH1L2 is the mitochondrial homolog of 10-formyltetrahydrofolate dehydrogenase. *J Biol Chem* **285**, 23056-23063 (2010).
93 Kim, Y.-I. Folic Acid Supplementation and Cancer Risk: Point. *Cancer Epidemiology Biomarkers & Prevention* **17**, 2220-2225 (2008).
94 Ebbing, M. *et al.* Cancer incidence and mortality after treatment with folic acid and vitamin B12. *Jama* **302**, 2119-2126 (2009).
95 Deghan Manshadi, S. *et al.* Folic acid supplementation promotes mammary tumor progression in a rat model. *PloS one* **9**, e84635 (2014).

96 Vollset, S. E. *et al.* Effects of folic acid supplementation on overall and site-specific cancer incidence during the randomised trials: meta-analyses of data on 50,000 individuals. *The Lancet* **381**, 1029-1036 (2008).
97 Qin, X. *et al.* Folic acid supplementation and cancer risk: A meta-analysis of randomized controlled trials. *International Journal of Cancer* **133**, 1033-1041 (2013).
98 Piskounova, E. *et al.* Oxidative stress inhibits distant metastasis by human melanoma cells. *Nature* **527**, 186-191 (2015).
99 Fan, J. *et al.* Quantitative flux analysis reveals folate-dependent NADPH production. *Nature* **510**, 298-302 (2014).
100 Luzzi, K. J. *et al.* Multistep nature of metastatic inefficiency: dormancy of solitary cells after successful extravasation and limited survival of early micrometastases. *Am J Pathol* **153**, 865-873 (1998).
101 Nakahata, K. *et al.* Aldehyde Dehydrogenase 1 (ALDH1) Is a Potential Marker for Cancer Stem Cells in Embryonal Rhabdomyosarcoma. *PloS one* **10**, e0125454 (2015).
102 Kreso, A. & Dick, J. E. Evolution of the cancer stem cell model. *Cell Stem Cell* **14**, 275-291 (2014).
103 Chen, J. *et al.* A restricted cell population propagates glioblastoma growth after chemotherapy. *Nature* **488**, 522-526 (2012).
104 Frank, N. Y., Schatton, T. & Frank, M. H. The therapeutic promise of the cancer stem cell concept. *The Journal of clinical investigation* **120**, 41-50 (2010).
105 Hong, W. K. *et al.* 13-cis-retinoic acid in the treatment of oral leukoplakia. *The New England journal of medicine* **315**, 1501-1505 (1986).
106 Yue, L. *et al.* Targeting ALDH1 to decrease tumorigenicity, growth and metastasis of human melanoma. *Melanoma Res* **25** (2015).
107 Ravindran Menon, D., Das, S., Krepler, C. & Vultur, A. A stress-induced early innate response causes multidrug tolerance in melanoma. **34**, 4448-4459 (2015).
108 Tirosh, I. *et al.* Dissecting the multicellular ecosystem of metastatic melanoma by single-cell RNA-seq. *Science* **352**, 189-196 (2016).
109 Lowe, E. D., Gao, G. Y., Johnson, L. N. & Keung, W. M. Structure of daidzin, a naturally occurring anti-alcohol-addiction agent, in complex with human mitochondrial aldehyde dehydrogenase. *J Med Chem* **51**, 4482-4487 (2008).
110 Morgan, C. A., Parajuli, B., Buchman, C. D., Dria, K. & Hurley, T. D. N,N-diethylaminobenzaldehyde (DEAB) as a substrate and mechanism-based inhibitor for human ALDH isoenzymes. *Chemico-biological interactions* **234**, 18-28 (2015).
111 Luo, M., Gates, K. S., Henzl, M. T. & Tanner, J. J. Diethylaminobenzaldehyde is a covalent, irreversible inactivator of ALDH7A1. *ACS chemical biology* **10**, 693-697 (2015).
112 Koto, K. S. *et al.* Antitumor activity of nifurtimox is enhanced with tetrathiomolybdate in medulloblastoma. *International journal of oncology* **38**, 1329-1341 (2011).
113 Moore, S. A. *et al.* Sheep liver cytosolic aldehyde dehydrogenase: the structure reveals the basis for the retinal specificity of class 1 aldehyde dehydrogenases. *Structure* **6**, 1541-1551 (1998).
114 Cen, D., Brayton, D., Shahandeh, B., Meyskens, F. L., Jr. & Farmer, P. J. Disulfiram facilitates intracellular Cu uptake and induces apoptosis in human melanoma cells. *J Med Chem* **47**, 6914-6920 (2004).
115 Zhou, L. *et al.* ALDH2 mediates 5-nitrofuran activity in multiple species. *Chemistry & biology* **19**, 883-892 (2012).

116 Liu, P. *et al.* Cytotoxic effect of disulfiram/copper on human glioblastoma cell lines and ALDH-positive cancer-stem-like cells. *Br J Cancer* **107**, 1488-1497 (2012).
117 Khanna, M. *et al.* Discovery of a Novel Class of Covalent Inhibitor for Aldehyde Dehydrogenases. *J Biol Chem* **286**, 43486-43494 (2011).
118 Yang, Y. *et al. NEK2 mediates ALDH1A1-dependent drug resistance in multiple myeloma*. (2014).
119 Viodé, C. *et al.* Enzymatic reduction studies of nitroheterocycles. *Biochemical Pharmacology* **57**, 549-557 (1999).
120 Rassi, A., Rassi, A. & Marin-Neto, J. A. Chagas disease. *The Lancet* **375**, 1388-1402 (2010).
121 WHO. World Health Organisation Model Lists of Essential Medicines. *19th edition* (2015).
122 Castro, J. A., de Mecca, M. M. & Bartel, L. C. Toxic side effects of drugs used to treat Chagas' disease (American trypanosomiasis). *Human & experimental toxicology* **25**, 471-479 (2006).
123 Vass, M., Hruska, K. & Franek, M. Nitrofuran antibiotics: a review on the application, prohibition and residual analysis. *Veterinarini Medicina* **53**, 469-500 (2008).
124 Spry, L. A., Zenser, T. V., Cohen, S. M. & Davis, B. B. Role of renal metabolism and excretion in 5-nitrofuran-induced uroepithelial cancer in the rat. *The Journal of clinical investigation* **76**, 1025-1031 (1985).
125 McCalla, D. R. Mutagenicity of nitrofuran derivatives: review. *Environmental mutagenesis* **5**, 745-765 (1983).
126 Saulnier Sholler, G. L. *et al.* A phase 1 study of nifurtimox in patients with relapsed/refractory neuroblastoma. *Journal of pediatric hematology/oncology* **33**, 25-30 (2011).
127 Nouws, J. F., Vree, T. B., Aerts, M. M., Degen, M. & Driessens, F. Some pharmacokinetic data about furaltadone and nitrofurazone administered orally to preruminant calves. *The Veterinary quarterly* **9**, 208-214 (1987).
128 Conklin, J. D. The pharmacokinetics of nitrofurantoin and its related bioavailability. *Antibiotics and chemotherapy* **25**, 233-252 (1978).
129 González-Martin, G., Thambo, S., Paulos, C., Vásquez, I. & Paredes, J. The pharmacokinetics of nifurtimox in chronic renal failure. *European Journal of Clinical Pharmacology* **42**, 671-673 (1992).
130 Boiani, M. *et al.* Mode of action of Nifurtimox and N-oxide-containing heterocycles against Trypanosoma cruzi: Is oxidative stress involved? *Biochemical Pharmacology* **79**, 1736-1745 (2010).
131 Saulnier Sholler, G. L., Kalkunte, S., Greenlaw, C., McCarten, K. & Forman, E. Antitumor activity of nifurtimox observed in a patient with neuroblastoma. *Journal of pediatric hematology/oncology* **28**, 693-695 (2006).
132 Saulnier Sholler, G. L. *et al.* Nifurtimox induces apoptosis of neuroblastoma cells in vitro and in vivo. *Journal of pediatric hematology/oncology* **31**, 187-193 (2009).
133 Du, M., Zhang, L., Scorsone, K. A., Woodfield, S. E. & Zage, P. E. Nifurtimox Is Effective Against Neural Tumor Cells and Is Synergistic with Buthionine Sulfoximine. *Scientific Reports* **6**, 27458 (2016).
134 Cabanillas Stanchi, K. M., Bruchelt, G., Handgretinger, R. & Holzer, U. Nifurtimox reduces N-Myc expression and aerobic glycolysis in neuroblastoma. *Cancer biology & therapy* **16**, 1353-1363 (2015).
135 Nelson, E. A. *et al. Nifuroxazide inhibits survival of multiple myeloma cells by directly inhibiting STAT3*. Vol. 112 (2008).

136 Yang, F. *et al.* Nifuroxazide induces apoptosis and impairs pulmonary metastasis in breast cancer model. *Cell death & disease* **6**, e1701 (2015).
137 Zhu, Y. *et al.* Nifuroxazide exerts potent anti-tumor and anti-metastasis activity in melanoma. *Scientific Reports* **6**, 20253 (2016).
138 Kamat, A. M. & Lamm, D. L. Antitumor activity of common antibiotics against superficial bladder cancer. *Urology* **63**, 457-460 (2004).
139 Kitson, T. M. The effect of 5,5'-dithiobis(1-methyltetrazole) on cytoplasmic aldehyde dehydrogenase and its implications for cephalosporin-alcohol reactions. *Alcoholism, clinical and experimental research* **10**, 27-32 (1986).
140 Nene, A., Chen, C.-H., Disatnik, M.-H., Cruz, L. & Mochly-Rosen, D. Aldehyde dehydrogenase 2 activation and coevolution of its εPKC-mediated phosphorylation sites. *Journal of Biomedical Science* **24**, 3 (2017).
141 Weiss, J. T. *et al.* N-alkynyl derivatives of 5-fluorouracil: susceptibility to palladium-mediated dealkylation and toxigenicity in cancer cell culture. *Frontiers in Chemistry* **2**, 56 (2014).
142 Amanuma, Y. *et al.* Protective role of ALDH2 against acetaldehyde-derived DNA damage in oesophageal squamous epithelium. *Scientific Reports* **5**, 14142 (2015).
143 Wojciechowska, S., van Rooijen, E., Ceol, C., Patton, E. E. & White, R. M. Generation and analysis of zebrafish melanoma models. *Methods in cell biology* **134**, 531-549 (2016).
144 Wojciechowska, S., Zeng, Z., Lister, J. A., Ceol, C. J. & Patton, E. E. Melanoma Regression and Recurrence in Zebrafish. *Methods Mol Biol* **1451**, 143-153 (2016).
145 Morgan, C. A. & Hurley, T. D. Characterization of two distinct structural classes of selective aldehyde dehydrogenase 1A1 inhibitors. *J Med Chem* **58**, 1964-1975 (2015).
146 Dolinsky, T. J. *et al.* PDB2PQR: expanding and upgrading automated preparation of biomolecular structures for molecular simulations. *Nucleic Acids Res* **35**, W522-525 (2007).
147 Li, H., Robertson, A. D. & Jensen, J. H. Very fast empirical prediction and rationalization of protein pKa values. *Proteins* **61**, 704-721 (2005).
148 O'Boyle, N. M. *et al.* Open Babel: An open chemical toolbox. *Journal of cheminformatics* **3**, 33 (2011).
149 Cosconati, S. *et al.* Virtual Screening with AutoDock: Theory and Practice. *Expert opinion on drug discovery* **5**, 597-607 (2010).
150 Huey, R., Morris, G. M., Olson, A. J. & Goodsell, D. S. A semiempirical free energy force field with charge-based desolvation. *Journal of computational chemistry* **28**, 1145-1152 (2007).
151 Boonyaratanakornkit, J. B. *et al.* Selection of tumorigenic melanoma cells using ALDH. *J Invest Dermatol* **130** (2010).
152 Morgan, C. A. & Hurley, T. D. Development of a high-throughput in vitro assay to identify selective inhibitors for human ALDH1A1. *Chem Biol Interact* **234**, 29-37 (2015).
153 McNeil, E. M., Ritchie, A. M. & Melton, D. W. The toxicity of nitrofuran compounds on melanoma and neuroblastoma cells is enhanced by Olaparib and ameliorated by melanin pigment. *DNA repair* **12**, 1000-1006 (2013).
154 Perez-Miller, S. *et al.* Alda-1 is an agonist and chemical chaperone for the common human aldehyde dehydrogenase 2 variant. *Nat Struct Mol Biol* **17**, 159-164 (2010).
155 Wang, M.-F., Han, C.-L. & Yin, S.-J. Substrate specificity of human and yeast aldehyde dehydrogenases. *Chemico-Biological Interactions* **178**, 36-39 (2009).

156 Eggert, M. W., Byrne, M. E. & Chambers, R. P. Kinetic Involvement of Acetaldehyde Substrate Inhibition on the Rate Equation of Yeast Aldehyde Dehydrogenase. *Applied Biochemistry and Biotechnology* **168**, 824-833 (2012).
157 Neubauer, R. *et al.* Potent Inhibition of Aldehyde Dehydrogenase-2 by Diphenyleneiodonium: Focus on Nitroglycerin Bioactivation. *Molecular Pharmacology* **84**, 407-414 (2013).
158 Canuto, R. A. *et al.* The effect of a novel irreversible inhibitor of aldehyde dehydrogenases 1 and 3 on tumour cell growth and death. *Chemico-Biological Interactions* **130–132**, 209-218 (2001).
159 Han, X. *et al.* A2780 human ovarian cancer cells with acquired paclitaxel resistance display cancer stem cell properties. *Oncol Lett* **6**, 1295-1298 (2013).
160 The Human Protein Atlas. *Tissue: Skin: ALDH1A3* (Accessed: 2016).
161 Dixon, S. J. *et al.* Ferroptosis: An Iron-Dependent Form of Non-Apoptotic Cell Death. *Cell* **149**, 1060-1072 (2012).
162 Xie, Y. *et al.* Ferroptosis: process and function. *Cell Death Differ* **23**, 369-379 (2016).
163 Yagoda, N. *et al.* RAS-RAF-MEK-dependent oxidative cell death involving voltage-dependent anion channels. *Nature* **447**, 865-869 (2007).
164 Cao, J. Y. & Dixon, S. J. Mechanisms of ferroptosis. *Cellular and Molecular Life Sciences* **73**, 2195-2209 (2016).
165 Jean, E. *et al.* Aldehyde dehydrogenase activity promotes survival of human muscle precursor cells. *Journal of Cellular and Molecular Medicine* **15**, 119-133 (2011).
166 Fadok, V. A., Bratton, D. L., Frasch, S. C., Warner, M. L. & Henson, P. M. The role of phosphatidylserine in recognition of apoptotic cells by phagocytes. *Cell Death Differ* **5**, 551-562 (1998).
167 Fadok, V. A. *et al.* A receptor for phosphatidylserine-specific clearance of apoptotic cells. *Nature* **405**, 85-90 (2000).
168 Magtanong, L., Ko, P. J. & Dixon, S. J. Emerging roles for lipids in non-apoptotic cell death. *Cell Death Differ* **23**, 1099-1109 (2016).
169 Friedmann Angeli, J. P. *et al.* Inactivation of the ferroptosis regulator Gpx4 triggers acute renal failure in mice. *Nature cell biology* **16**, 1180-1191 (2014).
170 Powell, W. S. & Rokach, J. The eosinophil chemoattractant 5-oxo-ETE and the OXE receptor. *Progress in lipid research* **52**, 651-665 (2013).
171 Jacobs, F. M. *et al.* Retinoic acid counteracts developmental defects in the substantia nigra caused by Pitx3 deficiency. *Development (Cambridge, England)* **134**, 2673-2684 (2007).
172 Galter, D., Buervenich, S., Carmine, A., Anvret, M. & Olson, L. ALDH1 mRNA: presence in human dopamine neurons and decreases in substantia nigra in Parkinson's disease and in the ventral tegmental area in schizophrenia. *Neurobiology of disease* **14**, 637-647 (2003).
173 Yao, L. *et al.* Inhibition of aldehyde dehydrogenase-2 suppresses cocaine seeking by generating THP, a cocaine use–dependent inhibitor of dopamine synthesis. *Nature medicine* **16**, 1024-1028 (2010).
174 Bacolod, M. D. *et al.* The gene expression profiles of medulloblastoma cell lines resistant to preactivated cyclophosphamide. *Current cancer drug targets* **8**, 172-179 (2008).
175 Bouree, P., Chaput, J. C., Krainik, F., Michel, H. & Trepo, C. [Double-blind controlled study of the efficacy of nifuroxazide versus placebo in the treatment of acute diarrhea in adults]. *Gastroenterologie clinique et biologique* **13**, 469-472 (1989).
176 Gao, F. *et al.* Residue depletion of nifuroxazide in broiler chicken. *Journal of the science of food and agriculture* **93**, 2172-2178 (2013).

177 Holmberg, L. *et al.* Adverse reactions to nitrofurantoin. *The American Journal of Medicine* **69**, 733-738 (1980).
178 Ali, B. H. Pharmacological, Therapeutic and Toxicological Properties of Furazolidone: Some Recent Research. *Veterinary Research Communications* **23**, 343-360 (1999).
179 Rabbani, G. H., Butler, T., Shahrier, M., Mazumdar, R. & Islam, M. R. Efficacy of a single dose of furazolidone for treatment of cholera in children. *Antimicrobial Agents and Chemotherapy* **35**, 1864-1867 (1991).
180 Jin, X. *et al.* Furazolidone induced oxidative DNA damage via up-regulating ROS that caused cell cycle arrest in human hepatoma G2 cells. *Toxicology Letters* **201**, 205-212 (2011).
181 Tavares, L. C., Chiste, J. J., Santos, M. G. & Penna, T. C. Synthesis and biological activity of nifuroxazide and analogs. II. *Bollettino chimico farmaceutico* **138**, 432-436 (1999).
182 Masunari, A. & Tavares, L. C. A new class of nifuroxazide analogues: synthesis of 5-nitrothiophene derivatives with antimicrobial activity against multidrug-resistant Staphylococcus aureus. *Bioorganic & medicinal chemistry* **15**, 4229-4236 (2007).
183 Tavares, L. C., Penna, T. C. & Amaral, A. T. Synthesis and biological activity of nifuroxazide and analogs. *Bollettino chimico farmaceutico* **136**, 244-249 (1997).
184 Pramanik, B. N., Bartner, P. L., Mirza, U. A., Liu, Y. H. & Ganguly, A. K. Electrospray ionization mass spectrometry for the study of non-covalent complexes: an emerging technology. *Journal of mass spectrometry : JMS* **33**, 911-920 (1998).
185 Los, G. V. *et al.* HaloTag: a novel protein labeling technology for cell imaging and protein analysis. *ACS chemical biology* **3**, 373-382 (2008).
186 Hertzman Johansson, C. & Egyhazi Brage, S. BRAF inhibitors in cancer therapy. *Pharmacology & therapeutics* **142**, 176-182 (2014).
187 Wagle, N. *et al.* Dissecting Therapeutic Resistance to RAF Inhibition in Melanoma by Tumor Genomic Profiling. *Journal of Clinical Oncology* **29**, 3085-3096 (2011).
188 Cheng, Y., Zhang, G. & Li, G. Targeting MAPK pathway in melanoma therapy. *Cancer metastasis reviews* **32**, 567-584 (2013).
189 Inamdar, G. S., Madhunapantula, S. V. & Robertson, G. P. Targeting the MAPK Pathway in Melanoma: Why some approaches succeed and other fail. *Biochemical pharmacology* **80**, 624-637 (2010).
190 Wellbrock, C. MAPK pathway inhibition in melanoma: resistance three ways. *Biochemical Society transactions* **42**, 727-732 (2014).
191 Chapman, P. B. Mechanisms of resistance to RAF inhibition in melanomas harboring a BRAF mutation. *American Society of Clinical Oncology educational book. American Society of Clinical Oncology. Meeting* (2013).
192 Grossman, D. & Altieri, D. C. Drug Resistance in Melanoma: Mechanisms, Apoptosis, and New Potential Therapeutic Targets. *Cancer and Metastasis Reviews* **20**, 3-11 (2001).
193 Homet, B. & Ribas, A. New drug targets in metastatic melanoma. *The Journal of pathology* **232**, 134-141 (2014).
194 Bhadury, J. *et al.* Hypoxia-regulated gene expression explains differences between melanoma cell line-derived xenografts and patient-derived xenografts. *Oncotarget* **7**, 23801-23811 (2016).
195 Wilson, W. R. & Hay, M. P. Targeting hypoxia in cancer therapy. *Nat Rev Cancer* **11**, 393-410 (2011).

Appendix I

Sanger melanoma cell line panel growth information

Cell line	Flask size	Passage	Date frozen	Relevant lesions	Media	Split rate	Comments on growth
A04	T25	P6	15-08-14	-	RPMI1640	1:3 - 1:4	medium growth rate
C008	T75	P9	17-08-15	NF1 negative	RPMI1640	1:3	slow growth rate
C021	T75	P9	06-02-15	NF1 negative	RPMI1640	1:3 - 1:4	medium growth rate
C022	T25	P6	22-07-14	BRAF translocation	RPMI1640	1:2 - 1:3	very slow, attach slowly, tricky to seed homogenously in MW96 (pipette well)
C025	T75	P13	18-05-15	NF1 negative	RPMI1640	1:3	slow; generally resistant to most of the drugs
C037	T75	P12	30-01-15	BRAF translocation	RPMI1640	1:3 - 1:4	medium growth rate
C052	T75	P9	06-02-15		RPMI1640	1:3	slow; change media every 2-3 days
C067	T75	P9	31-07-15	NF1 negative	RPMI1640	1:3	medium-slow growth, quite big cells
C077	T75	P13	05-05-15	BRAF S467L; NF1 neg	RPMI1640	1:3 - 1:4	medium growth rate
C084	T75	P14	08-05-15		RPMI1640	1:3 - 1:4	medium growth rate
C086	T25	P6	21-05-14	NF1 negative; KIT G826R	RPMI1640	1:3 - 1:4	medium growth rate
C089	T75	P12	30-01-15	BRAF V600E	RPMI1640	1:4-1:6	medium-fast growth rate, small
C092	T25	P6	01-04-14	-	RPMI1640	1:3 - 1:4	medium growth rate, cell line with the lowest number of lesions (mut and CNV)
CHL-1	T25	P8	28-04-14	KIT E640K	DMEM/F12	1:5 - 1:10	very fast growth
Colo-792	T75	P11	30-01-15	NF1 negative	DMEM/F12	1:5 - 1:8	fast growth rate
D10	T75	P15	18-05-15	KIT M541L	RPMI1640	1:3 - 1:4	medium growth rate
D22	T25	P6	22-04-14	-	RPMI1640	1:3 - 1:4	medium growth rate
D24	T75	P17	18-05-15	NF1 negative	RPMI1640	1:3 - 1:4	medium growth rate
D35	T75	P9	30-06-15	-	RPMI1640	1:3 - 1:4	medium growth rate
D38	T75	P13	16-04-15	-	RPMI1640	1:3 - 1:4	medium growth rate
MeWo	T75	P12	16-05-15	NF1 negative	RPMI1640	1:5 - 1:8	fast, very stretched shape

Sanger melanoma cell line panel seeding information

Cell line	6day assay	72hr assay	siRNA transfection
MW96	cell/well	cell/well	cell/well
A04	5000	15000	16500
C008	3000	9000	9900
C021	3500	10500	11550
C022	4000	12000	13200
C025	3500	10500	11550
C052	3000	9000	9900
C067	1000	3000	3300
C077	3000	9000	9900
C084	5000	15000	16500
C086	3500	10500	11550
C089	2500	7500	8250
C092	2500	7500	8250
C037	3000	9000	9900
CHL-1	500	1500	1650
Colo-792	2500	7500	8250
D10	5000	15000	16500
D22	2000	6000	6600
D24	3500	10500	11550
D35	3500	10500	11550
D38	2500	7500	8250
M002	3000	9000	9900
MeWo	3000	9000	9900

Appendix II

Sanger melanoma cell line panel ALDH Expression (RNA_{seq}) – Performed by Dr Marco Ranzani (Sanger Institute, Cambridge, UK)

	A04	C008	C021	C025	C037	C052	C067	C077	C084	C086	C089	C092	CHL-1	COLO-792	D10	D22	D24	D38	M002	MEWO
ALDH1A1	334.3889	26.56243	9.581963	3.507376	114.2107	13.95971	0.29079	2.283137	3.363288	13.8035	7.586397	0.054671	0.077577	3.8070827	7.092818	0.093786	1.5599581	18.9118	160.619	4.842421
ALDH1A2	3.812738	23.12301	0.123749	16.16446	5.627982	10.21814	0.47233	0.385264	0.21353	9.845608	0.102203	0.019791	0.007423	0.7252329	0.587517	0.024513	24.552633	0.9208293	0.307968	1.629807
ALDH1A3	63.88532	0.339993	143.4239	0.384956	21.29148	5.147514	629.1024	312.634	0.3236	202.1175	61.7181	22.58277	0.40215	174.80283	21.72953	12.20283	1265.8197	47.27347	7.317165	4.885375
ALDH1B1	36.98992	9.822547	10.03827	33.25124	11.70621	16.1401	18.43911	5.976208	0.373012	8.414438	20.8363	8.554065	11.54573	33.622315	13.59367	11.85966	5.5084666	9.3911461	12.06943	13.50829
ALDH1L1	0.231684	0.008203	0	0	35.07555	0.004314	0	0.021551	0.043516	0.09434	0.175148	0.073268	0.004428	0.0223309	0.195848	0.02681	0.0346281	0.0512962	0.144973	0.018759
ALDH1L2	14.51429	0.122748	0.168012	30.19767	3.828581	39.17514	0.094183	0.424219	0.029138	0.032595	0.225638	3.704774	18.78739	0.0962185	72.83752	0.45272	5.7678777	15.142141	0.107918	0.312372
ALDH2	0.307307	0.218045	0.339716	7.468295	18.53243	0.807075	0.353793	1.7152	0.07128	0.303755	0.874582	3.996286	27.40965	0.0517552	43.66951	0.129491	0.0683501	5.1937979	0.131046	0.033111
ALDH3A1	0.065158	0.126599	0.014031	0.251379	0.089872	0.006004	0.00857	0.054246	0	0	0.255546	0.059039	0.497683	0.7123002	0.0937	0	0.8079353	0.0150068	0.032281	0.00821
ALDH3A2	30.74007	27.97154	26.56697	18.68896	15.42117	10.49295	32.36554	54.6453	23.69337	0.952893	54.36657	19.70016	31.93639	39.992979	17.53233	20.13902	97.384585	25.079128	8.924886	35.4449
ALDH3B1	3.80625	5.972396	12.42268	23.07749	0.278026	9.096022	35.14028	14.07838	15.51818	8.081205	12.98594	16.02599	5.894044	16.071152	10.21353	19.40413	28.312896	4.2982987	3.082425	25.07162
ALDH3B2	1.133068	0.085323	86.32294	4.774931	0.056936	0.353845	0.01261	0.49196	0.600421	0.370251	0.048592	0.002444	0	2.1633269	0.156703	0.00687	0	0.0071097	19.17246	0.039968
ALDH4A1	10.59333	5.233102	7.768549	17.17236	3.38862	11.38132	3.854832	11.06419	12.54001	10.50709	4.897874	5.846582	7.490439	14.956618	10.18472	7.941782	6.2463469	5.3722725	37.26175	8.417984
ALDH5A1	11.85201	0.551076	3.984271	8.043175	8.789863	6.356714	0.403175	0.525989	0.024147	4.985864	14.72562	3.683074	9.889199	18.198813	12.90234	7.585425	2.8245954	3.9329018	3.848972	1.724769
ALDH6A1	5.882529	6.959225	7.273771	15.31742	11.9926	17.32032	23.38827	18.45164	7.673927	20.49994	21.66782	12.77455	11.52897	4.9862398	21.7427	4.348227	14.757503	4.6678878	5.318022	10.40178
ALDH7A1	61.87025	35.74744	63.42438	33.75924	61.89622	48.78037	85.26293	102.0255	46.36889	61.75107	76.4987	78.58636	26.92053	52.398989	31.89971	41.99787	54.779774	104.31369	60.08238	56.74447
ALDH9A1	92.11546	131.3017	86.33794	58.43186	146.7694	92.31622	51.7616	67.74004	105.7785	96.43331	29.9512	60.03402	74.43012	134.86874	50.63851	63.95581	39.66163	32.91405	40.07535	87.91001
ALDH8A1	0.675895	0.227795	0.095049	0.108938	1.082511	0.204235	0.261852	0.114876	0.686982	0.84913	0.128431	0.796763	0.428442	0.1523744	0.031276	0.033337	0.2853351	0.1270171	0.250245	0.128807
ALDH16A1	14.43383	12.00804	14.05996	13.37542	9.643836	26.82486	5.145173	19.94117	13.51909	12.86327	17.45192	8.028629	14.7634	8.8068131	6.738047	9.08198	4.0916353	17.637988	27.74042	13.14779
ALDH18A1	36.02603	33.3916	92.00518	74.24234	23.0686	68.24825	67.3893	63.78105	72.97821	73.29433	60.7429	86.14501	66.22901	46.952855	78.72875	46.43044	76.428854	32.698774	46.1027	68.44273

RNAseq data expressed as heat-map for each cell line, including all 19 ALDH isoforms. Higher numbers (red) indicate higher ALDH RNA expression. Lower numbers (green) indicate lower RNA expression.

Appendix III

Primer references used for design in RT-qPCR in ALDH characterisation by OakLabs (Berlin, Germany)

Gene	TaqMan Assays:	RefSeq	GenBank mRNA	Amplicon Length
ALDH1A1	Hs00946916_m1	NM_000689.4	AK302168.1;K03000.1;AK293176.1;AK026641.1;AF003341.1;BC001505.2;AY390731.1;M26761.1;AB209821.1;BT006921.1;AK000118.1	61
ALDH1A2	Hs00180254_m1	NM_170697.2;NM_170696.2;NM_003888.3;NM_001206897.1	BC030589.2;AK303057.1;BX443600.2;AK128709.1;AK294981.1;AB015228.1;AB015227.1;AB015226.1	70
ALDH1A3	Hs00167476_m1	NM_000693.2 updated to NM_000693.3	U07919.1;BC069274.1;BX538027.1;AK312303.1;AK302607.1;AK303441.1;DB480234.1;AL110109.1	60
ALDH1B1	Hs00377718_m1	NM_000692.4 was missing	BT007418.1;DB256700.1;AK313344.1;AK225950.1;BE889810.1;BC001619.1	85
ALDH1L1	Hs00201836_m1	NM_001270364.1;NM_012190.3;NM_001270365.1;NR_072979.1	AK294392.1;AF052732.1;AK222535.1;AK222694.1;CR749807.1;BC027241.1;AB209299.1;AK308112.1	94
ALDH1L2	Hs00402876_m1	NR_027752.1;NM_001034173.3	BC103935.1;AK095827.1;BC103934.1;AK300373.1	63
ALDH2	Hs01007998_m1	NM_001204889.1;NM_000690.3	AK301375.1;AY621070.1;CR456991.1;BC071839.1;AK223373.1;X05409.1;Y00109.1;BC002967.1;DC353712.1	66
ALDH3A1	Hs00964880_m1	NM_001135167.1;NM_001135168.1;NM_000691.4	M74542.1;AK093755.1;BC004102.2;AK091272.1;BC021194.2;AK225513.1;AK292193.1;S61044.1;AK314584.1;AK093877.1;BC004370.1;M77477.1;BT007102.1;BC008892.2	71
ALDH3A2	Hs00166066_m1	NM_001031806.1;NM_000382.2	AK025677.1;BC002430.2;AB208894.1;AK315096.1;CR457422.1;CR749559.1;L47162.1;AK292381.1;U46689.1	99
ALDH3B1	Hs00997594_m1	NM_001161473.1 updated to NM_001161473.2;NM_001030010.1 updated to NM_001030010.2;NM_000694.2 updated to NM_000694.3	AK291505.1;BC014168.2;BT009832.1;BC033099.1;EF411198.1;AB209651.1;U10868.1;BC013584.2	67
ALDH3B2	Hs02511514_s1	NM_000695.3;NM_001031615.1	BG009508.1;BC007685.2;AK299956.1;AK092464.1	90
ALDH4A1	Hs01013142_m1	NM_001161504.1;NM_003748.3;NM_170726.2	U24266.1;AK222486.1;AK294552.1;BC007581.1;FJ462711.1;AK289972.1;BC023600.2;U24267.1;BM856369.1	70
ALDH5A1	Hs00542449_m1	NM_001080.3;NM_170740.1	BC034321.1;AK294699.1;AJ427355.2;AJ427354.2;Y11192.1;AK314357.1;AK290800.1;AK315380.1;L34820.1	79
ALDH6A1	Hs00194421_m1	NM_005589.3;NM_001278593.1;NM_001278594.1	M93405.1;AK312389.1;AK311478.1;AJ249994.1;AK223244.1;AW418653.1;BC004909.1;AK222687.1;AF148505.1;AF159889.1;BC032371.1;AK294243.1	131
ALDH7A1	Hs00609622_m1	NM_001202404.1;NM_001182.4;NM_001201377.1	BC071712.1;BC002515.2;AU135961.1;BC073174.1;DC375277.1;AK312459.1;S74728.1;AK297365.1	113
ALDH8A1	Hs00988965_m1	NM_170771.2;NM_022568.3;NM_001193480.1	AK074266.1;AK290784.1;BC113862.1;AF303134.1;BC114473.1;DA635162.1;AK298325.1;AK222848.1	56
ALDH9A1	Hs00997881_m1	NM_000696.3	BC151141.1;AK302191.1;BC070030.1;U34252.1;AK312751.1;BC151140.1;AK301767.1;U50203.1;X75425.1;AK302183.1;AF172093.1;AK293520.1	60
ALDH16A1	Hs01035457_m1	NM_153329.3;NM_001145396.1	AK297101.1;AY007096.1;BC035641.1;BC014895.2;BC042142.1;AK298587.1	81
ALDH18A1	Hs00913261_m1	NM_001017423.1;NM_002860.3	BC117242.1;BC143930.1;BC106054.1;X94453.1;BC117240.1;AK295487.1;U68758.1;U76542.1;AK299557.1;AK312271.1	71
GAPDH	Hs03929097_g1			58
18S	Hs99999901_s1			187
TBP	Hs00427621_m1			65